DEVELOPMENT OF NOVEL EFFICIENT HETEROCYCLIC BASED CYTOFECTINS: EVALUATION AND STRUCTURE ACTIVITY STUDIES

Thesis Submitted for the Degree of

DOCTOR OF PHILOSOPHY

(In Chemistry)

To

NATIONAL INSTITUTE OF TECHNOLOGY WARANGAL

By

MALLIKARJUN GOSANGI

(Roll No. 701121)

Department of Chemistry
National Institute of Technology
Warangal-506004, India

June 2017

ACKNOWLEDGEMENT

It has been a long and a wonderful journey since I started my research career in Research lab II, Department of Chemistry, National Institute of Technology, Warangal (NITW). Although the first year of my Ph.D. was a bit challenging due to new working atmosphere but I was fortunate to join a team that helped me to overcome and improved my curiosity towards the research. Completion of this thesis was impossible without the support and guidance of these people.

It gives me an immense pleasure and pride to express my sincere gratitude and respect for my supervisor **Dr. Srilakshmi V. Patri**, Associate Professor, Department of Chemistry, National Institute of Technology, Warangal for her guidance and unconditional support scientific or otherwise throughout different stages of my doctoral studies.

I express my sincere thanks to the **Director**, National Institute of Technology, Warangal, for having given me the opportunity to carry out the work and allowing me to submit my investigations in the form of thesis.

I express my deep heartfelt gratitude to Head Department of Chemistry present (**K. V. Gobi**) and past (**B. Rajitha, V. Rajeswer Rao, K. Laxma Reddy and G. V. P. Chandramouli**) for their timely help to get fellowship and provided facilities in time to my research.

I proclaim my indebtedness to **Dr. Vijaya Gopal**, Senior Principal Scientist, Centre for Cellular and Molecular Biology, Hyderabad for extending her lab facilities and her motivational words towards successful completion of biological studies of my research work. I will remain ever grateful to **Dr. Arabinda Chauduri**, chief scientist,

IICT Hyderabad for his support and timely help to get scientific collaboration with Dr. Vijaya Gopal.

I express my sincere thanks to my DSC members **Prof. Y. Pydishetty**, Chemical Engineering Department, National Institute of Technology, Warangal and **Prof. V. Rajeswar Rao**, Chemistry Department, National institute of technology for their suggestions and assessing my work progress for every six months for institute academic proceedings during my tenure.

I take this opportunity to express thanks to **Prof. A. Ramachandraiah, Prof. I. Ajith Kumar Reddy, Prof. P. Nageswar Rao, Prof. B. Rajitha, Dr. Vishnu Shankar, Dr. Venkatathri Narayanan, Dr. Kashinath, Dr. B. Srinivas, Dr. L. Hariprasad** Department of Chemistry, National Institute of Technology, Warangal for their valuable advice, encouragement and moral support in my Ph. D tenure.

The thesis would not have come to a successful completion, without the help of my past and present lab members **Dr. K. Bhavani, Dr. V. Amarnath, R. Hithavani, R. Venkatesh, S. Nagaraju, B. Papulal** and **my friends**.

I also gratefully acknowledge the unstinted support of Dr. Vijaya gopal lab members **Dr. Thasneem, M. Mehamood Haroon, and Durga jeyalaxmi** for their helping hands to finish my biological experiments in CCMB.

I am also grateful to **Council of Scientific and Industrial Research (CSIR)** for providing me the CSIR-JRF/SRF fellowship during my Ph.D.

Finally I owe a lot to my family members, for their undying support, selfless love and sacrifice to see this dream come true.

(Mallikarjun Gosangi)

CONTENTS

CHAPTER 4

Design, Synthesis and Transfection Efficiencies of Novel 1, 2, 3 Triazolium Head Group Based Cationic Lipids

CHAPTER 5

Evolution of New "Bolaliposomes" Using Novel α-Tocopheryl Succinate Based Cationic Lipids and 1, 12-Disubstituted Dodecane Based Bolaamphiphile for Efficient Gene Delivery

Synopsis

Publications

Chapter 1

Introduction to the Thesis

-"Development of Novel Efficient Heterocyclic Based Cytofectins: Evaluation and Structure Activity Studies"

1.1 INTRODUCTION

A number of common human diseases have been linked directly to the gene regulation can be carrying forwarded to the next generation and also resulted from mutations. To cure these diseases at its genetic root, the concept of gene manipulation by using a corrected copy of gene sequence was introduced as "gene therapy" during the period from late 1960's to early 1970's.[1] As many pharmacological treatments are falling short of curing many diseases, quest for alternate unique approaches turns the gene therapy to become an attractive concept to treat both inherited and acquired diseases. This has created a lot of attention on gene therapy to improvise further advancements in the fields of medicine, biochemistry and biotechnology etc. The primary goal of gene therapy when it has been initiated was to restore the function of deficient gene in inherited diseases with functional copy of gene sequence has now broadened to applicable in curing acquired diseases and cancers including the delivery of genetic vaccines to induce both cell-mediated and humoral immune responses.[2] The multifaceted application of gene therapy can be defined as following functions like to replace defective genes, substitute missing genes, silence unwanted gene expression and introduce new cellular bio-functions. Although, gene therapy is a versatile approach, its therapeutic success has not yet met the expectations.

The objectives and principles of gene therapy has greatly been relies on two important criteria like (i) development of suitable oligo nucleic acid strands that can provide required functions in targeted cells[3] and (ii) their efficient intracellular delivery in to selected cells.[4] Many genes capable of expressing required functions have been identified, and it is now possible to produce engineered DNA that carries therapeutic phenotype in sufficient quantities for clinical trials. The methods to deliver the drug mimics, where their expression is to be needed is majorly hindering the clinical success of gene therapy. Among the wide range of methods to deliver oligonucleotide established so far,[5] vector mediated gene delivery are at forefront and mandates further advancements for ideal delivery.

1.2 BRIEF HISTORY & SUCCESS:

Research on gene therapy has been carrying for decades to bring the concept to clinic, yet very few patients have received significant benefits of gene-therapy treatments. Since the gene therapy concept arose initially during 1960s, only 1843 clinical trials have been completed, are ongoing or have been approved till June, 2012.[6] In 1983, a retroviral vector was used to transfer a functional gene into murine bone marrow,[7] 3T3 cells,[8] or a human HPRTB-lymphoblast cell line.[9] The first human gene therapy experiment was conducted on September 14, 1990, on four year-old Ashanti Desilva who suffered from ADA deficiency. Dr. W. French Anderson and Michael Blaese[10] were succeeded in infusing the white blood cells by performing experimental therapy (with correct copy of gene composition) into Ashanti to correct her immunodeficiency and proved that the concept could work tentatively. In 2000 the successful treatment of children suffering from a rare form of X-linked severe combined immunodeficiency (SCID-X1) characterized by an early block in differentiation of T and natural killer (NK) lymphocyte was lifted the morale of community.[11] The first non-viral clinical trials assessed the safety and efficacy of liposomes derived from DC-Chol:DOPE complexed with plasmid DNA containing the CFTR cDNA under the transcriptional control of the SV40[12]or RSV 3'LTR promoters[13] via single nasal delivery. In detail, the significant success achieved from gene therapy has been discussed with respect to the disease origin as follows.

A. Immune deficiencies: Several inherited immune deficiencies have been treated successfully with gene therapy. Notably, Severe Combined Immune Deficiency (SCID) and Adenosine deaminase deficiency (ADA) are the first two immune based disorders, which have been treated successfully by delivering the functional copies of genes using retroviral vectors. In both the cases the *ex vivo* experimental therapy was used, which involves the transduction of blood stem cells using virus and DNA complex outside the patient body and then administered into the patient after corrected functions established. In case of SCID treatments some of trials[14] experienced the triggered

leukemia symptoms but with ADA treatments majority of the patients no further injections needed for ADA enzyme and none of them developed leukemia[15].

B. Hereditary blindness: Inherited blindness treatment using gene therapy is in infancy which was being focused to develop due to some encouraging results from animal models show that potential to reverse vision loss. Retina is a part of eye plays an important role in vision is easy to access and also partially protected from the immune system. Hence, virus/DNA complex can enter easily and can't move to other organs. Leber congenital amaurosis (LCA) is one of the degenerative forms of blindness which was treated successfully using AAV (adeno-associated virus) based gene therapy treatment.[16] In another trial, 6 out of 9 patients with the degenerative disease choroideremia had improved vision after a virus was used to deliver a functional REP1 gene.[17]

C. Hemophilia: The missing clotting protein, Factor IX, is responsible for most severe forms of diseases by losing blood either internally or even small cut. This protein function was successfully accomplished by delivering the Factor IX gene using adeno-associated viral vector to liver cells.[18] After treatment, most of the patients made at least some Factor IX, and they had fewer bleeding incidents.

D. Blood disease: β-Thalassemia is a disease relates to the red blood cells arise due to the defect in β-globin gene, which codes for an oxygen carrying protein in red blood cells. People who have been suffering from this disease depend on regular blood transfusions due to lack of enough red blood cells.[19] In 2007, a patient received *ex vivo* experimental gene therapy for sever β-Thalassemia which included blood stem cells from bone marrow of patient were taken and treated with a retrovirus to transfer a working copy of the β-globin gene.[20] The modified stem cells were returned to his body, and gave rise healthy red blood cells. The patient required no blood transfusions even after seven years of the procedure. A similar approach could be used to treat patients with sickle cell disease.

E. Fat metabolism disorder: Lipoprotein lipase (LPL) is a gene responsible for a protein that helps break down of fats in the blood to prevent fat concentrations from rising to toxic levels. In 2012, Glybera became the first viral gene-therapy treatment to be

approved in Europe in which the working copy of LPL gene was successfully delivered using an adeno-associated virus to muscle cells.[21]

F. Cancer: Cancer is one of the dangerous diseases responsible for most of the recent human deaths in different forms throughout the world. Several gene-therapy treatments are under development for cancer.[22] T-VEC is an effective treatment for melanoma (a skin cancer) based on gene therapy experimentation using modified version of the herpes simplex 1 virus (normally causes cold sores).[23] The virus is injected directly into the patient's tumors which replicates inside the cancer cells until they burst, releasing more viruses that can infect additional cancer cells except healthy ones.

G. Parkinson's disease: Parkinson's disease is a brain related disorder arises due to the gradual loss of brain cells that are responsible to produce signaling molecule, dopamine. As the disease advances, patients lose the ability to control their movements. A small group of patients with advanced Parkinson's disease were treated with a retroviral vector to introduce three genes into cells in a small area of the brain.[24] These genes gave cells that don't normally make dopamine the ability to do so. After treatment, all of the patients in the trial had improved muscle control.

The success of the gene therapy mainly relies on the development of delivering devices that can transport nucleic acids from extracellular to intracellular. Many different kinds of vectors are in use and still have been developing to propagate the gene delivery approach towards success.

1.3 METHODS OF GENE DELIVERY:

Great efforts have been witnessed in many prior investigations to establish successive delivery of gene into selective cells using various strategies with different kind of power full tools. All these strategies were categorized mainly into three different methods based on the tools used for nucleic acid delivery. They are

1. Naked DNA delivery
2. Virus mediated gene delivery
3. Non-viral mediated gene delivery

1.3.1 Naked DNA delivery:

Naked DNA delivery is one of the broad classes of delivering methods of nucleic acid in to cell which involves the delivery of simple DNA into the local tissues or into the systemic circulation using specialized instruments or physical methods. Based on the instruments and physical techniques used for delivery have been discussed as follows.

a. Electroporation: Electroporation is a method that uses to create temporary pores throughout cell membrane, allowing DNA molecules to pass through. A high voltage of electric short pulses are used to supply in cell culture would responsible for pore formation including high rate of cell death. This method is suitable to perform transfection even in difficult cell types. This application is so limited in clinical trials due to its high rate of cell death.[25]

b. Gene Gun: The use of particle bombardment, or the gene gun, is another physical method of DNA transfection. In this technique, DNA is coated with gold particles and loaded into a device which generates a force to achieve penetration of DNA/gold into the cells. This technique is fast, simple and safe and has been successfully employed to deliver nucleic acids to cultured cells as well as to cells in vivo especially gene transfer to skin[26]and superficial wounds.

c. Sonoporation: Sonoporation uses ultrasonic frequencies to deliver DNA into cells. The process of acoustic cavitations is thought to disrupt the cell membrane and allow DNA to move into cells.

d. Magnetofection: In a method termed Magnetofection, DNA is complexed to magnetic particles and a magnet is placed underneath the tissue culture dish to bring DNA complexes into contact with a cell monolayer.

e. Microinjection: In this method, the DNA is directly injected into the nuclei of target cells using a fine glass needle under microscope. Although this method is simple, it is the most difficult to apply clinically. While this method of gene transfer is nearly 100% efficient it is laborious and time-consuming, typically allowing only a few hundred cells (e.g., < 500) to be transfected per experiment.[27]

The naked DNA delivery methods have so many limitations towards its successful application in clinic. Most frequently discussed drawbacks in earlier reports are as follows.

* Systemically administered naked DNA significantly inhibited by the barriers size, shape and polyanionic charge of DNA, thus inhibiting the cell permeability of DNA.
* It shows very little dissemination and transfection into the deeply sited cells following delivery and can be re-administered multiple times.
* Every approach in physical methods depends on a special kind of instrumentation to deliver the DNA which would responsible for lot of cell death happens in almost all techniques.
* Degradation of DNA is one more common drawback usually insists the *in vivo* application of physical methods.

These insisting drawbacks have given an idea to protect the DNA with a specialized material and allowed for delivery into maximum number of cell count. Viruses are the first materials have been used for packing of DNA and followed by delivery which in turn referred as viral mediated gene delivery.

1.3.2 Virus mediated DNA delivery:

Viral vectors are a tool commonly used by molecular biologists to deliver genetic material into cells. This process can be performed inside a living organism (*in vivo*) or in cell culture (*in vitro*). Viruses have evolved specialized molecular mechanisms to efficiently transport their genomes inside the cells they infect. Delivery of genes by a virus is termed transduction and the infected cells are described as transduced. Molecular biologists first harnessed this machinery in the 1970s. Paul Berg used a modified SV40 virus containing DNA from the bacteriophage lambda to infect monkey kidney cells maintained in culture.[28] There are different types of viral vectors have been used as vectors so far as mentioned as follows.

I. Retroviruses: Retroviruses are being used as vectors in many gene therapy clinical trials. Moloney murine leukemia is one of the recombinant retrovirus have the

ability to integrate into the host genome in a stable fashion. They contain a reverse transcriptase that allows integration into the host genome[29]having limited DNA payload capacities. The primary drawback to use of retroviruses involves the requirement for cells to be actively dividing for transduction. There is concern that insertional mutagenesis due to integration into the host genome might lead to cancer or leukemia.

II. Lentivirus: These types of viruses are capable of integrating into the genome of both dividing as well as non-dividing cells.[30] The viral genome in the form of RNA is reverse-transcribed when the virus enters the cell to produce DNA, which is then inserted into the genome at a random position by the viral integrate enzyme. However, studies have shown that lentivirus vectors have a lower tendency to integrate in places that potentially cause cancer than gamma-retroviral vectors.[31]

III. Adenovirus: They carry the genetic material in the form of double-stranded DNA of approximately 36 kb. In contrast to lentiviruses, adenoviral DNA does not integrate into the genome and is not replicated during cell division.[32] They cause respiratory, gastrointestinal and eye infections and trigger a rapid immune response with potentially dangerous consequences.

IV. Adeno-associated viruses: These are small viruses with a genome of single stranded DNA of approximately 4.7 kb surrounded by a protein coat.[33]The wild type AAV can insert genetic material at a specific site on chromosome 19 with near 100% certainty. There are a few disadvantages to using AAV, including the small amount of DNA it can carry and the difficulty in producing it.

V. Herpes Simplex Virus: The Herpes simplex virus is a human neurotropic virus. This is mostly examined for gene transfer in the nervous system.[34]

Although viruses are the most efficient gene transfer vehicles available to date, their widespread clinical success has been impeded by a number of major drawbacks associated with their use. The drawbacks are as follows:

* The strong immune response in host cells due to viral proteins (preventing virus reuse), endogenous viral recombination, oncogenic effects and possible large-scale contamination of the engineered viruses and high cost of production.

* The tragic death of an 18-year-old viral gene therapy research subject (in Sept. 1999, USA), who was being treated for partial ornithine transcarbamylase (OTC) deficiency,[35] was believed to be triggered by a severe immune response to the adenoviral vector used.
* The therapy-turned-setback situation in which two out of eleven children developed a blood disorder similar to leukemia following an adenoviral treatment against SCID by a French gene therapy team.

Thus with these complications viral gene therapy has come under severe scrutiny, provoking a sense of urgency to search for safer alternatives to viral vectors.

1.3.3 Non Viral mediated DNA delivery:

Non-viral methods present certain advantages over viral methods, viz., simple large scale production, no insert size limit and low host immunogenicity. Previously, low levels of transfection and expression of the gene held non-viral methods at a disadvantage. However, recent advances in vector technology have yielded molecules and techniques with transfection efficiencies similar to those of viruses.

i. Polymeric Vectors: Cationic polymers are the promising safe, predictable, biodegradable and non-toxic alternative vectors to viral gene therapy. Synthetic polymer-based carriers conjugated to the targeted gene or other biological molecules could provide successful delivery relying on endocytosis.[36] Many kinds of polymers have therefore been investigated for gene delivery, such as chitosan, PEI, polylysine, polyamino ester and so on.[37]

ii. Dendrimer-Based Vectors: Dendrimers are a class of macromolecules with highly branched spherical species that are readily soluble in aqueous solution and have a unique surface of primary amino groups.[38] Dendrimers can disperse uniformly in comparison with many other kinds of polymers investigated recently.[39] The structure starts from a core molecule and grows through stepwise polymerization process generating new layer on one another by increasing the exact number of surface amines conveniently binds to antibodies, contrast agents, and radio pharmaceuticals for applications in a number of different areas of biology and medicine.[40] PAMAM

dendrimers have therefore been extensively explored as non-viral gene carriers because of their unique characteristics, such as narrow molecular distribution, defined size and shape, high molecular uniformity and highly functionalized terminal surface.[41]

iii. Proteins and Peptides: Proteins and Peptides offer a unique strategy of delivering method of genetic material by direct conjugation to olegonucleotide with high efficiencies and cell-specificities. These efficient potentials of peptide vectors are due to utilizing short sequences of basic amino acid residues which can readily cross the plasmamembrane. These amino acid sequences, called protein transduction domains or cell-penetrating peptides, are generally divided into two classes: (1) lysine-rich peptides (e.g. MPG peptide and transportan) and (2) arginine-rich peptides, (e.g. antennapedia (Antp), trans-activating transcriptional activators (TAT).[42] Generally, in peptide-oligonucleotide delivery strategies, the peptide is covalently linked to the oligonucleotide construct rather than complexed via electrostatic interactions. Synthesis of these peptide-oligonucleotide complexes follows several strategies. Haralmbidis et al. first synthesized peptide-oligonucleotide constructs by solid phase synthetic approaches.[43]

iv. Nano particles:

iv.a Quantum Dots: Quantum dots are the nano-sized materials can emit fluorescence when they exposed to light and electricity, significantly helpful in labeling and tracking of proteins inside of the cell.[44] One major reason for the interest in using quantum dots (QD) over other organic fluorophores like fluoroscein, is that quantum dots can be excited over a wider range of wavelength and the emission spectra is more narrow and symmetrical. Additionally, quantum dots are less prone to photobleaching and have significantly longer fluorescence lifetimes when compared to organic fluorophores.[45] Finally, fluorescently labeled DNA complexes can show the association of the carrier and DNA, determining the point of dissociation is hindered by the fact that the two components must diffuse to a certain distance before being detected as distinct entities. Quantum dot-based FRET analysis of protein shows donor-acceptor separation distances of less than 100 Å, indicating potential for monitoring the unpacking of DNA nanoplexes after endocytosis.[46] Burgess et al. first showed that quantum dots could be covalently conjugated to plasmid DNA for transfection studies.[47]

iv.b Gold nano particles: Gold nanoparticles (AuNPs) are the attractive materials for nucleic acid delivery applications[48] due to their advantages like able to fabricate in a scalable fashion with low size dispersity, functional diversity can be achieved by the creation of multifunctional monolayers and allowing multiple functional moieties like nucleic acids and targeting agents to be placed onto the particle surface.[49] Additionally, the properties like cytotoxicity, bio-distribution and in vivo excretion can be modulated by regulating the particle size and surface functionality.[50]

v. Cationic lipids: Cationic lipids are the surfactant kind of materials can produce bilayer membrane type vesicles whenever they dispersed in aqueous solution. These artificially prepared vesicles made of from lipid bilayer used to refer as Liposome. Liposomes are the mimics of biological membranes can easily diffuse with cell plasma membranes and enter into the cell cytosol. Due to their structure, chemical composition and colloidal size, all of which can be well controlled by preparation methods, liposomes exhibit several properties which may be useful in various applications. The most important properties are colloidal size, i.e. rather uniform particle size distributions in the range from 20 nm to 10μm, and special membrane and surface characteristics. They include bilayer phase behavior, its mechanical properties and permeability, charge density, presence of surface bound or grafted polymers, or attachment of special ligands, respectively. Additionally, due to their amphiphilic character, liposomes are powerful solubilizing systems for a wide range of compounds. In addition to these physicochemical properties, liposomes exhibit many special biological characteristics, including (specific) interactions with biological membranes and various cells.[51]

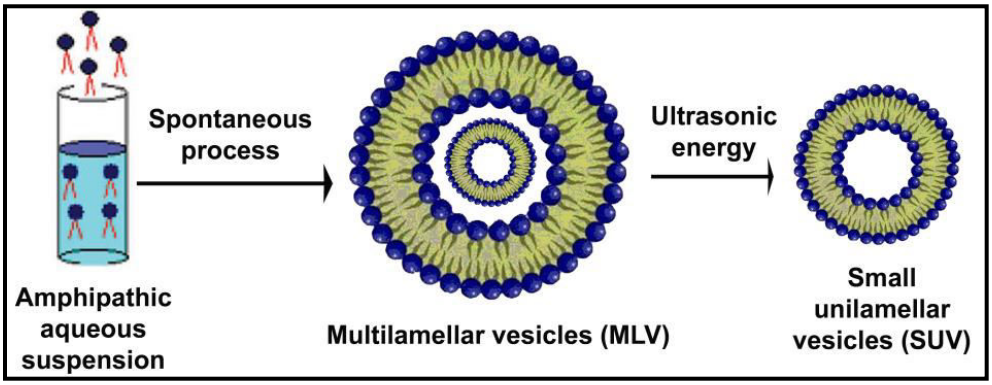

Fig. 1 Formation of Liposomes.

Liposomes are used for drug delivery due to their unique properties. A liposome encapsulates a hydrophilic molecule in the aqueous region inside a hydrophobic membrane, while the dissolved hydrophilic solutes cannot readily pass through the lipids. Hydrophobic chemicals can be dissolved into the membrane, and in this way liposome can carry both hydrophobic molecules and hydrophilic molecules. To deliver the molecules to sites of action, the lipid bilayer can fuse with other bilayer such as the cell membrane, thus delivering the liposomal contents. There are three types of liposomes – MLV (multilamellar vesicles), SUV (Small Unilamellar Vesicles) and LUV (Large Unilamellar Vesicles). These are used to deliver different types of drugs. Liposomes can deliver various types of biomolecules viz., plasmid DNA, RNA, oligonucleotides, DNA-RNA chimeras, synthetic ribozymes, antisense molecules etc. Targeted delivery could also be achieved by cationic liposomes through covalent attachment of receptor-specific ligands to the liposomal surface. The encapsulation of DNA into conventional liposomes could be a technical problem due to the plasmid size, representing a poor transfection system. On this basis, an alternative technology based on cationic lipids and PE was developed in the late 1980s.[52] The idea was to neutralize the negative charge of plasmids with positively charged lipids to capture plasmids more efficiently and to deliver DNA into the cells. Generally, this is a simple procedure requires mixing of the cationic lipids with the DNA and adding them to the cells. This results in the formation of aggregates composed of DNA and cationic lipids.

Non-viral cationic lipid mediated gene transfer was first described by Felgner et al., through the synthesis of a cationic lipid DOTMA.[52] This lipid, either alone or in combination with other neutral lipids, spontaneously forms multilamellar vesicles (MLV) which may be sonicated to form small unilamellar vesicles (SUV). DNA interacts spontaneously with DOTMA to form lipoplexes with 100% of the DNA becoming associated. It is presumed that complex formation simply results from ionic interactions between the positively charged headgroup of DOTMA and the negatively charged phosphate groups of DNA. DOTMA is commercialized (Lipofectin., Gibco-BRL, Gaithersburg, MD) as a one to one mixture with DOPE and has been widely used to

transfect a wide variety of cells.[53] In an effort to reduce the cytotoxicity of DOTMA, a series of metabolizable quaternary ammonium salts have been developed whose efficiency is comparable to that of Lipofectin when dispersed with DOPE.[54]

1.3.3.1 Cationic Lipids: Important Structural Parameters

The molecular architecture of cationic transfection lipids consists of a hydrophobic domain, linker functionality and a cationic head-group (Figure 2).It is important to recognize that the transfection efficiency is not determined solely by one part of the cationic lipid but by a combination of them. The characteristics of the hydrophobic moiety, head group and their linker segments that determine optimal gene transfer depend upon the overall structure of the lipid. Different types of lipids may have unrelated structural requirements towards transfection in terms of the optimal length of the hydrocarbon chains, chemical nature of the linkages and the polar head groups. Therefore a modular approach is useful for the plan and the design of new vectors. Trends in the aggregation properties of the liposomes can be obtained by studying the effect of variations in the chemical structures of the cationic lipids. The systematic modification of each part and understanding of the structure–activity relationship (SAR) are important determinants to achieve optimal performance.

a. Hydrophobic Domain: The hydrophobic domains of cationic transfection lipids are mainly derived from either simple aliphatic hydrocarbon chains or steroid. Majority of the commonly used cationic transfection lipids contain two linear aliphatic chains in their hydrophobic domains such as DOTMA[52] and SAINT.[55] In general, lipids containing one hydrocarbon chain tend to form micelles, transfect poorly, and are toxic,[56] whereas, cationic lipids containing three aliphatic chains tend to be poorly transfecting than those with two hydrocarbon chains.[57] In contrast, number of cationic lipids are reported as best transfecting agents having either a single cholesterol or a tocopherol moieties in hydrophobic regions which could sufficient to act as hydrophobic part to participate in self assembly and produce unilamellar vesicles.

b. Head-Group Domain: The polar headgroups of cationic transfection lipids usually consist of a single quaternary ammonium group (DOTMA, Figure 3), polyamine moieties (DOSPA,[58] Figure 4), and guanidinium salts (BGBH,[59] Figure 5) are examples of cationic transfection lipids with positively charged nitrogen head groups linked to hydrophobic tails. In addition, several cationic lipids with heterocyclic head groups such as pyridinium, piperizine, imidazolium (SAINT,[55] NCC10[60] & $(C_{16}Im_2)C_2$,[61] Fig. 3 & Fig. 4) and amino acid head-groups (e.g., lysine, arginine, ornithine, Histidine and tryptophan)[62] have also been reported.

c. Linker Bonds: The relative orientation of the cationic head group and hydrocarbon anchor is governed by the nature of linker bond bridging them. The linker group controls the conformational flexibility, degree of stability, biodegradability, and hence, the gene transfer efficacy of a cationic amphiphile. Most commonly used linker groups include ethers, esters, carbamates, amides, carbonates, phosphonates, disulfides, etc. Carbamate (as in DC-Chol,[63] Fig. 3) and amide (e.g., DOSPA, Fig.5) are stable chemically but biodegradable. Ethers (e.g., DOTMA, Fig. 3) are chemically stable but non-biodegradable, and are found to impart better transfection efficacies causing toxicities due to their strong persistence after transfection. Esters (e.g., DOTAP,[64] Fig. 3) are biodegradable and less toxic but not stable chemically. The length of the linker determines the level of hydration of a lipid. Incorporating ester function as a linker in tocopherol derived lipids aimed to establish least toxic better potentiate transfecting reagents. The phosphate di-ester bond (as in DOPE) is biodegradable and has chemical stability higher than esters but lower than amides. On the other hand, phosphonates are hydrolytically more stable than phosphates and presumably biodegradable.[65]

1.3.3.2 Classification of Cationic Transfection Lipids

The pioneering report by Felgner et al.[52] on the use of cationic liposomes-based formulation in transfecting cultured cells spurred the development of a wide range of cationic lipid-based reagents for use in gene therapy.[66] Cationic transfection lipids could be classified into various groups and sub-groups depending on the nature of the head group, hydrocarbon anchor, or the linker bonds. They can be conveniently classified into

four categories depending on the orientation of head group with respect to the hydrophobic back bone as follows:

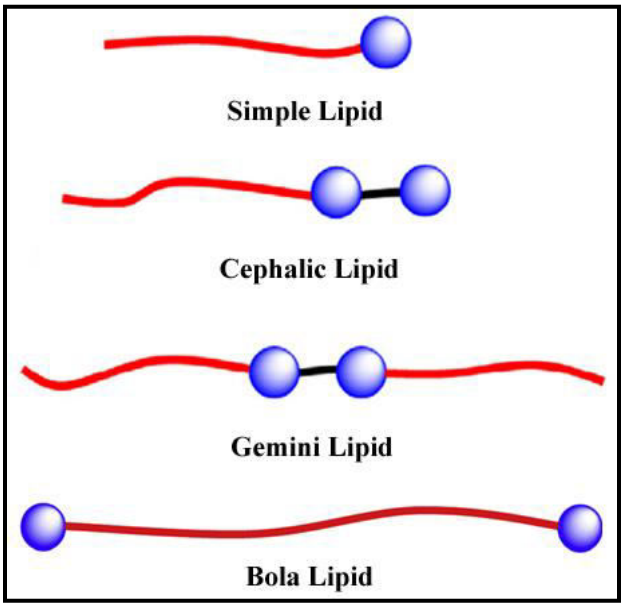

Fig. 2 Classification of cationic lipids

Spherical bead: Hydrophilic head group; cylindrical shape: Hydrophobic back bone.

a. Simple cationic lipids: Simple surfactants that can able to produce bilayer membrane vesicles while expose to hydration, commonly made up of from one cationic charge either simple (DOTMA) or delocalized (SAINT) as hydrophilic head group connects to a hydrophobic back bone usually arises from dialkyl long aliphatic chain or one steroidal skeleton from cholesterol (NCC10, DC-Chol) or vitamin-E[67] (AETHET)[67a] considered as simple cationic lipids.

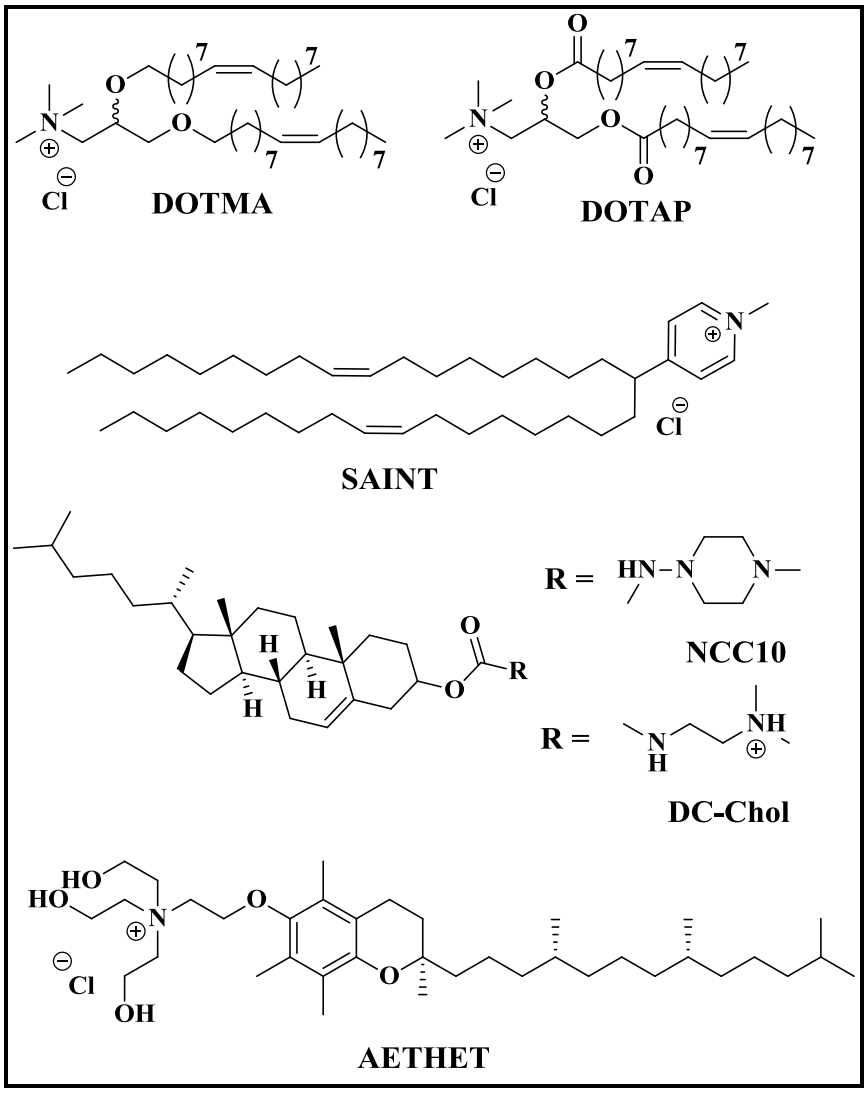

Fig. 3 Representative structures of mono cationic lipids having the head groups like simple quaternary ammonium cations (DOTMA, DC-Chol & AETHET) and delocalized cations (SAINT) with hydrophobic back bone like aliphatic long alkyl chain (DOTMA, SAINT) cholesterol (NCC10, DC-Chol) and tocopherol (AETHET).

b. Gemini cationic lipids: There are several lipids, that have been developed as better transfection reagents with the name of gemini cationic lipids, which is a term used to refer a dimeric lipid generated from two similar lipid molecules that are connected each other by a spacer functionality at their head group region.[68] The structural entity which is helpful to connect two similar lipid molecules plays crucial role in determining transfection along with the other common lipid constituents. Some of the achievements

using this kind of lipid molecules towards gene delivery mentioned in Fig. 4 such as cardiolipin analogue based gemini surfactants (lipid A),[69a] cholesterol based gemini lipids (Chol 5L)[69b] and tocopherol as anchoring group (T3T, T8T & DTEC)[69c,d]with localized positive charge density whereas the $(C_{16}Im)_2C_3$[70]gemini lipid is made up of from delocalized charge density using imidazolium cation.

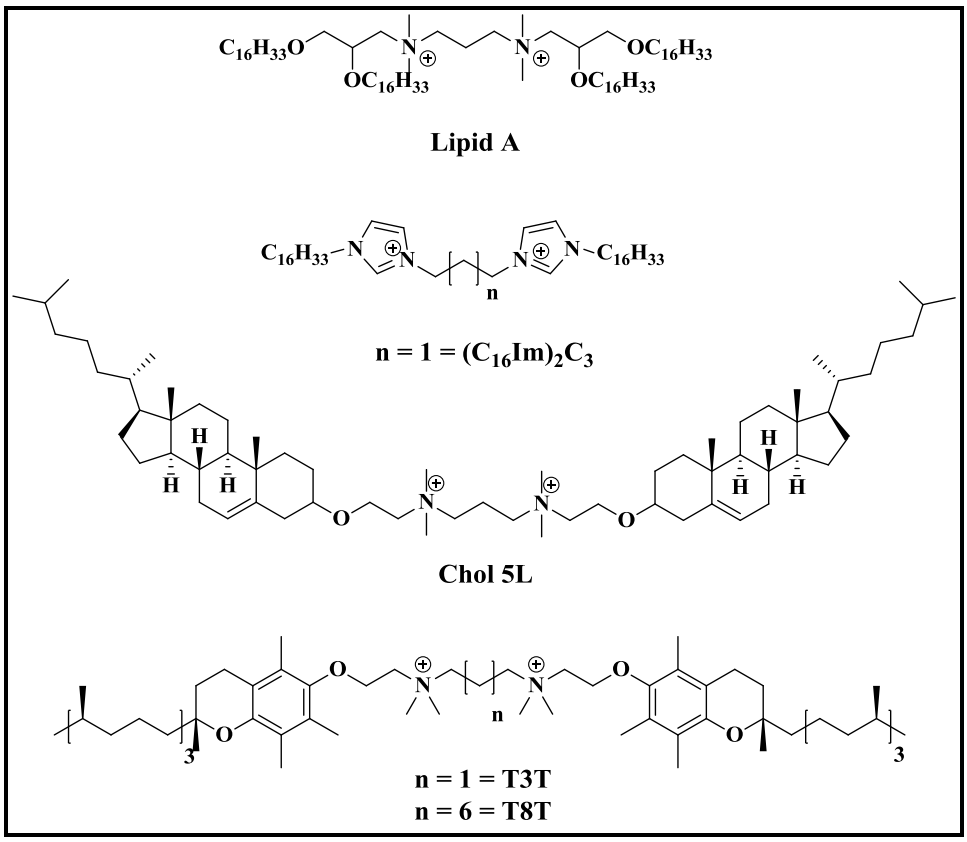

Fig. 4 Representative structures of gemini cationic lipids derived from simple quaternary ammonium cation (lipid A) and delocalizable cationic ($(C_{16}Im)_2C_3$) head groups linked to anchoring groups like long aliphatic alkyl chains (lipid A, $(C_{16}Im)_2C_3$), cholesterol (Chol 5L) and tocopherol (T3T, T8T).

c. Polycephalic lipids: Cephalic lipids are nothing but simple lipids which have more than one cationic head groups either of similar or dissimilar in structure. Increase in number of cationic charge can facilitate the strong charge-charge interactions with less amount of lipid and provide better transfection results. Usually two or more number of cationic head groups connect to a single hydrophobic back bone generates bicephalic and

poly cephalic lipids respectively. Fig. 5 represents the structures of cationic lipids having multiple cations in their head groups generated from simple protonated amines (DOSPA), trimethyl amines (lipid 1) and guanidinum groups (BGBH).[59]

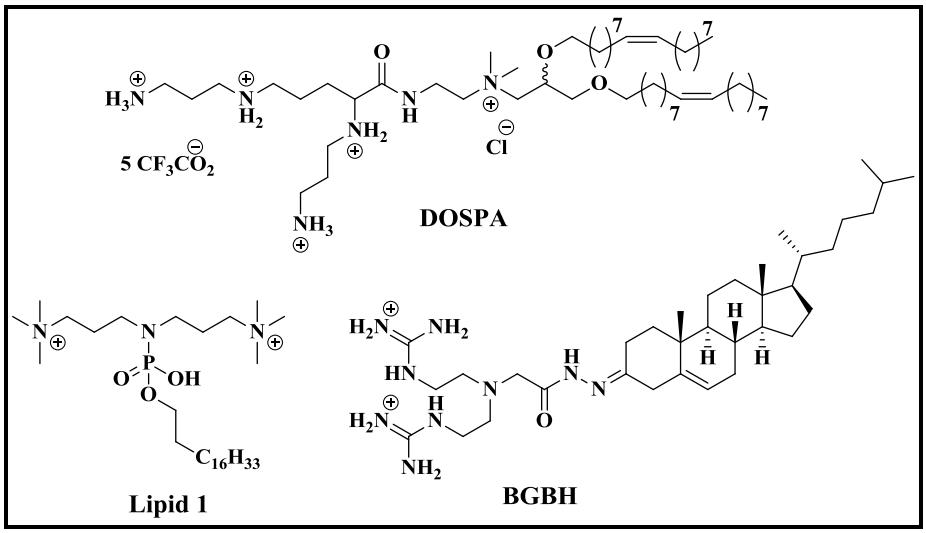

Fig. 5 Representative structures of cationic lipids having multiple cationic charges (protonated amines: DOSPA, trimethylammonium: lipid 1, and guanidinium:BGBH) of hydrophilic region connects to single hydrophobic anchoring group (aliphatic chain & cholesterol).

d. Bolaamphiphile: Some of recent reports for better transfection performances have been witnessed using the surfactants which consists of two hydrophilic centers having similar or dissimilar structures connects together by a long hydrophobic chain and are popularized with the name of bolaamphiphiles or bolalipids.[71] Bolalipids can be fabricated in to different kinds of aggregations such as hydrogelators, monolayered membrane vesicles and nano fibers, which can be helpful in successful delivery of olegonucleotide in intracellular.[72] The rapid usage of these particular molecules in cutting edge developments of drug and gene delivery is due to the significant features of surfactants that could develop chemically stable aggregations leads to proper packing and unwrapping of DNA while transporting from extracellular to intracellular respectively. An unsymmetrical bolaamphiphile, Orn-C20-G (Jain, N.et al,[73a] Fig. 6), symmetrical multivalent head group derived diaminododecane based bolaamphiphile (Khan, M. et

al,[73b] Fig. 6) and unsymmetrical vitamin b derived bolalipid (Patil, S. P. et al,[73c] Fig. 6) are the successful recent outcomes in the gene delivery using bolalipid kind of surfactants.

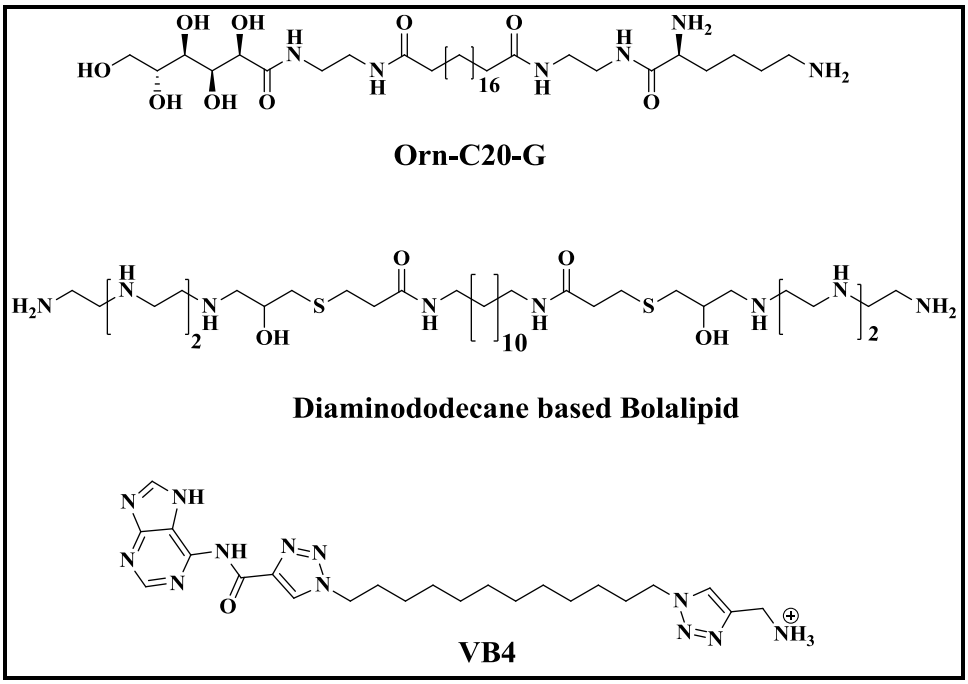

Fig. 6 Representative structures of cationic bolaamphiphiles having unsymmetrical (Orn-C20-G and VB4) and symmetrical (Diaminododecane based bolalpid) hydrophilic head groups.

1.4 LIPOFECTION PATHWAY

Lipofection is a process to inject desired functional material like active nucleotide in to the cells using liposomal membranous vesicles across the cell membrane which includes various steps like (a) formation of lipid-DNA complex (lipoplex); (b) adhesion of lipoplex to the cell surface; (c) endocytotic internalization of the lipid-DNA complex; (d) escape of lipoplex from the endosome compartment to the cytosol; (e) transport of the endosomal released DNA to the nucleus followed by its transgene expression (Figure **7**). Each step in the lipofection pathway is met with barriers thereby affecting the efficiency of the overall process.

(a) ***Formation of a Lipoplex*****:** Lipoplex is a supramolecular aggregate, generates from the electrostatic attraction between positively charged lipid vesicle and negative termini of plasmid DNA. It was initially suggested that several liposomes might associate with a single plasmid molecule to render its charge become neutral, condensing the DNA to form a small dense lipoplex.[74a] However, electron micrograph studies have produced images of lipoplexes with a range of diameters 100–200 nm macromolecular structures.[74b-d] The small size of the lipoplexes would be due to the complexation or condensation of DNA which results elongated, 'spaghetti'-shaped lipoplexes and thought to represent DNA sandwiched between lipid uni and or bilamellar layer.[74e] Large aggregates or 'meatball' lipoplexes are also observed, and thought to comprise numerous lipid and DNA molecules. Precisely which of these represents the most transfection-efficient fraction is not clear.

(b) ***Cellular internalization of lipid-DNA complex*****:** It was originally thought that cationic amphiphile–DNA complexes enter cells by absorption of net positive charge on to the negatively charged cell surface due to certain types of exposed cell membrane components.[52] Studies on cell entry and intracellular trafficking have been established that nonviral vector derived lipoplexes were being engulfed by the bilayered plasma membrane commonly termed as endocytosis[75] which has been classified as different types based on mechanism and participating proteins. Among the many types of endocytotic routes few of them were recognized and well documented such as clathrin-mediated endocytosis via coated pits, adsorptive mediated endocytosis via proteoglycon fusion,[76a] caveolae-mediated endocytosis via caveolae vesicles and or lipid-raft,[76c] phagocytosis and macropinocytosis.[76c]

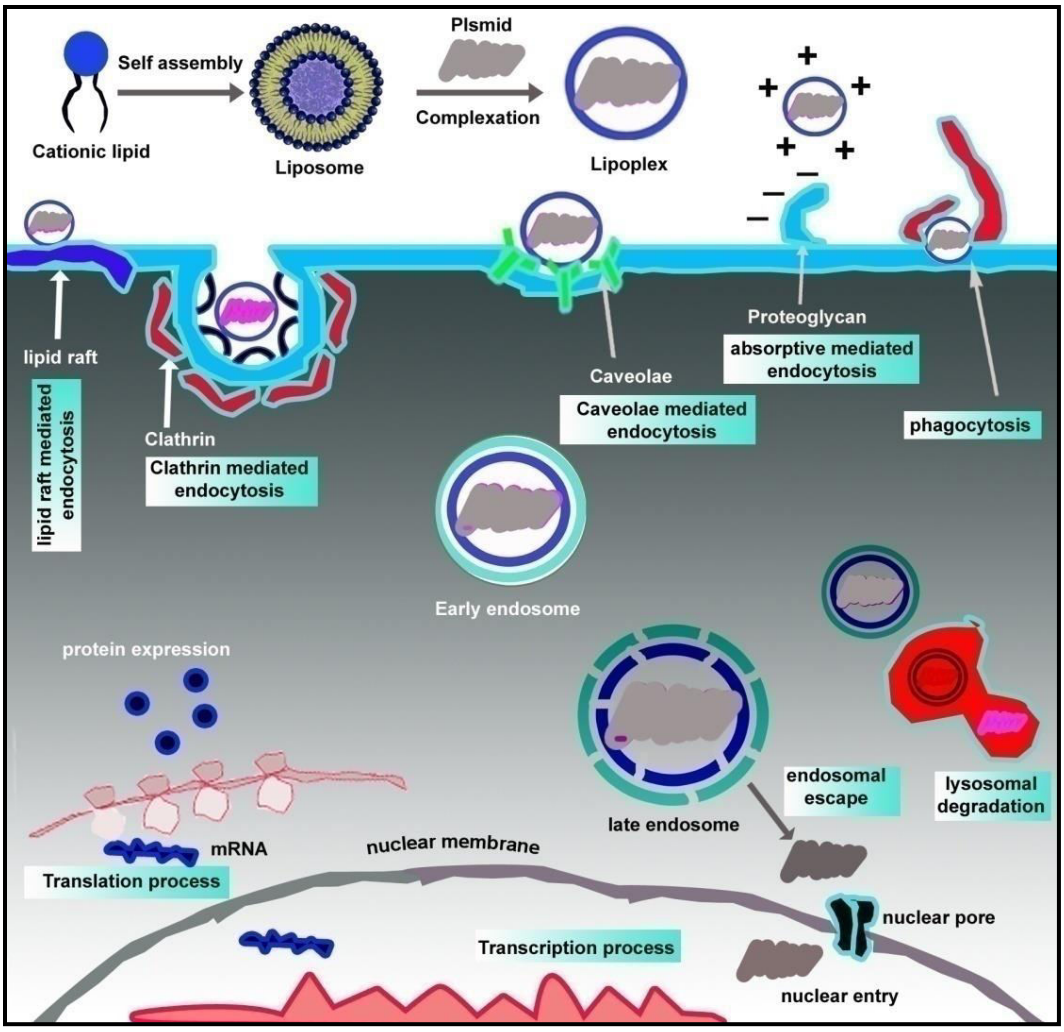

Fig. 7 Lipofection Pathway

As demonstrated in the Fig. 7, lipoplex can be taken up either by any one of the aforementioned pathways or multiple paths. Each of the endocytotic mechanism is involved with several types of distinct proteins and drives the lipoplex in to the early endosome stage where the internal pH is more than five. Several molecular biology studies have been succeeded to find the inhibitors which can selectively inhibit the expression of particular proteins would result the blocking of corresponding path way. While chlorpromazine (CPZ) inhibits clathrin-mediated endocytosis,[76a,b] methyl-β-cyclodextrin (m-β-CD) or filipin-III inhibits caveolae-mediated endocytosis.[76c] Cytochalasin D inhibits macropinocytosis by affecting actin polymerization and membrane ruffling.[76d] Wortmannin, an inhibitor of PI 3-kinase which contributes to

vesicle fusion is involved in vesicle trafficking.[76e] Blockage of transport of complexes from endosomes to lysosomes by nocodazole is known to prevent accumulation of complexes in the endosomes.[76f] Bafilomycin A1 is a specific inhibitor of vacuolar ATPase, which is involved in maintaining the acidic pH of lysosomes.[76g] Sequestration of cholesterol with nystatin was also used to assess the mode of internalization.[76b] All the inhibitors corresponds to specific endocytosis route and their optimized concentrations are listed in table 1.

Table 1 Endocytosis route inhibitors and their optimized concentrations

	Inhibitor	**Pathway**	**Concentration**
1.	Chlorpromazine	Clathrin	10 g/ml
2.	Filipin-III	Caveolae	5 g/ml
3.	Cytochalasin D	Actin	5 M
4.	Wortmannin	Macropinocytosis	25M
5.	Nystatin	Caveolae	25 g/ml
6.	Methyl-β-cyclodextrin	Clathrin and caveolae	7.5 M
7.	Nocadazole	Microtubules	10 M
8.	Bafilomycin A1	Vacuolar-type H(+)-ATPase	2.5 nM

(c) ***Endosomal Escape:*** It is the one of the critical steps to determine the transfection efficiency which involves endosome rupture or unfolds to release the packaged DNA material in to the cytoplasm prior to its degradation in lysosome. Following internalization, the coated vesicle transforms into an early endosome where accompanies acidification of vesicular lumen to get transformed to late endosome stage. Although the DNA release from this state of endosome to cytosol is not well understood, a few models have been proposed to explain the mechanistic insight. Xu & Szoka[77a] proposed a model in which local endosomal membrane destabilization occurs due to the electrostatic interactions between the cationic lipids and anionic lipids of endosomal membrane induce the displacement of anionic lipids from the cytoplasm and form a

charge neutral ion pair with the cationic lipid.[77b] This can induce destabilization of endosome membrane causes subsequent decomplexation of the DNA, by way of the so-called flip-flop mechanism. Additionally, non-cationic helper lipids such as neutral DOPE could facilitate membrane fusion and helps to increase the rate of destabilization of endosomal membrane.[78a-c] It is indeed known that DOPE has a tendency to form an inverted hexagonal phase, often observed when membranes are fusioned.

(d) ***Nuclear entry of DNA:*** The transport of DNA from the cytoplasm to the nucleus may be the most significant limitation to successful gene transfer. After endosomal escape, the nucleic acid must traffic through the cytoplasm and enter the nucleus by overcoming the hurdles like degradation due to cytoplasmic nucleases and mobility of DNA extremely low in cytoplasm. The cytoplasmic *p*DNA can enter nucleus by two possible hypotheses such as mixing of cytoplasm after the loss of nuclear membrane during mitosis[80a] and direct entry through the nuclear pore complex.[80b] Consistently, gene transfer in cultured cells has been shown to be greatly enhanced by mitotic activity for the lipoplexes. This would mean that tumor cells are more targeted due to their multiple mitosis and non-dividing cells are rarely transfected like healthy brain cells have no or low dividing activity. However, for delivery to non-dividing cells, nuclear localization sequences (NLS) can be incorporated into the DNA complexes in order to deliver the plasmid into the nucleus. NLS are short peptide sequences (5–25 amino acids) necessary and sufficient for nuclear localization of their respective proteins.[80b] These sequences can be incorporated into complexes with cationic lipids,[80c] or can be directly linked to the plasmid.[80d] Nevertheless, the transfection results of non-dividing endothelial cells gave with and without incorporation of a NLS is 5% positive and 80% positive respectively.[80c]

1.5 PRESENT THESIS

In general any synthetic cationic lipid consists of three basic building blocks such as positively charged hydrophilic part usually arises from nitrogen, phosphorus and arsenic atoms, hydrophobic part comes from simple aliphatic long alkyl chains, steroidal skeleton like cholesterol and vitamins like α-tocopherol. These two distinguished parts link together either by a functional moiety like ester, ether, sulfide and carbamate or directly by a covalent bond. Each of the lipid constituent could influence the gene delivering properties with their individual properties like fluidity, orientation, cleavage sensitivity of linker and hydration potentials etc. Several studies have been addressed in many structure activity relationships by modifying each of the constituent domains and how it could influence gene delivery efficiencies. The established activity investigations proved that the successful attributes obtained so far is due to the presence of multiple amines and various types of amines such as quaternary, protonated and tertiary amines. Hence, the presence of these amines is an important aspect in the design of gene delivery vectors, as these enhance DNA condensation and endosomal buffering capacity. Ever since Solodin et al. reported imidazolium as head group (DOTIM),[81] interest of research has been shifted to focus in using heterocyclic functionalities as head groups in cationic lipid mediated gene delivery.

Development of new vectors with alternative structural types is necessary to built better efficient transfection vectors to upgrade the non-viral gene therapy towards clinic. Tocopherol (Vitamin E) being a natural amphiphilic molecule consists of a group of isoprenoid compounds of plant origin which were described initially as essential micronutrients for normal fertility in rats.[82a-d] Subsequent studies have established a wide range of functions to it especially the RRR-tocopherol stereoisomer, the most biologically active form.[83] Besides its well documented role as a free radical chain-breaking antioxidant, α-tocopherol can also modulate directly cellular signaling pathways viz., protein kinase C, leading to diverse biological responses in different cell types.[84] Many analogues of alpha-tocopherol are proved to be efficient anti proliferative agents in wide range of cell types.[85] Tocopherol has been used for drug delivery with significant

success.[86] In addition, cationic lipid self-assemblies formulations including tocopherol were used for targeted gene delivery.[87]

Recent reports that established efficient transfection reagents using alpha-tocopherol as backbone via structure activity relationship represented in Fig. 8. **Lipids 1a-e** having single alpha-tocopherol as its aliphatic backbone and linked to quaternary ammonium cations which have various substitutions like protonated, methylated, mono-hydroxyethylated, di-hydroxyethylated and tri-hydroxyethylated head groups. The DNA delivering potentials using these lipids were reported that the increasing number of hydroxyl substitution in head group of lipid increased their DNA condensation potential which has led to increase delivering potentials. The same backbone has also used in another interesting study that the minor orientation change in lipid back bone having same functional lipid units **Lipid 2a-b** were synthesized and studied how could it affects the DNA delivering potentials with respect to the physicochemical properties were interpreted. Apart from many key steps in lipofection pathway, endosomolysis has significant role in successive nucleic acid delivery. Most of the recent reports have been developed in favor of endosomolysis by adding pH sensitive groups like 1H-imidazole to cationic head group for improved transfection results. To achieve this, **Lipid 3a-b** and **Lipid 4a-b** were synthesized to show the effectiveness of histidine and tocopherol groups toward overcoming the barriers like endosomolysis and serum sensitivities. The serum compatible nature of tocopherol has also proved again using in a series of gemini lipids such as **Lipid 5a-c** in siRNA delivery. Based on these successful outcomes tocopherol was being used as a lipid back bone in almost all studies of present thesis.

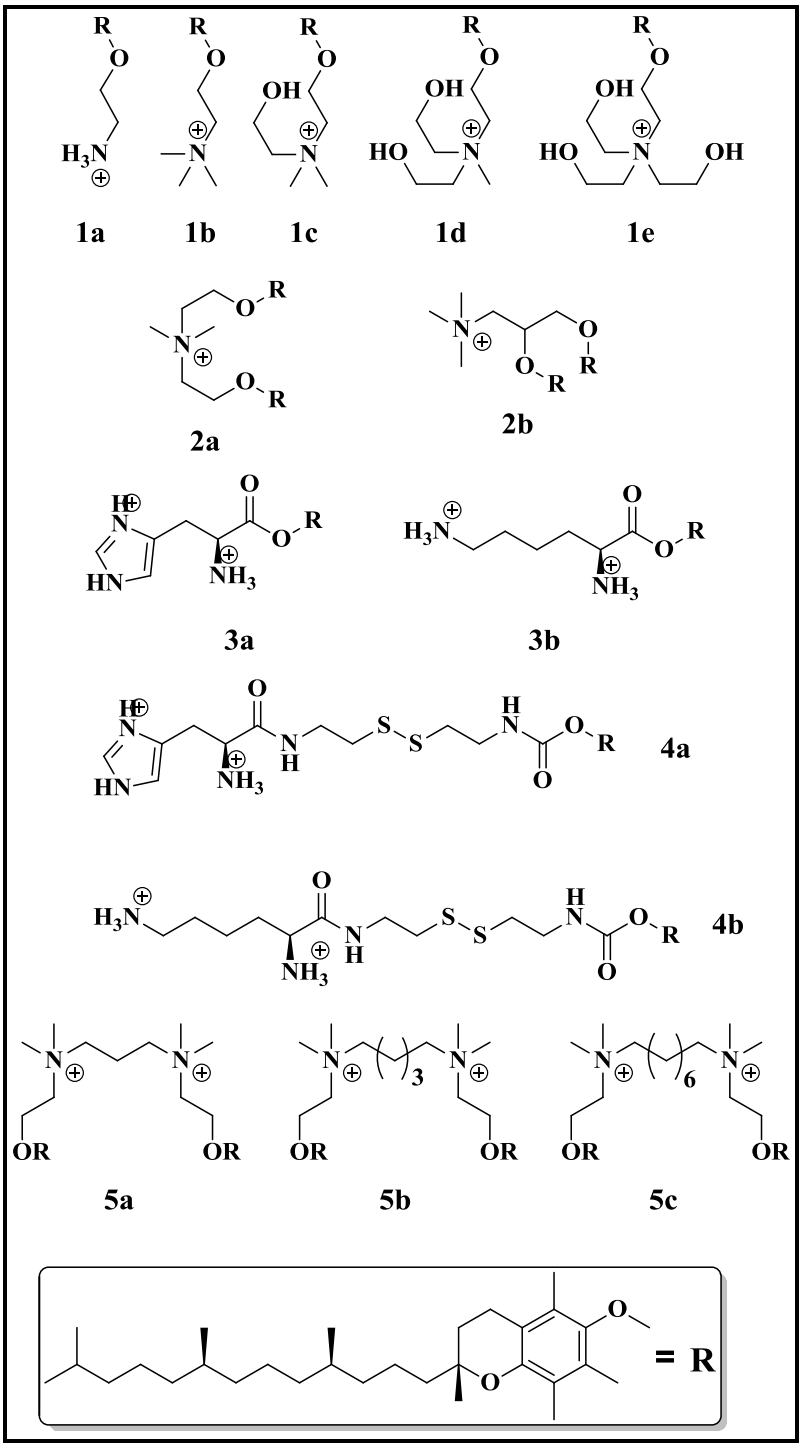

Fig. 8 Representative molecular structures of tocopherol back bone based cationic lipids reported in recent literature.

Among the all various counter parts of the lipid, head group has drawn lot of attention in many recent studies due to its close proximity towards the negative dipole of nucleic acid and significant role in self assembly of bilayered membranes. The systematic modification of head group structure with various linkages to quaternary 'N' atom of a head group, proper structure activity correlation study was envisaged. Accordingly, seven cationic lipids were synthesized using different tertiary amines from various heterocyclic functionalities, which were tethered to an anchoring back bone, alpha-tocopherol. In **chapter 2** the synthesis, characterization and transfection potentials of these different head group modified tocopherol lipids were discussed. A detailed structure activity study of these lipids on transfection potentials with respect to their physicochemical properties was discussed.

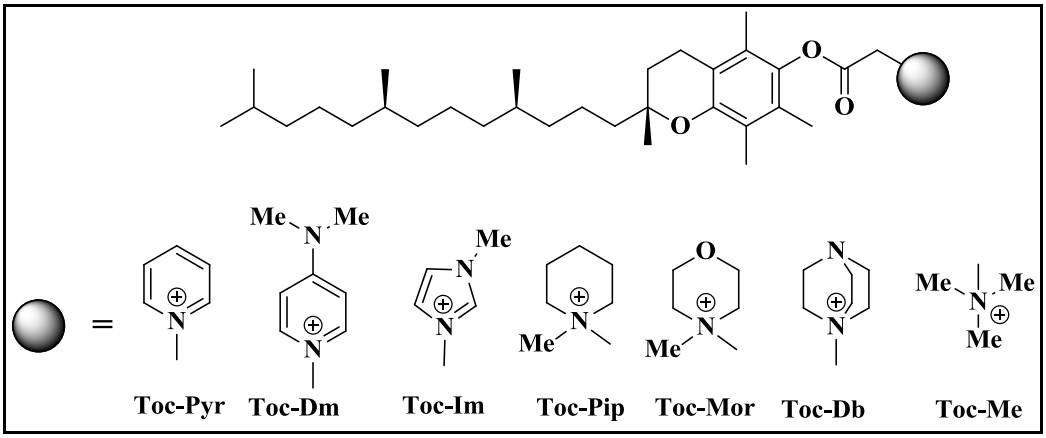

Fig. 9 Molecular structures of heterocyclic based tocopherol derived cationic lipids

The gemini cationic lipids are the well known class of non viral lipid based systems for inducing better transfection profiles than a simple one due to their dimeric lipid nature and low cellular toxicities. In tandem to develop better transfection reagents, alpha-tocopherol is used along with delocalizable charge density. In fact, delocalisable charged functionalities like imidazolium and pyridinium as head groups have been reported in recent studies towards liposomal mediated gene delivery. These lipids have interesting features like soft cationic nature, lesser hydration potentials and lower cytotoxicity. Based on these facts, a series of delocalizable cationic charge head group based, tocopherol derived, dimeric cationic lipids were designed. These lipids consists of

two tocopherol groups as anchoring groups and varying alkyl chain lengths as spacers between two imidazolium head groups. The varying spacer length may affect the DNA binding, hence the transfection. The synthesis, characterization and evaluation of transfection potentials of delocalizable cationic charged imidazolium head group based tocopherol derived gemini cationic lipids were discussed in **chapter 3** in detail with the support of physicochemical and lipid/DNA interaction studies.

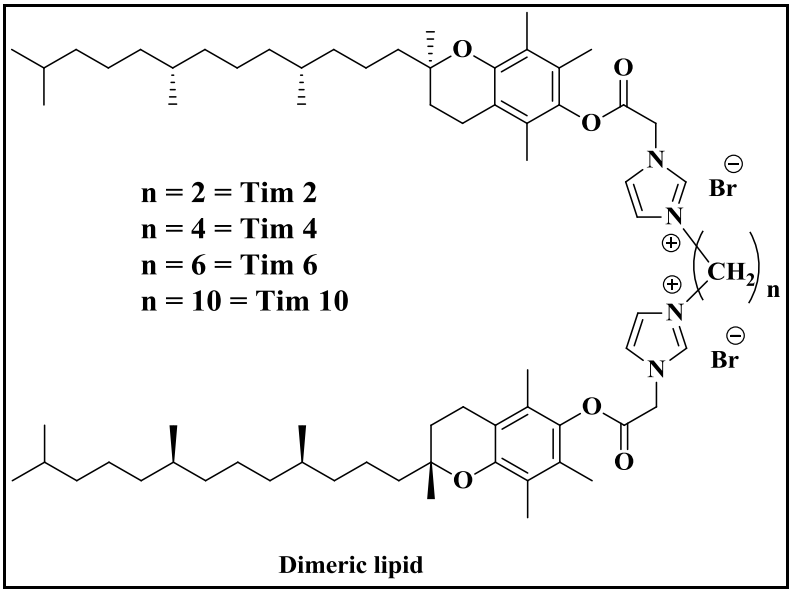

Fig. 10 Molecular structures of tocopherol derived dimeric lipids

Despite of many structure activity investigations towards the successful establishment of better cytofectins to deliver the genes, exact structural requirement for stable transfection are obscure. In attempts to develop better transfection reagents new motifs toward the structure based analysis have been used. To this end, we developed a new delocalisable cation by using a heterocyclic 1, 2, 3 triazole ring instead of imidazole and pyridine which were already used extensively in many prior studies. The heterocyclic 1, 2, 3 triazole ring was synthesized by using Huisgen 1, 3 dipolar cycloaddition is so called click chemistry.[88a] Click chemistry refers that a connecting strategy of two individual groups having terminal dipoles to produce regiospecific pure heterocyclic product with high yields.[88b,c] This strategy was used to develop 1, 2, 3 triazole heterocyclic aromatic ring has already been used as a core ring in many biologically

potent libraries due to its unique properties like stability towards acidic and basic environments as well as viable to neither oxidative nor reductive hydrolysis.[89a]. These features make the use of 1, 2, 3-triazole as a linker in cationic amphiphiles vector design.[89b,c]

The triazolium cation is a delocalisable cation, which could derive from the quaternization of 1, 2, 3 triazole, was used in two different studies and discussed their results separately under section A and section B of **chapter 4**. In an effort to study the effect of covalent grafting of a delocalisable cation to a head group of unshared positive charge of cationic lipid, a series of three lipids as shown in Fig. 11 were developed. The detailed structure activity investigation of these lipids in comparison with control lipid DDAB, which has no delocalisable cation on its head group, was discussed with various supporting experimental results under section A.

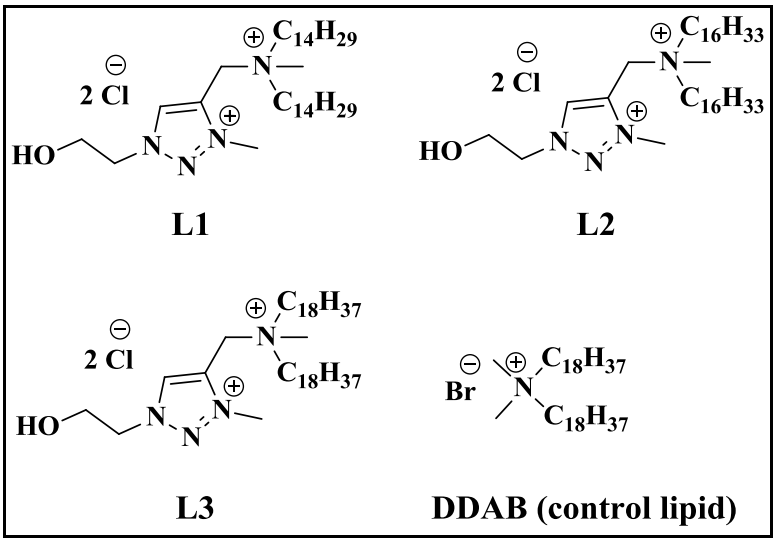

Fig. 11 Molecular structures of 1, 2, 3 triazolium dicationic lipids

Understanding the structural parameters of cationic amphiphiles which can influence their gene transfer properties is important for designing efficient liposomal gene delivery reagents. To this end we focused to study the effect of nature of side chain substitution of a delocalisable cation present in head group region of cationic lipid. The gene transfection properties were evaluated in comparison to a lipid which has similar heterocyclic core ring with unshared positive charge on its head group structure. In

consideration of preferred structural features and the successful attributes of enhancing transfection efficiencies of 1, 2, 3 triazolium delocalized cation discussed in section A, three cationic lipids with the structures as shown in Fig. 12 were designed. The synthesis, characterization of these designed lipids with consistent analytical data and comparative transfection profile were elaborated in detail by providing consistent experimental results in section B of chapter 4.

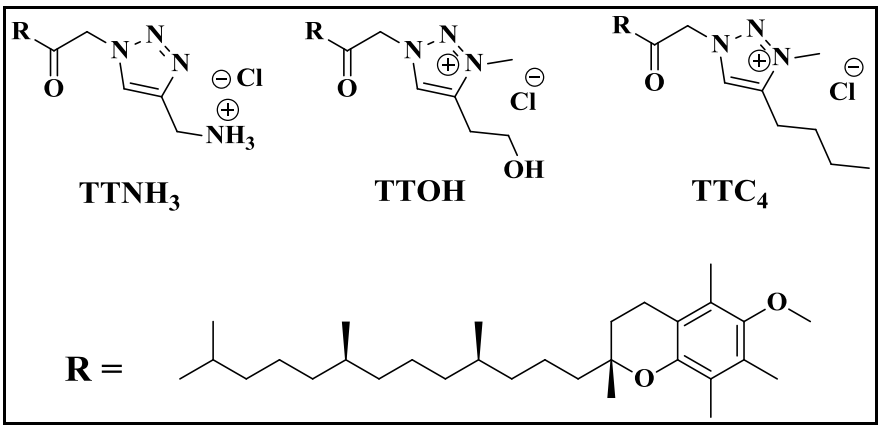

Fig. 12 Molecular structures of 1, 2, 3 triazolium based tocopherol derived lipids

Alpha-tocopherol succinate (TOS), esterified compound of tocol family, is a redox silent and well known for its selective apoptotic induction in cancer cells.[90a,b] This was further enhanced by making the molecule more hydrophilic using PEG like conjugates.[90c] In a quest to develop novel efficient nucleic acid delivery agents two different cationic amphiphiles were developed as shown in Fig. 12 using tocopheryl succinate as a common anchoring agent. In a trial to optimize better transfection formulation using these TOS derived lipids, these lipids were mixed with a novel cationic bolaamphiphile having C12 hydrophobic backbone. Bolaamphiphiles are emerging as new class of gene delivering cationic surfactants commonly made of two hydrophilic polar groups were connected to a long hydrophobic back bone unit on its both the ends.[91]

The mixed formulation of lipid/bolalipid has given better transfection potentials than the both individually derived neat aqueous formulations. This new outcome was extensively studied using various physicochemical investigations and transfection supporting experimental results. Overall study of structure activity investigation

including synthesis and characterization of cationic lipids and bolalipid were discussed in **chapter 5**.

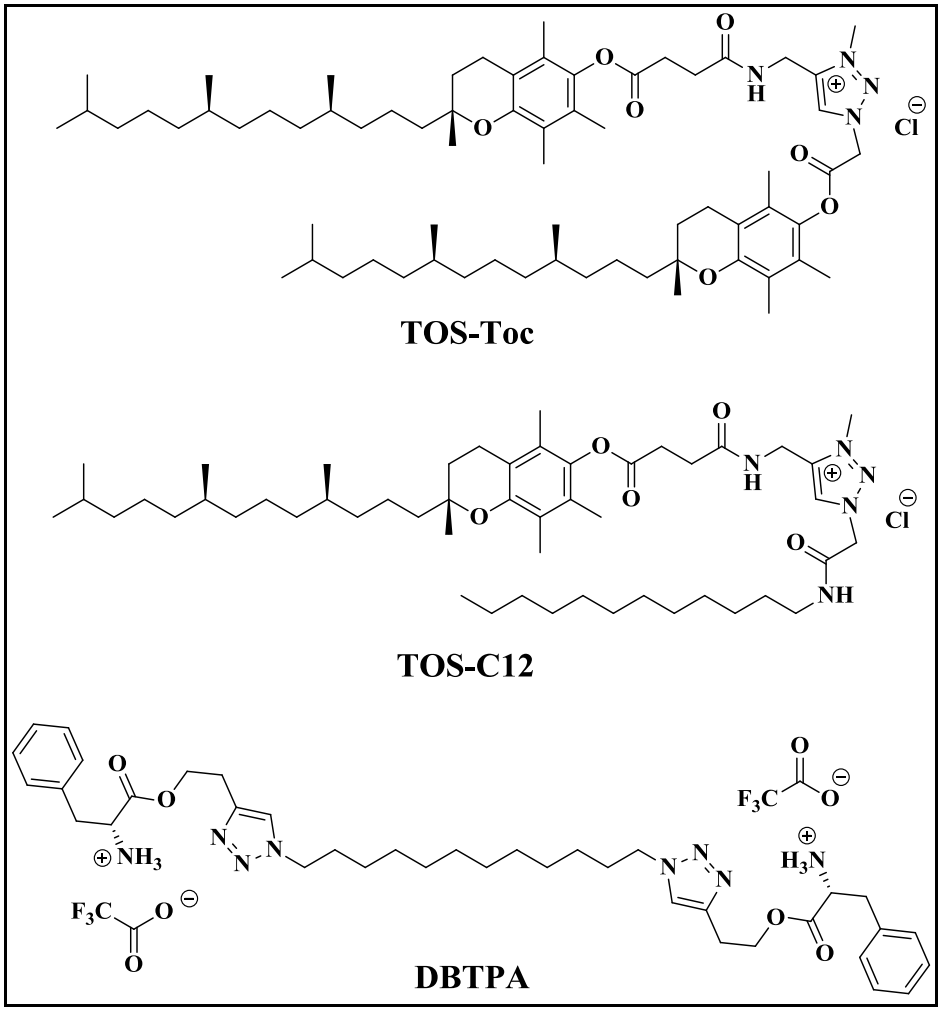

Fig. 13 Molecular structures of TOS based lipids and phenylalanine based bolalipid

1.5 REFERENCES

1. (a) Tatum, E. L. *Perspect Biol Med.* **1966**, *10(1),* 19. (b) Sinsheimer, R. L. *Am Sci*. **1969,** *57(1),*134. (c) Davis, B. D. *Science*. **1970**, *170,* 1279. (d) Friedmann, T.; Roblin, R. *Science.* **1972**, *175,* 949. (e) Morrow, J. F. *Science*. **1976**, *265*, 13.

2. (a) Ledley, F. D., *Pharm Res.,* **1996**, 13, 1595. (b) Garmory, H. S.; Brown, K. A.; Titball, R. W. *Genet Vaccines Ther.* **2003**, *1*, 2.
3. Vacik, J.; Dean, B. S.; Zimmer, W. E.; Dean, D. A., *Gene Ther.* **1999**, *6*, 106.
4. Schaffer, D. V.; Lauffenburger, D. A., *J. Biol. Chem.* **1998,** *273*, 28004.
5. (a) Mintzer, M. A.; Simanek, E. E., *Chem Rev*. **2008**, *2*, 259. (b) Morille, M.; Passirani, C.; Vonarbourg, A.; Clavreul, A.; Benoit, J. P., *Biomaterials*, **2008**, *24*, 3477.
6. Ginn, S. L.; Alexander, I. E.; Edelstein, M. L.; Abedi, M. R.; Wixon, J., *J Gene Med*. **2013**, *2*, 65.
7. Joyner, A.; Keller, G.; Phillips, R. A.; Bernstein, A. *Nature*. **1983**, *305*, 556.
8. Miller, A. D.; Jolly, D. J.; Friedmann, T.; Verma, I. M. *Proc. Natl. Acad. Sci. U.S.A.* **1983**, *80*, 4709.
9. Willis, R. C.; Jolly, D. J.; Miller, A. D. *J. Biol. Chem*. **1984,** *259*, 7842.
10. Blaese, R. M.; Culver, K. W.; Miller, A. D.; Carter, C. S.; Fleisher, T. *Science.* **1995,** *270*, 475.
11. Cavazzana-Calvo, M.; Hacein-Bey, S.; de Saint Basile, G. *Science.* **2000,** *288,* 669.
12. Caplen, N. *J. Nat. Med.* **1995**, *1*, 39.
13. Gill, D. R. *Gene. Ther*. **1997**, *4,* 199.
14. Hacein-Bey-Abina, S.; Garrigue, A.; Wang, G. P.; Soulier, J.; Lim, A.; Morillon, E.; Clappier, E.; Caccavelli, L.; Delabesse, E.; Beldjord, K.; Asnafi, V., *J Clin Invest.* **2008**, 9, 3132.
15. (a) Aiuti, A.; Slavin, S.; Aker, M.; Ficara, F.; Deola, S.; Mortellaro, A.; Morecki, S.; Andolfi, G.; Tabucchi, A.; Carlucci, F.; Marinello, E., *Science*, **2002**, *5577*, 2410. (b) Aiuti, A.; Cattaneo, F.; Galimberti, S.; Benninghoff, U.; Cassani, B.; Callegaro, L.; Scaramuzza, S.; Andolfi, G.; Mirolo, M.; Brigida, I.; Tabucchi, A., *N Engl J Med.* **2009**, *5*, 447.
16. Cideciyan, A. V.; Jacobson, S. G.; Beltran, W. A.; Sumaroka, A.; Swider, M.; Iwabe, S.; Roman, A. J.; Olivares, M. B.; Schwartz, S. B.; Komáromy, A. M.; Hauswirth, W. W., *Proc. Natl. Acad. Sci. U.S.A.* **2013**, *6*, 517.

17. MacLaren, R. E.; Groppe, M.; Barnard, A. R.; Cottriall, C. L.; Tolmachova, T.; Seymour, L.; Clark, K. R.; During, M. J.; Cremers, F. P.; Black, G. C.; Lotery, A. J., *The Lancet*, **2014**, *9923*, 1129.
18. (a) LoDuca, P. A.; Hoffman, B. E.; Herzog, R. W., *Curr. Gene Ther.* **2009**, *2*, 104. (b) Nathwani, A. C.; Tuddenham, E. G.; Rangarajan, S.; Rosales, C.; McIntosh, J.; Linch, D. C.; Chowdary, P.; Riddell, A.; Pie, A. J.; Harrington, C.; O'beirne, J., *N Engl J Med.* **2011**, *365*, 2357.
19. Niemeyer, G. P.; Herzog, R. W.; Mount, J.; Arruda, V. R.; Tillson, D. M.; Hathcock, J.; van Ginkel, F. W.; High, K. A.; Lothrop, C. D., *Blood*, **2009**, *4*, 797.
20. (a) Nienhuis, A. W. and Persons, D. A., *Cold Spring Harb Perspect Med.* **2012,** *11*, a011833. (b) Persons, D. A. *Nature*, **2010,** 7313, 277.
21. Ylä-Herttuala, S. *MolTher.* **2012**, *10*, 1831.
22. Amer, M. H. *Mol Cell Ther*. **2014**, *1*, 27.
23. Johnson, D. B.; Puzanov, I.; Kelley, M. C. *Immunotherapy*, **2015**, *6*, 611.
24. Palfi, S.; Gurruchaga, J. M.; Ralph, G. S.; Lepetit, H.; Lavisse, S.; Buttery, P. C.; Watts, C.; Miskin, J.; Kelleher, M.; Deeley, S.; Iwamuro, H., *The Lancet*, **2014**, *9923*, 1138.
25. (a) Heller, R. *FEBS Lett.* **1996**, *389,* 225. (b) Heller, L. *Gene Ther*. **2000**, *7*, 826. (c) Dujardin, N. *Pharm. Res*. **2001**, *18,* 61.
26. Benn, S. I. *J. Clin. Invest.* **1996**, *98*, 2894.
27. Hengge, U. *Nat. Genet*. **1995**, *10*, 161.
28. Goff, S. P.; Berg, P. *Cell*. **1976**, *9*, 695.
29. Miller, A. D. *Methods. Enzymol.* **1993**, *217*, 581.
30. Zufferey, R. *Nat. Biotech*. **1998**, *15*, 871.
31. Cattoglio, C.; Facchini, G.; Sartori, D. *Blood*. **2007**, *110,* 1770.
32. Schneider, G. *Nat. Genet.* **1998**, *18,* 180.
33. Xiao, W. *J. Virol*. **1999**, *73,* 3994.
34. Neve, R. L.; Geller, A. I. *Clin. Neurosci*. **1995**, *3*, 262.
35. Zhang, S.; Xu, Y.; Wang, B.; Qiao, W.; Liu, D.; Li, Z. *J. Control. Release*. **2004,** *100*, 165.

36. (a) Zhang, B.; Ma, X. P.; Murdoch, W.; Radosz, M.; Shen, Y. Q., *Biotechnol Bioeng.* **2013**, *110*, 990. (b) Schaffert, D.; Troiber, C.; Wagner, E., *Bioconjugate Chem.* **2012,** *6*, 1157.
37. (a) Pfeifer, B. A.; Burdick, J. A.; Little, S. R.; Langer, R., *Int J Pharm.* **2005**, *304*, 210. (b) Anderson, D. G.; Akinc, A.; Hossain, N.; Langer, R., *Mol Ther.* **2005**, *3*, 426. (c) Hwang, S. J.; Bellocq, N. C.; Davis, M, E., *Bioconjugate Chem.* **2001**, *2*, 280. (d) Kean, T.; Roth, S.; Thanou, M., *J Control Release*. **2005**, *3*, 643. (e) Thanou, M.; Florea, B. I.; Geldof, M.; Junginger, H. E.; Borchard, G., *Biomaterials*, **2002**, *1*, 153.
38. (a) Navarro, G.; de Ilarduya, C. T., *Nanomedicine,* **2009**, *3*, 287. (b) Wen, Y. T.; Guo, Z. H.; Du, Z.; Fang, R.; Wu, H. M.; Zeng, X.; Wang, C.; Feng, M.; Pan, S. R., *Biomaterials,* **2012**, *32*, 8111. (c) Yin, Z.; Liu, N.; Ma, M. S.; Wang, L.; Hao, Y. L.; Zhang, X. N., *Int J Nanomedicine,* **2012**, *7*, 4625.
39. (a) Yang, J.; Zhang, Q.; Chang, H.; Cheng, Y., *Chem Rev.***2015**, *6*, 5274. (b) Hu, J.; Hu, K.; Cheng, Y., *Actabiomaterialia*, **2016**, *35*, 1.
40. (a) Han, M. H.; Chen, J.; Wang, J.; Chen, S. L.; Wang, X. T., *J Biomed Nanotechnol,* **2013**, *9*, 1736. (b) Cao, D.; Qin, L.; Huang, H.; Feng, M.; Pan, S.; Chen, J., *Mol Biosyst*. **2013**, *9*, 3175.
41. Daneshvar, N.; Abdullah, R.; Shamsabadi, F. T.; How, C. W.; MH, M. A.; Mehrbod, P., *Cell Biol Int.* **2013**, *37*, 415.
42. Gupta, B.; Levchenko, T. S.; Torchilin, V. P., *Adv. Drug Delivery Rev.* **2005**, *57*, 637.
43. Haralambidis, J.; Duncan, L.; Tregear, G. W., *Tetrahedron Lett.* **1987**, *28*, 5199.
44. Park, J.; Lee, J.; Kwag, J.; Baek, Y.; Kim, B.; Yoon, C. J.; Bok, S.; Cho, S. H.; Kim, K. H.; Ahn, G. O.; Kim, S., *ACS nano*, **2015**, *9*, 6511.
45. Alivisatos, A. P.; Gu, W.; Larabell, C. *Ann. Rev. Biomed. Eng.* **2005**, *7*, 55.
46. Clapp, A. R.; Medintz, I. L.; Mauro, J. M.; Fisher, B. R.; Bawendi, M. G.; Mattoussi, H. *J. Am. Chem. Soc.* **2004**, *126*, 301.
47. Srinivasan, C.; Lee, J.; Papadimitrakopoulos, F.; Silbart, L. K.; Zhao, M.; Burgess, D. J. *Mol. Ther.* **2006**, *14*, 192.

48. (a) Ghosh, P.; Han, G.; De, M.; Kim, C. K.; Rotello, V. M. *Adv Drug Deliv Rev.* **2008**, *60*, 1307. (b) Rana, S.; Bajaj, A.; Mout, R.; Rotello, V. M. *Adv Drug Deliv Rev.* **2012***, 64*, 200. (c) Jewell, C. M.; Jung, J. M.; Atukorale, P. U.; Carney, R. P.; Stellacci, F.; Irvine, D. J., *Angew Chem Int Ed Engl*. **2011,** *50*, 12312.
49. (a) Boisselier, E.; Astruc, D. *Chem Soc Rev.* **2009,** *38*, 1759. (b) Gindy, M. E.; Prud'homme, R. K. *Expert Opin Drug Deliv.* **2009,** *6*, 865. (c) Panyala, N. R.; Pena-Mendez, E. M.; Josef, H. *J Appl Biomed.* **2009**, *7*, 75. (d) Park, K.; Lee, S.; Kang, E.; Kim, K.; Choi, K.; Kwon, I. C. *Adv Funct Mater.* **2009**, *19*, 1553. (e) Beaux, M. F.; McIlroy, D. N.; Gustin, K. E. *Expert Opin Drug Deliv.* **2008**, *5*, 725. (f) Roca, M.; Haes, A. J., *Nanomedicine (Lond),* **2008**, *3*, 555.
50. (a) Daniel, M. C.; Astruc, D. *Chem Rev.* **2004**, *104*, 293. (b) Sun, Y.; Xia, Y. *Science,* **2002**, *298*, 2176. (c) Zhu, Z. J.; Carboni, R.; Quercio, M. J.; Yan, B.; Miranda, O. R.; Anderton, D. L. *Small,* **2010**, *6*, 2261. (d) De Jong, W. H.; Hagens, W. I.; Krystek, P.; Burger, M. C.; Sips, A. J.; Geertsma, R. E. *Biomaterials,* **2008**, *29*, 1912. (e) Wang, B.; He, X.; Zhang, Z.; Zhao, Y.; Feng, W. *Acc Chem Res,* **2013**, *46*, 761.
51. Lasic, D. D. *Am. Sci*. **1992**, *80*, 20.
52. Felgner, P. L.; Gadek, T. R.; Holm, M.; Roman, R.; Chan, H. W.; Wenz, M.; Northrop, J. P.; Ringold, G. M.; Danielsen, M. *Proc. Natl. Acad. Sci. U.S.A.* **1987**, *84*, 7413.
53. (a) Brigham, K. L.; Meyrick, B.; Christmann, B.; Berry, L. C.; King, G. *Am J Resp Cell Mol*. **1989**, *1*, 95. (b) Innes, C. L.; Smith, P. B.; Langenbach, R.; Tindall, K. R.; Boone, L. R. *J. Virol.* **1990**, *64,* 957. (c) Brant, M.; Nachmansson, N.; Norrman, K.; Regnell, A.; Bredberg, A. *DNA Cell Biol.* **1991**, *10*, 75. (d) Li, A. P.; Myers, C. A.; Kaminski, D. L. *In Vitro Cell Dev Biol Anim.* **1992**, *28,* 373.
54. Leventis, R.; Silvius, J. R. *(BBA) Biomembranes*. **1990**, *1023*, 124.
55. Van Der Woude, I.; Wagenaar, A.; Meekel, A. A.; TerBeest, M. B.; Ruiters, M. H.; Engberts, J. B.; Hoekstra, D. *Proc. Natl. Acad. Sci. U.S.A.* **1997**, *94*, 1160.
56. Pinnaduwage, P.; Schmitt, L.; Huang, L. *(BBA) Biomembranes*. **1989**, *985*, 33.
57. Byk, G.; Dubertret, C.; Escriou, V. *J. Med. Chem.* **1998**, *41*, 224.

58. Hofland, H. E.; Shephard, L.; Sullivan, S. M., *Proc. Natl. Acad. Sci.* **1996**, *93*, 7305.

59. Aissaoui, A.; Martin, B.; Kan, E.; Oudrhiri, N.; Hauchecorne, M.; Vigneron, J. P.; Lehn, J. M.; Lehn, P. *J Med Chem.* **2004**, *47*, 5210.

60. Gao, H.; Hui, K. M., *Gene Ther.* **2001**, *8*, 855.

61. Misra, S. K.; Muñoz-Úbeda, M.; Datta, S.; Barrán-Berdón, A. L.; Aicart-Ramos, C.; Castro-Hartmann, P.; Kondaiah, P.; Junquera, E.; Bhattacharya, S.; Aicart, E., *Biomacromolecules*, **2013**, *14*, 3951.

62. Heyes, J. A.; Niculescu-Duvaz, D.; Cooper, R. G.; Springer, C. J. *J Med Chem.* **2002**, *45*, 99.

63. Gao, X.; Huang, L. *Biochem Biophys Res Commun.* **1991,** *179*, 280.

64. Aberle, A. M.; Tablin, F.; Zhu, J. *Biochemistry*. **1998**, *37*, 6533.

65. Duvaz-N, D.; Heyes, J.; Springer, C. J. *Curr. Med. Chem.* **2003,** *10*, 1233.

66. (a) Miller, A. D. *Angew. Chem. Int. Ed.* **1998**, *37*, 1768. (b) Kumar, V. V.; Singh, R. S.; Chaudhuri, A. *Curr. Med. Chem.* **2003**, *10,* 1297.

67. (a) Kedika, B.; Patri, S. V. *J Med Chem,* **2010**, *54*, 548. (b) Kumar, K.; Maiti, B.; Kondaiah, P.; Bhattacharya, S. *Org Biomol chem*, **2015**, *13*, 2444. (c) Zheng, L. T.; Yi, W. J.; Su, R. C.; Liu, Q.; Zhao, Z. G. *ChemPlusChem*, **2016**, *81*, 125. (d) Kedika, B.; Patri, S. V.; *Bioconjug Chem,* **2011**, *22*, 2581.

68. Menger, F. M.; Keiper, J. S., *Angew Chem Int Ed,* **2000**, *39*, 1906.

69. (a) Bajaj, A.; Paul, B.; Kondaiah, P.; Bhattacharya, S. *Bioconjugate Chem*, **2008**, *19*, 1283. (b) Misra, S. K.; Naz, S.; Kondaiah, P.; Bhattacharya, S. *Biomaterials*, **2014**, *35*, 1334. (c) Kumar, K.; Maiti, B.; Kondaiah, P.; Bhattacharya, S. *Mol Pharm*, **2014**, *12*, 351. (d) Kedika, B.; Patri, S. V., *Mol Pharm*, **2012**, *9*, 1146.

70. Kumar, K.; Barrán-Berdón, A. L.; Datta, S.; Muñoz-Úbeda, M.; Aicart-Ramos, C.; Kondaiah, P.; Junquera, E.; Bhattacharya, S.; Aicart, E., *J Mater Chem B*, **2015**, *3*, 1495.

71. Fuhrhop, J. H.; Wang, T., *Chem Rev*, **2004**, *104*, 2901.

72. Blume, A.; Drescher, S.; Graf, G.; Köhler, K.; Meister, A., *Adv. Colloid Interface Sci.* **2014**, *208*, 264.

73. (a) Jain, N.; Arntz, Y.; Goldschmidt, V.; Duportail, G.; Mély, Y.; Klymchenko, A. S., *Bioconjug Chem.* **2010,** *21*, 2110. (b) Khan, M.; Ang, C. Y.; Wiradharma, N.; Yong, L. K.; Liu, S.; Liu, L.; Gao, S.; Yang, Y. Y. *Biomaterials,* **2012**, *33*, 4673. (c) Patil, S. P.; Kim, S. H.; Jadhav, J. R.; Lee, J. H.; Jeon, E. M.; Kim, K. T.; Kim, B. H.; *Bioconjug Chem*. **2014**, *25*, 1517.

74. (a) Felgner, P. L.; Ringold, G. M. *Nature*. **1989**, *337,* 387. (b) Zabner, J. *J Biol Chem.* **1995,** *270,* 18997. (c) Sternberg, B.; Sorgi, F. L.; Huang, L. *FEBS Lett.* **1994**, *356*, 361. (d) Gershon, H. *Biochemistry*. **1993**, *32,* 7143. (e) Safinya, C. R. *CurrOpinStructBiol,* **2001**, *11*, 440.

75. Wattiaux, R.; Laurent, N.; Wattiaux-De Coninck, S.; Jadot, M. *Adv Drug Deliv Rev*, **2000**, *41*, 201.

76. (a) Perumal, O. P.; Inapagolla, R.; Kannan, S.; Kannan, R. M. *Biomaterials*, **2008**, *29*, 3469. (b) Khalil, I. A.; Kogure, K.; Akita, A.; Harashima, H. *Pharmacol Rev.* **2006***, 58*, 32. (c) Parton, R. G.; Richards, A. A. Traffic, **2003**, *4*, 724. (d) Boleti, B.; Benmerah, A.; Ojcius, D. M.; Cerf-Bensussan, N.; Dautry-Varsat, A. *J Cell Sci.* **1999**, *112*, 1487. (e) Martys, J. L.; Wjasow, C.; Gangi, D. M.; Kielian, M. C.; McGraw, T. E.; Backer, J. M. *J Biol Chem.* **1996**, *271*, 10953. (f) Li, D.; Li, P.; Li, G.; Wang, J.; Wang, E. *Biomaterials*, **2009**, *30*, 1382. (g) Yamamoto, A.; Tagawa, Y.; Yoshimori, T.; Moriyama, Y.; Masaki, R.; Tashiro, Y. *Cell Struct Funct,* **1998**, *23*, 33.

77. (a) Xu, Y.; Szoka, Jr, F. C. *Biochemistry,* **1996,** *35*, 5616. (b) Zelphati, O.; Szoka, Jr, F. C. *Proc Natl Acad Sci U S A*, **1996**, *93*, 11493.

78. (a) Hafez, I. M.; Maurer, N.; Cullis, P. R. *Gene Ther*, **2001**, *15*, 1188. (b) Ellens, H.; Bentz, J.; Szoka, F. C. *Biochemistry*, **1986**, *2*, 285. (c) Gao, X.; Huang, L. *Gene Ther*, **1995**, *10*, 710.

79. (a) Escriou, V.; Carriere, M.; Bussone, F.; Wils, P.; Scherman, D. *J Gene Med*, **2001**, *2*, 179. (b) Brunner, S.; Furtbauer, E.; Sauer, T.; Kursa, M.; Wagner, E. *Mol Ther*, **2002**, *1*, 80.

80. (a) Tseng, W. C.; Haselton, F. R.; Giorgio, T. D. *(BBA)-Gene.* **1999,** *1445*, 53. (b) Jans, D. A.; Chan, C. K.; Huebner, S. *Med. Res. Rev.* **1998,** *18,* 189. (c) Subramanian, A.; Ranganathan, P.; Diamond, S. L. *Nat. Biotechnol*. **1999,** *17,*

873. (d) Sebestyen, M. G.; Ludtke, J. J.; Bassik, M. C.; Zhang, G.; Budker, V. *Nat. Biotechnol.* **1998,** *16,* 80. (b) Zanta, M. A.; Belguise-Valladier, P.; Behr, J. P. *Proc. Natl. Acad. Sci. USA*. **1999,** *96*, 91.

81. Solodin, I.; Brown, C. S.; Bruno, M. S.; Chow, C. Y.; Jang, E. H.; Debs, R. J.; Heath, T. D. *Biochemistry*, **1995**, *34*, 13537.

82. (a) Tucker, J.; Townsend, D. *Biomed Pharmacother,* **2005**, *59*, 380. (b) Duhem, N.; Danhier, F.; Préat, V. *J Control. Rel.* **2014**, *182*, 33. (c) Nishina, K.; Unno, T.; Uno, Y.; Kubodera, T.; Kanouchi, T.; Mizusawa, H.; Yokota, T. *Mol Ther,* **2008**, *16*, 734. (d) Uno, Y.; Piao, W.; Miyata, K.; Nishina, K.; Mizusawa, H.; Yokota, T. *Hum Gene Ther,* **2010**, *22*, 711.

83. (a) Burton, G. W.; Traber, M. G. *Annu Rev Nutr.* **1990**, *10*, 357. (b) Brigelius-Flohe, R.; Traber, M. G. *FASEB J.* **1999**, *13*, 1145.

84. Azzi, A.; Ricciarelli, R.; Zingg, J. M. *FEBS Lett.* **2002**, *519*, 8.

85. (a) Birringer, M.; Eytina, J. H.; Salvatore, B. A.; Neuzil, J. *Br. J. Cancer.* **2003**, *88,* 1948. (b) Dong, L. F.; Swettenham, E.; Eliasson, J.; Wang, X. F.; Gold, M.; Medunic, Y.; Stantic, M.; Low, P.; Prochazka, L.; Witting, P. K.; Turaned, J.; Akporiaye, E. T.; Ralph, S. J.; Neuzil, J. *Cancer Res.* **2007**, *67*, 11906. (c) Nikolic. K. M. *J Mol Graph* ***Model***. **2008**, *26*, 868.

86. (a) Jizomoto, H.; Kanaoka, E.; Hirano, K. *Biochim. Biophys. Acta*. **1984**, *1213*, 343. (b) Neuzil, J.; Donga, L. F.; Wang, X. F.; Zinggc, J. M. *Biochem. Biophys. Res. Commun.* **2006**, *343*, 1113. (c) Turanek, J.; Wang, X. F.; Knotigova, P.; Koudelka, S.; Donga, L. F.; Vrublova, E.; Mahdavian, E.; Prochaka, L.; Sangsura, S.; Vacek, A.; Salvatore, B. A.; Neuzil, J. *Toxicol Appl Pharmacol*. **2009**, *237*, 249.

87. (a) Zhdanov, R.; Bogdanenko, E.; Moskoytsey, A.; Podobed, O.; Duzgu nes, N. *Methods Enzymol.* **2003**, *373*, 433. (b) Zhdanov, R.; Buneeva, O. A.; Podobed, O. V.; Kutsenko, N. G.; Tsvetkova, T. A.; Lavrenova, T. P. *Voprosy Meditsinskoi Khimii*. **1997**, *43(4)*, 212. (c) Nishina, K.; Unno, T.; Uno, Y.; Kubodera, T.; Kanouchi, T.; Mizusawa, H.; Yokota, T. *Mol Ther*. **2008**, *16(4),* 734. (d)Takanori, Y.; Kazutaka, N.; Hidehiro, M.; Toshinori, U. PCT Int Appl. 2009, WO 2009069313 A1 20090604.

88. (a) Kolb, H. C.; Sharpless, K. B. *Drug Discov Today,* **2003**, *8*, 1128. (b) Rostovtsev, V. V.; Green, L. G.; Fokin, V. V.; Sharpless, K. B. *Angew. Chem.* **2002**, *114*, 2708. (c) Tornøe, C. W.; Christensen, C.; Meldal, M. *J. Org. Chem.* **2002**, *67*, 3057.

89. (a) Lauria, A.; Delisi, R.; Mingoia, F.; Terenzi, A.; Martorana, A.; Barone, G.; Almerico, A. M. *Eur. J. Org. Chem.* **2014**, *16*, 3289. (b) Patil, S. P.; Kim, S. H.; Jadhav, J. R.; Lee, J. H.; Jeon, E. M.; Kim, K. T.; Kim, B. H. *Bioconj Chem.* **2014**, *25*, 1517. (c) Barnard, A.; Posocco, P.; Pricl, S.; Calderon, M.; Haag, R.; Hwang, M. E.; Shum, V. W.; Pack, D. W.; Smith, D. K. *J Amer Chem Soc.* **2011**, *133*, 20288.

90. (a) Noh, S. M.; Han, S. E.; Shim, G.; Lee, K. E.; Kim, C. W.; Han, S. S.; Choi, Y.; Kim, Y. K.; Kim, W. K.; Oh, Y. K. *Biomaterials*, **2011**, *32*, 849. (b) Prasad, K. N.; Kumar, B.; Yan, X. D.; Hanson, A. J.; Cole, W. C. *J Amer Coll Nutr.* **2003,** *22*, 108. (c) Youk, H. J.; Lee, E.; Choi, M. K.; Lee, Y. J.; Chung, J. H.; Kim, S. H.; Lee, C. H.; Lim, S. J. *J Control Release*, **2005**, *107*, 43.

91. (a) Fuhrhop, J. H.; Wang, T. *Chem Rev.* **2004,** *104*, 2901. (b) Khan, M.; Ang, C. Y.; Wiradharma, N.; Yong, L. K.; Liu, S.; Liu, L.; Gao, S.; Yang, Y. Y. *Biomaterials,* **2012,** *33*, 4673.

Chapter 2

Effect of Heterocyclic Based Head Group Modifications on the Structure-Activity Relationship of Tocopherol-Derived Mono-cationic Lipids for Non-viral Gene Delivery

2.1 INTRODUCTION

The basics of gene therapy have originated along the concept of manipulation of the genetic material, in order to ameliorate various pathological conditions.[1] This genetic modulation encompasses the transfer and subsequent expression of therapeutic nucleic acids in disease specific or target cells. The non-viral vectors were sought to condense, protect and chaperone the genetic material to target cells.[2,3] Among non-viral vectors, cationic lipids have emerged as a safer alternative to its viral equivalents due to the ease of synthesis in addition to combining the desired features of biocompatibility, stability, lower immunogenicity and ease of large scale production.[4] Despite of strong influences of each basic building block of a lipid like hydrophilic head group, hydrophobic back bone and a functional linker on transfection properties, the head group demands particular attention as it forms a major determinant of the charge density of liposomes and the subsequent self-assembly and complexation with polyanionic nucleic acids mediated by charge-charge interactions.[5,6] Often, the nature, density and orientation of head functional groups in relation to the backbone can dictate the lipoplex dissociation kinetics in the cytoplasm, in addition to the observed toxicity patterns.[7]

Though the numerous efforts to synthesize novel amphiphiles were performed using domain modifications, the exact structural features required for stable transfection still remains obscure.[7,8] In these circumstances, structure-activity investigations can provide valuable insight to the correlation between structure, efficacy and toxicity of cationic lipids. This in turn helps to delineate the complexities of transfection pathway and dictate the behavior of newly synthesized lipid formulations for clinical applications.[9-11] The fat soluble vitamins have provided a new dimension to the synthetic glycerol-dominated field of lipid-mediated gene delivery.[12-14] Indeed, the features of biocompatibility, minimal toxicity, serum stability and solvent capacity has further led to the development of vitamin-E based nanomedicines for cancer therapy.[15,16] Recently, several studies have been witnessed the use of alpha-tocopherol in developing efficient cytofectins for both *in vitro* and *in vivo* delivery of nucleic acids have inspired us to choose tocopherol as the preferred hydrophobic domain in the synthesis of diverse set of cationic lipids whose activity was explored through this study.[17,19]

Hence, in tandem to our ongoing programme of developing stable tocopherol based cytofectins, a systematic modification of the head group was performed using

seven different heterocyclic systems. Further, the effects of structure variation of head groups of the synthesized tocopherol based cationic lipids were carefully examined for their transfection potential *in vitro* in mouse neuroblastoma (Neuro-2a), hepatocarcinoma (HepG2), human embryonic kidney (HEK 293) and Chinese hamster ovarian (CHO) cell lines, representing cells of different origin.

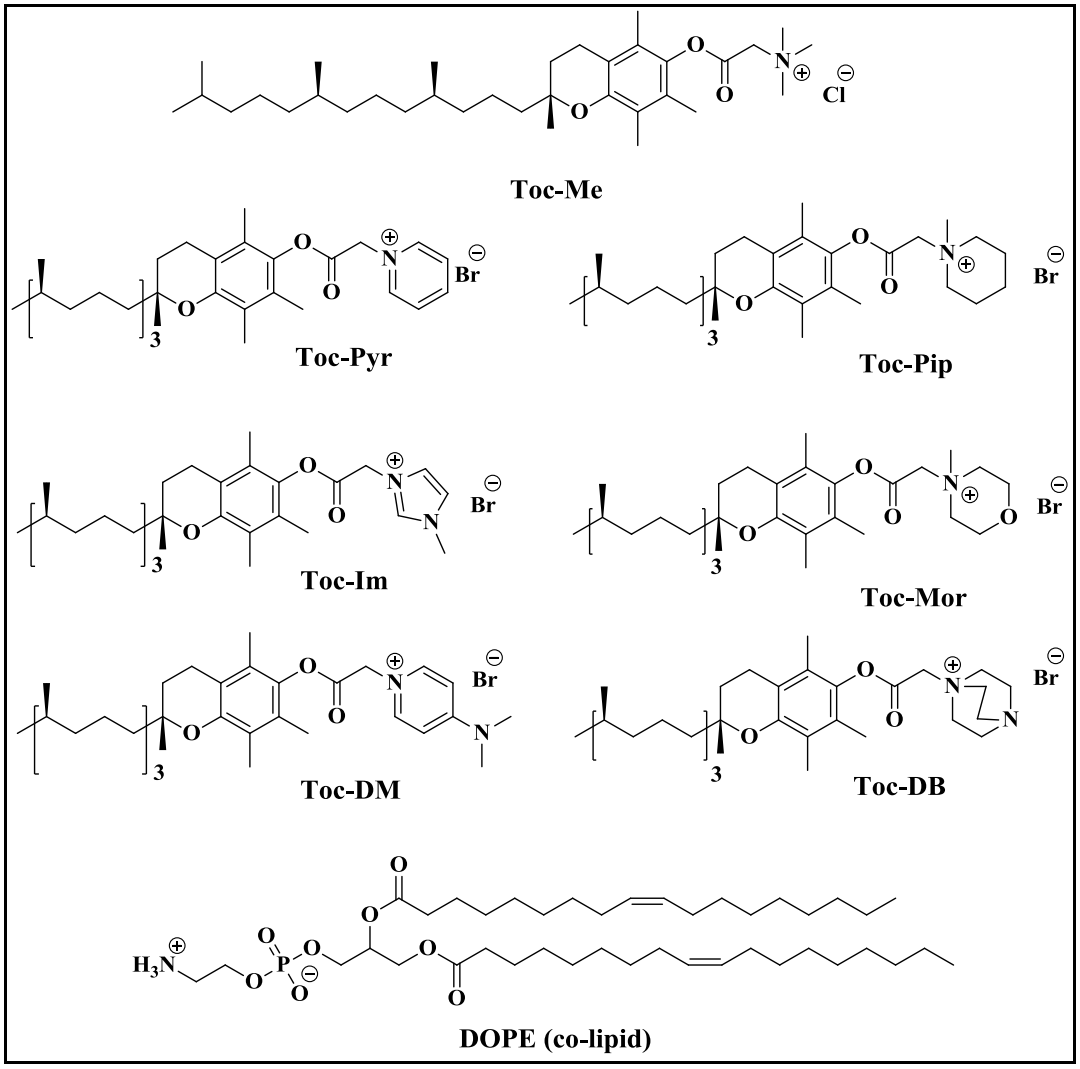

Fig. 1 Molecular structures of alpha-tocopherol based cationic lipids and co-lipid.

2.2 RESULTS AND DISCUSSION

2.2.1 Chemistry: The study was actually aimed to screen the transfection activities of i.e. quaternary 'N' atom of head group embedded with different kind of structural arrangements such as simple acyclic quaternary ammonium, simple cyclic quaternary ammonium, cyclic substituted quaternary ammonium, bicyclic quaternary ammonium and aromatic quaternary ammonium. Towards this, different tertiary amine structures containing heterocyclic nitrogenous bases have been chosen to synthesize seven monocationic tocopherol based lipids. These were synthesized by following the steps mentioned in Scheme 1. Initially, a common tocopherol intermediate such as tocopheryl-2-bromoacetate (Toc-Br) was developed by the esterification of alpha-tocopherol. On treatment with various heterocyclic organic bases the tocopherol intermediate yielded different monocationic tocopherol based lipids. All the mono cationic lipids were purified under solvent precipitation methods and analyzed using the spectroscopic data generated from ^{1}H NMR, ^{13}C NMR and HRMS.

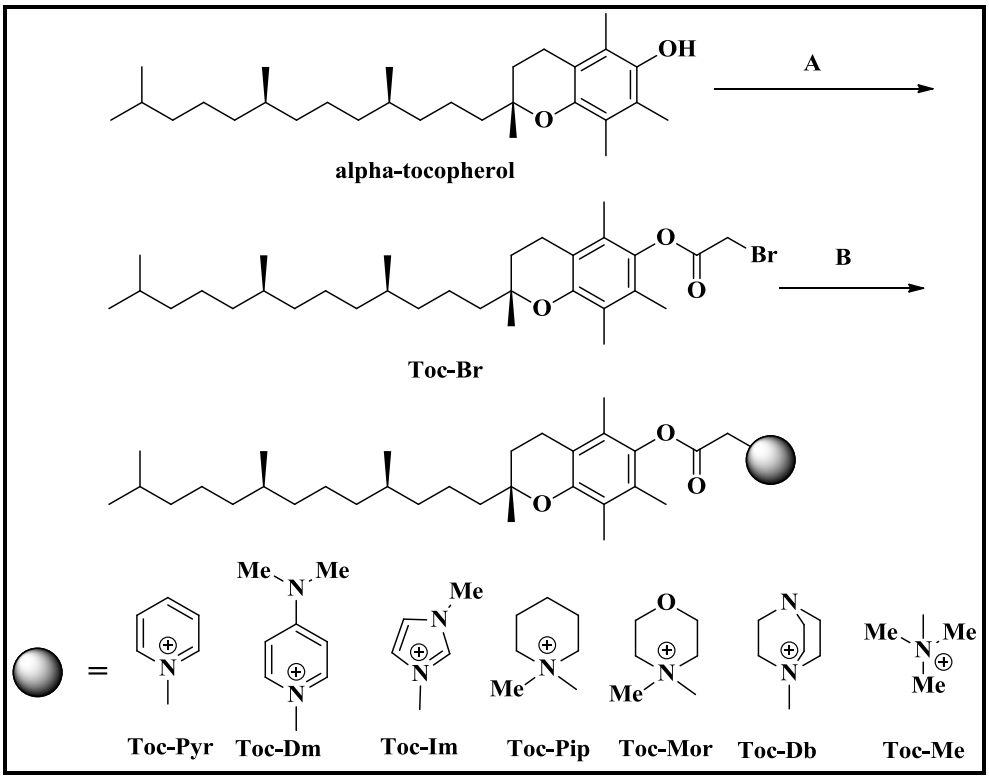

Scheme 1 Synthetic route and molecular structures of mono-cationic lipids.

Reagents & conditions: A) 2-bromoacetylbromide, pyridine, dichloromethane, 0 °C, 3 h; B) Organic base, acetonitrile, sealed tube, 80 ^{o}C, 24 h.

Liposomes were prepared as described in methods and formulated with co-lipid, 1, 2-dioleoyl-sn-glycero-3-phosphoethanolamine, DOPE at 1:1 molar ratio. Being fusogenic, DOPE offers the desired properties upon endosomal fusion with membranes at low pH and hence aids in release of DNA from the lipoplex.[20] All the different tocopherol based liposomes yielded optically transparent, stable aqueous suspensions without any apparent turbidity upon storage at 4 °C.

2.2.2 Physicochemical characterization of liposome (lipid/DOPE) & lipoplex (lipid/DOPE:DNA): A rational design of *in vivo* gene delivery vector mandates the characterization of various physicochemical aspects such as size, charge, shape and plasmid binding potential of lipid nano particles and DNA derived complexes. Towards this, initially lipoplexes with plasmid DNA were prepared and determined the size of the complexes at different N/P charge ratios (1:1, 3:1). The size of lipoplexes is an additive function of the different forces (Vander Waals, repulsive electrostatic and hydrophilic-hydrophobic) that exists between the lipid bilayer and the DNA molecule. Fig. 2A depicts that the size of all liposomal formulations were in the range ~50 – 120 nm. Among these, the lipids Toc-Pip and Toc-Dm led to the formation of particles of contrasting dimensions. Following complexation with plasmid at 1:1 charge ratio, a 2-fold increase in size was observed (Fig. 2A). The hydrodynamic diameter of lipoplexes varied from 195 nm to 330 nm range for Toc-Dm and Toc-Pyr respectively. Based on earlier established kinetics of lipoplex formation[21] larger dimensions at 1:1 charge ratio is not surprising.

In the presence of excess cationic lipids at 3:1 charge ratios, the probability of DNA condensation and liposome restructuring is high and thus must result in the decrease in lipoplex size. However, the observed increase in size of lipoplexes prepared with Toc-Pip, Toc-Mor, Toc-Im and Toc-Dm lipids at 3:1 charge ratios, can be explained in terms of polyanion induced aggregation of cationic head groups. The other reason for the resultant increase in size at higher charge ratios may be the dilution of lipoplexes in

bicarbonate ion enriched media, (DMEM) it can as such promote the growth of lipoplexes during standard incubation procedures.[22]

In addition to size, surface charge is a significant parameter that influences the stability of lipoplexes in the physiological milieu. In Fig. 2B, the zeta potential values of the formulated lipoplexes at the above mentioned charge ratios indicates the general transition from a negative to a more positive potential at higher N/P ratio. The observed negative potential at equimolar charge ratio is suggestive of the minimal aggregation tendency and possible non-toxic nature of these lipoplexes.

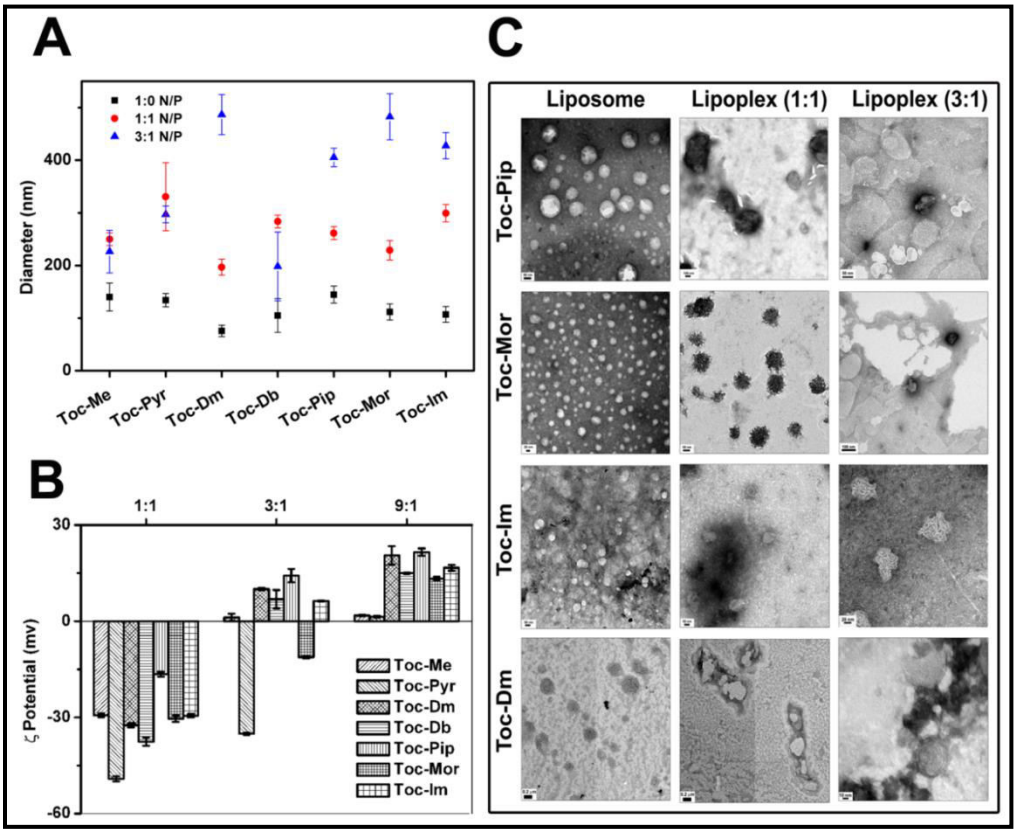

Fig. 2 Physicochemical characterization of liposomes and lipoplexes: A) Hydrodynamic diameter of liposomes (■) and lipoplexes at two different N/P charge ratios 1:1(●) and 3:1(▲) were measured by dynamic light scattering in DMEM minus serum. B) Zeta potential of lipoplexes at varying N/P charge ratios as denoted on the top axis using a constant amount of DNA (1 µg) suspended in Milli-Q. C) Transmission electron

micrographs of transfection active co-liposomal formulations and lipoplexes at 1:1 and 3:1 of Toc-Pip, Toc-Mor, Toc-Im and Toc-Dm.

To gain insight into the topological conformations of liposomes following the binding of pDNA, directly visualized the macroscopic structure of lipoplexes at different charge ratios by TEM (Fig. 2C). Liposomes bound by a unilamellar membrane appear as compact vesicles. This vesicular nature was maintained even after plasmid complexation at 1:1 and 3:1 ratios, thus confirming the condensation of DNA and fused nature of lipoplexes following polyelectrolyte interactions.[23] An interesting supra-molecular structure was observed in case of Toc-Mor, at 1:1 charge ratio where the lipoplex surface had distinct corrugations which had transformed to a more spherical morphology at higher 3:1 lipid ratios. Such protrusions in the rough-edged spherical lipoplexes were earlier reported by Sternberg and co-workers.[24] However, their significance under *in vitro* conditions is unknown. Importantly, the sizes of all the liposomes correlated well with particle dimension. However, the dried status of lipoplex can induce some vesicle fractionation and the related size variations become more obvious at higher 3:1 lipid ratios.

The association of cationic lipids with DNA was also examined qualitatively to determine the extent of binding and migration upon gel electrophoresis. Lipoplexes were prepared with all the tocopherol based lipids at varying charge ratios and electrophoresed (Fig. 3). It was observed for all the tocopherol based lipids that binding to plasmid DNA led to retarded mobility at increasing lipid concentrations. Further, at 9:1 N/P ratio, due to net neutralization of lipoplexes did not migrate and were retained in the well. The ratio of the cationic lipid:DNA required for complete charge neutralization varied among the different tocopherol based lipids. Among these, Toc-Pip and Toc-Im exhibited excellent DNA binding at 3:1 charge ratio which corresponds to the point at which a positive zeta potential was acquired (Fig. 2B). However, Toc-Mor acquired a positive zeta potential at higher charge ratio of 9:1 where almost complete binding was observed. The lipoplexes of remaining lipids also acquired positive potentials which was clearly been supported by the electrophoresis images at the highest 9:1 charge ratio. Nevertheless, for Toc-Db and Toc-Dm, retention of lipoplexes and lack of migration was well initiated at 3:1 charge

ratio, irrespective of the visible DNA bands in the gel. Probably, this corresponds to the co existence of naked DNA, partially masked and net neutral lipoplexes, at this particular ratio.[25]

We further determined the extent of plasmid binding in an EtBr titration experiment which is a fluorescence-based assay sensitive to the charge ratios of lipoplexes. In this assay, the binding strength can be interpreted by correlating the decrease in fluorescence intensity upon addition of the lipid following EtBr exclusion from EtBr:DNA complex. For all the tocopherol derived lipids, a concomitant decrease in the EtBr fluorescence from the initial intensity was observed upon sequential additions of cationic lipids. Eventually, the lipoplex tended to attain equilibrium at the highest 9:1 charge ratio (Fig. 3) as seen by the drop in the fluorescence intensity.

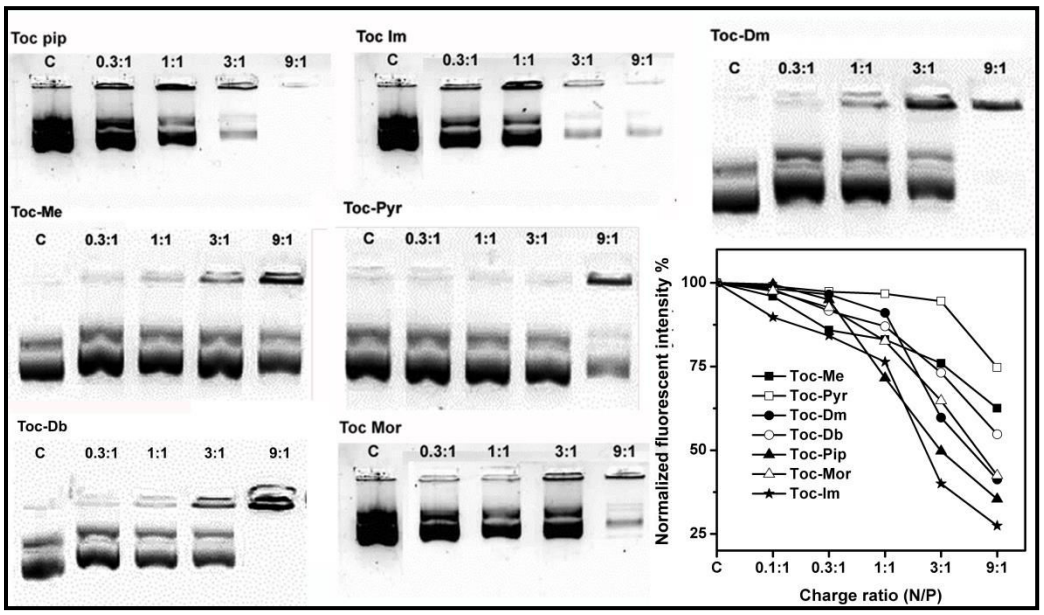

Fig. 3 Agarose gel electrophoresis of lipoplexes prepared with Toc-Pip, Toc-Im, Toc-Dm Toc-Me, Toc- Pyr, Toc- Db, and Toc-Mor. Lipoplexes were prepared with the corresponding co-liposomal formulation and complexed with *p*CMV-βgal plasmid DNA (0.4 µg) at varying (N/P) charge ratios (0.3:1 to 9:1). Naked DNA, denoted as "C" served as the control in each panel. Normalized fluorescent intensities of all lipid formulations were obtained on titration of CT-EtBr:DNA at various charge ratios of co-

liposomal suspensions. Fluorescence intensity of control EtBr:DNA complex was considered as 100%.

In agreement with the zeta potential and gel binding results, EtBr assay results pinpoints the degree of exclusion by Toc-Pip and Toc-Im, followed by Toc-Mor and Toc-Dm in the 1-3 range of charge ratios which indicates greater strength of interaction of these head groups with DNA. To be specific, the DNA binding strength among the various formulations follows the rank order Toc-Pip > Toc-Im > Toc-Mor > Toc-Db > Toc-Dm > Toc-Pyr. However, a slight excess of positive charge > 3:1 ratio was required by these lipids to acquire equilibrium (less than 50% quenching of EtBr:DNA complex fluorescence).

2.2.3 Transfection biology: Following initial characterization of the lipoplexes, we then ascertained the potential to transfect adherent cells in culture. We transiently transfected cells with pEGFP-N_3, which enables rapid screening of different tocopherol based formulations for their activity to determine the relative efficiency by flow cytometry. We observed that the geometric mean at 1:1 ratio was highest for Toc-Pip followed by Toc-Im and Toc-Dm in Neuro-2a cells as determined by fluorescence microscopy and flow cytometry (Fig. 4A-C). However, at 3:1 ratio, Toc-Mor has excelled over other formulations. The percentage of GFP positive cells measured using flow cytometry as depicted in Fig. 4C, indicate the following rank order i.e. Toc-Pip: ~45% > Toc-Dm: 39% > Toc-Im: 36% at 1:1 charge ratio. In the case of Toc-Mor, at 3:1, 34% cells were GFP positive. The data clearly demonstrate that direct visualization of GFP expression by fluorescence microscopy as provided in Fig. 4A, enabled comparative representation which together with flow cytometry data, enabled quantitating the extent of gene expression.

The data clearly discerned the higher efficacy observed with lipids Toc-Pip, Toc-Im, Toc-Mor and Toc-Dm in comparison to Toc-Pyr, Toc-Db and Toc-Me.

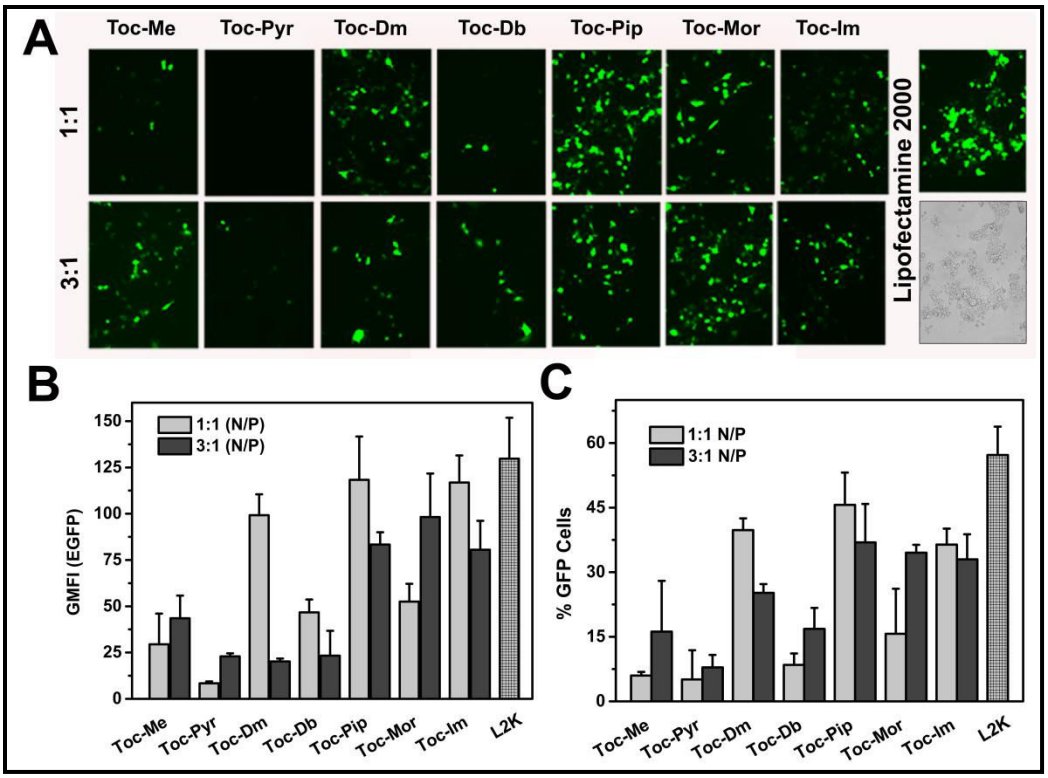

Fig. 4 Transient transfection using the reporter gene, *p*EGFP-N_3 plasmid in Neuro-2a cells: A) Representative Green fluorescence protein expression images of lipids at the two indicated charge ratios (1:1 and 3:1). Complexes were incubated for 4 h in presence of 10% serum; images were acquired 48 h post transfection. B) The graph represents geometric mean fluorescent intensity (GMFI) of GFP expression of transfected cells. C) Graph depicts the transfection efficiencies in terms of percentage GFP positive cells. The data shown is the mean and standard deviation of two different experiments.

We further monitored the efficiency of transfection using a second plasmid vector, harboring β-galactosidase reporter gene in a transient transfection assay. The relative *in vitro* gene delivery efficiency of all co-liposomal formulations were evaluated in Neuro-2a, CHO, HEK-293 and HepG2 cells at 1:1 and 3:1 (lipid:DNA) N/P charge ratios (Fig. 5) and compared with that of the commercial formulation L2K, used as a benchmark standard. An assay performed with these lipids indicated that Toc-Pip, among the series of lipids synthesized, emerged as the most efficient and closely followed by Toc-Im and Toc-Dm at 1:1 charge ratio across all the four types of cell lines studied. In

addition, Toc-Pip at 1:1 charge ratio is as efficient as the commercial formulation L2K, whereas at the 3:1 ratio Toc-Mor has excelled. The efficiency of these lipids is in sync with the specific charge ratios at which a more positive zeta potential and maximum binding efficiency was acquired. In contrast, Toc-Pyr is the least efficient followed by Toc-Me and Toc-Db at both charge ratios (Fig. 5).

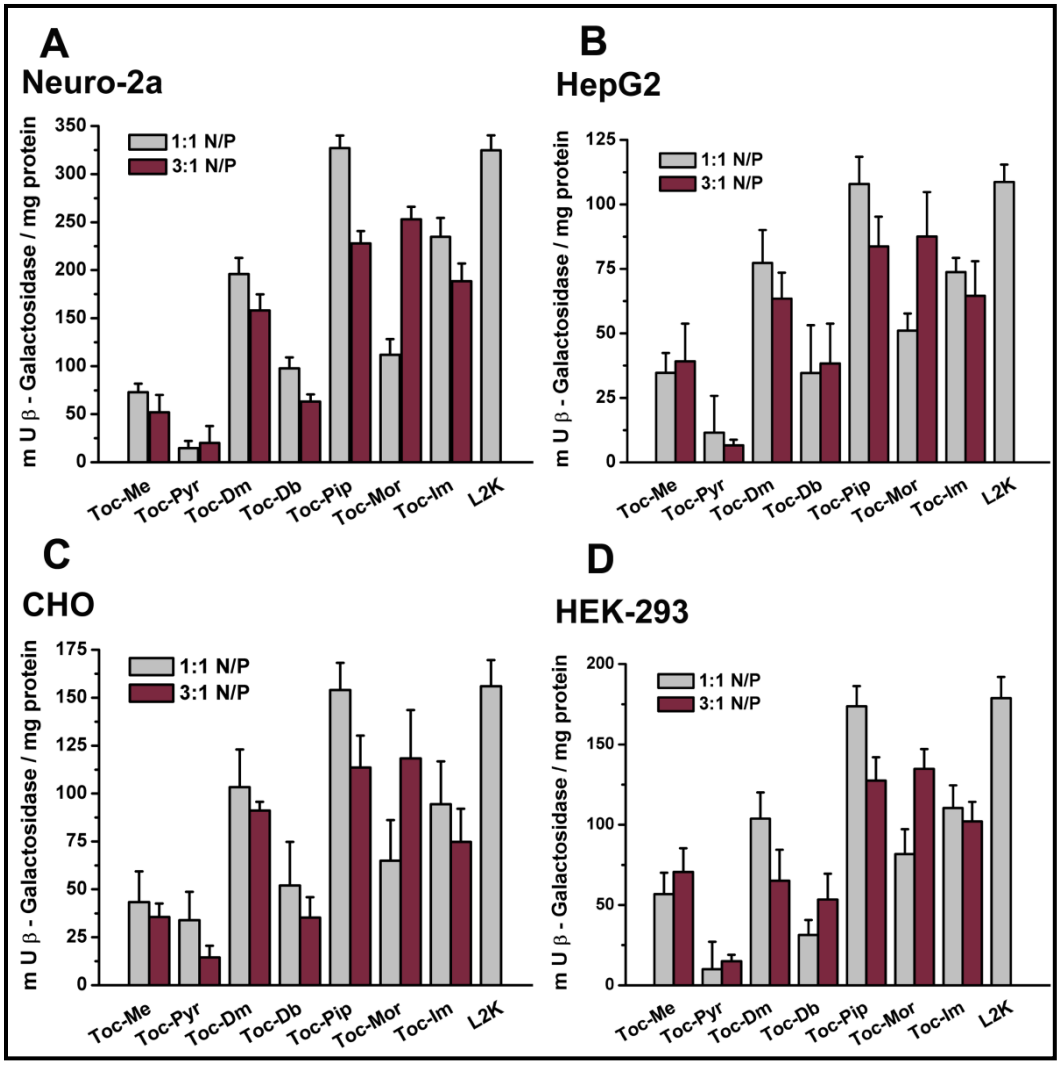

Fig. 5 *Transient* transfection *in vitro*: Graph depicts transfection efficiencies of all the co-liposomal formulations complexed with *p*CMV-βgal in A) Neuro-2a, B) HepG2, C) CHO and D) HEK-293. The charge ratios 1:1 (light gray); 3:1 (dark gray) were used to form complexes and incubated for 4 h in presence of 10% serum. Data represents normalized

miller units of β-galactosidase/mg protein was obtained from an average of three experiments. (Lipofectmine-2000: L2K).

The activity pattern of the seven tocopherol based formulations as estimated through β-galactosidase assay was similar to the EGFP expression profile. Thus, the comparative analysis of gene expression through the use of two different plasmid vectors, EGFP and β-galactosidase, complements each other and strengthen the reliability of this reported activity profile. Importantly this may indicate that these formulations may possibly target neuronal cells by lending their attributes essential for *in vivo* applications targeting the central nervous system. However further exploration is essential to confirm the *in vivo* efficacy of the formulations.

2.2.4 Uptake profile & co-localization: Endosomal escape of gene delivery candidates being another bottleneck in the development of efficient vectors, estimation of cell uptake and intracellular co-localization becomes significant. Hence, to further probe into the mechanistic details of transfection, intracellular trafficking of the lipoplexes was performed with the most efficient tocopherol based cationic lipids, namely Toc-Pip, Toc-Im, Toc-Mor and Toc-Dm. The four lipids were chosen based on the observed efficiency, Fig. 4A-C. Fig. 6 depicts the uptake proficiency of cells treated with all four formulations labeled with rhodamine-DHPE. This is punctuate cytoplasmic fluorescence clearly demonstrates the potential of all four lipoplexes in crossing the hydrophobic barrier, i.e. the plasma membrane. Following cellular uptake, endosomal escape is the other major rate limiting step for transfection complexes. To gain further insight into the intracellular distribution or endocytic route following internalization of lipoplexes, cells were treated with lysotracker-blue to label the lysosomal compartments. Following 2 h incubation, distinct fluorescence with no co-localization was observed. This is suggestive of the possible escape of all four lipoplexes from the endosome avoiding the lysosomes. Efficient escape of the tocopherol based formulations from these organelles may have clearly facilitated the translocation across the endosomal membrane and subsequent transport of the cargo into the nucleus for eventual transcription.

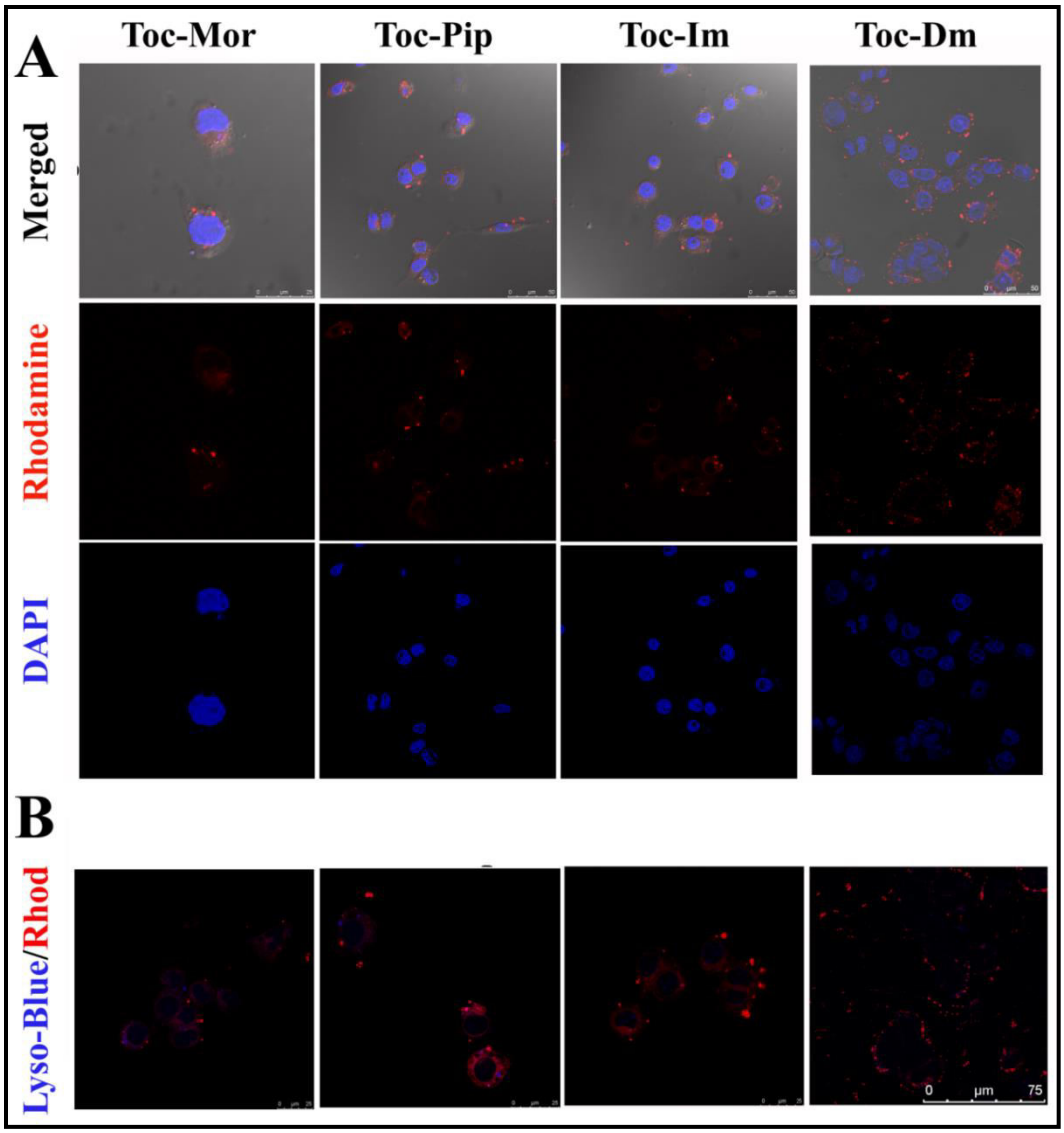

Fig. 6 Representative confocal images of cell uptake (A) and co-localization (B) of lipoplexes at 1:1 N/P in Neuro-2a cells: Rhodamine-DHPE labeled lipoplexes (Toc-Mor, Toc-Pip, Toc-Im and Toc-Dm) were incubated for 2 h and counter stained with DAPI (A). Lysotracker-Blue was used to stain lysosomal compartment after 2 h incubation of cells treated with rhodamine-DHPE labelled lipoplexes (B). Images in each panel were merged from five middle slices (0.5 µm each). Merged panels (A) depict internalization of lipoplexes (red punctuates) and depict nuclear staining with DAPI. Scale bar = 50 µm.

2.2.5 Cell viability: Cell viability analysis being a major limiting factor for the clinical application of liposomal gene delivery systems, we next evaluated this aspect by

an MTT assay to determine the safety of the lipids under investigation. The cell viability of all the tocopherol derived liposomes was hence evaluated (Fig. 7A-D). The experimental results in all the four cell lines studied indicate that the tocopherol based heterocyclic formulations are non toxic. The presence of biodegradable ester based linker group could further promote the non-toxic profile observed. Thus in comparison to the conventional cytofectins, the minimally toxic ester linked tocopherol derived lipids are way ahead in transfection efficiency which is an essential parameter towards designing and developing transfecting regents for *in vitro* and *in vivo* applications.

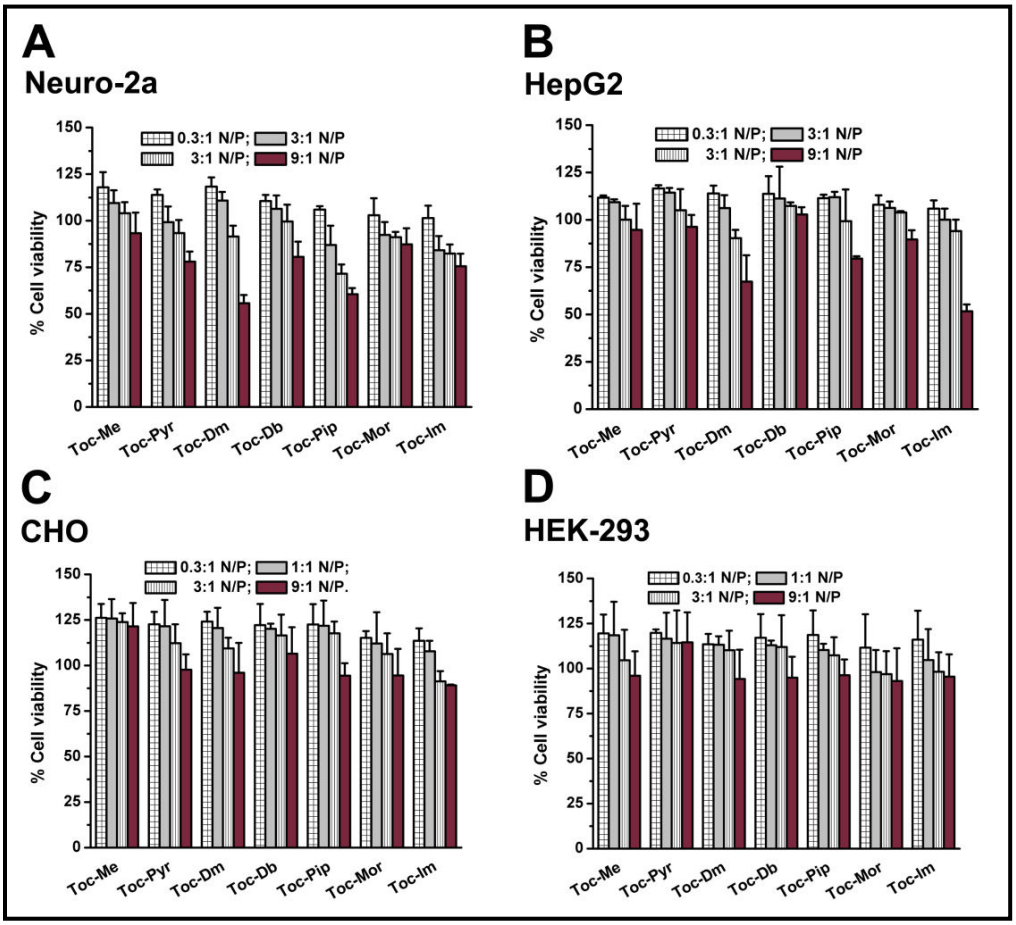

Fig. 7 % cell viability by MTT assay: Lipid:DNA complexes varying from 0.3:1 to 9:1 N/P charge ratios of all the co-liposomal formulations were prepared and cells treated as indicated in methods. Following incubation, cytotoxity was evaluated in four different

cell lines. A) Neuro-2a, B) HepG2, C) CHO and D) HEK-293. The data represents % viability from an average of three experiments.

2.3 STRUCTURE-ACTIVITY CORRELATION:

Structure-activity correlation of chemically synthesized cationic lipids designed to trigger their interaction with DNA is of paramount importance to the development of non-viral delivery systems. Exploring these aspects in depth facilitates the identification and determination of the chemical groups responsible for evoking optimal biological effect with minimal perturbation. In this connection, the transfection potential of tocopherol formulations evaluated in this study correlated with the chemical structure of each of the distinct heterocyclic head.

As a sequel to the vast expanse of heterocyclic compounds usage in cationic lipid construction,[26-28] we have attempted to optimize the structure of tocopherol based lipids with respect to the different nitrogen bases in order of reduced toxicity and increased gene transfer activity. Among the seven lipids synthesized, three lipids viz., Toc-Pip, Toc-Mor and Toc-Db possess non-aromatic heterocyclic head groups, the three more lipids viz., Toc-Pyr, Toc-Im and Toc-Dm have aromatic heterocyclic head groups and the last one lipid Toc-Me has no cyclic structure in back bone, treated as control lipid in the study. The less transfection efficiency of Toc-Me in comparison to the heterocyclic based lipids studied clearly emphasizes that heterocyclic groups enhance the transfection efficiency of tocopherol derived lipids. A recent study by Evanova et al has compared the positively charged head groups *N*-methylpiperidinium, *N*-methylmorpholinium and *N*-methylimidazolium by analyzing the structure-activity relatlionship.[27] This report highlights the maximum transfection potential of *N*-methylmorpholinium over the *N*-methylimidazolium, *N,N*-dimethylpyridinium based lipids. In other words, a non-aromatic based head group has excelled over the other aromatic substitutes. This justifies the higher transfection potential observed in case of the lipids with head groups bearing *N*-methylpiperidinium and *N*-methylmorpholinium. However, comparatively less active profiles of DABCO conjugated lipid draw special attention as a miscellaneous head group that is bulky in nature and capable of disrupting the proper wrapping of plasmid DNA. An interesting study by Bhargava et al has highlighted the higher hydration

potential and cross sectional area of DABCO head group with lithocholic acid,[29] over piperidine[30] based head groups. As hydrophobicity of head group favors cell membrane interactions,[31] steric hindrance and lower hydrophobicity rendered by the head group in DABCO could reduce their relative transfection potential. In addition, the omnipresent molecular skeleton of piperidine[32] can be considered as a structural mimic of glutamate and aspartate receptor agonist. Hence this confers better interactions with cellular membranes[33] as exemplified by the superior transfection potential. Finally, the relative lower transfection potential of pyridinium containing lipid (Toc-Pyr) may likely be due to the delocalization of the positive charge present on the nitrogen atom and hence may not foster lipid/DNA interactions. However, the comparatively higher transfection potential of Toc-Dm which is characterized by similar aromatic backbone like pyridinium could be justified by the presence of a tertiary amine on the ring. This exocyclic nitrogen atom can undergo protonation and thereby generate a stable cationic charge at physiological pH and there by lead to the proper condensation and delivery of DNA. Hence, the tocopherol based formulations with *N*-methylpiperidinium, *N*-methylimidazolium, *N*-methylmorpholinium and *N,N*-dimethylpyridinium as head groups turn out as the most efficient among the synthesized lipids.

2.4 CONCLUSIONS

In this study, the structure-function relationship of modified tocopherol-based formulations established that lipids with *N*-methylmorpholine, *N*-methylpiperidine, *N*-methylimidazolium and *N,N*-dimethylaminopyridinium head groups are promising candidates for gene delivery. Formulated lipids have the capacity for efficient endosomal release leading to efficient transfection *in vitro*. These lipoplexes were non-toxic and mediated good transfection efficiency as analyzed by the expression of two different reporter genes which established the superior activity of lipids whose structures correlate strongly with the transfection efficiency. The basis for superior activity is attributed to lipoplex size and stability in the presence of serum rendering these formulations suitable for *in vivo* applications, thus mandating further exploration.

2.5 EXPERIMENTAL SECTION

2.5.1 Materials: All the chemicals, reagents and solvents used for the synthesis were procured at highest purity from Sigma, Alfa Aeser and Spectrochem and used directly without further purification. Mass spectral data were acquired by using a commercial LCQ ion trap mass spectrometer (Thermo Finnigan, SanJose, CA, U.S.) equipped with an ESI source. ^{1}HNMR spectra were recorded on Bruker (2001). SAINT (Version 6.28a) & SMART (Version 5.625). 3-(4,5-dimethylthiazol-2-yl)-2,5-diphenyl-2H-tetrazolium bromide (MTT) was purchased from Calbiochem (Merck Millipore, USA), non-essential amino acids and sodium pyruvate supplements were purchased from Lonza. Lysotracker blue and Lipofecatmine 2000 (L2K) were procured from Life Technologies. Vectashield mounting media was obtained from DSS Takara (BioIndia, Delhi, India). Rhodamine-DHPE was a generous gift from IICT (Indian Institute of Chemical Technology, Hyderabad, India). Endotoxin free Plasmid *p*CMV-βgal and *p*EGFP-N_3 were obtained from laboratory stocks and purified using the Nucleo Bond Xtra Midi Plus EF (MACKAREY-NAGEL, Duren, Germany).

2.5.2 Synthesis: Alpha-tocopheryl-2-bromoacetate (Toc-Br): To an ice-cooled solution of alpha-tocopherol (3.5 g, 8.14 mmol) in pyridine (3 mL) and dichloromethane (5 mL), 2-bromoacetylbromide (3.27 g, 16.28 mmol) in 5 mL of dichloromethane was added slowly about 10 min. The reaction mixture was then allowed to stir at 0 °C for 3 h. The contents were diluted using 1 N HCl (50 mL) transferred in to 125 mL separating funnel. The compound was then extracted in to dichloromethane three times (3 X 20 mL). The fractions were collectively washed with saturated $NaHCO_3$ (2 X 25 mL), water (30 mL) and brine (30 mL). The organic layer was then separated and dried using anhydrous Na_2SO_4, followed by removal of the solvent under vacuum and the obtained residue was purified by column chromatography with 60-120 mesh silica gel using petroleum ether as the eluent. Yield: pale yellow liquid, 4.2 g (7.64 mmol, 93%). ^{1}H NMR (500 MHz,

$CDCl_3$) δ 4.07 (*s*, 2H), 2.59 (*t*, *J* = 5 Hz, 2H), 2.12 – 1.93 (*m*, 9H), 1.88 – 1.69 (*m*, 2H), 1.58 – 1.04 (*m*, 24H), 0.85 (*m*, 12H). ESI-MS: 551.30 $[M+H]^+$.

General method for the synthesis of cationic alpha-tocopheryl lipids: A 30 mL screw-top pressure tube was charged with magnetic stir bar and alpha-tocopheryl-2-bromo acetate (150 mg, 0.273 mmol) in 3 mL dry acetonitrile. The contents were refluxed for about 24 h at 80 °C after the addition of appropriate amount of tertiary amine of the corresponding heterocyclic head group, the reaction mixture was cooled and solvent was evaporated under vacuum. The residue was then washed repeatedly with the $CHCl_3$: EtOAc mixture to yield the pure compound (80-90% yield). The R_f ranged from 0.3-0.5 in 9:1 $CHCl_3$/MeOH. Seven new lipids were synthesized and characterized using ^{1}H-NMR, ^{13}C-NMR and ESI-MS (HRMS) analysis. Appropriate analytical and spectroscopic data are given below.

Toc-Me: brownish gummy solid, yield (123 mg, 85%). ^{1}H NMR (400 MHz, $CDCl_3$): *δ* 5.75 (*s*, 2H), 3.74 (*s*, 9H), 2.51 (*s*, 2H), 2.02 (*s*, 3H), 2.00 (*s*, 3H), 1.98 (*s*, 3H), 1.78 – 1.72 (*m*, 2H), 1.66 – 1.07 (*m*, 24H) 0.87 – 0.84 (*m*, 12H).^{13}C NMR (100 MHz, $CDCl_3$) δ 164.40, 149.96, 139.36, 126.28, 124.71, 123.34, 117.64, 75.27, 74.52, 62.67, 54.12, 39.37, 37.29, 32.78, 27.98, 24.81, 24.45, 23.75, 22.72, 21.04, 20.65, 19.69, 13.26, 12.38, 12.05, 11. ESI-MS (HRMS): Calcd for $[C_{34}H_{60}N^+O_3]$: 530.4568, Found: 530.4572.

Toc-Pyr: brownish oil, yield (143 mg, 95%). ^{1}H NMR (400 MHz, DMSO) *δ* 9.27 (*d*, *J* = 4 Hz, 2H), 8.76 (*t*, *J* = 8 Hz, 1H), 8.31 (*t*, *J* = 8 Hz, 2H), 6.21 (*s*, 2H), 2.56 (*t*, *J* = 8 Hz, 2H), 2.01 (*d*, *J* = 8 Hz, 9H), 1.75 (*m*, 2H), 1.52 – 1.05 (*m*, 24H), 0.84 – 0.80 (*m*, 12H). ^{13}C NMR (100 MHz, $CDCl_3$) δ 164.96, 149.84, 146.78, 145.86, 139.94, 127.68, 126.40, 124.85, 123.30, 117.66, 75.27, 60.96, 39.37, 37.41, 32.72, 27.98, 24.80, 24.45, 22.63, 21.03, 20.54, 19.68, 13.56, 12.78, 11.80. ESI-MS (HRMS): Calcd for $[C_{36}H_{56}N^+O_3]$: 550.4255, Found: 550.4271.

Toc-Dm: white wax, yield (152 mg, 94%). ^{1}H NMR (400 MHz, $CDCl_3$) δ 8.66 (*d*, *J* = 8 Hz, 2H), 6.88 (*d*, *J* = 8 Hz, 2H), 6.06 (*s*, 2H), 3.20 (*s*, 6H), 2.55 (*t*, *J* = 4 Hz, 2H), 2.05 (*s*, 9H), 1.75 – 1.65 (*m*, 2H), 1.62 – 1.06 (*m*, 24H), 0.87 – 0.83 (*m*, 12H). ^{13}C

NMR (100 MHz, $CDCl_3$) δ 166.22, 156.48, 149.76, 143.95, 140.04, 126.53, 124.99, 123.13, 117.58, 107.60, 75.22, 57.30, 40.38, 39.36, 37.39, 32.7, 30.89, 27.97, 24.80, 24.44, 22.63, 21.02, 19.75, 13.47, 12.68, 11.82. ESI-MS (HRMS): Calcd for $[C_{38}H_{61}N_2^+O_3]$: 593.4677, Found: 593.4680.

Toc-Db: brownish oil, yield (141 mg, 89%). ^{1}H NMR (400 MHz, DMSO) δ 4.98 (*s*, 2H), 3.60 – 3.49 (*m*, 6H), 3.14 – 3.01 (*m*, 6H), 2.62 – 2.55 (*m*, 2H), 2.03 – 1.90 (*s*, 9H), 1.76 (*m*, *J* = 4 Hz 2H), 1.51 – 1.06 (*m*, 24 H), 0.83 (*m*, 12H). ^{13}C NMR (100 MHz, $CDCl_3$) δ 168.92, 164.06, 149.99, 149.50, 140.11, 139.33, 126.49, 126.24, 124.67, 123.23, 117.57, 75.21, 52.97, 52.43, 45.12, 44.70, 39.36, 37.40, 32.78, 27.97, 24.81, 24.45, 23.70, 22.64, 21.03, 20.54, 19.69, 13.27, 12.46, 11.81. ESI- MS (HRMS): Calcd for $[C_{37}H_{63}N_2^+O_3]$: 583.4833, Found: 583.4817.

Toc-Pip: beige wax, yield (137 mg, 88%).^{1}H NMR (500 MHz, $CDCl_3$) δ 5.86 (*s*, 2H), 4.28 (*t*, *J* = 10 Hz, 2H), 4.03 (*d*, *J* = 10 Hz, 2H), 3.64 (*s*, 3H), 2.51 (*s*, 2H), 2.00 (*s*, 9H), 1.85 – 1.65 (*m*, 8H), 1.61 – 1.08 (*m*, 24H), 0.87 – 0.84 (*m*, 12H).^{13}C NMR (100 MHz, $CDCl_3$) δ 164.22, 149.86, 139.37, 126.35, 124.77, 123.21, 117.53, 75.21, 61.32, 46.60, 39.36, 37.45, 32.78, 30.91, 27.98, 24.81, 24.46, 22.73, 20.92, 20.81, 20.81, 20.36, 19.58, 13.40, 12.62, 11.75. ESI-MS (HRMS): Calcd for $[C_{37}H_{64}N^+O_3]$: 570.4881, Found: 570.5156.

Toc-Mor: brownish oil, yield (127 mg, 81%).^{1}H NMR (400 MHz, DMSO) δ 5.29 (*s*, 2H), 3.78 (*t*, *J* = 8 Hz, 4H), 3.46 (*s*, 3H), 3.43 (*t*, *J* = 8 Hz, 4H), 2.51 (*s*, 2H), 2.03 (*s*, 3H), 1.98 (*d*, *J* = 8 Hz, 6H), 1.76 (*s*, 2H), 1.51 – 1.06 (*m*, 24H), 0.85 – 0.81 (*m*, 12H). ^{13}C NMR (100 MHz, $CDCl_3$) δ 163.87, 150.07, 126.25, 124.66, 123.42, 117.73, 75.33, 63.61, 60.44, 53.55, 43.99, 39.37, 37.41, 32.79, 27.99, 24.81, 24.08, 23.50, 22.64, 21.78, 20.79, 19.66, 13.50, 12.27. ESI-MS (HRMS): Calcd for $[C_{36}H_{62}N^+O_4]$: 572.4673, Found: 573.4814.

Toc-Im: dark brown gummy solid, yield (132 mg, 88%). ^{1}H NMR (400 MHz, $CDCl_3$) δ 10.17 (*s*, 1H), 7.70 (*s*, 1H), 7.42 (*s*, 1H), 5.95 (*s*, 2H), 4.05 (*s*, 3H), 2.55 (*t*, *J* = 8 Hz, 2H), 2.06 – 2.01 (*s*, 9H), 1.75 – 1.69 (*m*, 2H), 1.52 – 1.08 (*m*, 24H), 0.87 – 0.83 (*m*, 12H). ^{13}C NMR (100 MHz, $CDCl_3$) δ 165.22, 149.92, 139.94, 138.51, 126.39, 124.86,

123.88, 123.31, 122.92, 117.70, 75.29, 50.13, 39.36, 37.15, 32.78, 30.95, 27.97, 24.80, 24.45, 22.73, 21.02, 20.55, 19.69, 13.42, 12.63, 11.83. ESI-MS (HRMS): Calcd for $[C_{35}H_{57}NN^{+}O_3]$: 553.4363, Found: 554.4666.

2.5.3 Preparation of SUVs: Cationic liposomes (SUVs) were prepared by the lipid hydration method as described before.[34,35] Small unilamellar liposomes were formulated from 1:1 (mole ratio) mixture of each of the differently modified cationic tocopherol lipid and co-lipid DOPE (1, 2-dioleoyl-*sn*-glycero-3-phosphoethanolamine). Briefly, lipid stocks in chloroform were mixed at the desired molar ratio (1:1) and dried uniformly under a thin flow of moisture-free nitrogen gas. The resulting thin films were subjected to reduced pressure for a limited time period of four hours. The dried lipid films were hydrated with deionized water to a final lipid concentration of 1 mM and were vortexed at room temperature. The resulting multi lamellar vesicles were subjected to sonication in an ice bath using a SONICS Vibra cell (25% Amplitude, pulse mode, 9 s on/off) until clarity. The newly formed small unilamellar vesicles or liposomes were stored at 4 °C until use.

Fluorescence labeled liposomes were also prepared separately by following the same method using 0.2 mol % of Rhodamine PE (20 µg/mL stock) at the time of thin film preparation along with the lipid and DOPE as described before.[36]

2.5.4 Hydrodynamic diameter & surface potential of SUVs and lipoplexes: Both SUVs and lipoplexes were characterized with respect to their size and zeta potential using a SZ-100 NEXTGEN (HORIBA) instrument, set at 25°C and equipped with a diode-pumped solid-state laser at λ 532 nm. Complexes were prepared immediately before analysis. Plain DMEM was used for sample dilutions and instrument auto correction prior to the sample measurements performed in a quartz cuvette. The instrument was programmed to sum the average of five different measurements done in general mode by using the software SZ-100, HORIBA.

The surface potential of the prepared complexes were also measured in the same instrument using Laser Doppler Electrophoretic Analysis using the provided SZ-100

software. Here, Milli-Q served as the blank control for instrument autocorrelation and sample dilutions.

2.5.5 Transmission electron microscopy: The morphology and particle size distribution of the cationic liposomes were examined using a JEOL JEM 2100 Transmission Electron Microscope operated at 120 kV. Briefly, a drop (4 μL) of the cationic liposome (1 mM) and the respective lipoplex formulation were separately applied on to a standard 300 mesh carbon coated copper grid and allowed to adsorb for about 60 sec. This was followed by negative staining using 2% uranyl acetate. The visualization of the vesicles was enabled by uranyl cation which binds to the phosphate group of the co-lipid, DOPE. Excess stain was removed after 45 sec and the grids were air dried at room temperature before the TEM analysis. The images were acquired on a Gatan camera, Digital Micrograph software.

2.5.6 Gel retardation assay: The DNA binding capacity of SUVs was examined in a gel binding assay using agarose gel electrophoresis. Lipid:DNA complexes were assembled from the cationic tocopherol based liposomes (1 mM) and plasmid *p*CMV-βgal (0.4 μg), at varying N/P charge ratios (0.3, 1, 3 & 9), in 0.5 X PBS (20 μL). The complexes were incubated for 30 min at room temperature, prior to the electrophoresis. Samples were loaded onto 1% agarose gel in a BROVIGA apparatus. Electrophoresis was carried out for 90 min at 70 V in TAE running buffer (40 mM Tris-Acetate, 1 mM EDTA, pH 8.2). Gels were stained with ethidium bromide (EtBr) (2 mg/mL mQ) for 30 min, post electrophoresis. Complexes were observed under transillumination at 300 nm. Images were captured on GENESYS imaging system.

2.5.7 Et-Br Displacement assay: The association of cationic lipids with plasmid DNA was studied using ethidium bromide as a probe in the displacement assay. Intercalation of the fluorescent probe with DNA exhibits an increase in the fluorescent quantum yield. The binding of lipids to nucleic acids by displacement of EtBr leads to a decrease in the fluorescence intensity. Fluorescence measurements were recorded using a Hitachi F-7000 fluorescence spectrophotometer at excitation and emission wavelength of 516 nm and 598 nm respectively (slit width 5 nm X 5 nm). Briefly, baseline fluorescence

(0%) was established using 0.23 µg EtBr in 20 mM Tris.HCl buffer (pH 7.4). Thereafter, *p*CMV-βgal DNA (2.3 µg) was introduced and this solution was used to set the instrument at 100% fluorescence value. Aliquots of cationic lipids corresponding to linear charge ratios (ranging from 0.1 to 9) were added sequentially and the readings were taken after thorough mixing at each step. The fluorescence values were normalized with respect to the EtBr-DNA complex, set at 100% intensity in the titration curve.

2.5.8 Amplification and purification of plasmid DNA: *p*CMV-βgal (7164bp) and *p*EGFP-N_3 (4729bp) control vectors encoding the β-galactosidase and Enhanced Green Fluorescent Protein were obtained from laboratory stocks. These plasmids were transformed into competent *Escherichia coli* DH-5α cells. Plasmids were amplified in LB broth media at 37 °C overnight. The endotoxin free plasmids were purified using the NucleoBond® Xtra Midi kit (MACKAREY-Nagel). The concentration and purity of the plasmids were quantified using the NanoDrop 2000 and agarose gel electrophoresis that confirmed the plasmid integrity and quality.

2.5.9 Cell Culture: Adherent mouse neuroblastoma derived Neuro-2a, human hepatocellular carcinoma derived HepG2, human embryonic kidney derived HEK-293 and Chinese hamster ovary derived CHO cell lines were used for all transfections. Cell lines were cultured in 25 cm^2 flasks in 6 mL of DMEM (Dulbecco's Modified Eagles medium, Invitrogen) containing 10% (v/v) Fetal Bovine Serum, 10 mM $NaHCO_3$, 60 µg/mL penicillin, 50 µg/ml streptomycin and 30 µg/ml kanamycin respectively. In addition, Neuro-2a cell culture media were supplemented with 1% sodium pyruvate and 1% non-essential amino acids (Lonza).

2.5.10 Transfection Biology: Briefly, the EGFP expression efficiency of the cationic lipoplexes was evaluated qualitatively and quantitatively in Neuro-2a cells using fluorescence microscopy and flow cytometry, respectively. Complexes were prepared using *p*EGFP-N_3 plasmid (1 µg per well) at 1:1 and 3:1 charge ratios and transfection was performed in 24 well plates as described above. A visual comparison 48 h later, using the microscope, was performed to monitor GFP fluorescence of cells treated with different

lipoplexes. Images were taken using Floid Cell Imaging Station in both fluorescence and transmittance mode.

In order to quantify the expression of EGFP reporter cassette via transfection, flow cytometry of cells treated with lipoplex formulations was performed after 48 h. Following this period of incubation, growth media was removed and cells were washed with PBS followed by the addition of 100 µL of 0.1% trypsin/EDTA. The detached cells were dispersed by pipetting, followed by resuspension in 400 µL of PBS supplemented with 10% serum. The pooled cells were analyzed using a FACS caliber system equipped with an argon ion laser at 488 nm for excitation and detection at 530 nm. 10,000 cells were analyzed for each sample using the software, CellQuest. Non transfected cells served as live cell controls for gate settings which in turn provided the cutoff thresholds for quantification of fluorescent cell population.

Further to evaluate the activity of the synthesized lipids, we examined the efficiency of transfection using the reporter gene, β-galactosidase. Briefly, Neuro-2a, HepG2, CHO and HEK-293 cells were seeded on to 96 well plates a day prior to transfection, at a density of 1×10^4 cells per well in complete medium. Here, the cell lines were selected on the basis of *in vivo* bio-distribution of tocopherol. Studies have shown that this fat soluble vitamin has a tissue specific distribution with highest levels in liver, prostate and whole brain. Other organs, such as kidney, prostate and ovary also rely on this lipophilic antioxidant for scavenging free radicals.[37,38] Correspondingly, a neural (Neuro-2a), hepatic (Hep-G2), kidney (HEK) and ovarian (CHO) cell lines, representing a fair selection of tissues, were chosen for evaluating the activity profile of tocopherol formulations in cell culture. Lipoplexes at charge ratios 1, 3 with respect to plasmid *p*CMV-βgal DNA (0.3 µg per well) were prepared in incomplete DMEM media. The complexes were incubated at room temperature for 30 min following which DMEM containing 10% serum was added to formulate the final transfection complex as described before.[39] DMEM and the commercially available cytofectin (Lipofectamine 2000) served as the controls. Prior to the addition of lipoplexes, the growth media from the cells were removed and were then washed with 1X PBS (100 µL). This was followed by the lipoplex addition and incubation for 3-4 h. Following incubation, the lipoplex containing media was replaced with DMEM containing 10% serum and incubated for 48 h and then

assayed for reporter gene expression. Briefly, 100 µL of lysis buffer (0.25 M Tris–HCl, pH 8.0, and 0.5% NP40) was added to each well and estimated for β-galactosidase activity as described.[40]

2.5.11 Cellular uptake & co-localization analysis: Briefly, Neuro-2a cells were seeded 24 h prior to the experiment at a density of 1×10^4 cells per coverslip (12 mm diameter) placed in the bottom of the well in a 12 well-plate. Here, the most efficient among the synthesized lipids were labeled with rhodamine-DHPE and the corresponding fluorescent liposomes were used for lipoplex assembly with the plasmid *p*CMV-β gal (1 µg per coverslip). Once the seeded cells attained 70% confluence, the cells were incubated with 100 µL of labelled lipoplexes at 1:1 charge ratio for 1 h and were done in duplicate. Following this, Lysotracker Blue DND-22 reagent (50-100 nM) was added to one of the duplicate coverslips containing the lipoplexes and incubated for an additional 30 min. DAPI (300 nM in PBS) was added for counterstaining the counterpart cells that were not labelled with the Lysotracker. After incubation, cells were washed twice with PBS and fixed with 4% paraformaldehyde for 10 min at room temperature and was followed by another PBS wash. Following washes, the coverslips were mounted on glass slides with 4 µL of Vectashield. Fluorescence was visualized under a confocal laser scanning microscope (Leica TCS S52) equipped with 63X oil immersion objective. The emission collection wavelengths were set at 373-422 nm for Lysotracker and 568-583 nm for RH-PE labelled lipoplexes, respectively. Co-localization of the fluorescent labels red (lipid)+blue (Lysotracker) were analyzed using LAS X imaging platform to determine the location of lipoplexes with respect to the nucleus and lysosomes.

2.5.12 Cell viability assay: Cytotoxicity screening is a mandatory protocol for the characterization of the synthesized tocopherol based gene delivery vectors. For this, cells were seeded at a density of 10^4 cells per well in 96 well plates. Lipid toxicities were evaluated by preparing lipoplexes at charge ratios 0.3, 1, 3 and 9 and incubating for 30 min at room temperature and then treating Neuro-2a, HepG2, CHO & HEK-293 cells with the prepared lipoplexes for 3 h at 37 °C in 10% serum containing DMEM. Following incubation, MTT [3-(4,5-dimethylthiazole-2-yl)-2,5-diphenyltetrazolium

bromide] was added to ascertain cell viability assay as described previously.[41] The assay was terminated following the completion of 21 h, by adding 100 µL of MTT (0.5 mg/mL) solution in serum less DMEM per well. Incubation continued for 3 more hours (37 °C, CO_2). The resulting purple colored granules were dissolved following cell lysis using 100 µL of MeOH: DMSO (1:1). The purple solution was spectroscopically read at 540 nm in a multiplate reader of multiscan spectrum and the untreated cells served as the controls. Results were expressed as percent viability = [A_{540} (treated cells)-background/A_{540} (untreated cells)-background] x 100.

2.6 REFERENCES

1. Friedmann, T. *Nat Genet.* **1992**, *2,* 93.
2. Thomas, C. E.; Ehrhardt, A.; Kay, M. A. *Nature Rev. Genet.* **2003**, *4,* 346.
3. Mintzer, M. A.; Simanek, E. E. *Chem Rev.* **2008**, *109*, 259.
4. Karmali, P. P.; Chaudhuri, A. *Med. Res. Rev.* **2007**, *27*, 696.
5. Gao, X.; Huang, L. *Gene Ther.* **1995**, *2*, 710.
6. Alton, E. W.; Boyd, A. C.; Porteous, D. J.; Davies, G.; Davies, J. C.; Griesenbach, U.; Higgins, T. E.; Gill, D. R.; Hyde, S. C.; Innes, J. A. *Am J Respir Crit Care Med.* **2015**, *192*, 1389.
7. Zhi, D.; Zhang, S.; Cui, S.; Zhao, Y.; Wang, Y.; Zhao, D. *Bioconjug Chem.* **2013**, *24*, 487.
8. Martin, B.; Sainlos, M.; Aissaoui, A.; Oudrhiri, N.; Hauchecorne, M.; Vigneron, J. P.; Lehn, J. M.; Lehn, P. *Curr Pharm Des.* **2005**, *11*, 375.
9. Niculescu-Duvaz, D.; Heyes, J.; Springer, C. J. *Curr Med Chem,* **2003**, *10*, 1233.
10. Bhattacharya, S.; Bajaj, A. *Chem Commun.* **2009**, *31,* 4632.
11. Le Gall, T.; Berchel, M.; Le Hir, S.; Fraix, A.; Salaün, J. Y.; Férec, C.; Lehn, P.; Jaffrès, P. A.; Montier, T. *Adv Healthc Mater.* **2013**, *2,* 1513.
12. Kumar, K.; Maiti, B.; Kondaiah, P.; Bhattacharya, S. *Mol Pharm.* **2014**, *12*, 351.
13. Kumar, K.; Maiti, B.; Kondaiah, P.; Bhattacharya, S. *Org Biomol chem.* **2015**, *13*, 2444.

14. Zheng, L. T.; Yi, W. J.; Su, R. C.; Liu, Q.; Zhao, Z. G. *ChemPlusChem*. **2016**, *81*, 125.
15. Tucker, J.; Townsend, D. *Biomed Pharmacother.* **2005**, *59,* 380.
16. Duhem, N.; Danhier, F.; Préat, V. *J Control. Release,* **2014**, *182*, 33.
17. Kedika, B.; Patri, S. V. *J Med Chem.* **2010**, *54*, 548.
18. Kedika, B.; Patri, S. V. *Bioconjug Chem.* **2011**, *22*, 2581.
19. Kedika, B.; Patri, S. V. *Mol Pharm.* **2012**, *9*, 1146.
20. Bajaj, A.; Mishra, S. K.; Kondaiah, P.; Bhattacharya, S. *Biochim. Biophys. Acta.* **2008**, *1778*, 1222.
21. Lai, E.; Van zanten, J. H. *J Pharm Sci.* **2002**, *91*, 1225.
22. Ross, P.; Hui, S. *Gene Ther.* **1999**, *6*, 165.
23. Pichon, C.; Billiet, L.; Midoux, P. *Curr Opin Biotechnol.* **2010**, *21,* 640.
24. Sternberg, B.; Sorgi, F. L.; Huang, L. *FEBS Lett.* **1994**, *356*, 361.
25. Zuidam, N. J.; Hirsch-Lerner, D.; Margulies, S.; Barenholz, Y. *BBA-Biomembranes.* **1999**, *1419*, 207.
26. Kedika, B.; Patri, S. V. *Eur J Med Chem.* **2014**, *74*, 703.
27. Ivanova, E. A.; Maslov, M. A.; Kabilova, T. O.; Puchkov, P. A.; Alekseeva, A. S.; Boldyrev, I. A.; Vlassov, V. V.; Serebrennikova, G. A.; Morozova, N. G.; Zenkova, M. A. *Org Biomol Chem.* **2013**, *11*, 7164.
28. Bajaj, A.; Mishra, S. K.; Kondaiah, P.; Bhattacharya, S. *Biochim. Biophys. Acta,* **2008**, *1778*, 1222.
29. Bhargava, P.; Singh, M.; Sreekanth, V.; Bajaj, A. *J Phy Chem B.* **2014**, *118*, 9341.
30. Westendorf, A. F.; Zerzankova, L.; Salassa, L.; Sadler, P. J.; Brabec, V.; Bednarski, P. J. *J Inorg Biochem.* **2011**, *105*, 652.
31. Singh, M.; Singh, A.; Kundu, S.; Bansal, S.; Bajaj, A. *BBA-Biomembranes.* **2013**, *1828*, 1926.
32. Siddiqui, N.; Andalip, S. B.; Ali, R.; Afzal, O.; Akhtar, M. J.; Azad, B.; Kumar, R. *J Pharm Bioallied Sci.* **2011**, *3*, 194.
33. King, D.; Mcbain, A. E.; Jais, M. M.; Roberts, C. J.; Collins, J.; Wheal, H.; Walker, R. *Comp Biochem Physiol C.* **1982**, *73*, 71.
34. Bangham, A.; Hill, M.; Miller, N. *Methods Membr Biol.* **1974**, *1*, 1.

35. Chandrashekhar, V.; Srujan, M.; Prabhakar, R.; Rakesh Reddy, C.; Sreedhar, B.; Kiran, R.; Sanjit, K.; Chaudhuri, A. *Bioconjug Chem.* **2011**, *22*, 497.
36. Gopal, V.; Xavier, J.; Dar, G. H.; Jafurulla, M.; Chattopadhyay, A.; Rao, N. M. *Int J Pharm.* **2011**, *419*, 347.
37. Stocker, A.; Zimmer, S.; Spycher, S. E.; Azzi, A. *IUBMB life*, **1999**, *48*, 49.
38. Uno, Y.; Piao, W.; Miyata, K.; Nishina, K.; Mizusawa, H.; Yokota, T. *Hum Gene Ther.* **2010**, *22*, 711.
39. Zuhorn, I. S.; Visser, W. H.; Bakowsky, U.; Engberts, J. B. F. N.; Hoekstra, D. *Biochim. Biophys. Acta.* **2002**, *25*, 1560.
40. Gopal, V.; Xavier, J.; Kamal, M. Z.; Govindarajan, S.; Takafuji, M.; Soga, S.; Ueno, T.; Ihara, H.; Rao, N. M. *Bioconj Chem.* **2011**, *22*, 2244.
41. Hansen, M. B.; Nielsen, S. E.; Berg, K. *J Immunol Methods.* **1989**, *119*, 203.

Chapter 3

●●●

Delocalizable Cationic Head Group Based alpha-Tocopherol Derived Gemini Cationic Lipids for Improved Plasmid Delivery

3.1 INTRODUCTION

Many setbacks are insisting the transformation of gene therapy from concept to clinic such as lower transfection of drug mimics, selective delivery of gene payloads and bio-safety issues arise from vector.[1] Despite of efficient induction of transfection of viral carriers, their application in clinic still have been suffering from many pharmacological issues like insertional mutagenesis through random integration into the host genome and immunogenic response.[2] In contrast the non-viral cationic lipid systems are evolving as promising future hope by satisfying the related issues with their bio-safety profiles. However, their clinical application is limited because of lower transfection abilities. Gemini cationic lipids are occupying a major space among the wide range of multimodular cationic lipid systems with their strong potentials of transfection and least toxic nature.[3]

Many reports of cationic lipid mediated gene delivery have been reported that each structural domain of cationic lipid has its own role to impact the aggregation as well as the transfection.[4] Numerous efforts have been made for the modification of molecular structural constitution of cationic lipids to attain the desirable activity.[5,6] The early established studies proved that a positively charged nitrogen atom is necessary to act as hydrophilic region of a lipid and to probe the buffering transformations in endosomal escape.[7,8] This cation resides on single atom and easily accessible to charge-charge interaction in most of the head group modification studies towards fruitful endeavors for improved efficacies.[9–18] Recently the delocalized cation has drawn attention as head group like pyridinium[19,20] and imidazolium[21,22] because of their lesser hydration potentials and soft cationic behavior and not been studied extensively. The structure–activity relation (SAR) studies of these delocalizable cation with different segments of cationic lipids may lead to desirable goals.[9,23] Recent developments in this non-viral lipid system also contain a prominent class of cationic lipids, i.e. gemini lipids, reported to be efficient cytofectins from various laboratories.[24–38]

The typical hallmarks of these gemini lipids are generally represented by having two polar head groups linked by a flexible or rigid spacer and two hydrophobic segments.

Towards developing synthetic cationic lipid formulations for elevating efficacy levels with no encircling limitations, we report here a new class of gemini lipids with exploiting a biologically active α-tocopherol based hydrophobic backbone. Tocopherol has earlier been employed for being chemically conjugated to ribonucleic acids and polymers for effective RNAi action.[39,40] Importantly, spacers which in turn used to link cationic head groups of lipids together through a moiety like simple alkyl chains varying in length,[41] disulfide bonds[42] and oligo-oxyethylene.[43] involve towards the successful transfection. In fact, transfection profiles of cationic amphiphiles are highly sensitive to even subtle changes of spacers such as the functional properties, chain lengths and orientation with head group.[44]

One more major influencing criterion regarding the cationic lipid mediated transfection is finding a suitable co-lipid which helps to enhance transfection potentials of cationic lipids.[45] In spite of number of different helper lipids are in use, DOPE has greatly been witnessed as a common most useful co-lipid in many prior investigations with its significant features like formation of non bilayer structure and fusogenicity.[46-48]

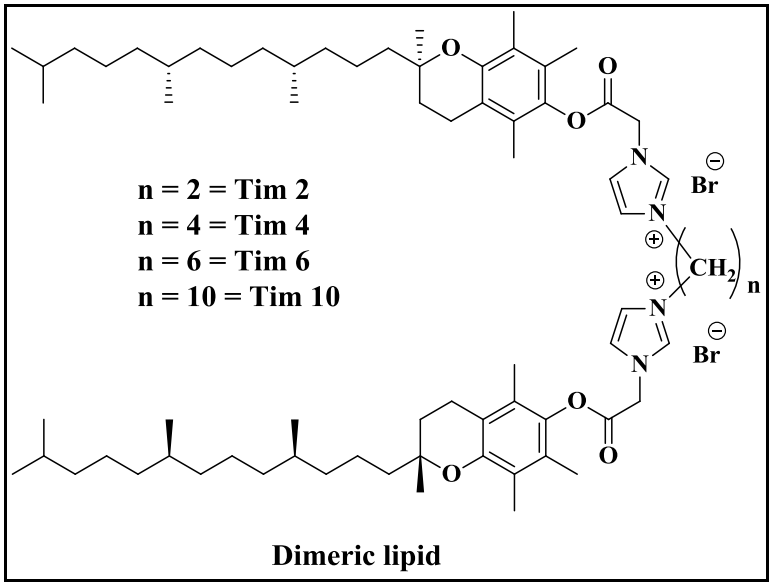

Fig. 1 Molecular structures of Dimeric lipids

In present investigation, we designed and synthesized a series of four different tocopherol derived delocalizable cation based dimeric lipids differ in length of the spacer.

As the spacer length increases from two methylene to ten methylene the two hydrophilic delocalized cations will move apart from each other. This in turn possibly affects the aggregation, interaction with DNA and ultimately the transfection profiles. These lipids were mixed with DOPE to produce clear aqueous suspensions. The lipid/co-lipid ratio which could give better transfection results were optimized using the β-galactosidase activity in HEK293 cells at single N/P charge ratio. This optimized molar ratio from each gemini lipid was further used to optimize for better N/P charge ratio and screened their potentials in comparison to lipofectamine 2000 (L2K) in three different cell lines. These optimized molar ratios, N/P charge ratios and varied activity potentials of four different lipids were carefully analyzed by the results of lipid/DNA interaction studies and physicochemical investigations of lipid aggregates and lipid/DNA complexes. These studies explored a structure activity correlation study in detail. Finally, the better activity performance of TIM 6 derived dimeric co-liposomal formulation was examined using fluorescent based uptake and co-localization studies.

3.2 RESULTS AND DISCUSSION

3.2.1 Synthesis: In tandem to our prior investigation of head group modified tocopherol based cationic lipids,[49] four different spacer length inserted dimeric delocalizable cationic lipids were synthesized by following the steps presented in Scheme 1.. Initially, ester conjugated tocopherol imidazole (Toc-Im) was synthesized from *N*-alkylation of 1H-imidazole with alpha-tocopheryl-2-bromoacetate which is isolated and used as common intermediate for all the final dimeric lipids. To produce dimeric lipid dibromides, each dibromoalkane was treated with Toc-Im intermediate separately and solvent precipitations were performed to get pure titled lipids. The structures of lipid and intermediates were analyzed by using the spectroscopic data generated from ^{1}H-NMR, ^{13}C-NMR and LC-MS.

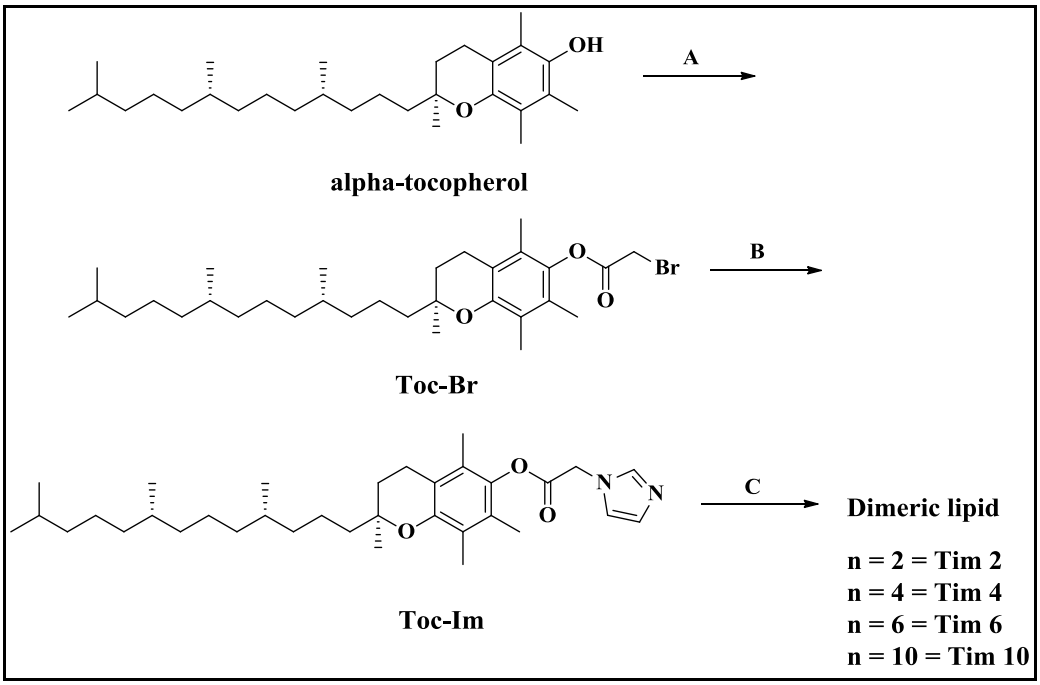

Scheme 1 Synthetic route and molecular structures of alpha-tocopherol based gemini cationic lipids.

Reagents & conditions: A) 2-bromoacetylbromide, pyridine, dichloromethane, 0 °C, 3 h; B) 1H-Imidazole, K_2CO_3, acetonitrile, 80 °C, 16 h; C) dibromoalkane, acetonitrile, sealed tube, 80 °C, 32 h.

3.2.2 Preparation of liposomal aggregates: Mixed liposomal suspensions were developed using the novel dimeric lipid and DOPE by following the protocol mentioned in earlier reports.[50,51] To optimize the better potential molar ratio of lipid/co-lipid, varying ratios of lipid/DOPE (1:1, 1:1.5, 1:2, 1:3 & 1:4) formulations using different concentrations of DOPE with respect to the constant dimeric lipid were prepared. All the rehydrated lipid thin films were vertexed to get multilamellar aggregates, subsequent sonication of these turbid suspension will provide clear aqueous suspensions stored at 4 ºC until use.

3.2.3 Lipid/DNA binding interaction studies: The DNA binding interactions of new dimeric co-liposomal formulations were characterized using gel electrophoresis and EtBr exclusion assays. In a typical gel based experiment complexes of DNA (*p*CMV-

βgal) were prepared using transfection optimized molar ratio (1:1.5; lipid/DOPE) at six different N/P charge ratios (0.5:1 – 8:1, lipid/DNA). Representative images obtained from each dimeric lipid demonstrated through Fig. 2A indicate that all the lipid formulation could efficiently condense the *p*DNA. Condensation potentials are observed to be increased with increase in spacer length and become saturated at spacer length 6. Among the present lipid series, TIM 6 is showing maximum binding by retarding plasmid completely at 1:1 ratio itself where as the other lipids started retardation of DNA at 2:1 charge ratio.

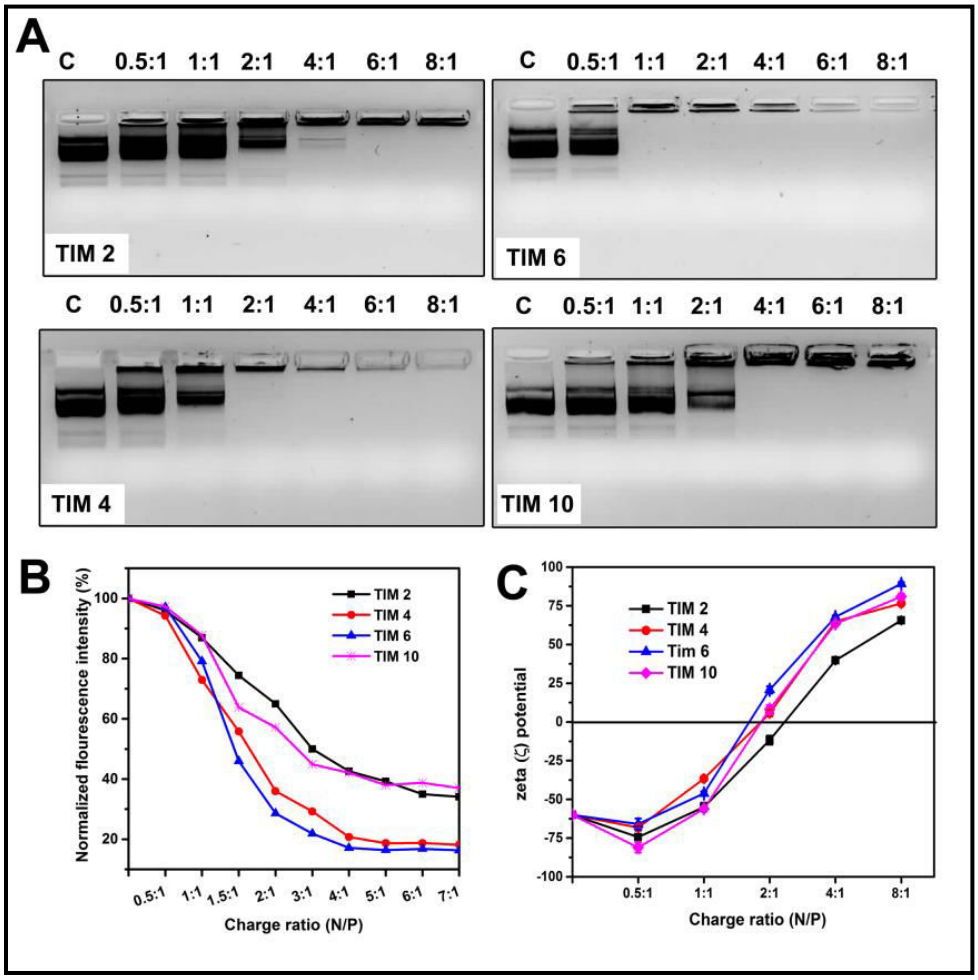

Fig. 2 DNA binding interaction studies of novel dimeric lipid formulations: A) Gel electrophoresis pictures of four different dimeric lipids was obtained using lipoplexes derived from *p*CMV-βgal plasmid (0.3μg/well) and optimized lipid/DOPE molar formulation across the varying charge ratios mentioned on top of each panel. Naked DNA

served as control indicated as 'C'. B) Normalized fluorescence intensities of four dimeric lipids acquired from a typical fluorescent based EtBr exclusion assay at varying charge ratios of lipid/DNA represented in the bottom of graph. C) Zeta potential of lipoplexes derived from four different dimeric lipids at varying ratios of N/P charge ratios depicted in the graph at the bottom.

The electrophoretic results were further sustained using the results from fluorescent based EtBr intercalation assay. On a sequential addition of each lipid formulation to a control EtBr-DNA complex which has been kept its fluorescent intensity as 100% has gradually dropped down to get neutralized. The concentration of lipid that could induce maximum dropdown of fluorescent value would responsible for better compaction and results maximum payloads. According to the results depicted in Fig. 2B, maximum compaction potentials were observed with TIM 6 followed by TIM 4, TIM 10 and TIM 2. The ratio 1.5:1 (N/P) was seemed to be maximum induced dropdown value of fluorescence irrespective of the lipids. All the lipoplexes derived from each co-liposomal formulation were also characterized in terms of zeta potentials represented through the Fig. 2C. The demonstrating results of zeta potential measurements were well corroborated with DNA retardation capacities such as the initial charge ratios like 0.5:1 and 1:1 N/P charge ratios showed negative potentials due to uneven binding of DNA which turned to positive on 2:1 N/P charge ratio where the DNA gets neutralized completely.

3.2.4 Physicochemical characterization of lipid aggregates: The transfection optimized dimeric co-liposomal formulations were characterized using DLS experiment to evaluate the aggregation properties in terms of suspended particle size. The results depicted through Fig. 3A revealed that the transfection optimized co-liposomes in all the gemini lipid formulations were in the range ~120 – 150 nm. Lipoplexes derived at optimized transfection N/P charge ratio 2:1 from each gemini lipid and plasmid complexation led to increase in size ranging from ~250 – 350 nm.. Significant observation was found that the size of lipid/DNA complex decreased with increase in spacer chain length up to TIM 6 and rose suddenly at TIM 10. This may supports the

proper compaction of DNA arrives with six methylene spacer containing TIM 6 and was further perturbed with ten methylene spacer length.

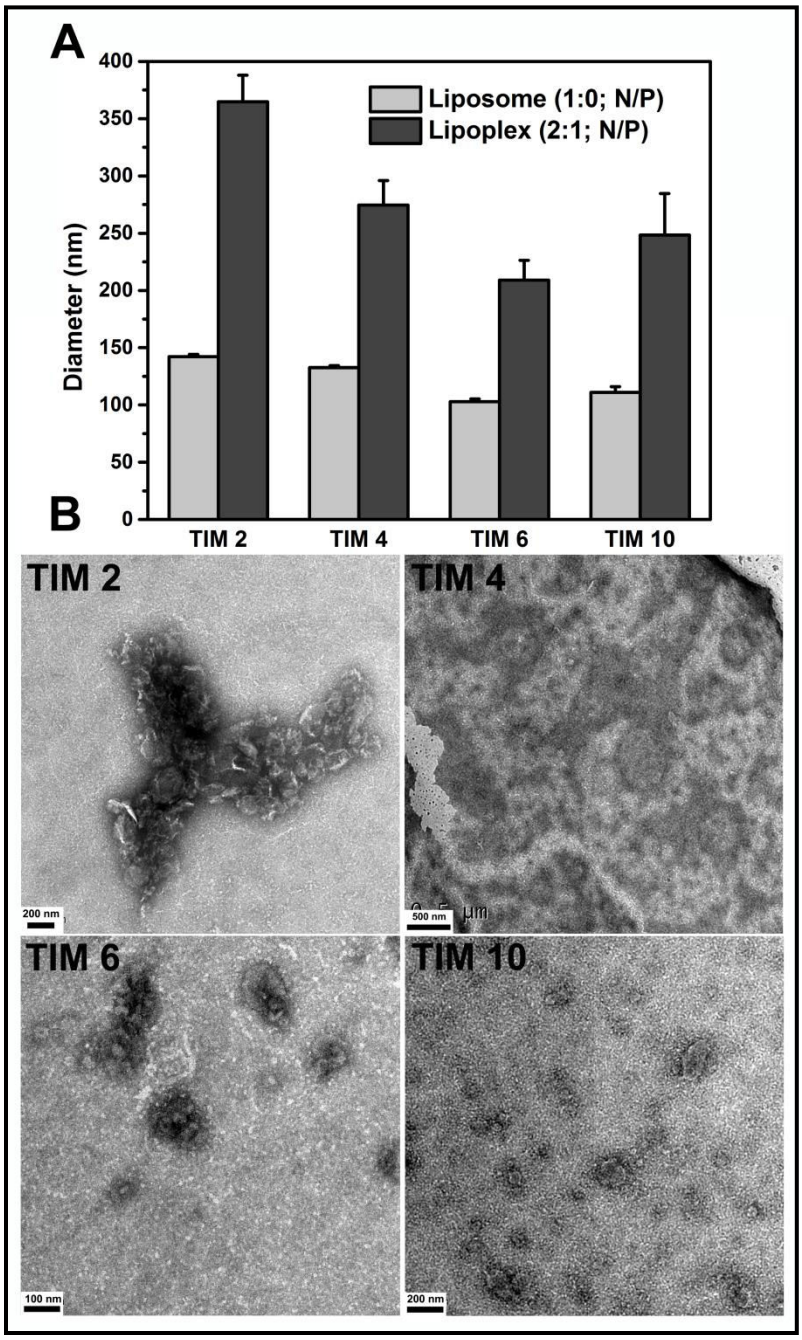

Fig. 3 Physicochemical characterization: A) Hydrodynamic diameter of liposomal aggregates (light gray) and their derived DNA complexes (gray) at 2:1 N/P ratio measured by dynamic light scattering technique. B) Representative transmission electron microscopy images of transfection optimized gemini co-liposomal formulations.

The observations found from DLS with respect to the co-liposomal formulations were visually interpreted by taking the images under transmission electron microscopy. The resulted images derived from each gemini lipid represented through Fig. 3B confirms the liposomal vesicular nature and surrounded by unilamellar membrane of each gemini lipid.

3.2.5. Transfection biology: *Optimization of dimeric lipid/DOPE molar formulation*: To find out better transfecting co-liposomal aggregate from various gemini lipid/DOPE molar formulations (1:1, 1:1.5, 1:2, 1:3 & 1:4), lipoplexes were generated using *p*CMV-βgal DNA at a single N/P charge ratio 2:1 and allowed for transfection in HEK293 cell line. Normalized results of β-galactosidase activity of 48 h post transfection were demonstrated through Fig. 4, indicates the molar ratio 1:1.5 was expelled maximum transfection among the all molar ratios. Based on these observations, 1:1.5 (gemini lipid/DOPE) mixed formulation was considered as optimized ratio for further investigations.

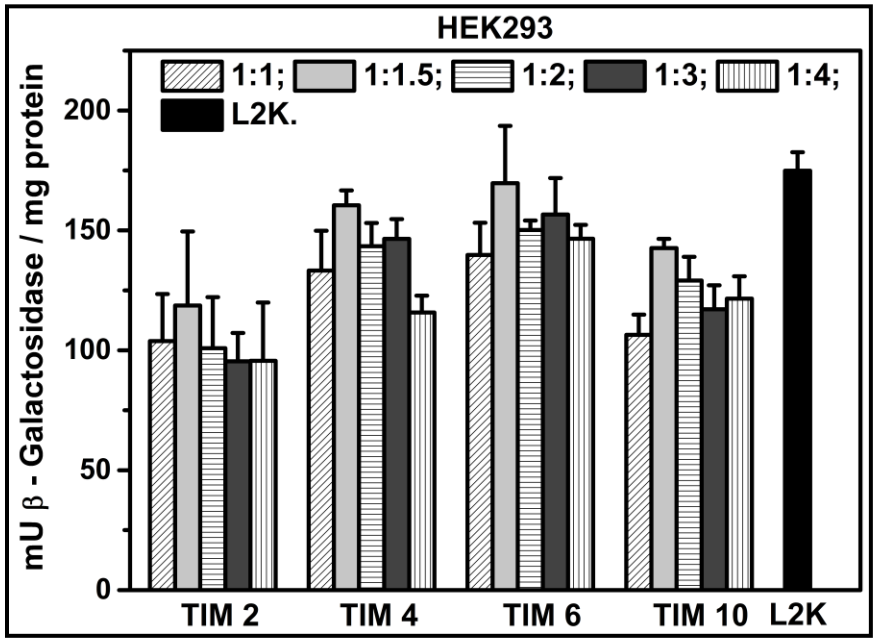

Fig. 4 Transient transfection results obtained from dimeric lipids in HEK293 cell line using *p*CMV-βgal DNA as a reporter plasmid: Optimization of molar ratio for maximum transfection potential using different molar combinations of lipid/DOPE (1:1, 1:1.5, 1:2, 1:3 & 1:4). Lipofectamine 2000 (L2K) served as bench mark standard.

One of the major setbacks of nonviral gene delivery for *in vivo* progress of gene therapy is the presence of serum, which will greatly influence the transfection properties of lipoplexes by disturbing its stability.[52] In order to evaluate the effect of serum on transfection properties of these novel lipid dimers, β-galactosidase assay was conducted using lipoplexes derived from *p*CMV-βgal and the four lipid formulations at varying charge ratios such as 0.5:1, 1:1, 2:1 & 4:1. The cells were incubated with the lipoplexes in presence of 10% FBS+DMEM for about 4 h. Normalized efficiencies of transfection were represented through the Fig. 5A shows that maximum activity was observed with 2:1 N/P charge ratio irrespective of the lipid. This particular observation have already supported by the lipid/DNA binding interaction results mentioned in previous sections. The transfection potentials of four different lipids followed a rank order indicate as TIM 6 > TIM > 4 > TIM 10 > TIM 2. The careful observation of relative transfection efficiencies indicates that the TIM 6 derived formulation has shown better performance among the lipid series studied and moreover the activity of TIM 6 is on par with the commercial formulation used (L2K) in the study.

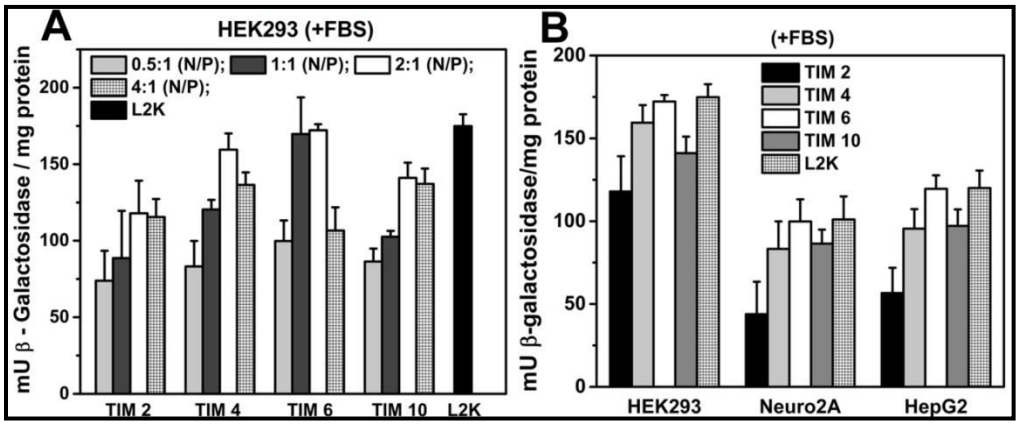

Fig. 5 Transfection using optimized molar ratio across the varying range of lipid/DNA (0.5:1, 1:1, 2:1 & 4:1) charge ratios (N/P). Normalized transient transfection results of lipid formulations at 2:1 lipid/DNA charge ratio compared to commercial transfection reagent lipofectamine in three different cell lines (HEK293, Neuro-2a and HepG2) using *p*CMV-βgal reporter gene. Lipofectamine 2000 (L2K) served as bench mark standard.

The tissue specific bio-distribution of tocopherol among the liver, renal and whole brain reported in previous findings[53,54] has driven us to probe the target oriented transfection potentials of these tocopherol derived lipid dimers. Towards this aim reporter gene expression was performed using the plasmid *p*CMV-βgal derived lipoplexes from four co-liposomal formulations at optimized transfection charge ratio 2:1 in three different cell lines such as HEK293, Neuro-2A and HepG2 derived from kidney, neuroblastoma and liver respectively. The normalized enzyme activity results were represented through Fig. 5B depicts the activity potentials were being fall among the three different cell lines as following rank order indicates HEK293 > HepG2 > Neuro-2A.

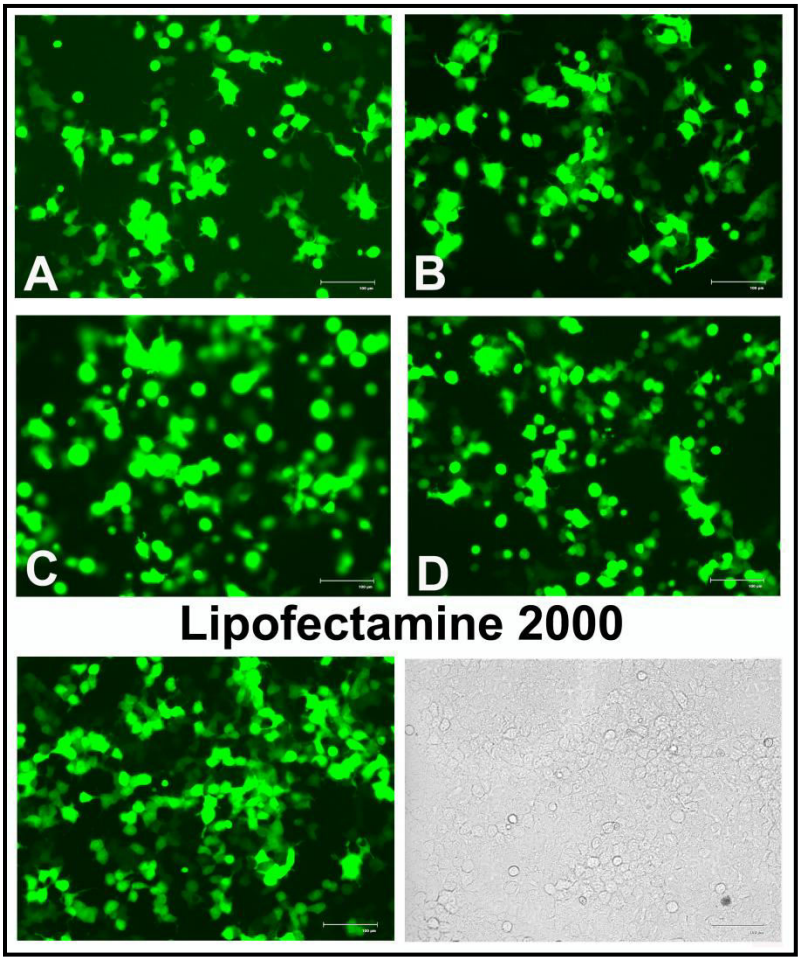

Fig. 6 Transfection in HEK293 cell lines using pEGFP-N_3 plasmid at optimized molar and N/P charge ratios of dimeric lipids A) TIM 2, B) TIM 4, C) TIM 6 and D)TIM 10.

The enhanced green fluorescent expression was captured under floid cell imaging system after 48 h post transfection.

Transient transfection results from *p*CMV-βgal reporter plasmid were sustained by qualitative analysis of fluorescence expression acquires through second reporter gene plasmid, pEGFP-N_3. Fig. 6 depicts fluorescent protein expression in HEK293 cells were transfected with four derived lipoplexes of *p*EGFP-N_3 using optimized co-liposomal formulations at optimized transfection charge ratio (2:1). The visual interpretation of captured images under floid cell image station represents the DNA delivery capacities of four newly generated mixed liposomal formulation at their optimized molar and charge ratios.

3.2.6. Cellular uptake & co-localization study: The efficient plasmid delivery capacities of TIM 6 have further been witnessed through their lipoplex internalization and co-localization studies using fluorescent labeled lipoplex derived from rhodamine-PE inserted liposome of TIM 6 and *p*CMV-βgal DNA. Although the transfection potentials of non viral vectors are directly influenced from many cellular events, internalization of lipoplex is a major determining step in entire plasmid delivery. To look at the uptake proficiency of lipoplex TIM 6, HEK293 cells were treated with *p*CMV-βgal derived lipoplex generated from rhodamine-PE tagged liposome and DNA. After 1 h of lipoplex incubation, cells were analyzed and imaged under confocal microscopy which is presented under Fig. 7 as Rhodamine.

The picture represents the punctuated red fluorescence parts in cell cytoplasm confirms the lipoplex internalization via cellular endocytosis. This analysis was further extended to ascertain whether lipoplexes are avoiding the lysosomal entry or not. The cell lysosomal regions were stained by using green fluorescent marker using lysotracker-green. The image lyso-green in Fig. 7 represents the cell lysosomal area as green punctuates. The merged image was obtained from merging of both rhodamine and lyso-green images, confirms that both characteristic fluorescent punctuates were not co-localized each other and the lipoplexes may not entering in to the lysosomal compartments. Probably, these findings support the higher transfection potentials of co-liposomal formulation derived from TIM 6.

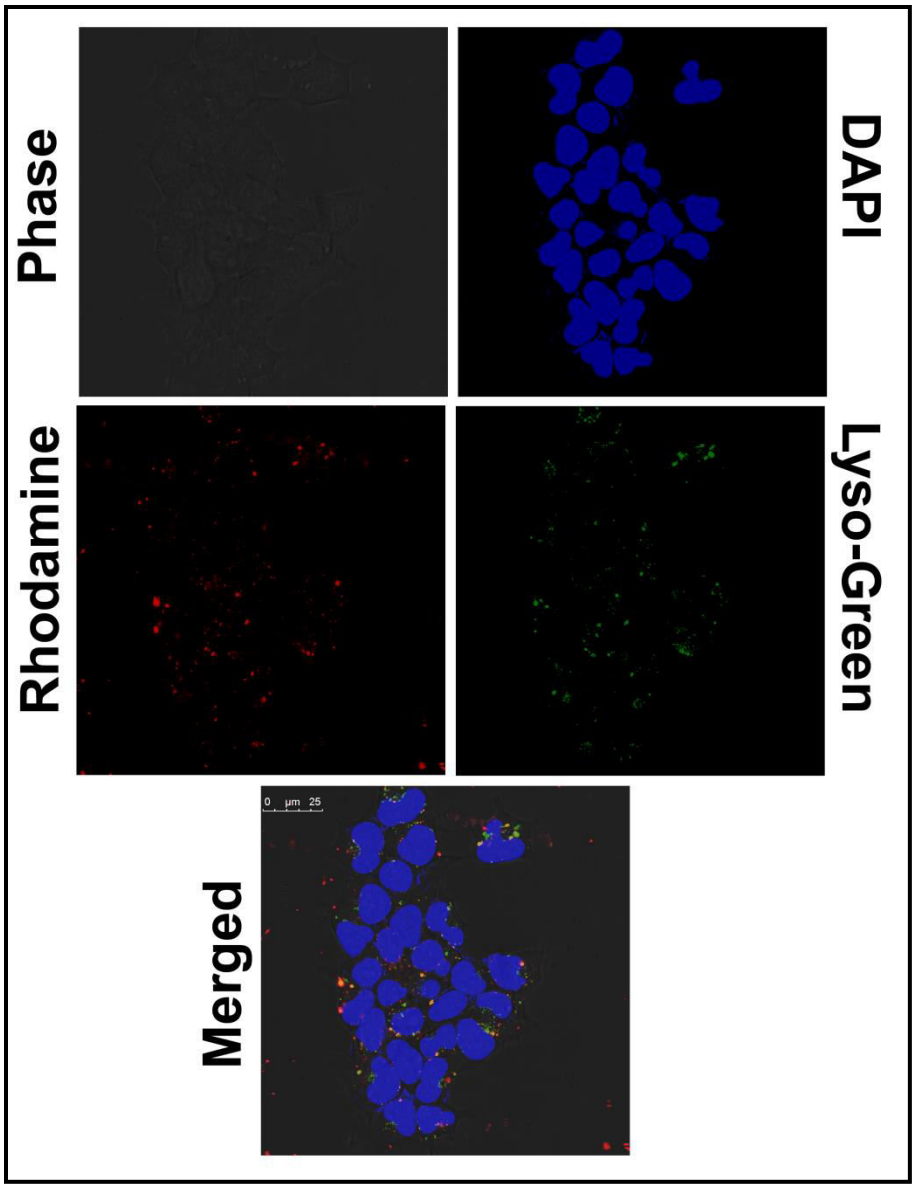

Fig. 7 Confocal laser scanning microscope images for endosomal co-localization of lipoplexes derived from rhodamine-PE labeled **TIM 6** formulation (lipid:DOPE:PE) and *p*CMV-βgal DNA. Acidic compartments and nuclear regions were stained with lysotracker green and DAPI blue respectively in HEK 293 cells.

3.2.7. Cell viability: To evaluate the toxicity profiles of co-liposomal formulations which were shown as efficient reagents for plasmid delivery, MTT cell based assay was performed as described.[55,56] The measured % cell viabilities are represented through Fig. 8, obtained from calorimetric quantification of developed purple

colored granules after 24 h transfection using derived lipoplexes from four dimeric lipid formulations and *p*CMV-βgal plasmid in all the transfection studied cell lines. Complexes were prepared using entire range of charge ratios (2:1, 4:1, 6:1 & 8:1) used in the reporter gene expression and incubated 4 h in 10% FBS+DMEM. The data clearly reveals that no formulation is more toxic than the commercial standard even at higher charge ratios like 8:1. All the formulations developed from novel dimeric tocopherol based lipids and DOPE showed maximum percent cell viabilities towards the studied cell lines.

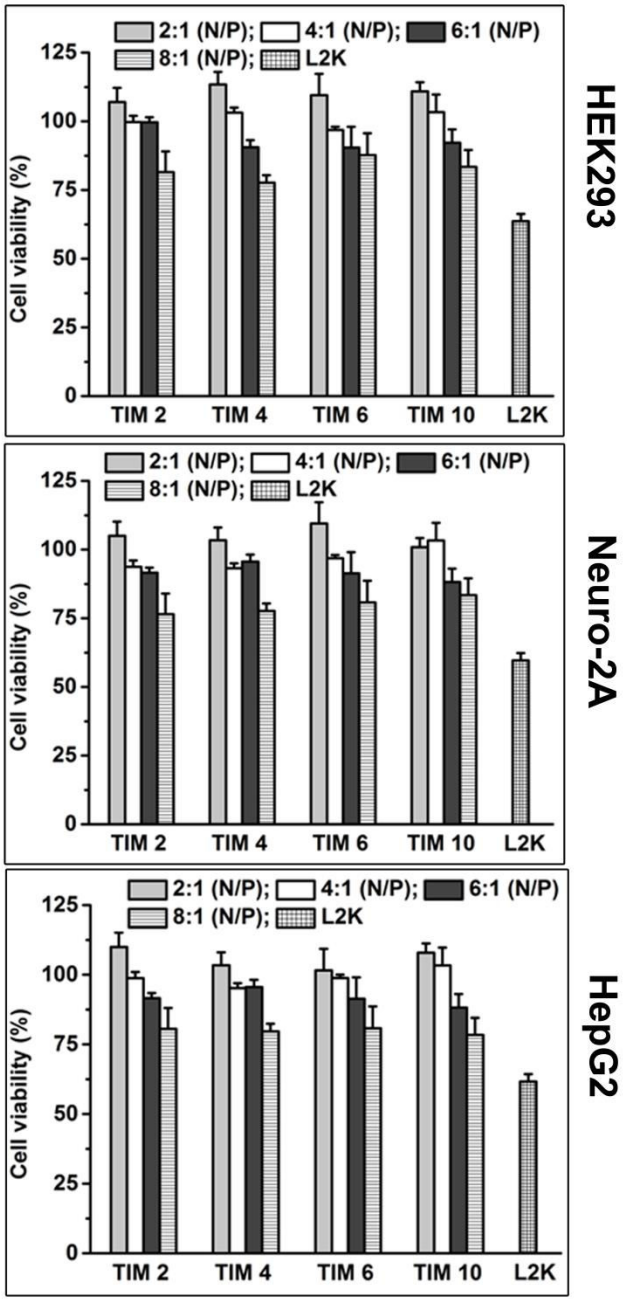

Fig. 8 Cell based MTT assay of lipoplexes derived from four dimeric lipid formulations and *p*CMV-βgal DNA at increasing range of charge ratios (2:1 to 8:1) mentioned in the figure. Complexes were incubated in 10%FBS+DMEM for 4 h, assay was terminated 24 h post transfection.

3.3 CONCLUSIONS:

The newly synthesized delocalisable head group based tocopherol derived dimeric lipids were able to produce small unilamellar vesicles on mixing with helper lipid DOPE and preferred molar ratio was optimized. The DNA binding potentials of these lipid membranes were thoroughly investigated using the techniques like gel electrophoresis and EtBr exclusion assays. The resulted data suggests spacer chain length is the major determining factor to condense the DNA which has led to affect the transfection further. The results derived from transfection of *p*CMV-βgal and *p*EGFP-N_3 plasmids in multiple cell lines demonstrate that the transfection efficiencies of the present series of lipids greatly dependent on the spacer chain length. All the experimental results support that the six methylene aliphatic spacer containing gemini lipid (TIM-6) has shown the maximum potential among the series of lipids studied in delivering plasmid DNA. The superior activity, DNA compaction potentials and least toxicity of these present dimeric lipids can be further explored in *in-vivo* systemic applications.

3.4 EXPERIMENTAL SECTION

3.4.1 Materials: All the reactions and experiments were carried out in this study using the reagents and solvents procured from Sigma, Spectrochem and Alfa Aeser at highest purity and used without further purification. ^{1}H-NMR and ^{13}C-NMR spectra were recorded on a Bruker WM-400 spectrophotometer at 400 MHz and 100 MHz respectively, in $CDCl_3$ with TMS as an internal standard. The chemical shifts were reported in ppm (δ). Mass spectral data were acquired by using a commercial LCQ ion trap mass spectrometer (Thermo Finnigan, SanJose, CA, U.S.) equipped with an ESI source. 3-(4,5-dimethylthiazol-2-yl)-2,5-diphenyl-2H-tetrazolium bromide (MTT) was purchased from Calbiochem (Merck Millipore, Massachusetts, USA), Lipofecatmine 2000 (L2K) were procured from Life Technologies. Lysotracker green and PE (Lissamine Rhodamine B) was a generous gift from IICT (Indian Institute of Chemical Technology, Hyderabad, India). Endotoxin free Plasmid *p*CMV-βgal and *p*EGFP-N_3

were obtained from laboratory stocks and purified using the Nucleo Bond Xtra Midi Plus EF (MACKAREY-NAGEL, Duren, Germany).

3.4.2 Synthesis: Alpha-tocopheryl-2-bromoacetate (Toc-Br): As followed by our previous published protocol[49] 3.5 g of alpha-tocopherol (8.14 mmol) in pyridine (3 mL) and dichloromethane (5 mL) was cooled to 0 ºC on stirring. A solution of 2-bromoacetylbromide (3.27 g, 16.28 mmol) in 5 mL of dichloromethane was added slowly about 10 min to above stirred suspension at 0 ºC and continued to stir further 3 h at same temperature. The contents were diluted using 1 N HCl (50 mL) and extracted in to dichloromethane three times (3 X 20 mL). The fractions were collectively washed with saturated $NaHCO_3$ (2 X 25 mL), water (30 mL) and brine (30 mL). The organic layer was then separated and dried using anhydrous Na_2SO_4, followed by removal of the solvent under vacuum. The resultant residue was purified by column chromatography with 60-120 mesh silica gel using petroleum ether as the eluent. Yield: pale yellow liquid, 4.2 g (7.64 mmol, 93.82%). ^{1}H NMR (500 MHz, $CDCl_3$) δ 4.07 (*s*, 2H), 2.59 (*t*, *J* = 5 Hz, 2H), 2.12 – 1.93 (*m*, 9H), 1.88 – 1.69 (*m*, 2H), 1.58 – 1.04 (*m*, 24H), 0.85 (*m*, 12H). ESI-MS: 551.30 $[M+H]^+$.

Alpha-tocophryl-2-(1H-imidazol-1-yl) acetate (Toc-Im): The suspension resulted from mixing the Toc-Br (1.1 g, 2 mmol), 1H-imidazole (0.2 g, 3 mmol) and K_2CO_3 (0.83 g, 6 mmol) in 6 mL of acetonitrile was refluxed at 80 °C for about 16 h. After getting confirmed with TLC that the reactants were consumed totally, solvent was removed under the reduced pressure and dissolved the crude in 100 mL of water to extract the organic compound in to ethyl acetate with the almost three fractions (3X30 mL) were collectively washed with brine (30 mL) and water. The dissolved residue was obtained by removing the solvent under rota evaporation followed by drying on to the anhydrous sodium sulphate. The resulted crude was loaded on to the 60-120 mesh chromatographic column to isolate the compound having the Rf 0.5 in MeOH: $CHCl_3$ (1:20) which was isolated using the solvent mixture MeOH: $CHCl_3$ (1-2%) as eluent. Yield: colorless solid, 0.86 g (1.6 mmol, 83.98%). ^{1}H NMR (500 MHz, $CDCl_3$) δ 7.39 (*s*, 1H), 6.93-6.90 (*d*, *J* = 15 Hz, 2H), 5.15 (*s*, 2H), 2.68 (*t*, *J* = 6.5 Hz, 2H), 2.25 – 2.14 (*m*,

9H), 1.82 – 1.73 (*m*, 2H), 1.57 – 1.10 (*m*, 24 H), 0.89 – 0.86 (*m*, 12 H). ESI-MS: 539 $[M+H]^+$.

General method for the synthesis of cationic dimeric lipids: A 30 mL screw-top pressure tube was charged with magnetic stir bar, alpha-tocopheryl-2-(1H-imidazol-1-yl) acetate (Toc-Im) (150 mg, 2.78 mmol) and appropriate dibromoalkane (1 mmol) in 3 mL of dry acetonitrile. The contents were refluxed for about 72 h at 80 °C, after the completion of starting materials the reaction mixture was cooled and solvent was evaporated under vacuum. The residue was then washed repeatedly with the $CHCl_3$: EtOAc mixture to yield the pure compound (80-90% yield) which have the R_f ranged from 0.3 - 0.5 in 9:1 $CHCl_3$/MeOH. Four new lipids were synthesized and characterized using ^{1}H-NMR, ^{13}C-NMR and LC-MS analysis. Appropriate analytical and spectroscopic data are given below.

TIM 2: colorless solid, yield (258 mg, 83.93%). ^{1}H NMR (400 MHz, $CDCl_3$) δ 10.02 (*s*, 2H), 8.27 (*s*, 2H), 7.51 (*s*, 2H), 5.59 (*s*, 4H), 5.22 (*s*, 4H), 2.52 (*s*, 4H), 2.04 (*s*, 6H), 1.99 (*d*, *J* = 10Hz, 12H) 1.55 – 1.48 (*m*, 4H), 1.42 – 1.04 (*m*, 48H), 0.87 – 0.83 (*m*, 24H). ^{13}C NMR (101 MHz, $CDCl_3$) δ 165.01, 149.95, 139.95, 138.39, 126.32, 124.79, 123.63, 123.34, 117.73, 75.28, 60.43, 50.25, 48.88, 39.37, 37.40, 32.79, 27.98, 24.81, 24.47, 22.69, 20.80, 19.83, 14.20, 13.38, 12.59, 11.83. LC-MS: Calcd for $[C_{70}H_{112}N_4O_6]^{2+}$/2: 552.43 Found: 552.65.

TIM 4: brownish gummy solid, yield (286 mg, 90.79%). ^{1}H NMR (400 MHz, $CDCl_3$) δ 9.98 (*s*, 2H), 7.90 (*s*, 2H), 7.58 (*s*, 2H), 5.75 (*s*, 4H), 4.49 (*s*, 4H), 2.52 (*t*, *J* = 6.4 Hz, 4H), 2.04 (*d*, *J* = 9.6 Hz, 12H), 1.98 (*s*, 6H), 1.76 – 1.71 (*m*, 4H), 1.55 – 1.05 (*m*, 48H), 0.87 – 0.83 (*m*, 24H). ^{13}C NMR (101 MHz, $CDCl_3$) δ 165.36, 149.86, 139.96, 137.88, 126.44, 124.90, 123.89, 121.90, 117.64, 75.25, 50.24, 39.21, 37.41, 32.72, 30.94, 29.61, 27.98, 25.47, 24.45, 22.64, 21.03, 20.55, 19.69, 13.43, 12.64, 11.82. LC-MS: Calcd for $[C_{72}H_{116}N_4O_6]^{2+}$/2: 566.44 Found: 566.65.

TIM 6: yellowish gummy solid, yield (299 mg, 92.56%). ^{1}H NMR (400 MHz, $CDCl_3$) δ 10.46 (*s*, 2H), 7.63 (*s*, 2H), 7.51 (*s*, 2H), 5.84 (*s*, 4H), 4.41 (*t*, *J* = 6.4 Hz, 4H), 2.56 (*d*, *J* = 5.6Hz, 4H), 2.07 – 2.02 (*m*, 18H), 1.77 – 1.70 (*m*, 8H), 1.53 – 1.05 (*m*, 52H),

0.87 – 0.83 (*m*, 24H). ^{13}C NMR (101 MHz, $CDCl_3$) δ 165.39, 149.87, 140.00, 137.85, 126.44, 124.89, 123.62, 123.26, 122.39, 117.67, 75.26, 50.12, 39.37, 37.42, 32.78, 30.99, 29.16, 27.97, 25.01, 24.81, 22.64, 21.03, 20.55, 19.69, 13.40, 12.60, 11.82. LC-MS: Calcd for $[C_{74}H_{120}N_4O_6]^{2+}/2$: 580.46 Found: 566.90.

TIM 10: yellowish solid, yield (310 mg, 91.17%). ^{1}H NMR (400 MHz, $CDCl_3$) δ 10.26 (*s*, 2H), 7.74 (*s*, 2H), 7.54 (*s*, 2H), 5.97 (*s*, 4H), 4.29 (*t*, *J* = 6.4 Hz, 4H), 2.53 (*t*, *J* = 6 Hz, 4H), 2.04 – 2.00 (*m*, 18H), 1.76 – 1.71 (*m*, 4H), 1.54 – 1.07 (*m*, 60H), 0.87 – 0.83 (*m*, 24H). ^{13}C NMR (101 MHz, $CDCl_3$) δ 165.63, 149.78, 140.01, 137.49, 126.50, 124.97, 123.70, 123.14, 122.84, 117.61, 75.25, 50.09, 49.21, 39.37, 37.44, 32.74, 30.93, 27.97, 26.46, 24.81, 22.74, 21.04, 20.51, 19.75, 13.37, 12.59, 11.79. LC-MS: Calcd for $[C_{78}H_{128}N_4O_6]^{2+}/2$: 608.49 Found: 608.70.

3.4.3 Preparation of dimeric lipid aggregates: All aqueous mixed lipid suspensions were produced from each lipid and various concentrations (1:1, 1.5:1, 2:1. 3:1 & 4:1) of DOPE. The resulted mixed combinations from mixing desired volumes of lipid and DOPE chloroform stacks were exposed to thin flow of moisture free nitrogen gas to get uniform lipid film. These were exposed to drying under high vacuum for about 4 h to remove remaining traces of solvents followed by rehydration using autoclaved water to maintain the final lipid concentration as 1 mM. The samples were allowed to disturb by vortexing after overnight hydration at 4 ºC, and subjected to sonication in an ice bath using a SONICS Vibra cell until get clarity. These optically clear aqueous suspensions were stored at 4 ºC until use.

3.4.4 Gel electrophoresis: Gel electrophoresis is one of the useful assays to visually predict the exact DNA binding capacities of lipid suspensions. In a typical experiment, complexes were prepared using *p*CMV-βgal DNA (0.3 µg/well) with varying ratios (0.5:1, 1:1, 2:1, 4:1, 6:1 & 8:1) of dimeric lipid suspensions. Complexes were incubated for about 30 min in presence of Milli-Q by maintaining the final volume 20 µL, before loading on to 1% agarose gel. The gels were allowed for electrophoresis for a period of 90 min in TAE running buffer at 75 V. The *p*DNA retardation ability of each lipid was assessed by analyzing the gels under fluorescent illumination after fluorescent

staining of *p*DNA with EtBr. Finally, gels were captured under GENESYS imaging system at 900 nm transillumination.

3.4.5 EtBr intercalation assay: The exact lipid/DNA association can also be assessed by a fluorescent based assay, i.e. EtBr displacement assay. The high quantum yields of DNA on association with EtBr could act as a probe to develop lipid/DNA biding interaction by displacing the EtBr from complex while adding the lipid suspension has led to decrease in fluorescent value. Briefly, Hitachi F-7000 fluorescence spectrophotometer was used to measure and record the fluorescent changes at excitation and emission wavelength of 516 nm and 598 nm respectively (slit width 5 nm X 5 nm). Initially, control fluorescence was obtained by mixing 2.3 µg *p*DNA with 0.23 µg EtBr in 20 mM Tris.HCl buffer (pH 7.4). Aliquots of dimeric lipid suspensions correspond to charge ratios were allowed to mix with CT-EtBr:DNA complex and measured the resulted dropdown fluorescence.

3.4.6 Dynamic light scattering and zeta potential measurements: Hydrodynamic sizes of dimeric lipid aggregates and resulted complexes from *p*DNA were measured using a SZ-100 NEXTGEN (HORIBA) instrument equipped with a diode-pumped solid-state laser at λ 532 nm set at 25°C. Prior to the measurements, freshly prepared samples (liposome & lipoplex) were diluted to 800 µL using Milli-Q in a quartz cuvette. Complexes were prepared using 1 µg *p*DNA (*p*CMV-βgal) at 2:1 charge ratio of each co-liposomal formulation. The average of five different measurements which were done in general mode by using the software SZ-100 (HORIBA) was considered.

The zeta potentials resulted from the complexes of dimeric lipid suspensions and *p*CMV-βgal were also measured in the same instrument by using separate zeta cuvette at 25°C with a fixed angle 93°. Complexes were prepared using 5 µg *p*DNA (*p*CMV-βgal) at 0.5:1, 1:1, 2:1, 4:1 and 8:1 charge ratios before 20 min to the each measurement. Samples were diluted to 800 µL of final volume using Milli-Q water and subjected to the instrument. The values were considered from each sample from the average of five different measurements.

3.4.7 Transmission electron microscopy: The morphology and particle size distribution of the dimeric liposomes were examined using a JEOL JEM 2100 Transmission Electron Microscope operated at 120 kV. Briefly, 4 µL of each lipid suspension was dropped on to the surface of standard 300 mesh carbon coated copper grid, and allowed to adsorb for 1 min then excess sample was wicked off using a sterile tissue paper. This was allowed for negative staining by adding 5 µL of 2% uranyl acetate then excess stain was removed after 45 sec. This was followed by air drying at room temperature before the TEM analysis. The images were acquired on a Gatan camera, Digital Micrograph software.

3.4.8 Cell culture: All the adherent cell lines chosen for transfection experiments were taken from laboratory maintained stacks. Cell lines were cultured in 25 cm^2 flasks in 6 mL of DMEM (Dulbecco's Modified Eagles medium, Invitrogen) containing 10% FBS (v/v, Fetal Bovine Serum), 10 mM $NaHCO_3$, 60 µg/mL penicillin, 50 µg/ml streptomycin and 30 µg/ml kanamycin respectively. Cell lines were incubated to grow under 37 °C with the level of 5 % CO_2 and 95 % humidity supply. Cells were passaged at regular intervals whenever proper confluence gets attained. Confluent cells were properly washed with PBS (phosphate buffered saline) and were detached by using 1 % trypsin-EDTA, simultaneously resuspended in to 10% FBS+DMEM.

3.4.9 Plasmids: Two different plasmid vectors were used in this entire study, they are *p*CMV-βgal and pEGFP-N_3 plasmids were encodes b-galactosidase and enhanced green fluorescent protein respectively. Both the plasmids under a CMV promoter were amplified using *Escherichia. coli* DH-5α cells and purified using the NucleoBond® Xtra Midi kit (MACKAREY-Nagel). The purified plasmids were checked for concentration and purity using the NanoDrop 2000 and 1% agarose gel electrophoresis that confirmed the plasmid integrity and quality.

3.4.10 Transfection biology & MTT assay: All the transfections were done using the multiple culture cell lines such as HEK293, Neuro-2A and HepG2. To assess the transfection potentials of new gemini co-liposomal formulations reporter gene transfections were conducted using two different plasmids *p*CMV-βgal and pEGFP-N_3 to

obtain the activity potentials in terms of miller units of β-galactosidase and enhanced green fluorescence protein expression respectively. The assay using *p*CMV-βgal DNA, multiple 96 well plate was seeded with the cells at a density of 10,000/well a day before the transfection. Complexes were prepared using *p*DNA (0.3µg/well) and lipid suspensions at varying charge ratios (mentioned at results) incubated for 30 min in serum less media. These complexes were transferred to cells in 96 well plate after formulating final transfection complex. Cells were allowed to incubate for 4 h at 37 °C with complex media which was replaced with fresh 10% FBS+DMEM. Plates were again placed back in to the incubator to complete 48 h incubation. The assay was terminated and estimated for normalized β-galactosidase activity as described earlier.[59]

The second plasmid reporter gene expressions were analyzed qualitatively using the enhanced green fluorescence expression resulted from the transfection assay using the complexes derived from pEGFP-N_3 plasmid and dimeric lipid suspension. Briefly, in this assay HEK293 cells were seeded on to a 24 well tissue culture plate at a density of 40,000 per well a day before the complex treatment. Complexes of gemini lipid suspensions using pEGFP-N_3 (0.8 µg/well) plasmid at optimized charge ratio (2:1) were incubated with the cells for about 4 h. The complex media was replaced with fresh 10%FBS+DMEM (400 µL/well) after the incubation. The plate was allowed to incubate for further 44 h and the expressed fluorescence was visually analyzed and captured under floid cell imaging station.

To screen the toxicity profiles associated with these novel co-liposomal formulations towards the studied cell lines (HEK293, Neuro-2A and HepG2) a cell based MTT assay was performed using the *p*CMV-βgal derived lipoplexes prepared from increased pattern of charge ratios from 2:1 to 8:1. Initially, the transfection was initiated by following the steps mentioned at β-gal activity and allowed complexes for 4 h incubation after the addition. Complex media was replaced with fresh 10%FBS+DMEM and continued the incubation for 16 h in incubator. MTT [3-(4, 5-dimethylthiazole-2-yl)-2, 5-diphenyltetrazolium bromide] (0.5 mg/mL) solution in serum less DMEM was added and continued the incubation for 3 h in incubator (37 °C, CO_2). This was followed by cell lysis using MeOH:DMSO (v/v, 1:1, 100 µL/well) after 24 h gets completed. The resultant

purple coloured suspensions were read at 540 nm in a multiplate reader, Multiscan spectrum and the untreated cells served as the controls. Results were expressed as percent viability = [$A_{(540)}$treated cells – background/$A_{(540)}$untreated cells – background] X 100.

3.4.11 Uptake & co-localization: The qualitative intracellular trafficking of fluorescent labeled lipoplex was achieved via live cell analysis and imaging in confocal microscopy. Briefly, HEK293 cells were seeded on to a two chambered coverglass (Nunc™ Lab-Tek™) 50,000 cells/chamber a day prior to transfection. Lipoplexes were prepared using *p*CMV-βgal DNA (1 µg/chamber) complexing with fluorescent (rhodamine-PE) labelled dimeric liposomes of TIM 6 in serum free DMEM. After 30 min incubation at room temperature the lipid/DNA complex was formulated to final transfection complex to be in 10%FBS+DMEM was transferred to coverglass chambers in duplicates and allowed 1 h incubation in incubator (37 ºC, CO_2). The fluorescent reagents for cell counter parts like DAPI (blue, nucleus) and Lysotracker (green, lysosome) were mixed in required quantity in one aliquot of serum+DMEM and transferred to each chamber of coverglass after incubation of complex. This was followed by 30 min incubation (37 ºC, CO_2) and then analyzed under confocal laser scanning microscope (Leica TCS S52) at various emission collection wavelengths corresponds to three different fluorescent probes as described before.[60] Localisation of the fluorescent labels red (lipid), green (Lysotracker) and blue (DAPI) were analysed using LAS X imaging platform to determine the location of lipoplexes with respect to the nucleus and lysosomes.

3.5 REFERENCES

1. Jones, C. H.; Chen, C. K.; Ravikrishnan, A.; Rane, S.; Pfeifer, B. A. *Mol. Pharm.* **2013**, *10*(11), 4082.
2. Thomas, C. E.; Ehrhardt, A.; Kay, M. A. *Nat Rev Gene.* **2003**, *4*(5), 346.
3. Karmali, P. P.; Chaudhuri, A. *Med Res Rev*, **2007**, *27*, 696.
4. Menger, F. M.; Keiper, J. S. *Angew Chem Int Ed*, **2000**, *39*, 1906.
5. Bhattacharya, S. and Biswas, J. *Langmuir*, **2010**, *26*, 4642.

6. Martin, B.; Sainlos, M.; Aissaoui, A.; Oudrhiri, N.; Hauchecorne, M.; Vigneron, J. P.; Lehn, J. M. and Lehn, P. *Curr. Pharm. Des.* **2005**, *11*, 375.
7. Behr, J. P. *Chimia Int J Chem*, **1997**, *51*, 34.
8. Bhattacharya, S.; Bajaj, A. *Chem Comm*, **2009**, *31*, 4632.
9. Zhi, D. F.; Zhang, S.; Wang, B.; Zhao, Y.; Yang, B. and Yu, S. *Bioconjugate Chem.* **2010**, *21*, 563.
10. Aissaoui, A.; Martin, B.; Kan, E.; Oudrhiri, N.; Hauchecorne, M.; Vigneron, J. P.; Lehn, J. M. and Lehn, P. *J. Med. Chem.* **2004**, *47*, 5210.
11. Bajaj, A.; Kondaiah, P. and Bhattacharya, S. *Bioconjugate Chem.* **2008**, *19*, 1640.
12. Dileep, P. V. and Bhattacharya, S. *Bioconjugate Chem*. **2004**, *15*, 508.
13. Bajaj, A.; Kondaiah, P. and Bhattacharya, S. *Bioconjugate Chem.* **2007**, *18*, 1537.
14. Bajaj, A.; Mishra, S. K.; Kondaiah, P. and Bhattacharya, S. *Biochim. Biophys. Acta*, **2008**, *1778*, 1222.
15. Smisterova, J.; Wagenaar, A.; Stuart, M. C. A.; Polushkin, E.; Ten Brinke, G.; Hulst, R.; Engberts, J. B. F. N. and Hoekstra, D. *J. Biol. Chem.* **2001**, *276*, 47615.
16. Ghosh, Y. K.; Visweswariah, S. S. and Bhattacharya, S. *FEBS Lett.* **2000**, *473*, 341.
17. Zhi, D.; Zhang, S.; Cui, S.; Zhao, Y.; Wang, Y. and Zhao, D. *Bioconjugate Chem.* **2013**, *24*, 487.
18. Bajaj, A.; Kondaiah, P. and Bhattacharya, S. *J. Med. Chem.* **2008**, *51*, 2533.
19. Van Der Woude, I.; Wagenaar, A.; Meekel, A. A.; Ter Beest, M. B.; Ruiters, M. H.; Engberts, J. B.; Hoekstra, D. *Proc Natl Acad Sci,* **1997**, *94*,1160.
20. Parvizi-Bahktar, P.; Mendez-Campos, J.; Raju, L.; Khalique, N. A.; Jubeli, E.; Larsen, H.; Nicholson, D.; Pungente, M. D.; Fyles, T. M. *Org Biomol Chem*, **2016**, *14*, 3080.
21. Kumar, K.; Barrán-Berdón, A. L.; Datta, S.; Muñoz-Úbeda, M.; Aicart-Ramos, C.; Kondaiah, P.; Junquera, E.; Bhattacharya, S.; Aicart, E. *J Mater Chem B*, **2015**, *3*, 1495.
22. Misra, S. K.; Muñoz-Úbeda, M.; Datta, S.; Barrán-Berdón, A. L.; Aicart-Ramos, C.; Castro-Hartmann, P.; Kondaiah, P.; Junquera, E.; Bhattacharya, S.; Aicart, E. *Biomacromolecules*, **2013**, *14*, 3951.
23. Bhattacharya, S. and Bajaj, A. *Chem. Commun.* **2009**, 4632.

24. Bajaj, A.; Kondaiah, P. and Bhattacharya, S. *Biomacromolecules*, **2008**, *9*, 991.
25. Bajaj, A.; Kondiah, P. and Bhattacharya, S. *J. Med. Chem.* **2007**, *50*, 2432.
26. Biswas, J.; Mishra, S. K.; Kondaiah, P. and Bhattacharya, S. *Org. Biomol. Chem.* **2011**, *9*, 4600.
27. Munoz-ubeda, M.; Misra, S. K.; Barran-Berdon, A. L.; Aicart-Ramos, C.; Sierra, M. B.; Biswas, J.; Kondaiah, P.; Junquera, E.; Bhattacharya, S. and Aicart, E.; *J. Am. Chem. Soc.*, **2011**, *133*, 18014.
28. Misra, S. K.; Naz, S.; Kondaiah, P. and Bhattacharya, S. *Biomaterials*, **2014**, *35*, 1334.
29. Bombelli, C.; Faggioli, F.; Luciani, P.; Mancini, G. and Sacco, M. G. *J. Med. Chem.*, **2005**, *48*, 5378.
30. Rosenzweig, H. S.; Rakhmanova, V. A. and MacDonald, R. C. *Bioconjugate Chem.*, **2001**, *12*, 258.
31. Chien, P. Y.; Wang, J.; Carbonaro, D.; Lei, S.; Miller, B.; Sheikh, S.; Ali, S. M.; Ahmad, M. U. and Ahmad, I. *Cancer Gene Ther.*, **2005**, *12*, 321.
32. Damen, M.; Aarbiou, J.; van Dongen, S. F.; Buijs- Offerman, R. M.; Spijkers, P. P.; van den Heuvel, M.; Kvashnina, K.; Nolte, R. J.; Scholte, B. J. and Feiters, M. C. *J. Controlled Release*, **2010**, *145*, 33.
33. Zhao, Y. N.; Qureshi, F.; Zhang, S. B.; Cui, S. H.; Wang, B.; Chen, H. Y.; Lv, H. T.; Zhang, S.-F. and Huang, L. *J. Mater. Chem. B*, **2014**, *2*, 2920.
34. Sharma, V. D.; Aifuwa, E. O.; Heiney, P. A. and Ilies, M. A. *Biomaterials*, **2013**, *34*, 6906.
35. Wettig, S. D.; Verrall, R. E. and Foldvari, M. *Curr. Gene Ther.,* **2008**, *8*, 9.
36. Wettig, S. D.; Badea, I.; Donkuru, M.; Verrall, R. E. and Foldvari, M. *J. Gene Med.*, **2007**, *9*, 649.
37. Badea, I.; Verrall, R.; Baca-Estrada, M.; Tikoo, S.; Rosenberg, A.; Kumar, P. and Foldvari, M. *J. Gene Med.*, **2005**, *7*, 1200.
38. Donkuru, M.; Wettig, S. D.; Verrall, R. E.; Badea, I. and Foldvari, M. *J. Mater. Chem.*, **2012**, *22*, 6232
39. Uno, Y.; Piao, W.; Miyata, K.; Nishina, K.; Mizusawa, H. and Yokota, T. *Hum. Gene Ther.*, **2011**, *22*, 711.

40. Noh, S. M.; Han, S. E.; Shim, G.; Lee, K. E.; Kim, C. W.; Han, S. S.; Choi, Y.; Kim, Y. K.; Kim, W. K. and Oh, Y. K. *Biomaterials*, **2011**, *32*, 849.
41. Kumar, K.; Maiti, B.; Kondaiah, P. Bhattacharya, S. *Mol Pharm*, **2014**, *12*, 351.
42. Kedika, B.; Patri, S. V. *Mol Pharm*, **2012**, *9*, 1146.
43. Bajaj, A.; Kondaiah, P.; Bhattacharya, S. *Bioconjugate Chem*, **2007**, *18*, 1537.
44. Bajaj, A.; Kondaiah, P.; Bhattacharya, S. *J Med Chem*, **2008**, *51*, 2533.
45. Fasbender, A.; Marshall, J.; Moninger, T. O.; Grunst, T.; Cheng, S.; Welsh, M. J. *Gene Ther*, **1997**, *4*.
46. Du, Z.; Munye, M. M.; Tagalakis, A. D.; Manunta, M. D.; Hart, S. L.; *Sci Rep*, **2014**, *4*.
47. Mochizuki, S.; Kanegae, N.; Nishina, K.; Kamikawa, Y.; Koiwai, K.; Masunaga, H.; Sakurai, K. *(BBA)-Biomembranes*, **2013**, *1828*, 412.
48. Cheng, X.; Lee, R. J. *Adv Drug Deliv Rev*, **2016**, *99*, 129.
49. Gosangi, M.; Mujahid, T. Y.; Gopal, V.; Patri, S. V. *Org Biomol Chem*, **2016**, *14*, 6857.
50. Dua, J. S.; Rana, A. C.; Bhandari, A. K. *Int J Pharm Stud Res*, **2012**, *3*, 14.
51. Chandrashekhar, V.; Srujan, M.; Prabhakar, R.; Rakesh Reddy, C.; Sreedhar, B.; Kiran, R.; Sanjit, K.; Chaudhuri, A. *Bioconjug Chem,* **2011***, 22*, 497.
52. Zuhorn, I. S.; Visser, W. H.; Bakowsky, U.; Engberts, J. B.; Hoekstra, D. *(BBA)-Biomembranes*, **2002**, *1560*, 25.
53. Stocker, A.; Zimmer, S.; Spycher, S. E.; Azzi, A. *IUBMB life*, **1999**, *48*, 49.
54. Uno, Y.; Piao, W.; Miyata, K.; Nishina, K.; Mizusawa, H.; Yokota, T. *Hum Gene Ther*, **2010**, *22*, 711.
55. Lv, H.; Zhang, S.; Wang, B.; Cui, S.; Yan, J. *J. Control. Release.* **2006**, *114*, 100.
56. Hansen, M. B.; Nielsen, S. E.; Berg, K. *J. Immunol Methods,* **1989**, *119***,** 203.
57. Gopal, V.; Xavier, J.; Kamal, M. Z.; Govindarajan, S.; Takafuji, M.; Soga, S.; Ueno, T.; Ihara, H.; Rao, N. M. *Bioconjug Chem*, **2011**, *22*, 2244.
58. Meka, R. R.; Godeshala, S.; Marepally, S.; Thorat, K.; Rachamalla, H. K. R.; Dhayani, A.; Hiwale, A.; Banerjee, R.; Chaudhuri, A.; Vemula, P. K. *RSC Advances*, **2016**, *6*, 77841.

Chapter 4

●●●●

Design, Synthesis and Transfection Efficiencies of Novel 1, 2, 3-Triazolium Cation Head Group Based Cationic Lipids

4.1 INTRODUCTION

The cutting edge technology of therapeutic gene delivery and expression has long been dominated by the cationic lipid based non viral vectors.[1,2] The ease in construction and characterization of such cationic lipids has added to many intensive investigations for

optimizing their performance.[3,4] To date, cationic lipids form the non viral vector of choice for clinical trials, worldwide. Nevertheless, the many cytofectins reported so far, still needs modification to address the barriers in regards to direct *in vivo* transfection.[5] In short, the preferred structure promoting stable transfection still remains unresolved.[6] This has inspired the introduction of novel structural motifs in the lipid backbone with a view to excel the current transfection standards. Majority of cationic lipids addressed in various studies,[7] suggested that the common structural back bone of lipid consists of following basic building blocks; head group in polar form exposed to aqueous environment, hydrophobic back bone lying in the non-polar milieu of liposome and both are connected together either directly with covalent bond or by a functional unit called linker.

Great efforts have been witnessed to increase the transfection efficiencies of non-viral cationic lipids through the systematic modification of individual domains, mainly head group and hydrophobic region.[8,9] In many of recent successful outcomes in the field, the head group has drawn lot of attention due to its crucial roles in self aggregation to develop unilamellar vesicles and charge-charge electrostatic interaction with DNA while complexation. In fact, the self aggregation and DNA complexation are the two strong influencing characteristics of a head group of lipid by providing positive charge potentials and close proximity with DNA in lipoplex assembly lead to determine the efficiency of transfection.[10,11] Localized positive charge based mono cationic lipids and gemini lipids have thoroughly been used for different investigations to generate better gene delivery reagents,[12] but head groups with delocalized positive charge have not been studied extensively.

Ever since Solodin et al.[13] in 1995 reported the use of delocalisable cationic charge in the head group of cationic lipid (DOTIM) in liposomal mediated gene delivery, interest of research has been shifted to focus in using delocalized cation instead of unshared positive charge in head group. The delocalized cation head groups due to their soft cationic nature provide smart wrapping of DNA and low toxicities.[14] Consequently, the usage of heterocyclic functionalities such as pyridinium[15,16] and imidazolium[17,18] as head groups were provided better transfection efficiencies with low toxicity due to their

delocalizable cationic charge. This inspired us to find better heterocyclic constructs as head groups for better potentials.

Since the most of the reports have been used imidazolium and pyridinium aromatic heterocyclic delocalisable cations to produce better cytofectins through the structure activity investigation which reinstigate to establish more such constructs to produce better cytofectins and also would be helpful to understand the various structure related effects on transfection. Towards this 1, 2, 3-triazolium cation have been chosen to use as cationic head group in lipid back bone and studied activity potentials from the synthesized lipids and explored various structural influences on transfection properties.

4.2 RESULTS AND DISCUSSIONS

4.2.1 SECTION A

"Novel 1, 2, 3-Triazolium Based Dicationic Amphiphiles Synthesized by using Click-chemistry Approach for Efficient Plasmid Delivery"

The present work illustrates, screening of DNA transfection potentials of novel dicationic amphiphiles, in which head group of quaternary ammonium cation of cationic lipids was conjugated to delocalizable cation of a heterocyclic ring. The delocalizable cation is generated using a construct called 1, 4 disubstituted 1, 2, 3-triazole is synthesized by following the azide-alkynes Huisgen 1, 3 dipolar cycloaddition. This is an important reaction of a well known strategy of "Click chemistry"[19,20] and it was followed to couple acetylene and azide functions using established protocol of copper catalysed click reaction to produce 1, 2, 3-triazole intermediate in high yields.[21] This five membered 1, 2, 3 triazole heterocyclic aromatic ring has unique properties like stability towards acidic and basic environments as well as viable to neither oxidative nor reductive hydrolysis.[24] Because of these characteristics 1, 2, 3 triazole group has been used as a core ring in many biologically potent libraries and also as a linker in cationic amphiphilic vector design[22,23] As there are no reports on 1, 2, 3-triazolium as a head group for cationic lipid mediated gene delivery like pyridinium and imidazolium and considering

the above mentioned features of this group, hereby we report design, synthesis and biological evaluation of novel 1, 2, 3-triazolium based dicationic amphiphiles.

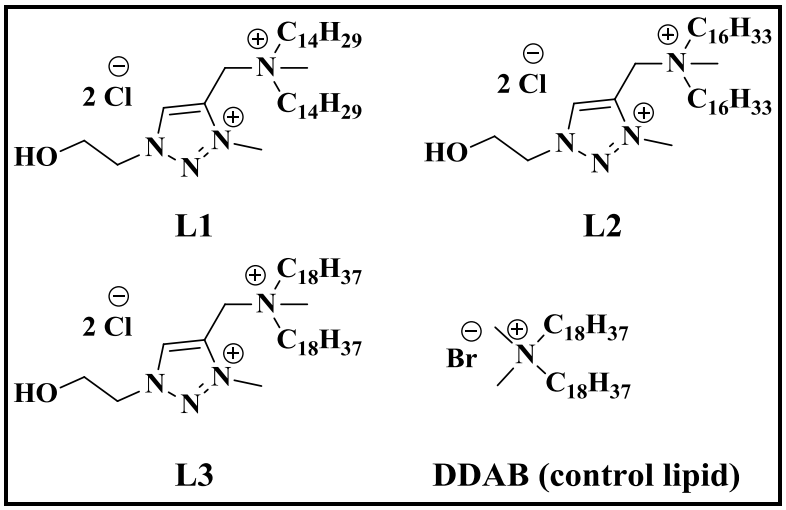

Fig. 1 Molecular structure of dicationic lipids and control lipid used in the study

4.2.1.1 Chemistry: A series of dicationic amphiphiles (L1, L2 and L3) were synthesized. These new lipids consists a head group of simple quaternary ammonium ion which is connected to aliphatic alkyl chains back bone (C14 orC16 or C18). Each lipid is individually further connected to a delocalizable cation having a 2-hydroxy ethyl chain as a substitution. Initially, acetylene derivatives of corresponding tertiary amines (1a-c) were obtained in high yields (approximately 90%) by alkylation of propargyl amine using respective alkyl bromides. The corresponding acetylene derivatives of the tertiary amine was then coupled with 2-azidoethanol to yield the click adduct via Copper (I) catalyzed 1, 3 dipolar cyclo addition. Finally, the obtained click adduct (2a-c) was allowed to quaternize using excess methyl iodide in a sealed tube under reflux for about 7 days and resulted 1, 2, 3-triazolium salts in ~50 % yield. This prolonged time for quaternization reaction to yield dication may be due to weak basic character of 1, 2, 3 triazole. Whereas the poor yields of iodide salts may be expected due to the elimination of water molecule (dehydration) from 2-hydroxy ethyl 1, 2, 3-triazole in presence of residual copper (Cu) at reflux temperature. The obtained dicationic iodide salts were subjected to chloride ion exchange to replace the iodide counter ion with chloride ion to afford titled lipids. All the

novel lipids and intermediates were purified and characterized using spectral (^{1}H-NMR, ESI-MS) and elemental analytical data.

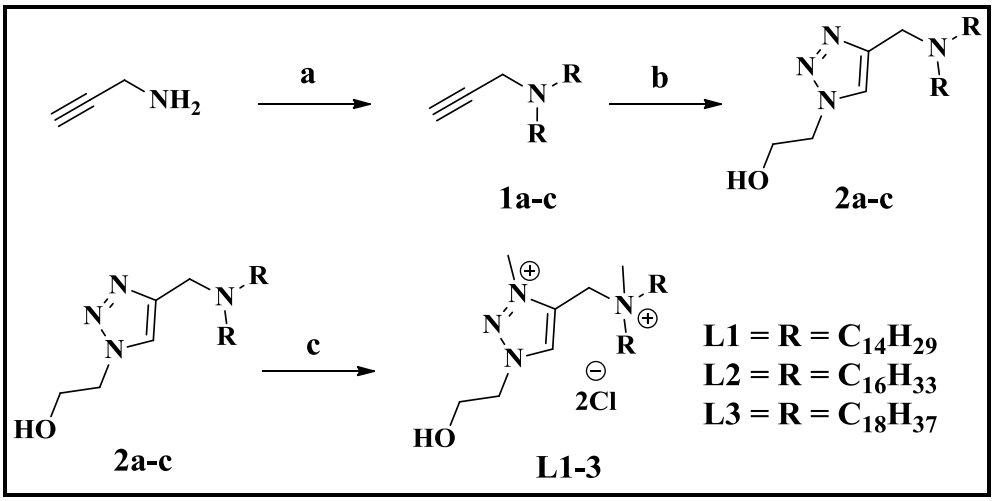

Scheme 1 Synthetic route and molecular structures of dicationic lipids.

Reagents & Conditions: a) Alkyl bromide, K_2CO_3, acetonitrile, 80 ºC, 48 h; b) 2-azidoethanol, $CuSO_4.5H_2O$, sodium ascorbate, *tert*-BuOH:H_2O, RT, 16 h; c) MeI, acetonitrile, sealed tube, 80 ºC, 72 h, amberlite anion exchange resin.

Small unilamellar vesicles were prepared by mixing the dicationic amphiphiles with one of the well known neutral co-lipid (DOPE) for enhanced transfection results in an equimolar ratio (1:1) by following the lipid hydration technique as described in previous.[25] These aqueous dispersions were stable and clear up to three months by storing at 4 ºC. Following the formulation, liposomal vesicles were characterized in terms of size, surface potential and DNA binding.

4.2.1.2 Physicochemical characterization of the particles (lipid: DOPE) and complexes (lipid: DOPE:DNA): The mean size of the dispersed vesicles in aqueous medium was determined by dynamic light scattering. The technique which involves a photon correlation spectroscopy will produce the value of hydrodynamic diameter of the suspended particles. The data shows that relative hydrodynamic diameters of liposomes of L1, L2 and L3 as 150 nm, 113 nm and 54.7 nm respectively. This clearly represents a

pattern of decrement in size from L1-L3 (Fig. 2A). To be specific, the vesicular diameter is decreasing with respect to the length of the hydrophobic long chain present in lipid back bone, in proportion. In the literature, Liang C. H. et al has reported this trend of shorter alkyl chain comprising cationic lipids producing larger hydrodynamic sphere owing to the higher surface potential and vice versa.[26] Importantly, the size of the lipoplexes generated from these lipids could also be correlated. At 1:1 N/P charge ratio (TE optimized ratio) the size of the lipoplexes increased at an average ratio of 2/3 rd diameter, with respect to the corresponding liposome. This indicates an optimal condensation of the DNA molecule and which might be facilitated the maximum transfection efficiency at 1:1 charge ratio.

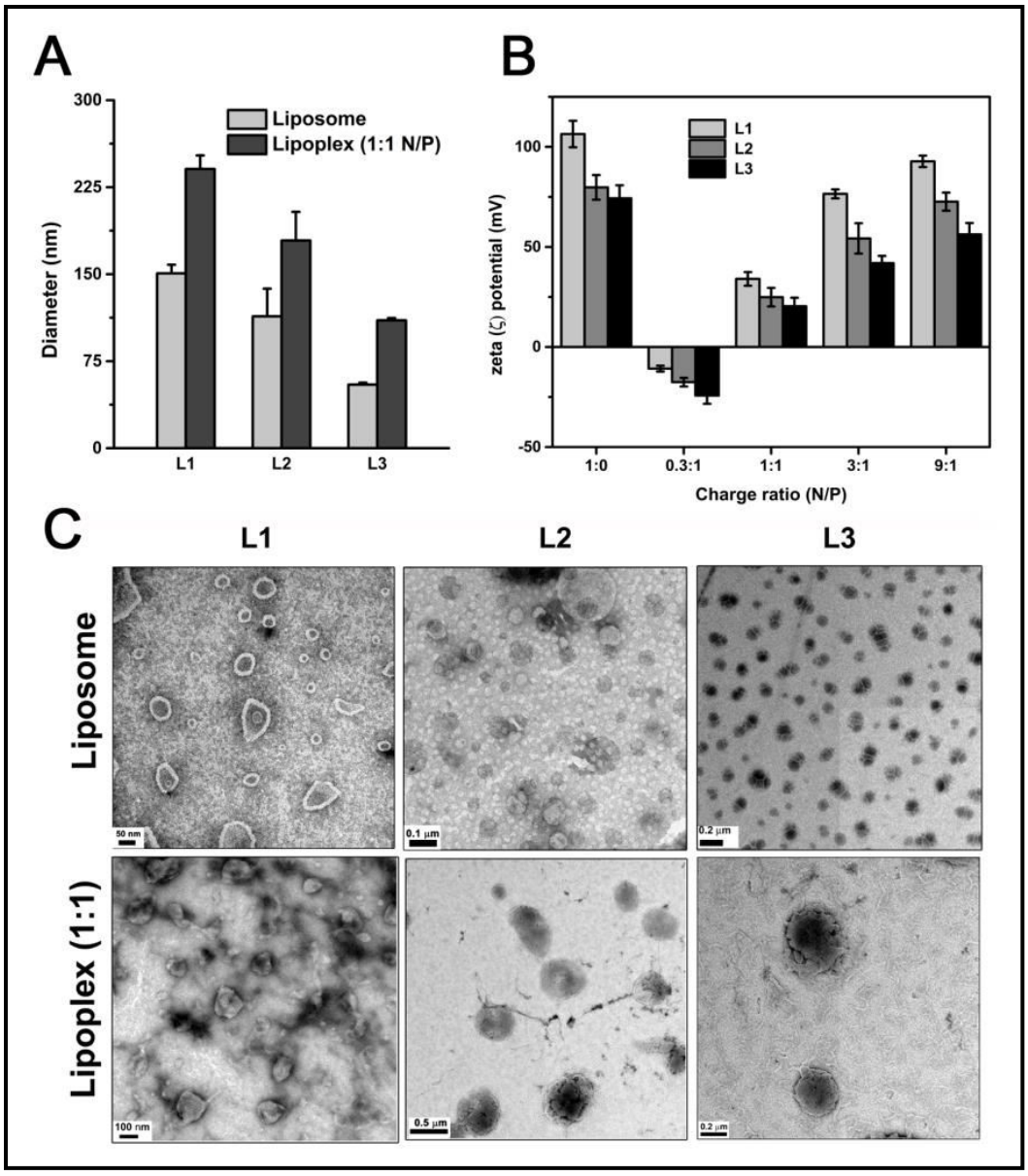

Fig. 2 A) Hydrodynamic diameter (nm) of the lipid vesicles (light gray) and lipid: DNA complexes (dark gray) at 1:1 N/P charge ratio using 5 µg pCMV-βgal DNA were measured by dynamic light scattering method. B) zeta-potentials of lipid formulations (1:0, L1-light gray, L2-gray and L3-black) and lipoplexes were prepared from lipid: DNA at varying N/P charge ratios (0.3:1-9:1) using constant amount of *p*CMV-βgal DNA (10 µg) in Milli-Q. C) Representative transmission electron microscopy images of negatively stained lipid: DOPE vesicles and liposome: DNA complexes at 1:1 N/P ratio.

To further confirm the size and to reveal the supra molecular structure of these vesicles and complexes, we have attempted the transmission electron microscopic analysis by using negative staining. Fig. 2C depicts that the liposomes were observed as compacted vesicles with distinct boundary. The corresponding complexes formed at the optimized transfection ratio also revealed a similar vesicular nature with irregular margin.

Significantly, zeta potential is one of the parameters used to determine the stability of the formulated complexes with DNA, and is mostly in proportion with the transfection potential. Fig. 2B represents the zeta potential of liposomes (1:0) and lipoplexes at different charge ratios (0.3:1, 1:1, 3:1 and 9:1). The negative zeta potential observed at 0.3:1 ratio got transformed to a positive value at the next higher 1:1 ratio, most probably following complete charge neutralization of the DNA.

4.2.1.3 Gel electrophoresis: The extent of DNA binding is a significant parameter to elucidate the transfection potential of these dicationic lipid formulations. To investigate the DNA binding capacity, a conventional gel electrophoresis was performed as a function of lipid: DNA charge ratio (N/P) as depicted in Fig. 3. The Fig. 3 confirms that the mobility of DNA was optimally retarded with all the lipid complexes, at 1:1 and 3:1 N/P charge ratios. It is also understood that all three lipids could retain the DNA in the wells at least 50-60 % at 1:1 charge ratio and 80 - 90 % of DNA at 3:1 charge ratio. Comparatively, at higher ratio 9:1 all the three lipids were capable of inhibiting completely the electrophoretic mobility of plasmid DNA. The results are in corroboration with the pattern of zeta potentials as described in the previous section. Thus the lipoplexes of lipids L1, L2 and L3 having optimal lipid-DNA interactions at 1:1 and 3:1 charge ratios may effectively facilitate the release of DNA into cytoplasm after the delivery. This is evident in the following reporter gene expression data.

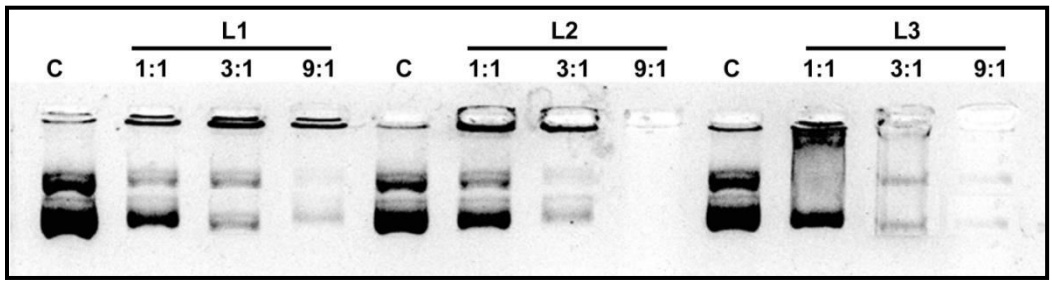

Fig. 3 DNA binding patterns of dicationic liposome formulations (L1, L2 and L3) on 1% agarose gel electrophoresis. L1, L2 and L3 represents liposome formulations prepared from lipid: DOPE at 1:1 molar ratio. Lipoplexes were prepared in 20 μL of 0.5X PBS by mixing the constant amount of pCMV-βgal DNA (0.4 μg/well) with varying lipid charge ratios (1:1, 3:1& 9:1) mentioned on top of each panel. DNA alone, depicted as "C" on each panel served as control.

4.2.1.4 Transfection biology: The relative transfection efficiencies of DOPE mixed liposomal formulations of lipids L1, L2 and L3 in different cell lines (HEK-293, HepG2, CHO and B16F10) across the N/P charge ratios (0.3:1 to 9:1) were analyzed using β-galactosidase reporter gene expression. Fig. 4 depicts the transfection efficiencies of the three lipid formulations (L1, L2 and L3) and it demonstrates that the maximum transfection is observed in case of all the three lipids at 1:1 and 3:1 charge ratios, irrespective of the cell lines studied. The maximum efficiencies of these lipid formulations at specified charge ratios have clearly been supported by the facts estimated in previous sections such as DNA binding, zeta potentials of lipid:DNA complexes and hydrodynamic sizes of DNA derived complexes.

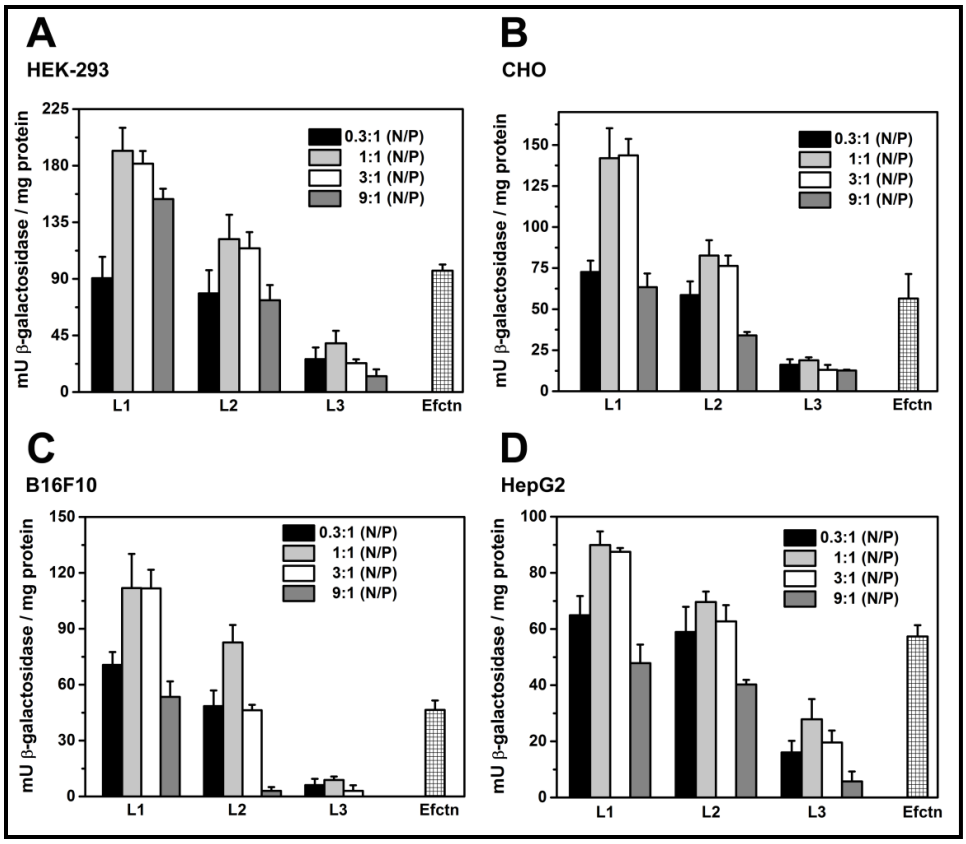

Fig. 4 *Transient* transfection *in vitro*: Graph depicts transfection efficiencies of dicationic lipid formulations (L1, L2 & L3) in four different cell lines A) HEK-293; B) CHO; C) B16F10; D) HepG2. The lipoplexes were prepared at varying charge ratios (N/P) of lipids 0.3:1 (black); 1:1 (light gray); 3:1 (white); 9:1 (gray) using constant amount of pCMV-βgal DNA (0.3μg/well). Complexes were incubated for 4 h in presence of serum less DMEM and the assay was performed 48 h post transfection. Representative data presents normalized miller units of β-galactosidase/mg protein and was obtained from an average triplicate of three individual experiments. (Effectene: Efctn).

Further, to investigate the effect of the designed construct (1, 2, 3-triazolium), which confer additional delocalized cationic charge to the unshared positive charge present on simple quaternary ammonium head group region, an interesting study was endeavored. For this purpose, an independent lipid that resembles the synthesized dicationic lipid in its structure except for the additional 1, 2, 3-triazolium group in the head group region is required. The commercially available cationic lipid, DDAB can fit

in as the required standard when compared along the rest of the synthesized lipids in the β-gal transfection activity profile.[27,28] Additionally, the transfection reagent effectene was used as the positive control (Efctn). Here again the charge ratio 1:1 has been considered due to its maximum activity at minimal charge ratio for reporter gene and the average of triplicate transfection results in the four different cell lines HEK-293, HepG2, CHO and B16F10in presence of 10% serum were depicted in Fig. 5. It becomes clear from the representative graph that the lipid L1 is the most effective in terms of transfection potential in all the studied cell lines,. Lipid L1 with the chain length C14 is on an average, two fold better active than both the control lipid DDAB and the commercial transfection reagent, effectene. Whereas lipid L3 with C18 chain as anchoring group was found be to least active among the studied lipids. The activity of lipid L2 having the chain length of C16 is found to be on par with the activity of control lipid and effectene. Here, the specificity of cell lines also plays a role in deciding the transfection potential of the synthesized lipids. In fact, the Fig. 5 also illustrate the cell line specific activity and shows that the activity of lipid L1 is maximum in HEK-293 cell lines then follows the order of activity in CHO and then in B16F10 cell lines and least active in HepG2 cell lines.

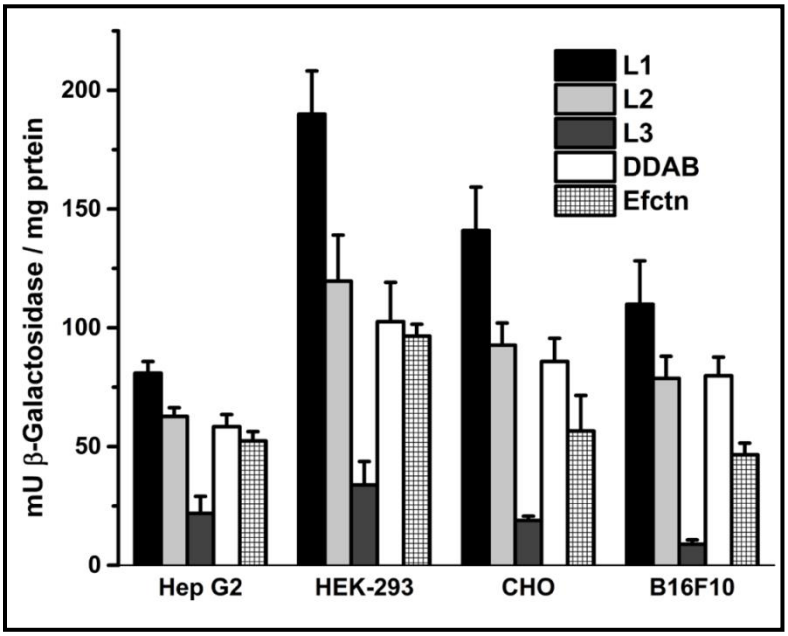

Fig. 5 Relative efficiencies of transfection of *p*CMV-βgal DNA in HepG2, HEK-293, CHO and B16F10 cell lines using three lipid formulations (L1, L2 & L3) at 1:1 N/P charge ratio. The cells were incubated with the complexes in 10% FBS+DMEM for 4 h and the assay was terminated after 48 h of complex addition. Efctn (effectene) and DDAB: DOPE (1:1) formulations were included as controls.

In the present investigation, as the length of the alkyl chain is varying from C14 to C16 to C18 of the dicationic lipid formulations, transfection activities were observed to be decreased. In fact many reports established a clear connection between the length of hydrophobic chain and the transfection efficiency. It is described that the shorter alkyl chain in hydrophobic backbone increases the fluidity of the bilayer, and helps in higher intermembrane transfer rate, results in potential disruption of the endosome and consequently enhanced DNA release.[26] In addition, the interesting outcome of this study describes the least activity of lipid L3 among the lipids studied and also compared with the control lipid which has same length of backbone. In spite of the associated features like delocalized cation along with hydroxyl functionality in the head group of L3, inferior activity of L3 is accounted in terms of plasmid delivery. This particular observation was being supported by the fact which has already been discussed in earlier investigation[29] on the basis of surface hydration of lipid membranes. Surface hydration is one of the parameters to determine the efficiency of liposome-DNA complexation has further led to the understanding of transfection patterns. The complexation of lipid-DNA molecules is mainly due to the electrostatic interaction between the head group of cationic lipid and phosphate backbone of plasmid DNA. According to the statements of Bajaj et al. (2008) as the surface hydration of a cationic lipid increases, the transfection efficiency will decrease. Probably, the combination of dicationic and hydroxyl functionality in the head group of lipid L3 might be responsible for its higher surface hydration in comparison to mono cationic DDAB lipid. This could be a reason behind the lower transfection activity of lipid L3 in spite of having the same back bone as present in the control lipid DDAB.

In addition, the results obtained from β-gal reporter gene expression were further supported by using another plasmid DNA in terms of fluorescent protein expression.

Subsequently, the Complexes were prepared using pEGFP-N_3 plasmid (0.8 µg) at optimized N/P charge ratio (1:1). The cells both HEK-293 and CHO were incubated with formulated lipoplexes in 10% FBS+DMEM for 4 h. The green fluorescent expression was visually observed under the fluorescent microscope, images were captured 48 h of post transfection for the qualitative analysis of gene expression. The representative florescent microscopic images demonstrated through Fig. 6, clearly depicts that the fluorescent gene expression obtained from HEK293 cells were relatively higher than the expression obtained from CHO cell lines. The GFP expression obtained using the lipids L1, L2 and L3 in comparison with the control lipid DDAB and commercial cytofectin Efctn followed a rank order indicated as L1 > L2 ≈ DDAB > Efctn > L3. These results are well consistent with the quantitative transfection data obtained from β-galactosidase gene expression.

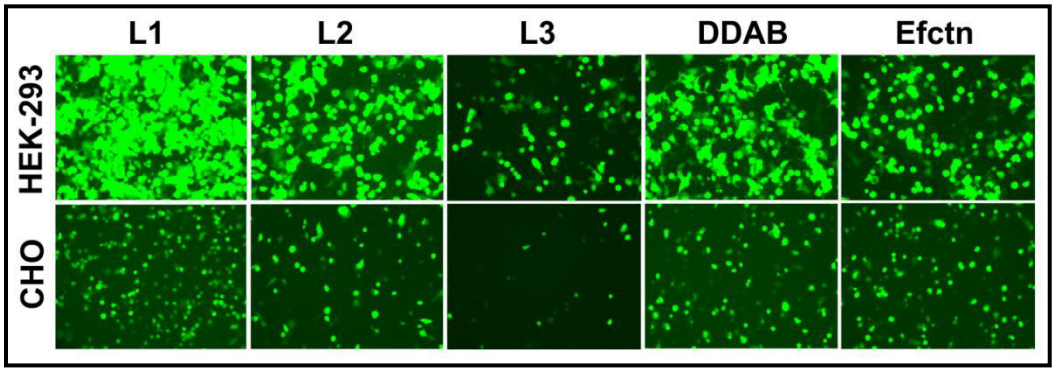

Fig. 6 Representative fluorescence microscopic images obtained from pEGFP-N3 transfection using co-liposomal formulations of L1, L2 and L3 in HEK-293 and CHO. Complexes were prepared from dicationic lipid formulations at 1:1 N/P charge ratio using pEGFP-N3 plasmid (0.8 µg) in serum minus DMEM. For visual comparison images were captured in Floid fluorescent imaging station at 48 h post transfection. DDAB and Efctn were served as positive controls for relative activity comparison.

4.2.1.5 Serum compatibility of lipoplex transfection: In spite of many setbacks in cationic lipid mediated gene delivery, serum is one of the well known modulating factors to disrupt the transfection efficiencies of novel cationic amphiphiles.[30,31] However, though a transfection reagent derived from any cationic lipid possessing

superior transfection activity, has to be serum compatible to mandate/execute its application in *in vivo*. In order to know the impact of serum on the stability of lipoplexes derived from dicationic lipid formulations, the assay was conducted in those two cell lines with the highest activity rank order (HEK-293, CHO). The complexes were prepared at an optimized N/P charge ratio (1:1) in order to formulate the final transfection complex using increasing concentrations of added serum (10-50%, v/v). Interestingly, as shown in the Fig. 7, the β-galactosidase gene expression pattern of all the three lipids in both the cell lines studied remains unaffected in presence of 10% added serum. However, upon increasing the serum concentrations to 30% and 50%, a corresponding activity decrease to 20% and 40% was observed respectively for all the three lipids.

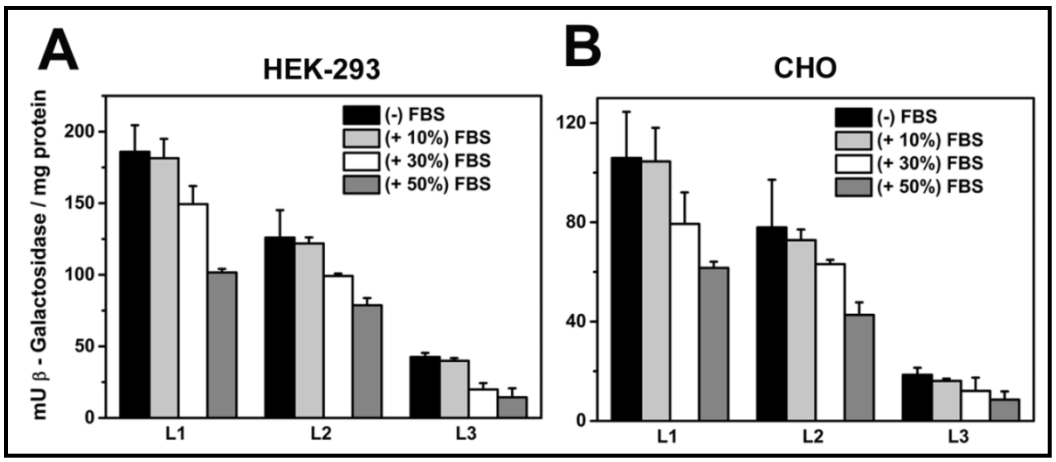

Fig. 7 Representative histograms depict the *transient* transfection results conducted in HEK-293 (A) and CHO (B) in presence of increasing added concentrations of serum: Complexes were prepared at optimized N/P charge ratio (1:1) in serum free DMEM, final transfection complex was formulated by using (–FBS (black), +10% FBS (light gray), +30% FBS (white) and +50% FBS (gray)) increasing concentrations of added serum containing DMEM. The results were measured in terms of β-galactosidase units per mg protein 48 h of post transfection.

4.2.1.6 Cell viability: The significance of efficient synthetic gene carriers is directly related to the cell compatibility and survival measures. Thus the cationic lipid toxicity posses a major limiting factor for the clinical application of liposomal gene

delivery.[33] Cell viabilities of the lipoplexes derived from novel dicationic lipids were assessed by using MTT cell based assay[34] by following the same conditions as followed in actual transfection studies. Fig. 8 displays the percentage of cell viability of the lipoplexes derived at varying lipid to DNA charge ratios i.e. 0.3:1, 1:1, 3:1 and 9:1. The toxicity profile of the lipoplexes in all the cell lines used for transfection were compared with control and standard formulations, DDAB & Efctn. The obtained data reveal that cell survivability is directly linked to the combined effect of both the lipid concentration as well as the dialkyl chain length present in the lipid backbone. Specifically, cell viability can be increased by decreasing the chain length and lipid concentration. Finally, the formulations of these 1, 2, 3-triazolium based lipids L1 and L2 were developed as potential transfection reagents having lesser toxicities than the available commercial transfection reagent effectene (Efctn).

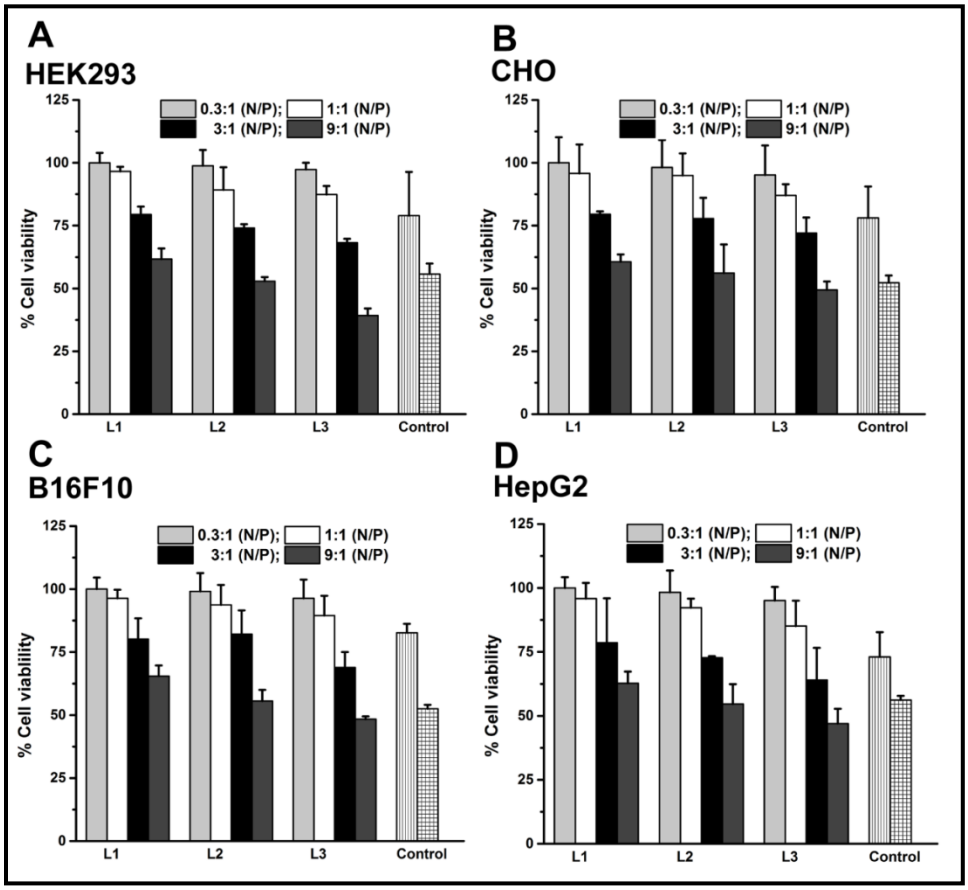

Fig. 8 % cell viability by MTT assay resulted from A) HEK-293, B) CHO, C) B16F10 and D) HepG2: Cells were treated with the complexes prepared in 10% FBS+DMEM from varying charge ratios (0.3:1/light gray, 1:1/white, 3:1/black and 9:1/gray) of dicationic lipid formulations L1, L2 and L3 along with control lipid (DDAB:DOPE/vertical stripes) and commercial transfection reagent (effectene/checks) at constant amount of pCMV-βgal DNA (0.3μg/well) as mentioned in methods. Complexes were incubated for 4 h and cells were assayed after 24 h of complex addition.

4.2.1.7 Conclusions: In summary, a series of aliphatic back bone with varying chain length-anchored dicationic lipids were synthesized by connecting the head group of quaternary ammonium to a delocalizable cation (1, 2, 3-triazolium) having a 2-hydroxy ethyl chain. These lipids were formulated to lipid vesicles using DOPE as a co-lipid (**L1**, **L2** & **L3**) and their transfection potentials in various cell lines were evaluated using reporter gene activity with two different plasmids, such as *p*CMV-βgal and *p*EGFP-N_3. The study also focused on the effects of additional heterocyclic construct on transfection by comparing the activity with a control formulation DDAB:DOPE. Comparative biological studies indicated that enhancement of transfection due to additional heterocyclic cation is in good agreement with all the experimental results. The results also demonstrate that the activities of these dicationic lipids are critically dependent on the chain length of the hydrophobic back bone. The lipoplexes produced from these dicationic lipids were stable in serum, least toxic and mediated good transfection. Hence, the present study endorses the triazole based dicationic head group with the C14 alkyl chain length as a better transfecting reagent for modulating the activity and toxicity profile.

4.2.1 SECTION B

"Effect of Nature of Substitution on Side chain of 1, 2, 3-Triazolium Delocalizable Head Group Containing α- Tocopherol Based Cationic Lipids on Gene Transfection"

Understanding the effect of structural modification of cationic lipid on gene transfection properties is prerequisite to upgrade the cationic lipid mediated gene

delivery. Taking the impressive gene transfer properties of many previously reported cationic amphiphiles with hydroxyalkyl head groups.[32,33] into account, it is envisaged that a hydroxyethyl group in the delocalized cationic head group region of tocopherol based cationic lipids discussed under section B of this chapter may be rewarding.

In this direction, the present work describe the synthesis, characterization and biological evaluation of a tocopherol based cationic lipid with delocalizable cationic (1, 2, 3-triazolium) head group having a substitution of hydroxyethyl chain (TTOH). To assess the effect of both delocalizable cation and hydroxyethyl chain substitution on transfection properties, two tocopherol based monocationic control lipids (TTC_4 & $TTNH_3$) were designed as shown in the Fig. 9. One of the control lipids TTC_4 has delocalizable cation having n-butyl chain as substitution without hydroxyl group and another lipid $TTNH_3$ having protonated cation has neither hydroxyl group nor delocalizable cation in its head group.

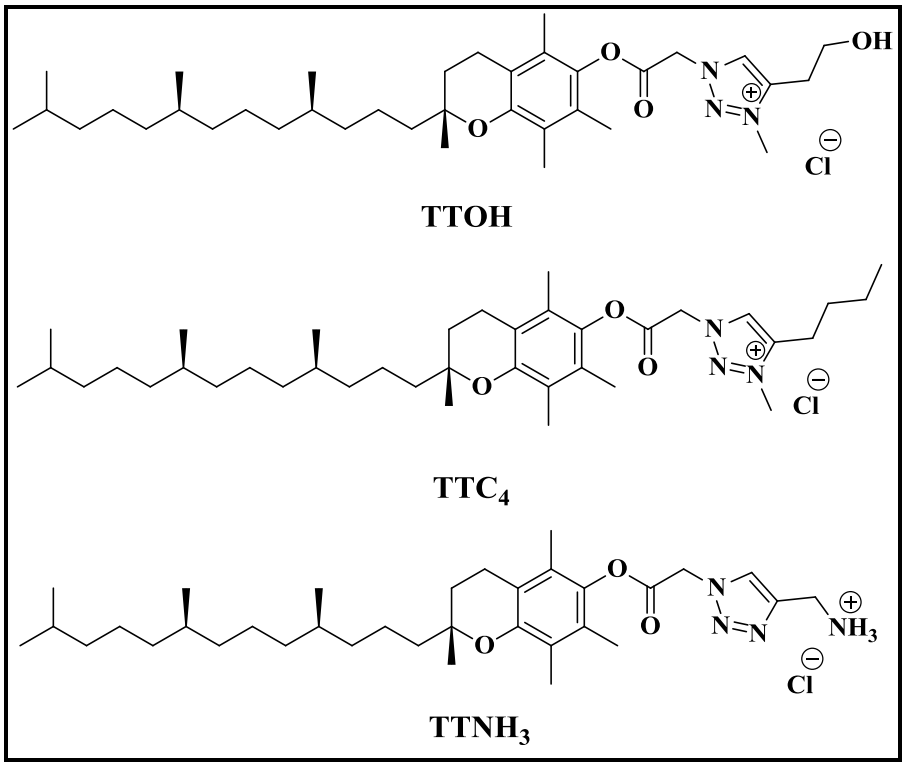

Fig. 9 Molecular structure of tocopherol based cationic lipids

To synthesize the designed lipids represented in Fig 9, a strategy called Huisgen 1, 3-dipolar cyclo addition was followed. The synthesized and purified three lipids were mixed with common co-lipid DOPE at various molar fractions to obtain better packing ratio that could perform better transfections. All the optimizations like lipid/DOPE molar ratio and lipid/DOPE: DNA (N/P) charge ratios were carried out using quantified reporter gene expression derived from the transfection of pEGFP-N_3 gene in HEK293 cells. The structure activity study of these lipids was carried out using another reporter gene (*p*CMV-βgal) based assay called beta-galactosidase in three different cell lines from three different origins. The biological studies of these lipids were correlated with the physicochemical characterization of liposomal cationic aggregates and DNA complexes using various techniques.

4.2.2.1 Chemistry: In tandem to our prior investigation of effect of head group modification on transfection efficiencies using tocopherol derived cationic lipids discussed in chapter 2 and chapter 4A, the effect of side chain nature at delocalizable head group on transfection properties was envisaged. To this end, the designed monocationic tocopherol based lipids were synthesized by following the steps mentioned in the scheme 2. As per the requirement of proposition, a common intermediate alpha tocopheryl-2-azidoacetate (Toc-N_3) was synthesized from alpha tocopheryl-2-bromoacetate which is used further to produce three different click intermediates Boc-$TTNH_3$, Int. TTOH and Int. TTC_4 on individual coupling with three different acetylene derivatives boc-propargylamine, but-3-yn-1-ol, and hex-1-yne respectively. This coupling reaction is followed by the protocol of copper (I) catalyzed Hiusgen 1, 3 dipolar cyclo addition. Isolated click intermediates of TTOH and TTC_4 are allowed for methyl iodide quaternization to produce iodide salts which were further subjected to chloride ion exchange resin to afford pure titled lipids such as TTOH and TTC_4. The lipid $TTNH_3$ which has similar core ring and unshared cation in its head group is produced by the deprotection of *N*-boc of Boc-$TTNH_3$ using triflouroacetic acid followed by chloride ion exchange resin. The structures of all lipids and intermediates were analyzed by using the spectroscopic data generated from ^{1}H-NMR, ^{13}C-NMR and ESI-HRMS.

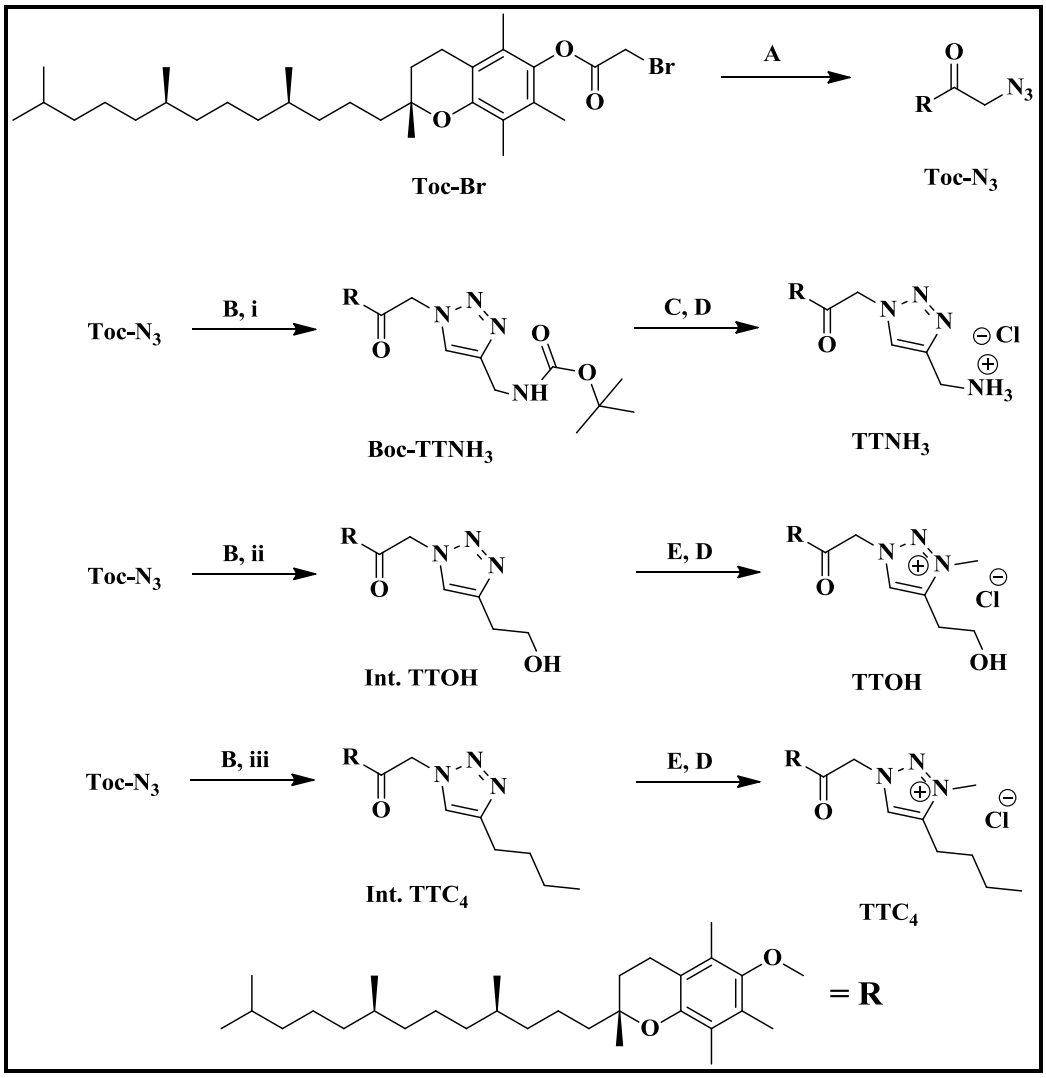

Scheme 2 Synthetic route and molecular structures of alpha-tocopherol based cationic lipids.

Reagents and conditions: A) NaN_3, acetonitrile, 80 ºC, 16 h; B) $CuSO_4.5H_2O$, sodium ascorbate, THF:H_2O: *tert*-BuOH (2:2:1), RT, 24 h, i) boc-propargylamine, ii) but-3-yn-1-ol, iii) hex-1-yne; C) DCM:TFA (2:1); D) Amberlite anion exchange resin; E) MeI, acetonitrile, sealed tube, 80 ºC, 48 h.

4.2.2.2 Preparation of liposomal aggregates: Cationic lipid aggregates were developed by mixing the cationic lipid with common neutral co-lipid DOPE at varying concentrations to obtain better molar ratio for maximum transfection potentials. Mixed

co-liposomal formulations such as 1:1, 2:1, 3:1 and 4:1 ratios of DOPE: lipid from each cationic lipid were prepared by following the protocol mentioned in earlier reports.[25] Optically clear aqueous suspensions were generated by sonication of turbid solutions prepared from mixed cationic thin lipid films and are stable and clear under sterile atmosphere at 4 ºC up to three months from the preparation without any turbidity and sedimentation.

4.2.2.3 Lipid/DNA binding interaction studies: The DNA binding potential screening of novel cationic lipid aggregates is the initial characterization of liposomal suspensions towards DNA delivery. Gel electrophoresis and EtBr exclusion assays are the better techniques to predict lipid/DNA binding interactions in exact. In a typical gel electrophoresis, complexes of DNA (*p*CMV-βgal) were prepared from transfection optimized molar ratio (2:1; DOPE/lipid) of each lipid at seven different N/P charge ratios (0.5:1–6:1, Lipid/DNA). Complexes were loaded on to 1% agarose gel and allowed for electrophoresis. Representative images obtained from each co-liposomal formulation demonstrated through Fig. 10A indicate the lipid formulations arose from TTOH and $TTNH_3$ could efficiently condense the *p*DNA even at lower charge ratios like 1.5:1 (N/P) where as the lipid TTC_4 started retardation of DNA electrophoretic mobility at 3:1 N/P charge ratio.

To sustain the visual interpretation of lipid/DNA binding interactions from gel electrophoresis images, a qualitative fluorescent based assay was conducted using optimized molar ratio of (1:2 lipid/DOPE) each lipid. EtBr intercalation assay is the one, well known fluorescent based assay to find the binding potentials of lipid aggregates. On a sequential addition and titration of each lipid formulation to a control EtBr-DNA complex which has been kept its fluorescent intensity as 100% has gradually dropped down to get quenched. The concentration of lipid at which maximum dropdown of fluorescent value is induced would responsible for better compaction of DNA and results maximum transfection. Representative graph in Fig 10B demonstrate the obtained drop down fluorescent curves generated from each co-liposomal formulation, reveal that the lipids TTOH and $TTNH_3$ have displaced almost 70 % of EtBr from CT-EtBr:DNA

complex at 1.5:1 N/P charge ratio. In contrast the lipid TTC_4 has shown maximum DNA compaction at 3:1 N/P charge ratio.

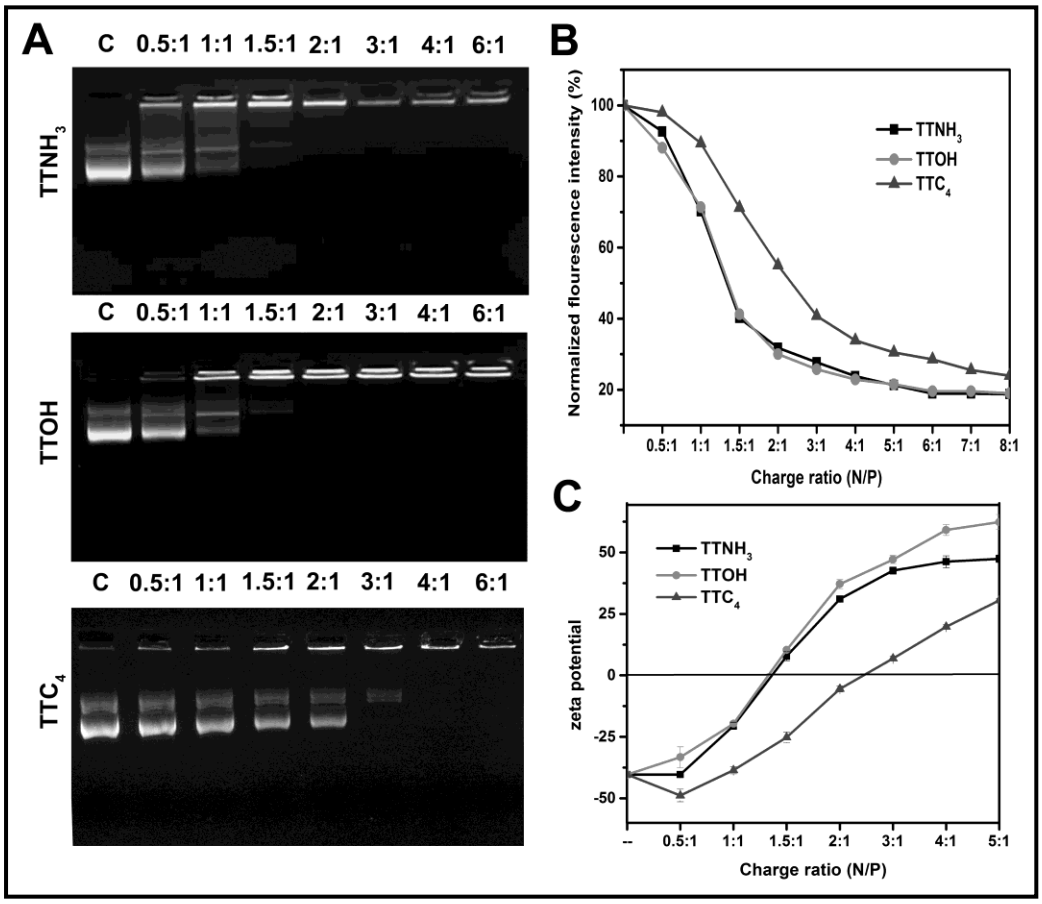

Fig. 10 A) 1% agarose gel electrophoresis of lipid/DNA complexes derived from $TTNH_3$, TTOH and TTC_4 using 0.3 µg (pCMV-βgal) DNA/well across the mentioned charge ratios on top of each panel, Naked DNA served as control represented as "C" B) Normalized fluorescence intensities of lipid $TTNH_3$ (square), TTOH (circle) and TTC_4 (triangle) at increased charge ratios mentioned at bottom of the graph with respect to the CT-EtBr:DNA was analyzed. C) Zeta potential of lipoplexes derived from lipid $TTNH_3$ (square), TTOH (circle) and TTC_4 (triangle) at varying N/P charge ratios depicted at the bottom of graph.

The zeta potentials of lipoplexes derived from each co-liposomal formulation and DNA were measured using laser doppler electrophoresis technique and the results are

represented through the Fig. 10C. The graph demonstrates that surface potentials are increased across the various charge ratios mentioned at the bottom of the graph and pattern is clearly resembles with the visual analysis of electrophoretic mobility retardation of DNA from gel electrophoresis assay. The DNA condensation of lipids $TTNH_3$ and TTOH were loosely held with the ratios like 0.5:1 and 1:1 charge ratios showed negative potentials which were then transformed to positive potential at the charge ratio 1.5:1 where the complete compaction of DNA could achieved. Similarly, the lipid TTC_4 has given the lower positive potentials than the other two lipid formulations at 3:1 charge ratio where the proper condensation of DNA was initiated.

4.2.2.4 Size and morphology of lipid aggregates: The optimized co-liposomal formulations (DOPE/lipid; 2:1) and the complexes derived at transfection active charge ratio (1.5:1; liposome/DNA; N/P) were characterized in terms of suspended particle size under DLS. Fig. 11A represents the hydrodynamic diameter of liposome derived from lipid TTOH is around 100 nm in size which is raised about $1/3^{rd}$ when complexed with DNA at optimized N/P charge ratio. Similar trend is observed for the lipid $TTNH_3$, having non- delocalized cation and aminoethyl functional substituent at the head group. In contrast the lipid (TTC_4) having delocalized charge and aliphatic butyl substitution at head group showed the lipid particle size is around 150 nm and its complex is around 200 nm in size.

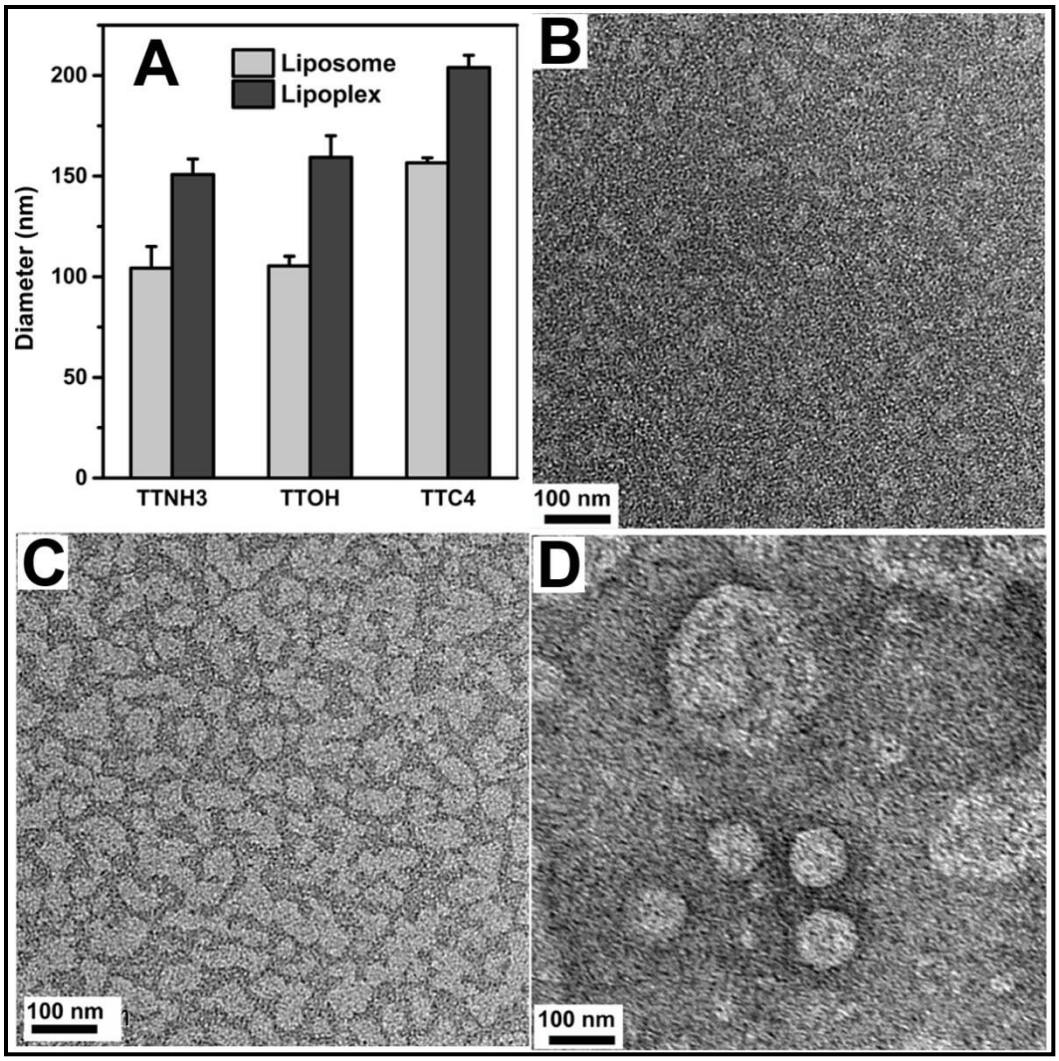

Fig. 11 A) Hydrodynamic diameter of liposomal aggregates (light gray) and their derived DNA (pCMV-βgal) complexes (gray) at 1.5:1 N/P ratio under DLS; Representative transmission electron microscopy images of co-liposomal formulations derived from lipid B) $TTNH_3$, C) TTOH and D) TTC_4.

The liposomal aggregates were also characterized in terms of morphology and particulate distribution in aqueous media using the images captured under transmission electron microscopy demonstrated through the Fig. 11B-D reveal that the lipids TTOH and $TTNH_3$ are seemed to be similar kind of particulate distribution and size whereas the lipid TTC_4 shows distinguished aggregate nature having different sizes of particulate distribution.

4.2.2.5 Transfection biology: *Optimization of lipid/DOPE molar formulation:* To find out better transfection potent molar ratio of lipid/DOPE, varying ranges of lipid formulations (DOPE:lipid; 1:1, 2:1, 3:1 and 4:1) were allowed for transfection using pEGFP-N_3 plasmid in HEK293 cell line. The transfection efficiencies in terms of expressed enhanced green fluorescent protein was analyzed qualitatively by capturing fluorescent images under floid cell imaging station at 48 h of post transfection and quantified the enhanced green fluorescence via flow cytometry. Both quantitative and qualitative results of GFP plasmid transfection were displayed in the Fig. 12 and Fig. 13 respectively. The quantitative transfection data provided from FACS based analysis, two particular statistics like % of GFP positive cells and extent of fluorescence intensity using geometric mean fluorescent intensity (GMFI) have been considered to evaluate the transfection potentials. Fig. 12a, 12c and 12e represent the derived transfection potentials from the varying molar formulations of lipids $TTNH_3$, TTOH and TTC_4 respectively confirms that the molar ratio of 2:1 (DOPE/lipid) has given maximum % of positive cells and highest mean intensities among the all studied molar combinations irrespective of the lipid. The mixing ratio of DOPE/lipid 2:1 have been considered as optimized and used for further experimentation.

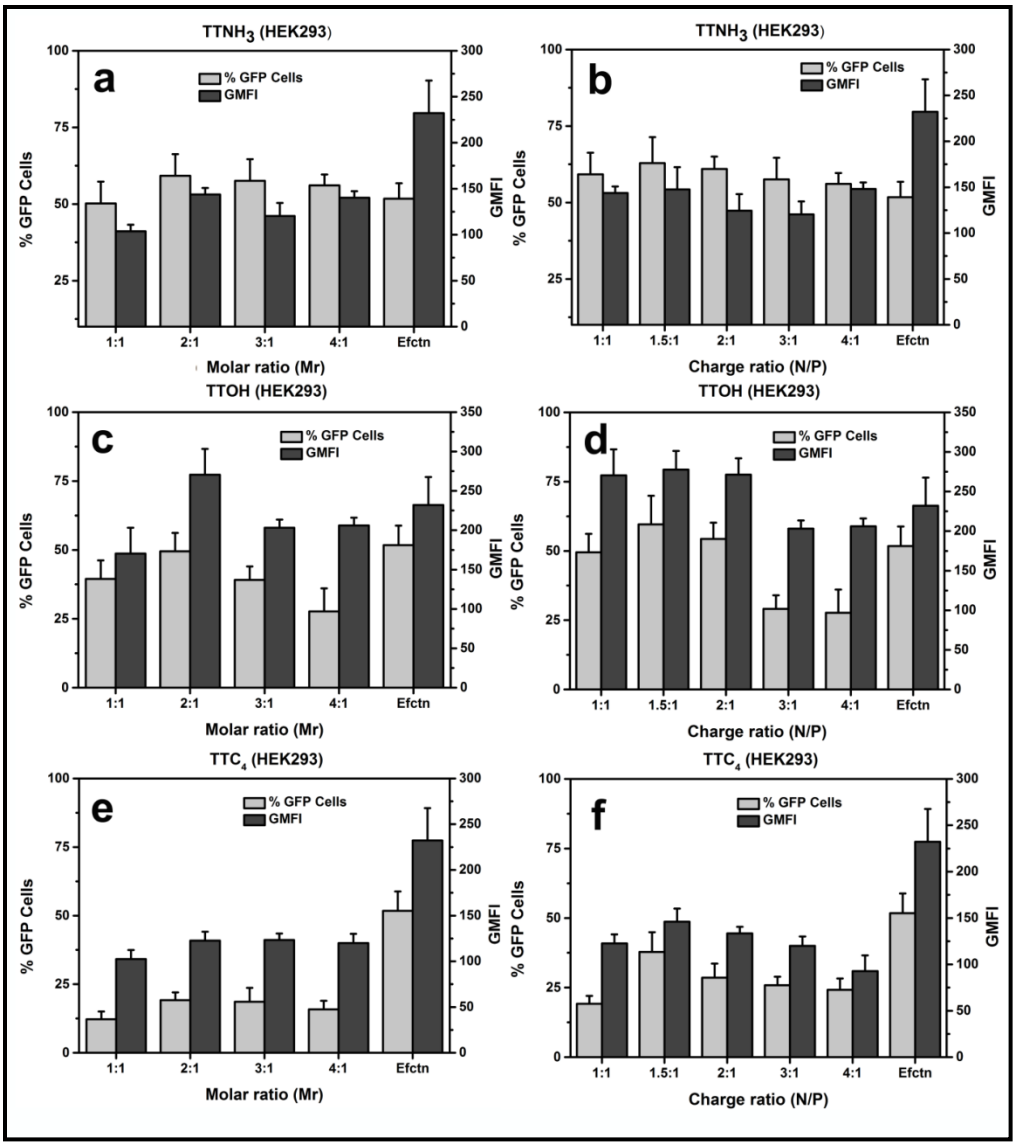

Fig. 12 Transfection of pEGFP-N_3 DNA in HEK 293 cells using lipoplexes of $TTNH_3$(a), TTOH(c) and TTC_4(e) at various molar combinations of DOPE/lipid (1:1, 2:1, 3:1 & 4:1) and lipoplexes derived from lipids $TTNH_3$(b), TTOH(d) and TTC_4(f) at various N/P charge ratios of lipid/DNA (1:1, 1.5:1, 2:1, 3:1 & 4:1). Effectene (Efctn) is served as positive control.

Optimization of lipid/DNA charge ratios: Considering the 2:1 (DOPE/lipid) molar ratio as optimized fraction for transfection, utilized further to optimize N/P charge ratio for maximum transfection potential. Fig. 12b, 12d and 12f illustrate the transfection

efficiencies of lipids $TTNH_3$, TTOH and TTC_4 respectively confirms that the 1.5:1 charge ratio has expelled maximum % of GFP positive cells and highest mean intensities among the varying range of charge ratios (1:1, 1.5:1, 2:1, 3:1 & 4:1) irrespective of the lipid. This has already been supported by the lipid/DNA binding interaction studies that the optimal binding nature of 1.5:1 charge ratio could condense the DNA properly and facilitates to higher transfections.

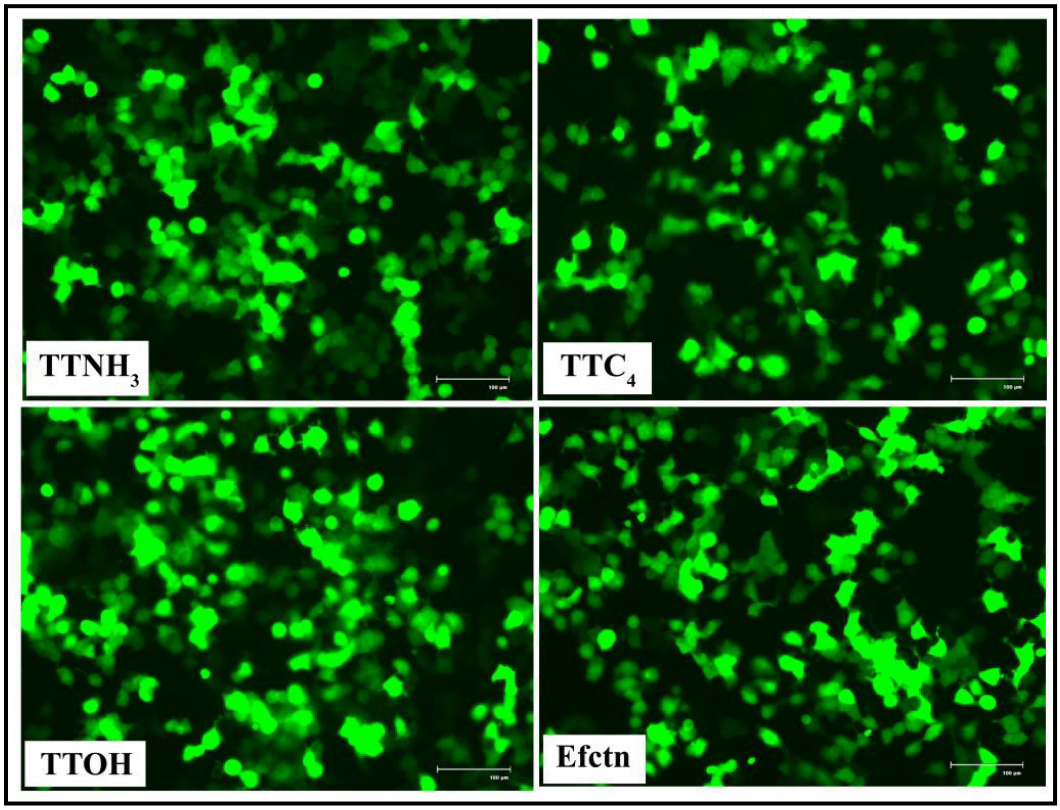

Fig. 13 Transfection of pEGFP-N_3 DNA using the lipoplexes ($TTNH_3$, TTOH & TTC_4) derived from optimized molar ratio and N/P charge ratio in presence of plane (-FBS) DMEM. Fluorescent images were captured under floid cell imaging station after 48 h of transfection. Effectene (Efctn) is served as bench mark standard.

The *in vivo* application of cationic lipid mediated gene delivery has majorly been insisted by the presence of serum which could disturb the stability of lipid/DNA complex while transfection. In order to find the stability of transfection in presence of serum and to get reliability in activity comparison, transfection assay was conducted in presence of

10% FBS+DMEM using another reporter gene *p*CMV-βgal in three different cultured cell lines derived from human embryonic kidney (HEK293), mouse neuroblastoma (Neuro-2A) and hepatocarcinoma (HepG2) which are significantly posses tocopherol distribution in their related tissues. Normalized miller units of β-galactosidase expressed by the treatment of three lipids at optimized N/P ratio (1.5:1) represented through Fig. 14. The transfection efficiencies of hydroxyl ethyl substituted delocalizable head group based tocopherol derived lipid (TTOH) and the control lipids ($TTNH_3$ and TTC_4) followed a rank order as TTOH > $TTNH_3$ > TTC_4 in all cell lines studied.

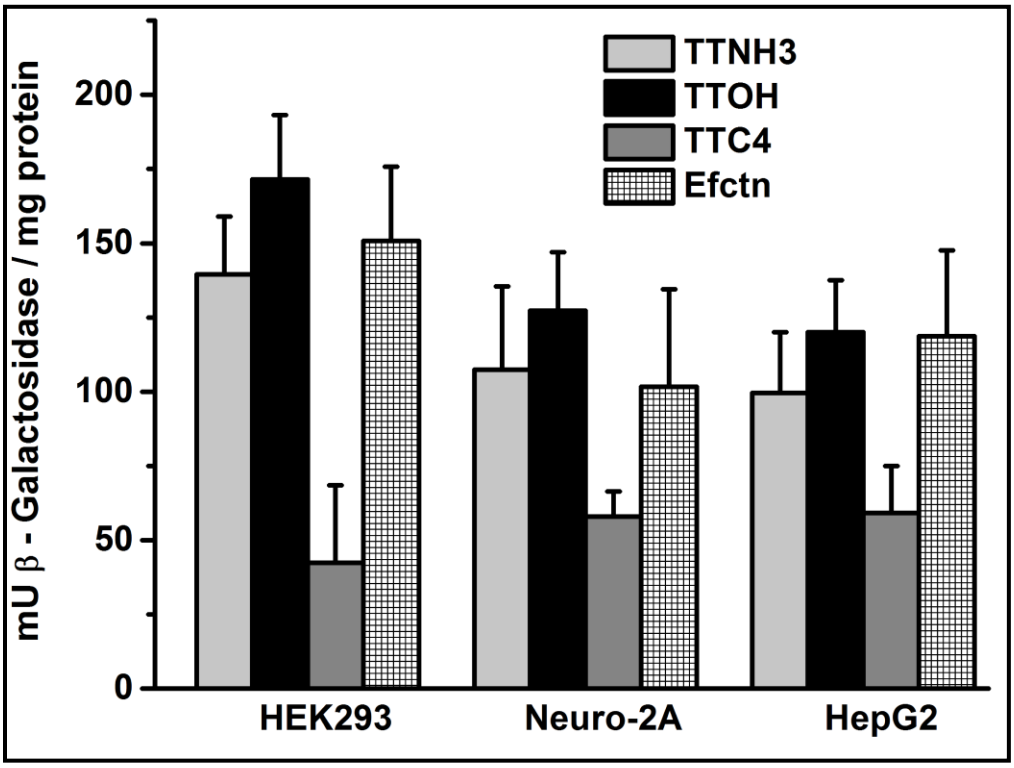

Fig. 14 Transient transfection of *p*CMV-βgal DNA using optimized molar and N/P charge ratios of lipoplexes derived from $TTNH_3$, TTOH and TTC_4 in HEK293, Neuro-2A and HepG2 cell lines. Complexes were incubated in 10% FBS+DMEM for 4 h and the assay is terminated at 48 h of post transfection. Effectene (Efctn) is served as positive control.

The consistent activity results derived from both the reporter gene activities convincingly supports the fact that the maximum transfection efficiency is associated

with the lipid TTOH. This is due to the presence of hydroxyl functional group on termini of side chain substitution at delocalizable head group might be induced more association with DNA during complexation with its providing hydrophilic nature. In addition, the soft cationic nature of delocalizable cation might also assist in efficient DNA release during endosomal escape. The lipid formulation has made up of from $TTNH_3$ has the cation which resides on single 'N' atom would be available for strong association with DNA negative charge and follows next to the lipid TTOH and similar to commercial cytofectin (Efctn) in transfection performance. The least activity of TTC_4 lipid formulation among the three lipid formulations studied and also in comparison with the positive control (Efctn) has clearly been revealed that the simple delocalized charge would not be enough to get accommodate maximum DNA payloads and hence the potential to delivery DNA into the cell lines studied.

4.2.2.6 Cellular uptake & co-localization study: Further to evidence the transfection potential patterns qualitatively, fluorescent labelled lipoplexes derived from three lipid formulations ($TTNH_3$, TTOH & TTC_4) were allowed for transfection in HEK293 cells and analyzed under confocal laser scanning microscope. Fig. 15 is included the representative images captured under confocal microscope at respective emission wavelengths after 1 h incubation of rhodamine-PE labelled lipoplexes to interpret the uptake efficiencies of lipoplexes obtained from *p*CMV-βgal and corresponding lipid formulation. In spite of many complicated steps involved in transfection process, avoiding of lysosomal counter parts of cell by lipoplexes plays significant role to determine efficiency of transfection. To interpret the same phenomenon with respective of these tocopherol derived lipoplexes, a qualitative co-localization study was endeavoured by staining the lysosomal regions of cell using another fluorescent probe, so called Lyso-Green.

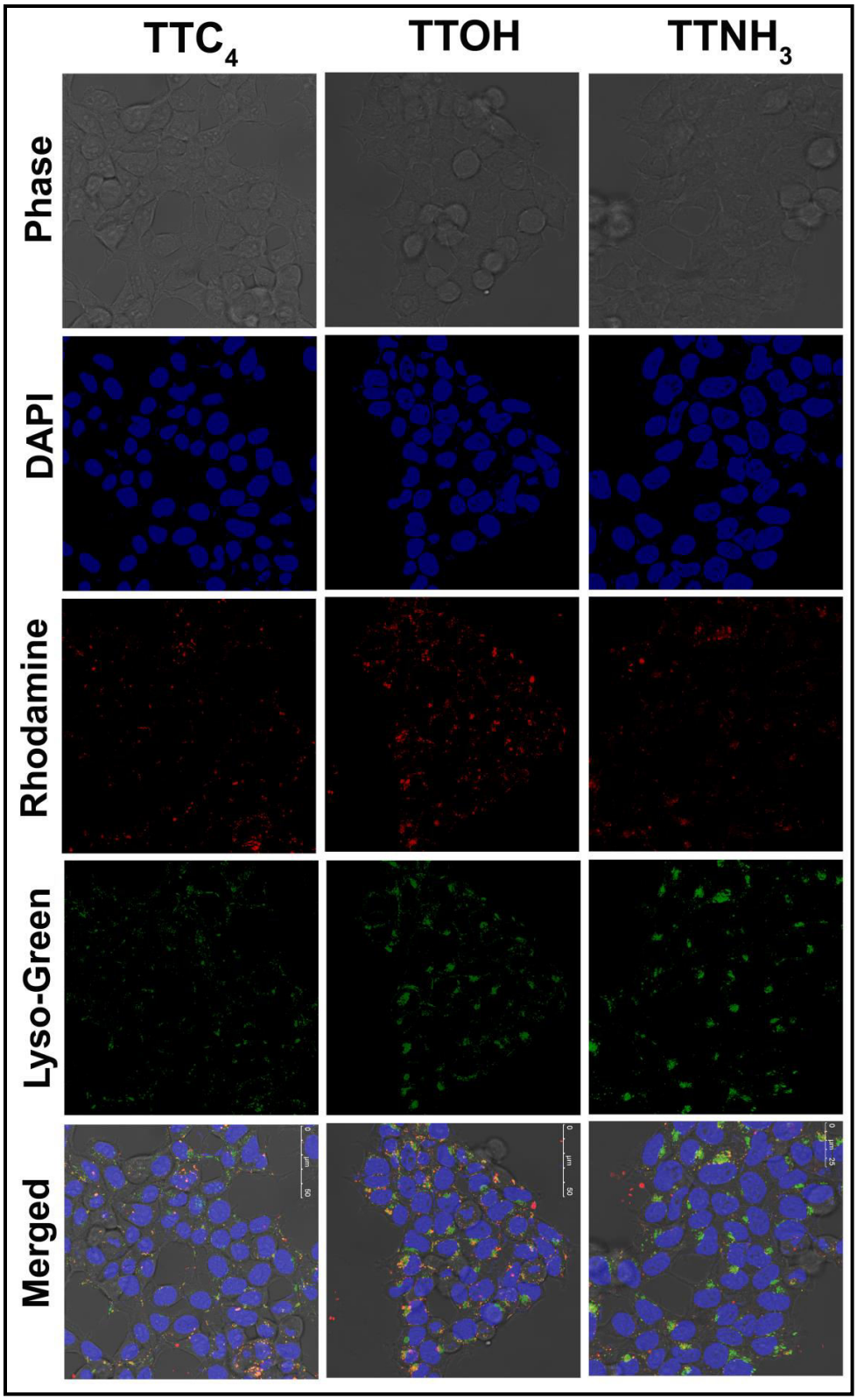
TTC4
TTOH
TTNH3
Phase
DAPI
Rhodamine
Lyso-Green
Merged

Fig. 15 Confocal laser scanning microscope images obtained from HEK293 cells after the transfection of pCMV-βgal DNA using rhodamine-PE labeled liposomal formulations derived from $TTNH_3$, TTOH and TTC_4. The images of Lyso-Green were captured after the treatment of lysotracker-green to represent cell acidic counter parts like lysosomes and the merged images were acquired from the both (red-fluorescent and green fluorescent) images. Cell nucleus parts were stained using the blue colored fluorescent dye (DAPI).

The careful observations of the Fig. 15 is indicating that red fluorescent punctuates acquired from rhodamine-PE labelled lipoplexes are placed under the label of Rhodamine which clearly demarcate the different uptake efficiencies fall among the three different lipid formulations. The green punctuates observed in the panels placed under the label Lyso-Green is representing that lysosomal cell counterparts (acidic regions) whereas the merged images obtaining from the merging of both red and green florescent images clearly distinguish the co-localization of lipoplexes with cell lysosomal regions.

4.2.2.7 Cell viability: The cytotoxicity associated with the new synthetic lipid formulations and DNA derived lipoplexes has to be measured and mandates to prove best cationic cytofectins in lipid mediated gene delivery.[34,35] MTT cell based assay is carried out in order to assess the toxicity profiles of lipoplexes at increasing charge ratios (1:1, 2:1, 4:1 & 8:1) of optimized co-liposomal formulation ($TTNH_3$, TTOH and TTC_4) and *p*CMV-βgal DNA. MTT assay is well established technique to determine the exact % cell viabilities after the transfection of lipoplexes at 24 h of post transfection. The resulted data is represented through the Fig. 16, which reveals that the lipoplexes prepared from TTOH and $TTNH_3$ are less toxic even at higher charge ratios like 8:1 with the cell viability ~80-85 % irrespective of the cell lines studied. Exceptionally the lipoplexes derived from the lipid TTC_4 which has aliphatic side chain substitution at delocalizable head group of lipid showed significant toxicities towards all the studied cell lines especially at 4:1 and 8:1 charge ratios.

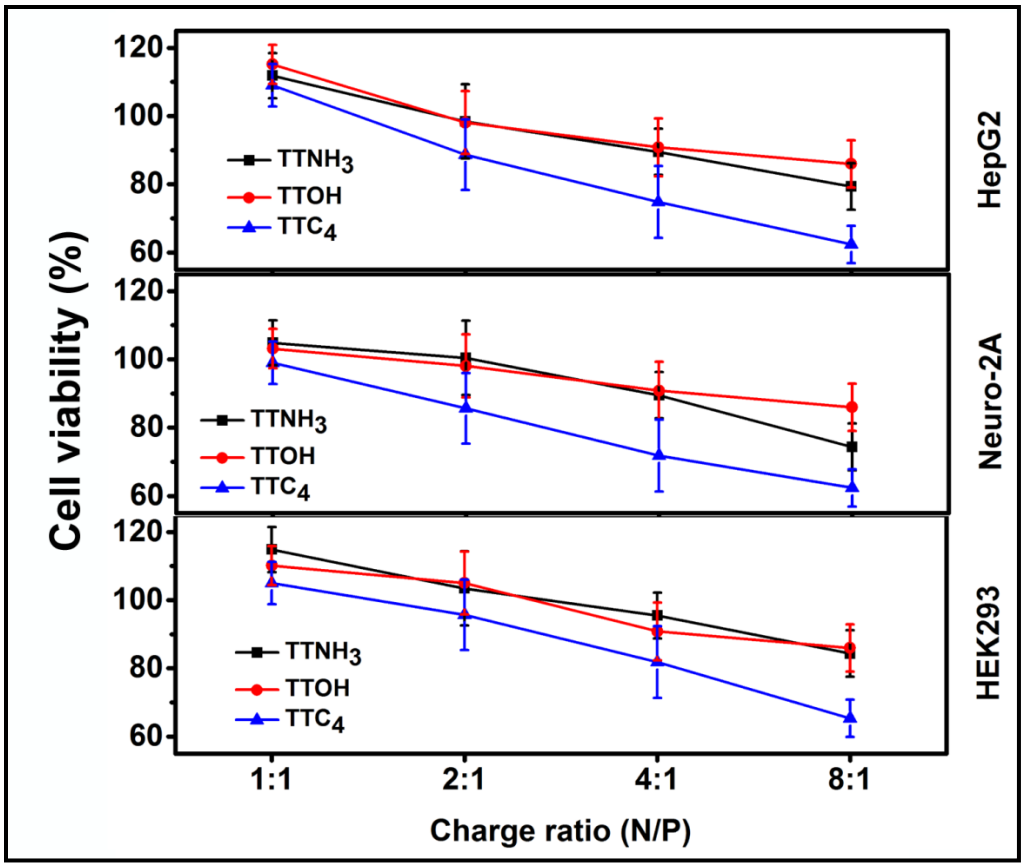

Fig. 16 Cell based MTT assay of lipoplexes derived from three optimized lipid formulations using pCMV-βgal DNA at increasing range of charge ratios (2:1 to 8:1) mentioned in the figure. Complexes were incubated in 10% FBS+DMEM for 4 h, assay was terminated 24 h post transfection.

4.2.2.7 Conclusions: The study highlights the delivery of plasmid DNA efficiently using new lipid motifs creates the interest towards development of new synthetic lipid vectors. The outcome of present study describes the lipid having delocalizable cation with hydroxyethyl chain substitution on the backbone of biocompatible vitamine-E provides inspiring transfection results with low toxicities. These results were analyzed on the basis of comparative assessment using control lipids in transfections and also the physicochemical investigation using various techniques. All the supportive findings evidenced that lipid formulation derived from TTOH facilitates better transfection with the aid of both hydroxy substitution and delocalizable cation, may

helps to find better cytofectins using various heterocyclic motifs in cationic vector design via structure activity phenomenon.

4.3 EXPERIMENTAL SECTION

4.3.1 Materials: All the chemicals, reagents and solvents used for the synthesis were procured at highest purity from Alfa Aeser, Spectrochem and used directly without further purification. Mass spectral data were acquired by using a commercial LCQ ion trap mass spectrometer (Thermo Finnigan, San Jose, CA, U.S.) equipped with an ESI source. ^{1}HNMR spectra were recorded on Bruker (2001), SAINT (Version 6.28a) & SMART (Version 5.625) Bruker AXS Inc., Madison, Wisconsin, USA. 3-(4,5-dimethylthiazol-2-yl)-2,5-diphenyl-2H-tetrazolium bromide (MTT) was purchased from Calbiochem (Merck Millipore, Massachusetts, USA), Endotoxin free Plasmid pCMV-βgal and pEGFP-N_3 were extracted from competent *E. coli* bacteria, the extraction being carried out using Nucleo Bond Xtra Midi Plus EF (MACKAREY-NAGEL, Duren, Germany), following a protocol previously described. The 1, 2-dioleoyl-sn-glycero-3-phosphatidylethanolamine (DOPE) was purchased from Avanti Polar Lipids. Fetal Bovine Serum (FBS) is procured from Thermo Fischer Scientific (Gibco®).

4.3.2 Synthesis (Scheme 1): General procedure for the synthesis of acetylene derivatives (1a-c): In a 50 mL round bottom flask, 1 g (18.16 mmol) propargyl amine, 12.54 g (90.78 mmol) anhydrous K_2CO_3 and corresponding alkyl bromide (38.136 mmol) were taken in to 15 mL of acetonitrile. The resulting mixture was allowed to reflux at 80 ºC for about 2 days for maximum disappearance of starting materials on TLC. The contents were cooled and exposed to rota evaporation to remove the solvent. The resulting crude was dissolved in excess amount of chloroform (100 mL) which is then washed three times with water (3X30 mL) and one time with brine (50 mL). The separated organic layer was removed under reduced pressure followed by drying upon anhydrous sodium sulphate to remove the remained water droplets. The resultant crude was subjected to 60-120 mesh silica gel column chromatography purification using 1% EtOAc: pet ether as eluent.

***N*-tetradecyl-*N*-(prop-2-yn-1-yl)tetradecan-1-amine (1a):** colorless oil, yield (5.6 g, 69%). ^{1}H NMR (400 MHz, $CDCl_3$) δ 3.40 (*s*, 2H, -N-C<u>H</u>$_2$-C≡), 2.44 (*t*, *J* = 8 Hz, 4H, -N-(C<u>H</u>$_2$)$_2$-), 2.15 (*s*, 1H, <u>H</u>C≡C-), 1.43 (*s*, 4H, -N-(CH$_2$)$_2$-(C<u>H</u>$_2$)$_2$-), 1.26 (*s*, 44H, -(C<u>H</u>$_2$)$_{22}$-(CH$_3$)$_2$), 0.88 (*t*, *J* = 8 Hz, 6H, -(CH$_2$)$_{22}$-(C<u>H</u>$_3$)$_2$). ESI-MS: 447 $[M+H]^+$.

***N*-hexadecyl-*N*-(prop-2-yn-1-yl)hexadecan-1-amine (1b):** colorless solid, yield (6.41 g, 70 %). ^{1}H NMR (400 MHz, $CDCl_3$) δ 3.41 (*s*, 2H, -N-C<u>H</u>$_2$-C≡), 2.44 (*t*, *J* = 8 Hz, 4H,-N(C<u>H</u>$_2$)$_2$-), 2.15 (*s*, 1H, <u>H</u>C≡C-), 1.44 (*t*, *J* = 8 Hz, 4H,-N-(CH$_2$)$_2$-(C<u>H</u>$_2$)$_2$-), 1.28 (*s*, 52H, -(C<u>H</u>$_2$)$_{26}$-(CH$_3$)$_2$), 0.88 (*t*, *J* = 8.0 Hz, 6H, -(CH$_2$)$_{26}$-(C<u>H</u>$_3$)$_2$). ESI-MS: 505 $[M+H]^+$.

***N*-octadecyl-*N*-(prop-2-yn-1-yl)octadecan-1-amine (1c):** colorless solid, yield (7.48 g, 73.5 %). ^{1}H NMR (400 MHz, $CDCl_3$) δ 3.40 (*s*, 2H, -N-C<u>H</u>$_2$-C≡), 2.44 (*t*, *J* = 8 Hz, 4H, -N-(C<u>H</u>$_2$)$_2$-), 2.15 (*s*, 1H, <u>H</u>C≡C-), 1.44 (*s*, 4H, -N-(CH$_2$)$_2$-(C<u>H</u>$_2$)$_2$-), 1.24 (*s*, 60H, -(C<u>H</u>$_2$)$_{30}$-(CH$_3$)$_2$), 0.88 (*t*, *J* = 8.0 Hz, 6H, -(CH$_2$)$_{30}$-(C<u>H</u>$_3$)$_2$). ESI-MS: 560 $[M+H]^+$.

General procedure for click reaction (2a-c): To a stirred solution of acetylene-derivative of 1 mmol (1a-c) and 2-azidoethanol (1 mmol) in *tert*-BuOH: H_2O (1:1; 20 mL) were added $CuSO_4.5H_2O$ (0.1 mmol) and sodium ascorbate (0.2 mmol). The resulting mixture was stirred at room temperature until complete conversion of the starting material, which was diluted with excess of water (100 mL) then, extracted in to ethyl acetate (3 X 50 mL) and removed the solvent under reduced pressure followed by drying upon anhydrous $NaSO_4$. The compound showing the R_f in the range 0.4 – 0.5 in 9:1 $CHCl_3$: MeOH, was purified using 60-120 mesh silica gel column chromatography using 2-3% MeOH: $CHCl_3$ as eluent.

2-(4-((ditetradecylamino)methyl)-1H-1,2,3-triazol-1-yl)ethanol (2a): yellowish gummy solid, yield (0.485 g, 91 %) ^{1}H NMR (400 MHz, $CDCl_3$) δ 7.66 (*s*, 1H, -N-<u>H</u>C=C-(CH$_2$)-), 4.48 (*t*, *J* = 4 Hz, 2H, HO-C<u>H</u>$_2$-CH$_2$-), 4.07 (*t*, *J* = 4 Hz, 2H, HO-CH$_2$-C<u>H</u>$_2$-), 3.83 (*s*, 2H, =C-C<u>H</u>$_2$-N-), 2.50 (*t*, *J* = 8 Hz, 4H, -N-(C<u>H</u>$_2$)$_2$-), 1.51 (*s*, 4H, -N-(CH$_2$)$_2$-(C<u>H</u>$_2$)$_2$-), 1.25 (*s*, 44H, -N-(C<u>H</u>$_2$)$_{22}$-), 0.86 (*t*, *J* = 12 Hz, 6H, -(CH$_2$)$_{22}$-(C<u>H</u>$_3$)$_2$). ESI-MS: 535 $[M+H]^+$.

2-(4-((dihexadecylamino)methyl)-1H-1,2,3-triazol-1-yl)ethanol (2b): yellowish gummy solid, yield (0.548 g, 93 %) ^{1}H NMR (400 MHz, $CDCl_3$) δ 7.61 (*s*, 1H, -N-HC=C-(CH_2)-), 4.50 (*t*, *J* = 4 Hz, 2H, HO-CH_2-CH_2-), 4.09 (*t*, *J* = 4 Hz, 2H, HO-CH_2-CH_2-), 3.81 (*s*, 2H, =C-CH_2-N-), 2.47 (*t*, *J* = 8 Hz, 4H, -N-(CH_2)$_2$-), 1.51 (*s*, 4H, -N-(CH_2)$_2$-(CH_2)$_2$-), 1.27 (*s*, 52H, -(CH_2)$_{26}$-(CH_3)$_2$), 0.90 (*t*, *J* = 8 Hz, 6H, -(CH_2)$_{26}$-(CH_3)$_2$). ESI-MS: 591 $[M+H]^+$.

2-(4-((dioctadecylamino)methyl)-1H-1,2,3-triazol-1-yl)ethanol (2c): yellowish gummy solid, yield (0.591 g, 91.5%) ^{1}H NMR (400 MHz, $CDCl_3$) δ 7.65 (*s*, 1H, -N-HC=C-(CH_2)-), 4.48 (*t*, *J* = 4 Hz, 2H, HO-CH_2-CH_2-), 4.06 (*t*, *J* = 4 Hz, 2H, HO-CH_2-CH_2-), 3.82 (*s*, 2H, =C-CH_2-N-), 2.50 (*t*, *J* = 4 Hz, 4H, -N-(CH_2)$_2$-), 1.51 (*s*, 4H, -N-(CH_2)$_2$-(CH_2)$_2$-), 1.25 (*s*, 60H, -(CH_2)$_{30}$-(CH_3)$_2$), 0.88 (*t*, *J* = 4 Hz, 6H, -(CH_2)$_{26}$-(CH_3)$_2$). ESI-MS: 647 $[M+H]^+$.

Synthesis of dicationic lipid (L1-L3): To an obtained click intermediate 2a-c (1 mmol) in 5 mL of acetonitrile was added 10 mmol of excess methyl iodide in a screw cap sealed tube. The resulting mixture was refluxed for about 7 days at 80 ºC, until the complete conversion of starting material monitored by TLC. Consequently, the residue was subjected to column chromatographic purification to yield pure quaternized iodide salt by using 3-4% MeOH: $CHCl_3$ as eluent. The pure dicationic iodide lipid was further subjected to repeated chloride ion exchange procedure to afford pure titled lipids (L1-3).

4-((ditetradecyl(methyl)ammonio)methyl)-1-(2-hydroxyethyl)-3-methyl-1H-1,2,3-triazol-3-ium, (lipid L1): brown gummy solid, yield (0.264 g, 47 %) ^{1}H NMR (400 MHz, $CDCl_3$) δ 8.81 (*s*, 1H, -N-CH=C-(CH_2)-), 5.16 (*s*, 2H, -CH=C-CH_2-N^+-), 4.59 (*t*, *J* = 8 Hz, 2H, HO-CH_2-CH_2-), 3.81 (*t*, *J* = 8 Hz, 2H, HO-CH_2-CH_2-), 3.46 – 3.37 (*m*, 7H, -N^+-(CH_3)(CH_2)$_2$-, -N^+(CH_3)=N-N-), 3.20 (*s*, 3H, -N^+-(CH_3)(CH_2)$_2$-), 1.82 – 1.74 (*m*, 4H, -N^+-(CH_3)(CH_2)$_2$-(CH_2)$_2$-), 1.36 – 1.26 (*m*, 44H, -CH_2)$_2$-(CH_2)$_{22}$-(CH_3)$_2$), 0.88 (*t*, *J* = 8 Hz, 6H, -(CH_2)$_{22}$-(CH_3)$_2$). ESI-MS: *m/z*: 564 $[M^+]$ for $[C_{35}H_{72}N_4O^{2+}]$. Elemental analysis: Calculated: %C: 74.41; %H: 12.85; %N: 9.92; %O: 2.83. Observed: %C: 74.01; %H: 12.5; %N: 9.98; %O: 2.63.

4-((dihexadecyl(methyl)ammonio)methyl)-1-(2-hydroxyethyl)-3-methyl-1H-1,2,3-triazol-3-ium, (lipid L2): white gummy solid, yield (0.275 g, 44.35%) ^{1}H NMR (400 MHz, $CDCl_3$) δ 8.78 (*s*, 1H, -N-C<u>H</u>=C-(CH_2)-), 5.10 (*s*, 2H, -CH=C-C<u>H_2</u>-N^+-), 4.59 (*t*, *J* = 4 Hz, 2H, HO-C<u>H_2</u>-CH_2-), 3.81 (*t*, *J* = 8 Hz, 2H, HO-CH_2-C<u>H_2</u>-), 3.46 – 3.37 (*m*, 7H, -N^+-(CH_3)(C<u>H_2</u>)$_2$-, -(C<u>H_3</u>)-N^+=N-N-), 3.20 (*s*, 3H, -N^+-(C<u>H_3</u>)(CH_2)$_2$-), 1.83 – 1.76 (*m*, 4H, -N^+-(CH_3)(CH_2)$_2$-(C<u>H_2</u>)$_2$-), 1.39 – 1.26 (*m*, 52H, -CH_2)$_2$-(C<u>H_2</u>)$_{26}$-(CH_3)$_2$), 0.88 (*t*, *J* = 8 Hz, 6H, -(CH_2)$_{26}$-(C<u>H_3</u>)$_2$). ESI-MS: *m/z*: 620 [M^+] for [$C_{39}H_{80}N_4O^{2+}$]. Elemental analysis: Calculated: %C: 75.42; %H: 12.98; %N: 9.02; %O: 2.58. Observed: %C: 75.41; %H: 12.85; %N: 9.2; %O: 2.38.

4-((dioctadecyl(methyl)ammonio)methyl)-1-(2-hydroxyethyl)-3-methyl-1H-1,2,3-triazol-3-ium, (lipid L3): creamy solid, yield (0.335 g, 49.5%) ^{1}H NMR (400 MHz, $CDCl_3$) δ 8.77 (*s*, 1H, -N-C<u>H</u>=C-(CH_2)-), 5.09 (*s*, 2H, -CH=C-C<u>H_2</u>-N^+-), 4.59 (*t*, *J* = 4 Hz, 2H, HO-C<u>H_2</u>-CH_2-), 3.81 (*t*, *J* = 4 Hz, 2H, HO-CH_2-C<u>H_2</u>-), 3.46 – 3.42 (m, 7H, -N^+-(CH_3)(C<u>H_2</u>)$_2$-, -N^+(C<u>H_3</u>)=N-N-), 3.37 (*s*, 3H, -N^+-(C<u>H_3</u>)(CH_2)$_2$-), 1.86 – 1.79 (*m*, 4H, -N^+-(CH_3)(CH_2)$_2$-(C<u>H_2</u>)$_2$-), 1.39 – 1.26 (*bs*, 60H, -(CH_2)$_2$-(C<u>H_2</u>)$_{30}$-(CH_3)$_2$), 0.88 (*t*, *J* = 4 Hz, 6H, -(CH_2)$_{30}$-(C<u>H_3</u>)$_2$). ESI-MS: *m/z*: 676 [M^+] for [$C_{43}H_{88}N_4O^{2+}$]. Elemental analysis: Calculated: %C: 76.27; %H: 13.10; %N: 8.27; %O: 2.36. Observed: %C: 76.41; %H: 13.15; %N: 8.2; %O: 2.38.

4.3.3 Synthesis (Scheme 2): Synthesis of alpha-tocopheryl-2-azidoacetate (Toc-N_3): To a vigorously stirred solution of alpha-tocopherol (1.075 g, 2.5 mmol) in pyridine (3 mL) and dichloromethane (5 mL) was added 2-bromoacetylbromide (1 g, 5 mmol) in 5 mL of dichloromethane slowly about 10 min. The resulting mixture was then allowed to stir at 0 °C for 3 h, which was diluted using 1 N HCl (50 mL). The diluted aqueous solution was extracted in to dichloromethane. The crude residue was obtained by removing the solvent under reduced pressure followed by washing with saturated $NaHCO_3$ (2 X 25 mL), water (30 mL) and brine (30 mL). The resultant residue was purified by column chromatography with 60-120 mesh silica gel using petroleum ether as the eluent. The obtained bromo derivative (1 g, 1.82 mmol) was further subjected in to reflux with stirring using sodium azide (0.59 g, 9.1 mmol) in acetonitrile (10 mL), the solvent was removed under vacuum after 16 h of reflux. The resultant residue was

dissolved in water and extracted in to ethyl acetate, the pure compound was obtained without any further purification by removing the solvent using rota evaporation. Yield: yellowish oil, 0.81 g (1.58 mmol, 87 %). ^{1}H NMR (400 MHz, $CDCl_3$) δ 4.16 (*s*, 2H), 2.59 (*t*, *J* = 8 Hz, 2H), 2.1 – 1.98 (*m*, 9H), 1.84 – 1.73 (*m*, 2H), 1.57 – 1.05 (*m*, 24H), 0.87 – 0.83 (*m*, 12H). ESI-MS: 514.3 $[M+H]^+$.

General procedure for click reaction: To a stirred solution of alpha-tocopheryl-2-azidoacetate (Toc-N_3) in THF:*tert*-BuOH:H2O (2:2:1; 20 ml) were added $CuSO_4.5H_2O$ (0.1 mmol), sodium ascorbate (0.4 mmol) and corresponding acetylene-derivative 1 mmol (boc-propargylamine (i), but-3-yn-1-ol (ii), hex-1-yne (iii)) separately. The resulting mixture was stirred at room temperature until complete conversion of the starting material, which was diluted with excess of water (100 mL) then extracted in to ethyl acetate (3X 50 mL) and dried upon anhydrous $NaSO_4$ followed by removing the solvent under reduced pressure. The compound showing the R_f in the range 0.3 – 0.6 in 9:1 $CHCl_3$: MeOH, was purified using column chromatography with the eluent 1-3% MeOH: $CHCl_3$.

Boc-TTNH$_3$: pale yellow liquid, yield (0.539 g, 80.63%) ^{1}H NMR (400 MHz, $CDCl_3$) δ 7.75 (*s*, 1H), 5.43 (*s*, 2H), 5.13 (*s*, 1H), 4.43 (*d*, *J* = 8 Hz, 2H), 2.57 (*t*, *J* = 8 Hz, 2H), 2.08 – 1.95 (*m*, 9H), 1.84 – 1.73 (*m*, 2H), 1.54 – 1.06 (*m*, 33H), 0.87 – 0.83 (*m*, 12H). ESI-MS: 669 $[M+H]^+$.

Int. TTOH: yellowish gummy solid, yield (0.5 g, 85.76%) ^{1}H NMR (400 MHz, $CDCl_3$) δ 7.68 (*s*, 1H), 5.44 (*s*, 2H), 4.03 (*s*, 2H), 2.98 (*s*, 2H), 2.58 (*t*, *J* = 8 Hz, 2H), 2.08 – 1.95 (*m*, 9H), 1.83 - 1.73 (*m*, 2H), 1.54 – 1.07 (*m*, 24H), 0.87 – 0.83 (*m*, 12H). ESI-MS: 584 $[M+H]^+$.

Int. TTC$_4$: white gummy solid, yield (0.48 g, 80.67%) ^{1}H NMR (400 MHz, $CDCl_3$) δ 9.3 (s, 1H), 5.95 (s, 2H), 2.70 (t, *J* = 8 Hz, 2H), 2.27 (t, *J* = 8 Hz, 2H), 2.01 – 1.92 (m, 9H), 1.78 – 1.62 (m, 4H), 1.54 – 1.12 (m, 28H), 0.91 – 0.83 (m, 12H). ESI-MS: 596 $[M+H]^+$.

Synthesis of lipid TTNH$_3$: To a stirred solution of boc-$TTNH_3$ (0.5 g, 0.75 mmol) in 10 mL of dry DCM was added 0.5 mL of TFA slowly at 0 ºC, and continued

the stirring at room temperature for about 6 h. To remove the excess TFA present in reaction mixture was exposed to repeated rota evaporations by adding excess ethyl acetate. Finally the pure title lipid was obtained by subjecting the quaternized triflouroacetate salt to repeated chloride ion exchange chromatography using Amberlyst A-26 chloride ion exchange resin and about 100 mL of chloroform as eluent. Yield: Colorless oil, 0.42 g (0.74 mmol, 98.82%). ^{1}H NMR (400 MHz, $CDCl_3$) δ 8.01 (*s*, 1H), 5.42 (*s*, 2H), 4.27 (*s*, 2H), 2.54 (*t*, *J* = 8 Hz, 2H), 2.05 – 1.90 (*m*, 9H), 1.76 – 1.69 (*m*, 2H), 1.54 – 1.01 (*m*, 24H), 0.87 – 0.83 (*m*, 12H). ^{13}C NMR (100 MHz, $CDCl_3$) δ 165.39, 149.79, 139.98, 126.32, 124.79, 123.25, 117.66, 75.21, 50.49, 39.37, 37.41, 34.50, 32.80, 30.97, 27.98, 24.82, 24.47, 22.74, 21.03, 20.12, 19.69, 12.77, 11.83. ESI-MS (HRMS): Calcd for $[C_{34}H_{57}N_4O_3^+]$: 569.4425, Found: 569.4507.

Synthesis of lipid TTOH: To an obtained click intermediate TTOH (0.45 g, 0.77 mmol) in 5 mL of acetonitrile was added 0.5 mL of methyl iodide. The resulting mixture was refluxed in sealed tube for about 48 h at 80 ºC, until the complete conversion of starting material monitored by TLC. Consequently, the pure quaternized iodide salt was obtained by removing the solvent under reduced pressure which was subjected to anion exchange resin to afford pure titled lipid. Yield: yellowish white gummy solid, 0.44 g (0.74 mmol, 95.65%). ^{1}H NMR (400 MHz, $CDCl_3$) δ 9.10 (s, 1H), 5.98 (s, 2H), 4.34 (s, 3H), 4.04 (s, 2H), 3.17 (t, *J* = 8 Hz, 2H), 2.59 (t, *J* = 8 Hz, 2H), 2.09 – 2.02 (m, 9H), 1.83 – 1.77 (m, 2H), 1.55 – 1.08 (m, 24H), 0.87 – 0.83 (m, 12H). ^{13}C NMR (100 MHz, $CDCl_3$) δ 163.98, 149.96, 142.99, 139.96, 126.41, 124.85, 123.34, 117.71, 75.30, 58.77, 53.65, 39.37, 38.51, 37.40, 32.79, 30.94, 29.71, 27.99, 27.19, 24.84, 24.64, 22.65, 21.03, 20.57, 19.69, 13.21, 12.41, 11.83. ESI-MS (HRMS): Calcd for $[C_{36}H_{60}N_3O_4^+]$: 598.4578, Found: 598.4690.

Synthesis of lipid TTC_4: To an obtained click intermediate TTC_4 (0.45 g, 0.76 mmol) in 5 mL of acetonitrile was added 0.5 mL of methyl iodide. The pure white amorphous solid was obtained by following the same procedure mentioned at lipid TTOH. Yield: white amorphous solid, 0.4 g (0.66 mmol, 86.95%). ^{1}H NMR (400 MHz, $CDCl_3$) δ 9.49 (s, 1H), 6.36 (s, 2H), 4.28 (s, 3H), 2.90 (m, *J* = 8 Hz, 2H), 2.57 (t, *J* = 8

Hz, 2H), 2.07 – 2.03 (m, 9H), 1.80 – 1.72 (m, 4H), 1.52 – 1.07 (m, 28H), 0.96 (t, J = 8 Hz, 3H), 0.87 – 0.83 (m, 12H). ^{13}C NMR (100 MHz, $CDCl_3$) δ 165.20, 149.88, 149.10, 139.91, 126.27, 124.63, 123.40, 122.01, 117.67, 75.26, 50.61, 39.38, 37.40, 32.79, 31.45, 30.94, 29.72, 27.99, 25.33, 24.83, 24.45, 22.65, 22.25, 21.02, 20.58, 19.70, 13.84, 12.99, 12.15, 11.84. ESI-MS (HRMS): Calcd for [$C_{38}H_{65}N_3O_3^+$]: 611.5020, Found: 611.5021.

4.3.4 Preparation of liposomes: Cationic liposomes were prepared by mixing the desired quantities of cationic lipid and co-lipid (DOPE) from separately dissolved chloroform stocks. The solvent was evaporated uniformly using a thin flow of moisture free nitrogen gas. The resulted thin films were rehydrated using appropriate volume of deionized water to swell the films by overnight. These films were converted to multilamellar vesicles by using a frequent vertex. At last, optically clear aqueous suspensions were obtained by subjecting the MLV's to sonication in an ice bath using SONICS Vibra cell (25% Amplitude, pulse mode, 9 s on/off). The newly prepared clear aqueous suspensions were stored at 4 ºC until use.

4.3.5 Size & zeta (ζ) potential measurements: Cationic liposomes derived from cationic lipid and co-lipid (DOPE), complexes derived from liposome and DNA both were characterized with respect to their size and zeta potential using the instrument called SZ-100 NEXTGEN (HORIBA) equipped with a diode-pumped solid-state laser at λ 532 nm calibrated at 25°C. The size of the particle in diameter obtained by an average of three different measurements was done in general mode. In order to gets the information regarding the stability and charge of the dispersed particles, measurement of zeta potentials have to be done. These measurements were also carried in the same instrument using Laser Doppler Electrophoresis analysis provided by SZ-100 software. Here, Milli-Q served as the blank control for instrument autocorrelation and sample dilutions.

4.3.6 Transmission Electron Microscope (TEM): The particle size distribution and morphological appearance of both SUV's and their derived complexes were examined under Transmission Electron Microscope. Briefly, 6 µL of a sample was

spreaded on to a Cu grid coated with Formvar-film. After 60 sec, the excess liquid was absorbed on to a filter paper and allowed to stain using 5 µL of 2% uranyl acetate. This was followed by removal of excess stain using fresh filter paper, and dried in atmospheric pressure at room temperature and visualized under JEOL JEM 2100 Transmission Electron Microscope operated at 120 kV. The images were acquired on a Gatan camera, Digital Micrograph software.

4.3.7 Agarose-gel electrophoresis: To assess the DNA binding abilities of optimized cationic co-liposomal formulations (lipid/DOPE) agarose gel retardation assay was performed. In a typical experiment, 400 ng of pCMV-βgal was complexed with each cationic formulation by maintaining different N/P (lipid/plasmid) charge ratios in 0.5 X PBS (20 µL). These complexes were loaded on to a freshly prepared 1% agarose gel after 25 min of complex incubation followed by adding 6X loading dye to each sample. Electrophoresis was done for about 90 min in 1mm TAE running buffer in an electrophoresis chamber set at 70 V. Gel images were captured under the gel documentation system in transillumination mode after the DNA staining using EtBr for 30 min post electrophoresis.

4.3.8 Amplification and purification of plasmid DNA: *p*CMV-βgal and *p*EGFP-N_3 plasmids were used in *in vitro* gene transfection studies which are being meant for β-galactosidase reporter gene expression and green fluorescent gene expression respectively. Both the plasmids were prepared from laboratory stocks, were initially transformed into competent *E. coli* DH-5α cells and amplified in LB broth media at 37 °C overnight. The endotoxin free pure plasmids were isolated using the NucleoBond® Xtra Midi kit (MACKAREY-Nagel). Then the resultant plasmids were dissolved in TE buffer solution and stored at -20 °C. The integrity, purity and concentrations of plasmids were confirmed by agarose-gel electrophoresis and Nano Drop 2000 respectively.

4.3.9 Cells & cell culture: B16F10 (human melanoma carcinoma derived), CHO (Chinese hamster ovary), HEK-293 (human embryonic kidney), HepG2 (human hepatocarcinoma derived) and Neuro-2A (mouse neuroblastoma) cell lines were used

from our laboratory maintenance cultures. Cells were cultured at 37 °C in Dulbecco's modified Eagle's medium (DMEM, invitrogen) supplemented with 10% (v/v) Fetal Bovine Serum (FBS), 10 mM $NaHCO_3$, 60 µg/mL penicillin, 50 µg/ml streptomycin and 30 µg/ml kanamycin in a humidified atmosphere containing 5% CO2.

4.3.10 Transfection biology: To investigate the DNA transfection capacities of all novel cationic co-liposomal formulations, two different reporter genes were used such as pCMV-βgal for beta galactosidase expression and pEGFP-N_3 for enhanced green fluorescence expression. The expressions of both reporter genes were quantified and reported in terms of miller units of β-galactosidase and statistics of Fluorescence-activated cell sorting (FACS) applied in flow cytometry. The experimental protocols were followed for two different plasmids were different.

Briefly, the β-gal assay using pCMV-βgal DNA was done in 96 well plate after seeding the cells at the density of 10,000/well a day prior to transfection. On the day of transfection lipoplexes were prepared using co-liposomal formulation and *p*CMV-βgal DNA (0.3 µg/well) at varying range of charge ratios in 100 µL of serum free media. These resulted complexes were incubated at room temperature for about 25 min, following which the serum containing media from cells was removed and washed with 1XPBS. After 25 min of incubation, the complexes were diluted to formulate the final transfection complex using serum free media. This was followed by addition of complexes in to the wells in a triplicate manner, and allowed the cells for incubation in an atmosphere where the 5% CO_2 and 95% humidity was supplied for about 4 h. The complex media was replaced by 10% serum media (0.3 mL/well) and continued the incubation for about 48 h in same atmosphere and assayed by following the protocol as mentioned earlier.[36]

In addition the second plasmid pEGFP-N_3 was used in transfection by allowing the cells to grow in 24 well plate to reach the confluence by 70%. Briefly, cells were seeded at a density of $4x10^4$ cells per well a day before the transfection. After reaching the cells required confluence, lipoplexes were prepared with *p*EGFP-N_3 plasmid (0.8µg/well) using the lipid formulations at varying range of N/P charge ratios mentioned in results and incubated for about 25 min in serum free media. Following

which the lipoplexes were formulated to final transfection complex using either – FBS+DMEM or +10% FBS+DMEM as per the requirement and transferred to cells. The complex containing cells were incubated in CO_2 incubator for about 4 h after the addition. The added complex media was replaced with 10% serum containing media and continued to incubate to complete 48 h of transfection period. DMEM (without any complex), lipoplex formulated with Effectene (commercially available formulation) and DDAB:DNA served as the controls. The transfection efficiencies were analyzed by capturing the images under the fluorescence microscope Floid cell imaging station for qualitative visual comparison and the cells were subjected to flow cytometry to analyze the fluorescence.

4.3.11 Transfection in Presence of Serum: In order to determine the sensitivity of the lipoplexes towards the serum, we performed the transfection in presence of increasing concentrations of serum using pCMV-βgal. Briefly, cells were seeded at a density of 10,000 cells per well in a 96-well plate 18-24 h before the transfection. Then the complexes were prepared using 0.3 μg/well of plasmid DNA was mixed with the lipids (L1-3) at transfection optimized charge ratio (1:1) in DMEM in presence of increasing concentrations of added serum (10-50% v/v).Then the final transfection complex was formulated by using the appropriate volume of DMEM and allowed to incubate for about 25 min. Further, the assay was performed similarly as mentioned in earlier sections.

4.3.12 Flow cytometry: In order to quantify the expression of EGFP reporter cassette via transfection, flow cytometry of cells treated with lipoplex formulations was performed after 48 h. Following this period of incubation, growth media was removed and cells were washed with PBS followed by the addition of 100 μL of 0.1% trypsin/EDTA. The detached cells were dispersed by pipetting, followed by resuspension in 400 μL of PBS supplemented with 10% serum. The pooled cells were analyzed using a FACS caliber system equipped with an argon ion laser at 488 nm for excitation and detection at 530 nm. 10,000 cells were analyzed for each sample using the software, CellQuest. Non transfected cells served as live cell controls for gate settings

which in turn provided the cutoff thresholds for quantification of fluorescent cell population.

4.3.13 Uptake & co-localization: The qualitative intracellular trafficking of fluorescent labelled lipoplex was achieved via live cell analysis and imaging in confocal microscopy. Briefly, HEK293 cells were seeded on to a two chambered coverglass (Nunc™ Lab-Tek™) 50,000 cells/chamber a day prior to transfection. Lipoplexes were prepared using pCMV-βgal DNA (1 µg/chamber) complexing with fluorescent (rhodamine-PE) labelled cationic liposome formulation of $TTNH_3$, TTOH and TTC_4 in serum free DMEM. After 30 min incubation at room temperature the lipid/DNA complex was formulated to final transfection complex to be in 10% FBS+DMEM was transferred to coverglass chambers in duplicates and allowed 1 h incubation in incubator (37 ºC, CO_2). The fluorescent reagents like DAPI (blue, nucleus) and Lysotracker (green, lysosome) were mixed in required quantity in one aliquot of serum+DMEM and transferred to each chamber of coverglass after incubation of complex to stain cell counter parts. This was followed by 30 min incubation (37 ºC, CO_2) and then analyzed under confocal laser scanning microscope (Leica TCS S52) at various emission collection wavelengths corresponds to three different fluorescent probes as described before.[37] Localisation of the fluorescent labels red (lipid), green (Lysotracker) and blue (DAPI) were analysed using LAS X imaging platform to determine the location of lipoplexes with respect to the nucleus and lysosomes.

4.3.14 MTT assay for cell viability: The cationic lipid formulations were screened for their toxicities by following the MTT based assay which involves the reduction of 3-(4, 5-dimethylthiazole-2-yl)-2, 5-diphenyltetrazolium bromide (MTT) by viable cells will produce purple colored insoluble formazan granules. The intensity of the color is related to the number of viable cells and it is measured by colorimetric analysis. In order to measure the viabilities of the complexes derived from these lipids, cells were seeded on to 96 well plate 18 to 20 h of prior to the complex addition. Followed by which cells were incubated for 4 h in CO_2 incubator, then the complexes were replaced by complete DMEM to continued the incubation further 24 h. MTT dye

(0.5 mg/ml) was prepared freshly in serum free DMEM was added 100 µL to each well and allowed for incubation, 3 h of prior to termination of the assay. Finally, the media was removed and added 100 µL of MeOH:DMSO (1:1, v/v) to each well. This dissolves purple colored dye, was then measured by spectroscopically at 540 nm in a multiplate reader, Multiscan spectrum and the untreated cells served as the controls. Results were expressed as percent viability =A_{540} (treated cells) - background/A_{540} (untreated cells) - background X 100.

4.4 REFERENCES

1. Mintzer, M. A.; Simanek, E. E. *Chem Rev.* **2008**, *109*, 259.
2. Jin, L.; Zeng, X.; Liu, M.; Deng, Y.; He, N. *Theranostics*, **2014**, *4*, 240.
3. Draghici, B.; Marc, A. I. *J. Med. Chem.* **2015**, *58*, 4091.
4. Junquera, E.; Aicart, E. *Curr. Top. Med. Chem*. **2014**, *14*, 649.
5. Jones, C. H.; Chen, C. K.; Ravikrishnan, A.; Rane, S.; Pfeifer, B. A. *Mol Pharm*. **2013**, *10*, 4082.
6. Bhattacharya, S. and Bajaj, A. *Chem. Commun.* **2009**, *31*, 4632.
7. Srinivas, R.; Samanta, S.; Chaudhuri, A. *Chem. Soc. Rev*. **2009**, *38*, 3326.
8. Zhi, D.; Zhang, S.; Cui, S.; Zhao, Y.; Wang, Y.; Zhao, D. *Bioconj Chem*. **2013**, *24*, 487.
9. Zhi, D.; Zhang, S.; Wang, B.; Zhao, Y.; Yang, B.; Yu, S. *Bioconj Chem.* **2010**, *21*, 563.
10. Rao, N, M.; Gopal, V. *Expert Opin. Ther. Pat.* **2006**, *16*, 825.
11. Karmali, P. P.; Choudary, A. *Med. Res. Rev.* **2007**, *27*, 696.
12. Maslov, M. A.; Syicheva, E. V.; Morozova, N. G.; Serebrennikova, G. A. *Russ. Chem. Bull*, **2000**, *49*, 385-401.
13. Solodin, I.; Brown, C. S.; Bruno, M. S.; Chow, C. Y.; Jang, E. H.; Debs, R. J.; Heath, T. D.; *Biochemistry*, **1995**, *34*, 13537.
14. Sharma, V. D.; Ilies, M. A. *Med. Res. Rev.* **2014**, *34*, 1.
15. Van Der, W. I.; Wagenaar, A.; Meekel, A. A.; Ter Beest, M. B.; Ruiters, M. H.; Engberts, J. B.; Hoekstra, D. *Proc. Natl. Acad. Sci.* **1997**, *94*, 1160.

16. Parvizi-Bahktar, P.; Mendez-Campos, J.; Raju, L.; Khalique, N. A.; Jubeli, E.; Larsen, H.; Nicholson, D.; Pungente, M. D.; Fyles, T. M. *Org. Biomol. Chem*. **2016**, *14*, 3080.
17. Kumar, K.; Barrán-Berdón, A. L.; Datta, S.; Muñoz-Úbeda, M.; Aicart-Ramos, C.; Kondaiah, P.; Junquera, E.; Bhattacharya, S.; Aicart, E. *J. Mater. Chem. B*. **2015**, *3*, 1495.
18. Misra, S. K.; Muñoz-Úbeda, M.; Datta, S.; Barrán-Berdón, A. L.; Aicart-Ramos, C.; Castro-Hartmann, P.; Kondaiah, P.; Junquera, E.; Bhattacharya, S.; Aicart, E. *Biomacromolecules*, **2013**, *14*, 3951.
19. Kolb, H. C.; Sharpless, K. B. *Drug. Discov. Today.* **2003**, *8*, 1128.
20. Rostovtsev, V. V.; Green, L. G.; Fokin, V. V.; Sharpless, K. B. *Angew. Chem.* **2002**, *114*, 2708.
21. Tornøe, C. W.; Christensen, C.; Meldal, M. *J. Org. Chem.* **2002**, *67*, 3057.
22. Patil, S. P.; Kim, S. H.; Jadhav, J. R.; Lee, J. H.; Jeon, E. M.; Kim, K. T.; Kim, B. H. *Bioconj. Chem.* 2014, **25**, 1517-1525.
23. Barnard, A.; Posocco, P.; Pricl, S.; Calderon, M.; Haag, R.; Hwang, M. E.; Shum, V. W.; Pack, D. W.; Smith, D. K. *J. Amer. Chem. Soc.* **2011**, *133*, 20288.
24. Lauria, A.; Delisi, R.; Mingoia, F.; Terenzi, A.; Martorana, A.; Barone, G.; Almerico, A. M. *Eur. J. Org. Chem.* **2014**, *16*, 3289.
25. Dua, J. S.; Rana, A. C.; Bhandari, A. K. *Int. J. Pharm. Stud. Res.* **2012**, **3**, 14.
26. Chia-Hua, L.; Tzung-Han, C. *Chem. Phys. Lipids.* **2009**, *158*, 81.
27. Ruozi, B.; Forni, F.; Battini, R.; Vandelli, M. A. *J. Drug Target*. **2003**, *11*, 407.
28. Hattori, Y.; Nakamura, A.; Arai, S.; Kawano, K.; Maitani, Y.; Yonemochi, E. *J. Liposome Res.* **2015**, *25*, 279.
29. Bajaj, A.; Paul, B.; Kondaiah, P.; Bhattacharya, S. *Bioconjug. Chem.* **2008**, *19,* 1283.
30. Zuhorn, I. S.; Visser, W. H.; Bakowsky, U.; Engberts, J. B.; Hoekstra, D. *Biochim. Biophys. Acta.* **2002**, *1560*, 25.
31. Kumar, K.; Maiti, B.; Kondaiah, P.; Bhattacharya, S. *Org. Biomol. Chem.* **2015**, *13*, 2444.
32. Majeti, B. K.; Karmali, P. P.; Madhavendra, S. S.; Chaudhuri, A. *Bioconjug Chem.* **2005**, *16*(3), 676.

33. Singh, R. S.; Mukherjee, K.; Banerjee, R.; Chaudhuri, A.; Hait, S. K.; Moulik, S. P.; Ramadas, Y.; Vijayalakshmi, A.; Rao, N. M. *Chem. Eur. J*, **2002**, *8*(4), 900.
34. Lv, H.; Zhang, S.; Wang, B.; Cui, S.; Yan, J. *J. Control. Releas*e. **2006**, *1*, 100.
35. Hansen, M. B.; Nielsen S. E.; Berg, K. *J. Immunol Methods.* **1989**, *119*, 203.
36. Gopal, V.; Xavier, J.; Kamal, M. Z.; Govindarajan, S.; Takafuji, M.; Soga, S.; Ueno, T.; Ihara, H.; Rao, N. M. *Bioconjug Chem.* **2011**, *22*, 2244.
37. Meka, R.R.; Godeshala, S.; Marepally, S.; Thorat, K.; Rachamalla, H. K. R.; Dhayani, A.; Hiwale, A.; Banerjee, R.; Chaudhuri, A.; Vemula, P. K. *RSC Advances*, **2016**, *81*, 77841.

Chapter 5

●●●●●

Evolution of New "Bolaliposomes" using Novel α-Tocopheryl Succinate Based Cationic Lipids and 1, 12-Disubstituted Dodecane Based Bolaamphiphile for Efficient Gene Delivery

5.1 INTRODUCTION

Gene therapy has fascinated researchers because of its increasing success rate in clinical trials during the last two decades.[1,2] However, the concept is yet to reach its maximum therapeutic goal in clinical conditions. Moreover, gene therapy is severely daunted by one major hurdle, i.e., successful delivery of the therapeutic material to the target cell. Cutting-edge technology has been used in the development of the most ideal carrier that can be either viral or non-viral-based carrying reagents. [3,4] Non-viral delivering reagents are more preferred than the viral reagents because the latter is associated with non-compiling features of virus like immunopathogenicity, expensive handling techniques, and low-scale production.[5,6] In fact, many diverse nano-vectorizations such as cationic vectors (DOTMA, DOSPA), polymeric vectors (PLL, PEI), dendrimer vectors (PAMAM, PPI), polypeptide-based vectors (TAT, MPG peptides), and nanoparticles (quantum dots, gold nanoparticles, carbon nanotube)[5,7] belong to non-viral category. These nano-vectorizations have been built to increase transfection of oligonucleotide sequences in various cell lines having diverse origins. Among the explored non-viral carrying systems, cationic lipids have drawn significant attention due to their ease of construction, lower toxicity, and large-scale productivity.[8-10]

Despite the associated barriers like lower transfection and toxicity of synthetic materials, much interest has been focused on developing new motifs to overcome these barriers. In general, cationic lipids can self assemble to produce nano-aggregates termed as '*liposome*'.[11] Liposomes of cationic lipids were developed in aqueous solution either by mixing with any one of the helper lipids like DOPE, DOPC, cholesterol, etc., or alone, called as '*co-liposomal formulation'*.[12,13] Most of the related literature have focused on the modifications of various backbones of cationic lipids and the development of novel formulations to achieve better performances.[14] Studies have also examined the safety and efficiency of nanomedicines in the multifaceted delivery of therapeutic molecules by using fat soluble 'tocol' family.[15-18] Given this background, the present study attempts to further develop efficient cytofectins using newly synthesized tocopherol-based cationic lipids by optimizing their concentrations so as to probe the stable transfection. Alpha-tocopheryl succinate (TOS, RRR-stereoisomer) is an esterified, redox-silent analog of vitamin E with unique biological properties like selective induction of apoptosis and can

act as a radio sensitizer, thus making it important in integrative cancer care.[19-22] Since Youk et al.[23] reported the enhancement of selective anticancer efficacy of TOS by increasing its polarity in 2004, TOS has become an interesting molecule in the developments of cancer care. Importantly, any cationic lipid for better transfection has to be composed either of multiple amines or various types of amines such as quaternary, protonated, and tertiary; this is an important aspect in the design of gene delivery vectors since these enhance DNA condensation and endosomal buffering capacity.[24] Moreover, the studies has also proved that the use of delocalizable charge in head group facilitates potential delivery of nucleic acid with reduced toxicities due to the soft cationic nature of delocalizable cation and creates lesser hydration potential while giving flexibility in binding and intracellular release of DNA.[25] Based on these findings of prior studies, two cationic lipids (TOS-Toc, TOS-C12) were synthesized using TOS as common lipid backbone and 1, 2, 3-triazolium as common lipid head group (Fig. 1).

In addition, the surfactants dissimilar with regular cationic lipid structure having dual hydrophilic centers on either side of single hydrophobic backbone became an interesting tool due to their impressive efficiencies in delivery of nucleotide.[26,27] These surfactants are referred to as '*bolaamphiphile'* and can produce aqueous suspended monolayer nano-aggregates termed as '*bolasome'*.[28-30] Among the natural amino acid residues, an aromatic amino acid-phenylalanine residue has distinct features like playing key roles in membrane channel gating functions and the formation of deleterious amyloid structures. Phenylalanine (Phe) residues in particular have been identified as a key component in the formation of amyloid structures.[31] In addition, Phe is a unique molecule in terms of its propensity for self-assembly. Furthermore, short peptides composed solely of phenylalanine are known to self-assemble into ordered nanostructures in water.[32] Considering the biological importance and self-assembling nature of phenylalanine, we designed and synthesized a disubstituted dodecane-based symmetrical bolaamphiphile. It constitutes l-phenylalanine conjugated on either side of dodecane chain via 1, 2, 3 triazole linker to produce dodecane-based cationic symmetrical bolaamphiphile (DBTPA) (Fig. 1).

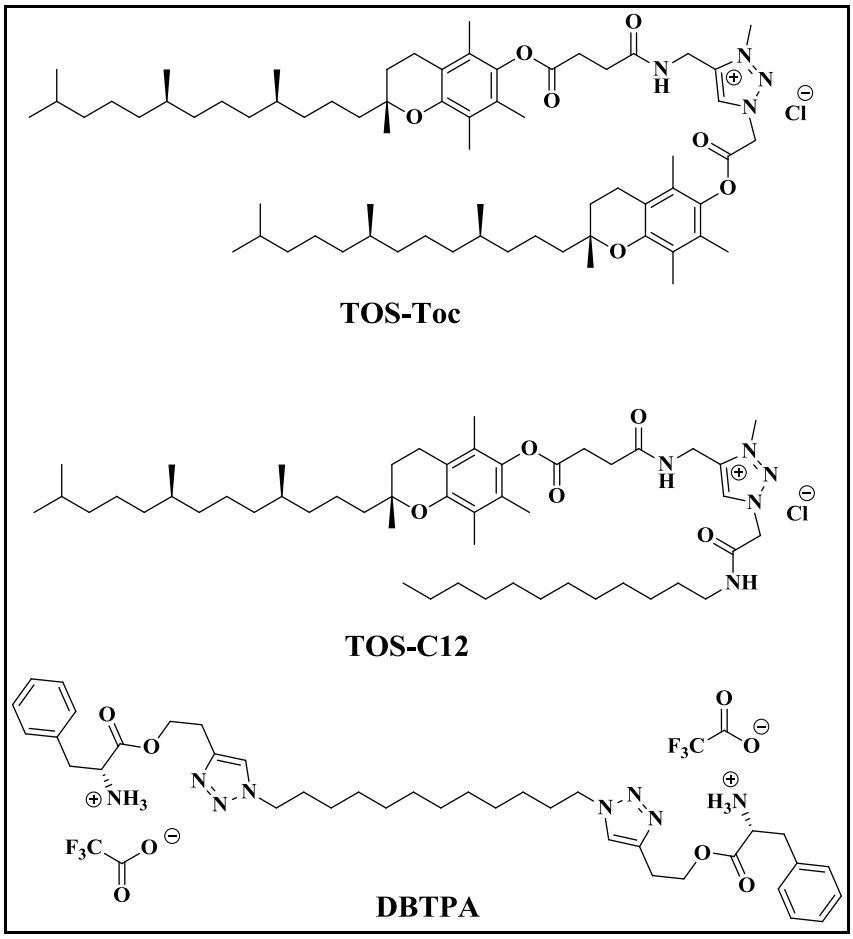

Fig. 1: Molecular structures of cationic lipids (TOS-Toc, TOS-C12) and cationic bolaamphiphile (DBTPA)

Herein, we report efficient transfection potentials of new cationic lipid formulation generated from two distinct cationic surfactants such as cationic lipid and bolalipid. Both newly synthesized bolalipid and cationic lipids were used to formulate vesicles using individual and mixed formulations. The aggregates were produced by mixing two distinct cationic surfactants and were better transfecting aggregates than the individually developed aggregates. These newly prepared mixed aggregates are termed as "*Bolaliposomes,*" which were characterized in terms of their size, shape and morphology using different physicochemical investigations. Their DNA complexation interactions were also studied using gel electrophoresis and EtBr intercalation assays. All the transfection studies were conducted using the plasmid *p*EGFP-N_3, and the quantified

expressed protein in terms of statistics (% GFP positive cells & GMFI's) derived from FACS based analysis were reported in the results. The uptake pathways of DNA-derived complexes were also studied with the help of transfection efficiencies using various endocytosis inhibitors at optimized concentrations. MTT assay was used to determine the toxicities of both neat individual formulations, and the DNA derived complexes of new bolaliposomes proved that these formulations are lower in creating toxicity towards all the studied cell lines.

5.2 RESULTS AND DISCUSSION

5.2.1 Chemistry: The molecular structures of cationic lipids (TOS-Toc, TOS-C12) and cationic bolaamphiphile (DBTPA) are shown in Fig. 1. Their synthesis process is detailed in Schemes 1 and 2, respectively. As demonstrated in Scheme 1, the alpha-tocopheryl succinate was coupled with propargylamine using a well-known peptide coupling reagent, i.e., EDCI.HCl was used for the acetylene derivative TOS-Ac. To introduce another hydrophobic moiety of the lipids, the acetylene derivative was further treated with an azide functional group of either alpha tocopheryl-2-azidoacetate or 2-azido-*N*-dodecylacetamide, followed by Huisgen 1, 3-dipolar cycloaddition strategy (click chemistry) so as to develop 1, 2, 3-triazole heterocyclic ring.[33] These click derived adducts (I and II) were subjected to methyl iodide quaternization to obtain iodide salts of 1, 2, 3-triazolium cation. Repeated passage of iodide salts on to the chloride ion exchange column yielded titled lipids TOS-Toc and TOS-C12 with chloride as a counter ion.

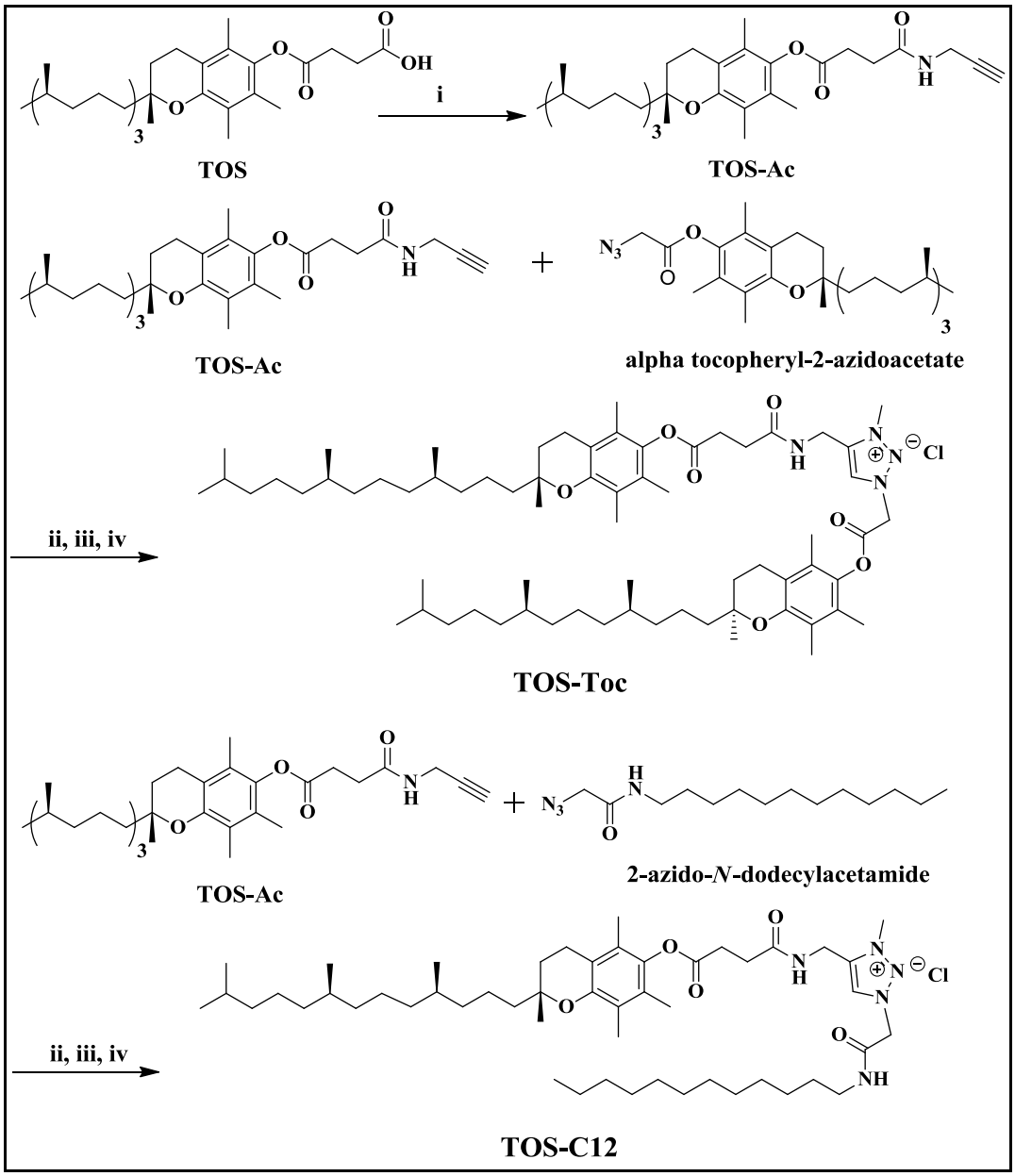

Scheme 1 Molecular structures and synthetic route of cationic amphiphile.

Reagents & conditions: i) Propargylamine, EDCI.HCl, DIPEA, DCM, 0 °C - RT, 16 h; ii) $CuSO_4.5H_2O$, sodium ascorbate, THF:H_2O:*tert*-BuOH (2:2:1), RT, 24 h; iii) Methyl iodide, acetonitrile, sealed tube, 80 °C, iv) amberlite chloride ion exchange resin.

On the other hand, cationic symmetrical bolaamphiphile (DBTPA) was synthesized by following the steps mentioned in Scheme 2, which includes synthesis of

acetylene derivative of boc-l-phenylalanine on an ester coupling reaction using 3-butyn-1-ol and DCC. The resulting acetylene derivative (1a) on cycloaddition reaction with azide functional group present on either side of 1, 12-diazidododecane by following the protocol (click chemistry) mentioned in Scheme 1 produced Boc-DBTPA (1c). The protected amines were protonated by removing the 'boc' on acidic conditions to afford titled bolalipid 'DBTPA,' having two protonated amines with trifluoroacetate as counter ion in hydrophilic part and dodecane in hydrophobic region. All the lipids and intermediates were characterized by using the spectroscopic techniques ^{1}H-NMR, ^{13}C-NMR and HRMS. The corresponding data is found to be consistent with its structures, and the purity of the lipids was confirmed by reverse phase analytical HPLC.

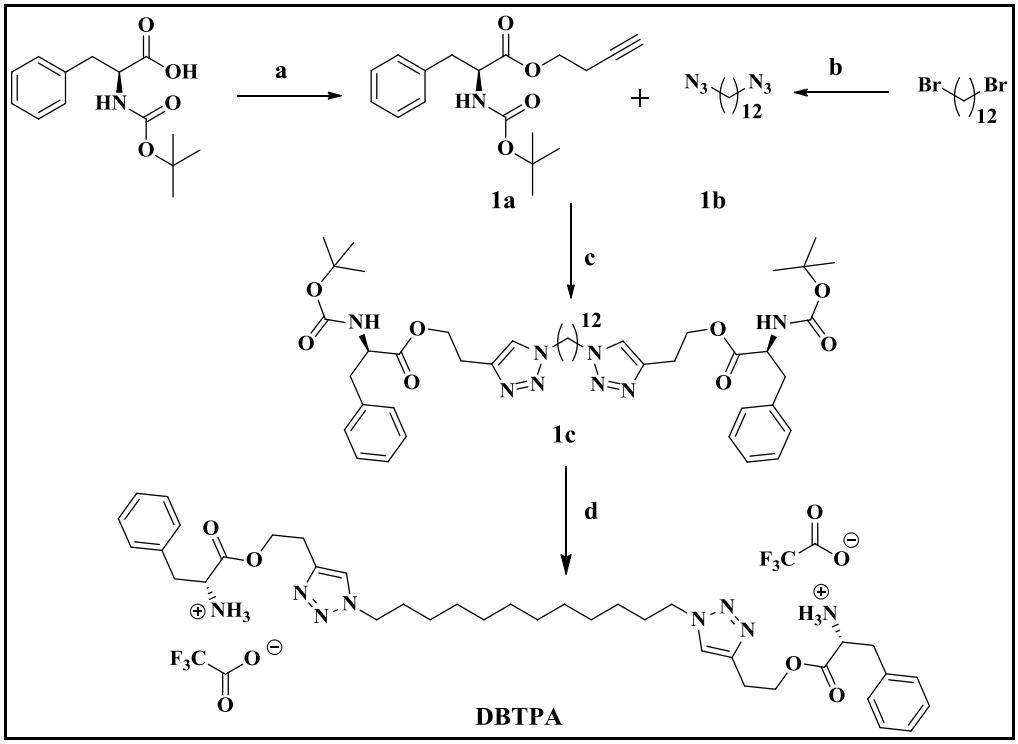

Scheme 2 Synthetic route and molecular structure of cationic bolaamphiphile.

Reagents and conditions: a) but-3-yn-1-ol, DCC, DCM, DMAP, RT, 24 h; b) NaN_3, ACCN, 80 °C, 16 h; c) $CuSO_4.5H_2O$, sodium ascorbate, THF:H_2O:*tert*-BuOH (2:2:1), RT, 24 h; d) 2:1 dry DCM: TFA.

5.2.2 Preparation of bolaliposomes: Preparation of bolaliposomes: Many prior establishments of non-viral vectors proved that mixed liposomal formulations (lipid/co-lipid) could enhance the transfection properties better than neat cationic formulation (lipid alone). [34] In fact, DOPE is a zwitter ionic phospholipid widely used as a helper lipid in most of the studies because of its fusogenic nature and non-bilayer structure formation that helps to disrupt the endosomal membrane after the cellular uptake of lipoplex into cytoplasm.[35] Initially, we aimed to develop lipid/DOPE (liposome) vesicles using various molar combinations of DOPE with both cationic lipids (TOS-Toc & TOS-C12), which resulted in suspensions that were neither clear nor effective in transfection (data not shown). To accomplish the plasmid delivery properties to these TOS derivatives, we extended our efforts to find better mixed formulation.

The common structural feature (C12 chain) of both the cationic lipids (TOS-Toc & TOS-C12) is interestingly found to be similar to the aliphatic backbone of newly synthesized bolalipid (DBTPA). This motivated us to make mixed formulations using these two diverse cationic lipids together. Considering the aggregation patterns discussed in previous studies, the patterns of self assembly of present formulations derived individually from cationic lipid, bolalipid and mixed cationic lipid/bolalipid were expected to form nano aggregates like liposome, bolasome, and bolaliposome, respectively, as represented in Fig. 2.

In order to get optimized transfection formulations, ten mixed formulations from each cationic lipid were prepared at varying concentration ranges from 1 to 10 mmol with 1 mmol of bolalipid (DBTPA) along with individual neat cationic liposomal and bolaliposomal formulations. The resulting dried thin lipid films were rehydrated by adjusting the final concentration as 1 mmol using autoclaved water and kept undisturbed overnight. According to the lipid hydration techniques mentioned earlier,[36] hydrated films were vortexed and sonicated at 0 °C to produce optically clear aqueous suspensions that were found to be stable even after 3 months when stored at 4 °C.

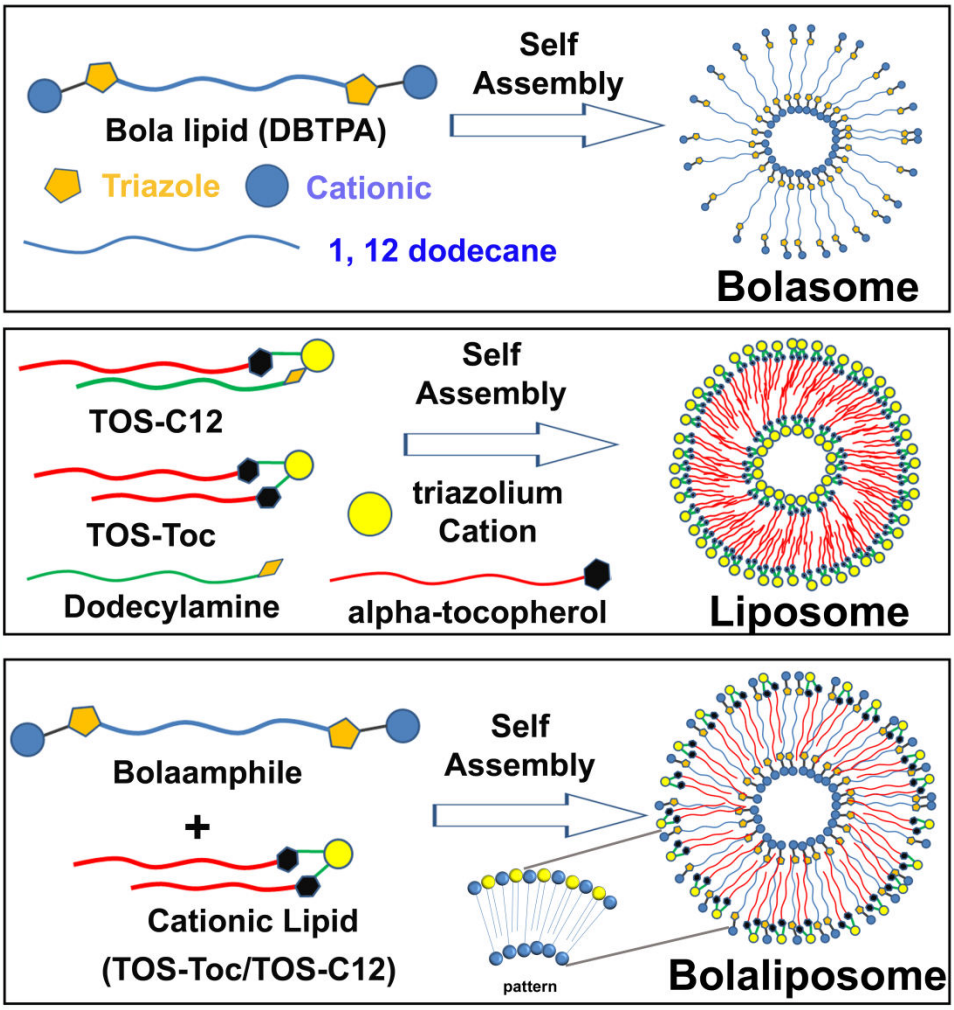

Fig. 2: Schematic of the distinct aggregates from cationic lipid and bolalipid

5.2.3 Transfection biology: Reporter gene expression assays are the most appropriate and useful techniques to determine the transfection capacities of newly produced lipid vesicles. To observe the DNA delivery capacities of all the formulations developed either by neat or mixed formulations, *p*EGFP-N_3 DNA was transfected into HEK293 cells using the lipoplexes derived from lipid suspension and DNA. Enhanced green fluorescence expression of transfected cells was visualized and captured under the fluorescent microscope (floid cell imaging station) for initial screening. These captured GFP fluorescent images are represented in Fig. 3 so as to assess the transfection efficiency qualitatively. Furthermore, the expressed fluorescence was quantified by

analyzing the cells using flow cytometry, which derived statistics such as % GFP positive cells and geometric mean fluorescence intensities (GMFI) as demonstrated in Fig. 4.

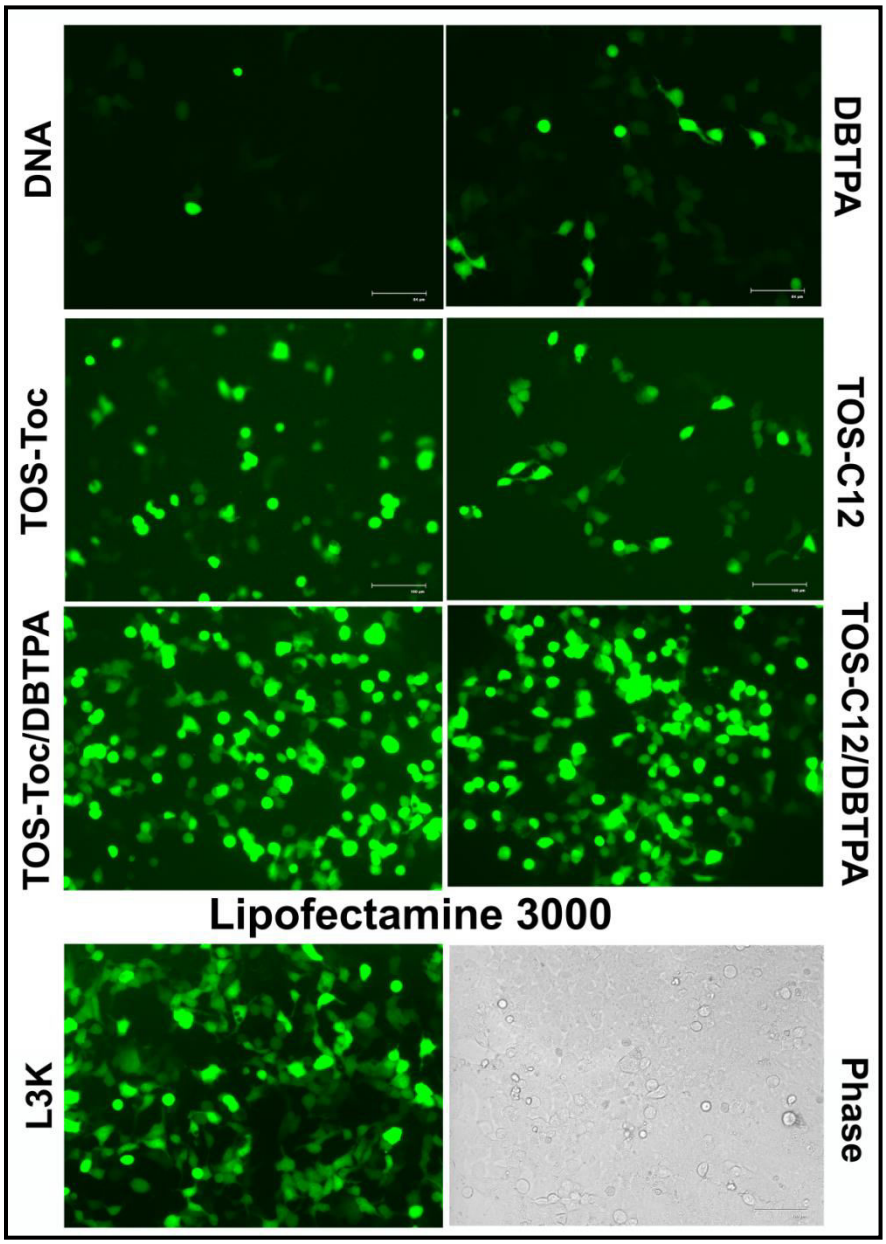

Fig. 3 Green fluorescence protein expression in HEK293 cell lines, treated with TOS-Toc and TOS-C12 at optimized mole ratio (4:1) and charge ratio (2:1) prepared with 0.8 µg pEGFP-N_3 plasmid. Images were captured under Floid cell imaging station 48 h of post transfection for visual comparison. Lipofectmine 3000 (L3K) was served as positive control.

As shown in Fig. 3 and Fig. 4, the transfection efficiencies of mixed formulations (lipid/bolalipid) are higher than the neat lipid formulations irrespective of cationic lipid (TOS-Toc/C12 & DBTPA). In Fig. 4, the % GFP positive cells and GMFI are important for the determination of the reporter gene activity by providing the number of transfected cells and the level of GFP expression of high intensity fluorescence of individual cells[37] respectively. The data confirmed that both mixed aggregates of cationic lipid:bolalipid (TOS-Toc/TOS-C12:DBTPA) exhibited efficiency almost at par with that of commercial golden standard, lipofectamine 3000 (L3K).

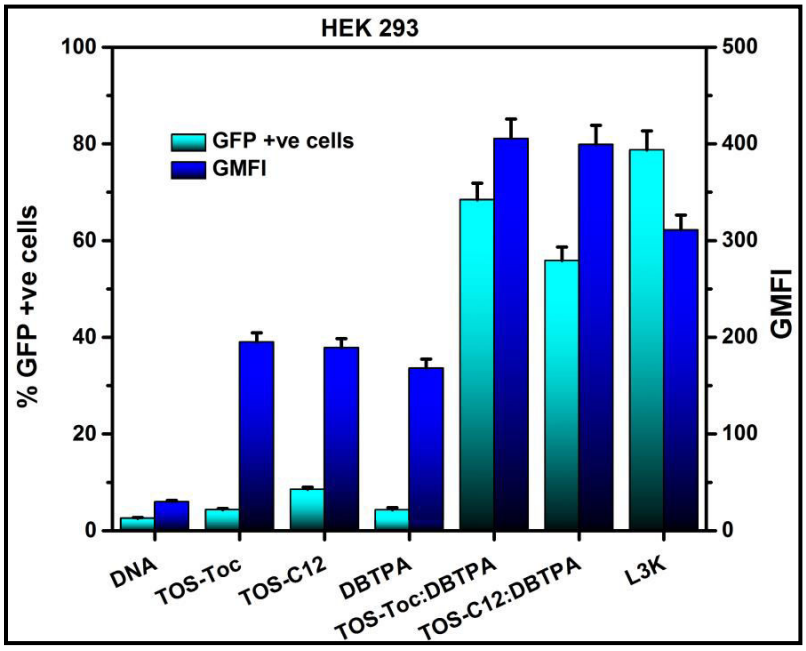

Fig. 4% positive GFP cells (cyan) and GMF intensities (blue) of *p*EGFP-N_3 plasmid transfection in HEK293 cell lines using TOS-Toc, TOS-C12, DBTPA and mixed formulations of TOS-Toc:DBTPA & TOS-C12:DBTPA at 2:1 N/P charge ratio. Complexes were prepared using 0.8 µg *p*EGFP-N_3 plasmid/well and incubated for 4 h in plain DMEM. Naked DNA and lipofectamine 3000 (L3K) were served as negative and positive controls respectively. All lipids were tested on the same day, and the data presented are the average of three experiments performed on three different days. The difference in the data obtained is statistically significant in all charge ratios.

Optimization of cationic lipid:bolalipid molar formulation and N/P charge ratio: The enhanced activity of transfection of lipid/bolalipid mixed aggregates relative to that of neat lipid formulations were thoroughly investigated by optimizing their molar and charge ratios. The exact mixing proportion of lipid/bolalipid, which is responsible for maximum transfection of *p*EGFP-N3 DNA, was scrutinized by considering the ten variety of formulations of each lipid ranging from 1:1 to 10:1 (TOS lipid: DBTPA; molar ratio) in HEK 293 cell line. The qualitative transfection analysis of these formulations infers that the maximum transfection efficiency is observed among the first four molar ratios, viz., 1:1, 2:1, 3:1 and 4:1 (Fig. 5). These particular molar ratios are further optimized for better transfection of N/P charge ratio by varying N/P charge ratios (2:1, 4:1, 6:1 and 8:1) with a constant amount (0.8 μg) of *p*EGFP-N_3 plasmid in HEK293 cell lines.

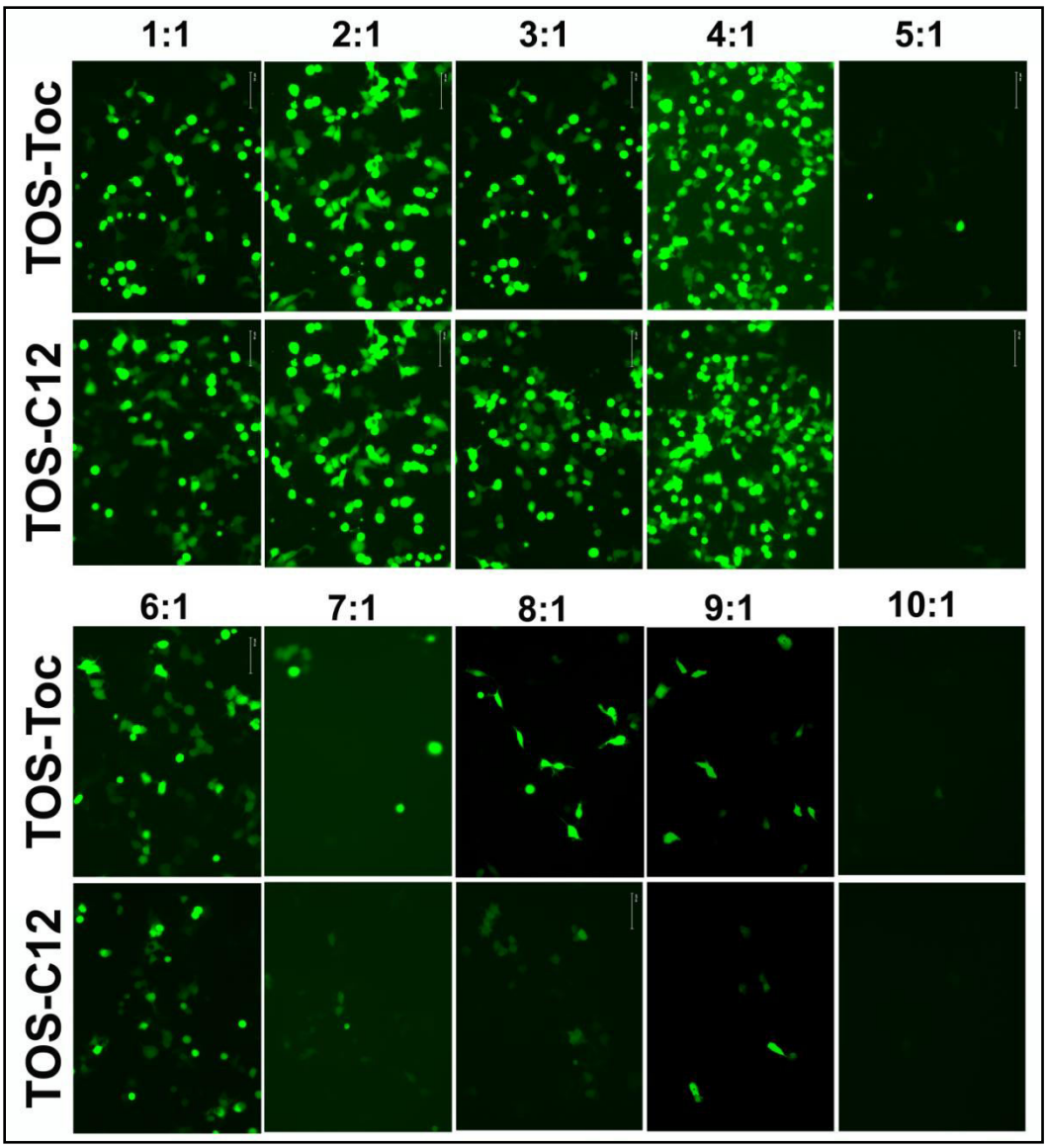

Fig. 5: Green fluorescence protein expression in HEK293 cell lines after the transfection using lipoplexes derived from pEGFP-N3 (0.8 µg/well) plasmid and mixed formulations developed from various molar ratios of TOS-Toc and TOS-C12 with constant DBTPA (1:1 to 10:1 lipid/bolalipid). Images were captured under Floid cell imaging station 48 h of post transfection for visual comparison.

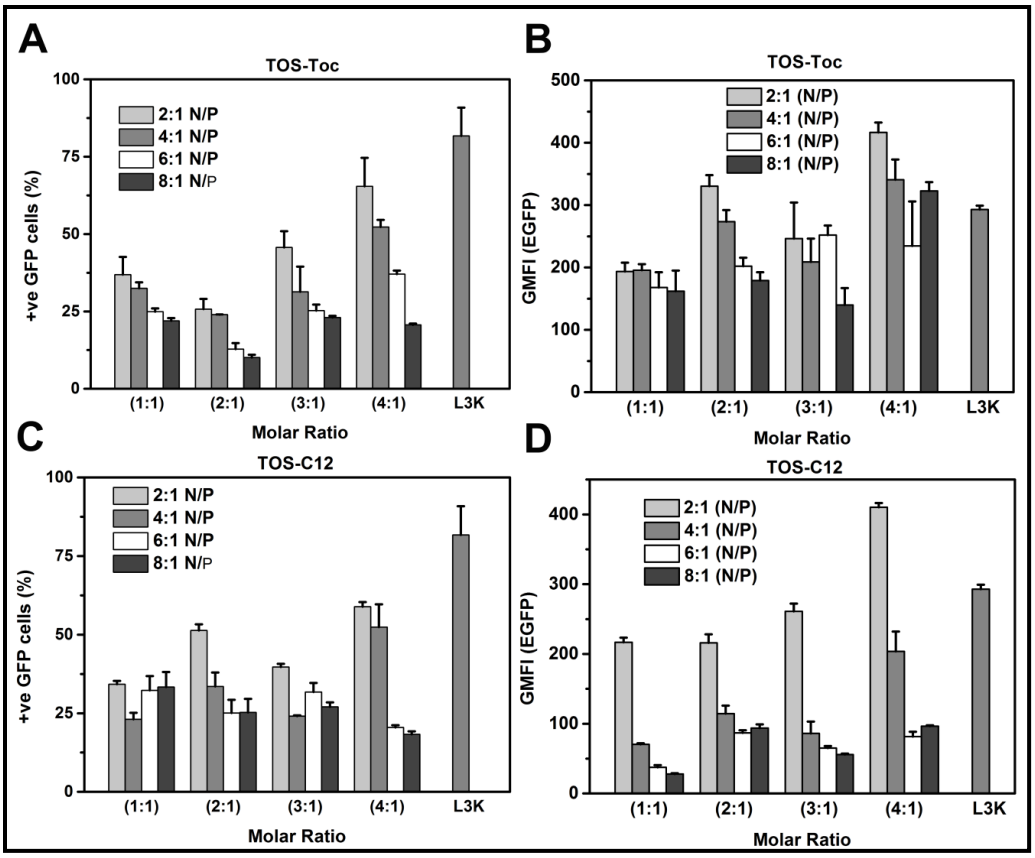

Fig. 6 Optimization of maximum transfecting molar and N/P charge ratios of bolaliposomes derived from TOS-Toc and TOS-C12 using transfection of *p*EGFP-N_3 plasmid in HEK293 cell line: A & B represents % GFP positive cells and GMF intensities of TOS-Toc and C & D represents % GFP positive cells and GMF intensities of TOS-C12 respectively obtained from flow cytometry after 48 h of transfection using *p*EGFP-N_3 plasmid (0.8 µg/well). (lipofectamine 3000:L3K). The data presented are the average of three experiments performed on three different days and the error bar represents the standard error.

The cell lines were analyzed to quantify the observed fluorescence under FACS and represented through Fig. 6(A-D). The two statistics of FACS (% GFP positive cells, GMFI) were considered to represent the gene expression activity, which summarizes that the maximum % GFP positive cells was observed for the formulation of 4:1 among the range (1:1-4:1) of molar varieties. Formulation 4:1 (molar ratio) of both cationic lipids exerts maximum transfection capacities by showing 68% of GFP positive cells, ~410 of

GMF intensity with TOS-Toc and 60% of GFP positive cells, ~400 of GMF intensity with TOS-C12. Particularly, it is found that at 2:1 N/P charge ratio, irrespective of molar formulation, both the lipids exerted maximum values of % GFP positive cells and GMF intensities. Therefore, it is confirmed that the 2:1 N/P ratio deserves the maximum potentials among all the studied N/P charge ratios. This would be further strengthened with the results of physicochemical characterization in the following sections. Certainly, the maximum transfection molar ratio 4:1 at 2:1 N/P charge ratio was considered as the optimized molar and charge ratios with both the cationic lipids.

Further evaluation of the transfection properties in different cell lines from different origin mandates the use of new delivering reagents towards the specific tissues for multipurpose delivery. It can be seen from the results shown in Fig. 7(a-d) that the GMF intensities of both the lipid formulations, TOS-Toc and TOS-C12, were found to be slightly better than the commercial standard, i.e., L3K, in all the cell lines studied except in Neuro 2A cell lines. However, the % GFP positive cells of both the lipid formulations were found to be similar to that of L3K in all the cell lines studied except HEK 293.

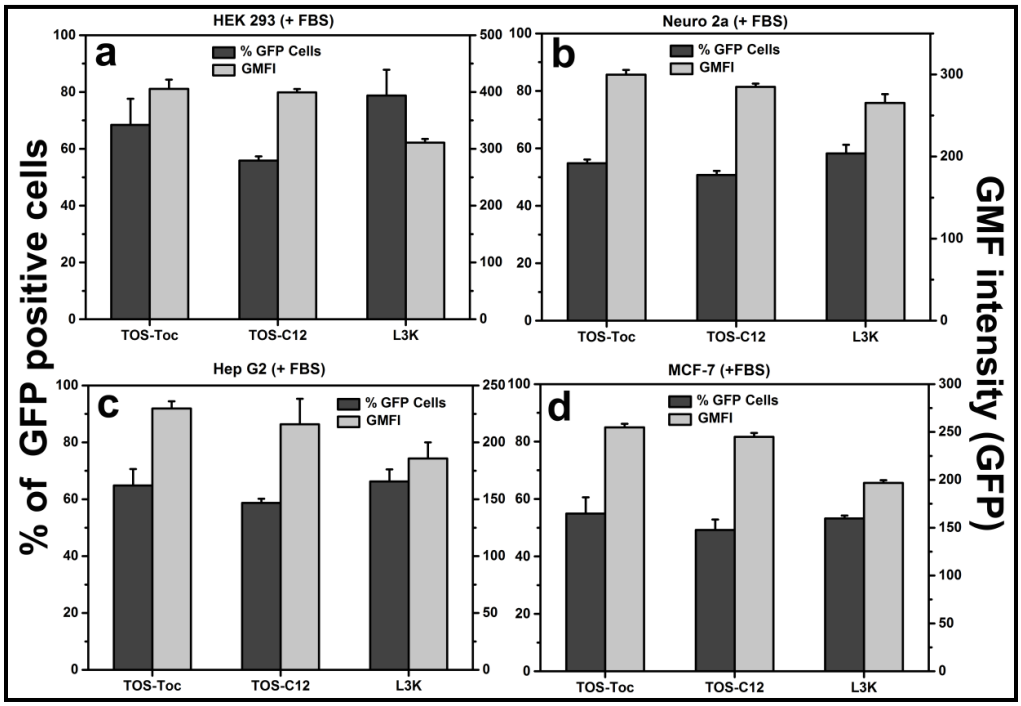

Fig. 7: Transfection efficiencies in terms of number of GFP positive cells (black) and GMF intensities (light gray) measured via FACS based analysis 48 h of post transfection carried out in a) HEK293, b) Neuro 2a, c) MCF-7 and d) HepG2 cell lines. Complexes were prepared from optimized molar ratio (4:1) of bolaliposome and pEGFP-N_3 plasmid (0.8 µg/well) at optimized N/P charge ratio (2:1) were incubated the cells in presence of 10% FBS containing DMEM.

5.2.4 Characterization of aggregates in terms of size and morphology: The study of physical aspects like size, shape and morphology of these suspended nano particles in water will provide the information regarding their pattern of self assembly for assessing their transfection potential and stability of particles. Fig. 8A demonstrates the particle diameters (nm) with respect to the varied mixed molar formulations of lipid/bolalipid at 1:0-4:1. The data indicates that the size of both the neat lipid formulations (1:0) (TOS-Toc/C12) is ~200 nm. As the concentration of the bolalipid is increased from 1:1 to 4:1, the size of bolaliposomes of both the lipids was observed to decrease. The saturation in size reduction is observed at 4:1, and further increase in the concentration of the bolalipid resulted in an increase in the size (data not shown for above 4:1). This may suggest the proper packing of bolaliposome was acquired at 4:1 ratio (~100 nm) of lipid/bolalipid. Thus, this supports the fact that maximum transfection results of both the lipids were optimized at this particular ratio.

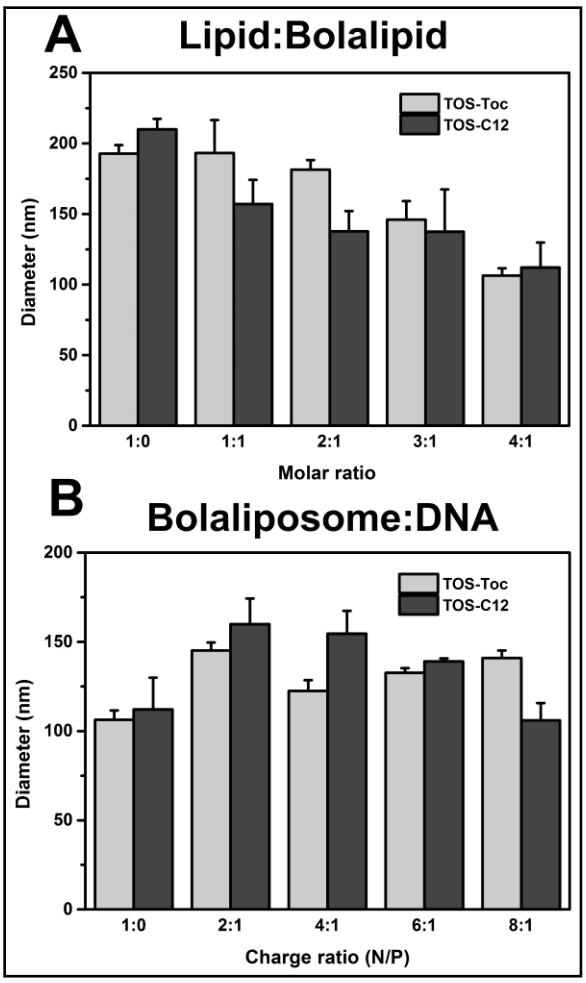

Fig. 8 Representative histograms A) depicts size in diameter of bolaliposomes were derived from mixing the various concentrations (1-4 mmol) of TOS-Toc (light gray) and TOS-C12 (black) with constant concentration (1 mmol) of bolalipid and (B) depicts the size in diameter of complexes were obtained by the mixing of bolaliposome (4:1 molar ratio) with constant amount of DNA (1 µg pEGFP-N_3) across the various (2:1, 4:1, 6:1 and 8:1) N/P charge ratios mentioned at the bottom.

Further, the hydrodynamic size of DNA derived complexes of optimized molar formulation (4:1) of both bolaliposomes (TOS-Toc:DBTPA & TOS-C12:DBTPA) were measured across the various charge ratios such as 2:1, 4:1, 6:1 and 8:1 at constant amount of DNA. The data represented in Fig. 8B indicates that the size of complexes at 2:1 (transfection active charge ratio) of both lipids is observed as 33 percent more in diameter

with its naked bolaliposome. The complex size of both lipids was slightly reduced at higher charge ratios like 6:1 and 8:1 due to the condensation of DNA. The maximum transfection capacities were observed particularly at 2:1 N/P ratio, where the optimal hydrodynamic diameters of the complexes were observed. This confirmed that the smooth wrapping of DNA at lower concentrations of lipids possibly helps to relieve DNA in cytoplasm.

Finally, to confirm the pattern of aggregations formed by different cationic species used in the present study, suspensions were directly visualized under the transmission electron microscope. The exact size, morphology and particulate distribution of liposomes, bolasomes and bolaliposomes derived from cationic lipids, bolalipid and cationic lipid/bolalipid can be assessed by the captured images represented in Fig. 9. The definite edge, particulate distribution, and range of size (100 nm to 200 nm) of all the neat aggregates except DBTPA clearly confirmed the bilayer membrane pattern. In contrast, the bolasome derived from DBTPA showed less than 50 nm size with particulate morphology, supporting the possibility of monolayer aggregation. The TEM images (Fig. 9D & 9E) of new mixed aggregates of lipid/bolalipid (bolaliposomes) were depicted as circular vesicles with definite edge showing compacted unilamellar boundary around the particle.

Therefore, based on size, shape and morphology results obtained for new bolaliposomal mixed aggregates, the proposed rationale for pattern of new aggregation may be justified in Fig. 2.

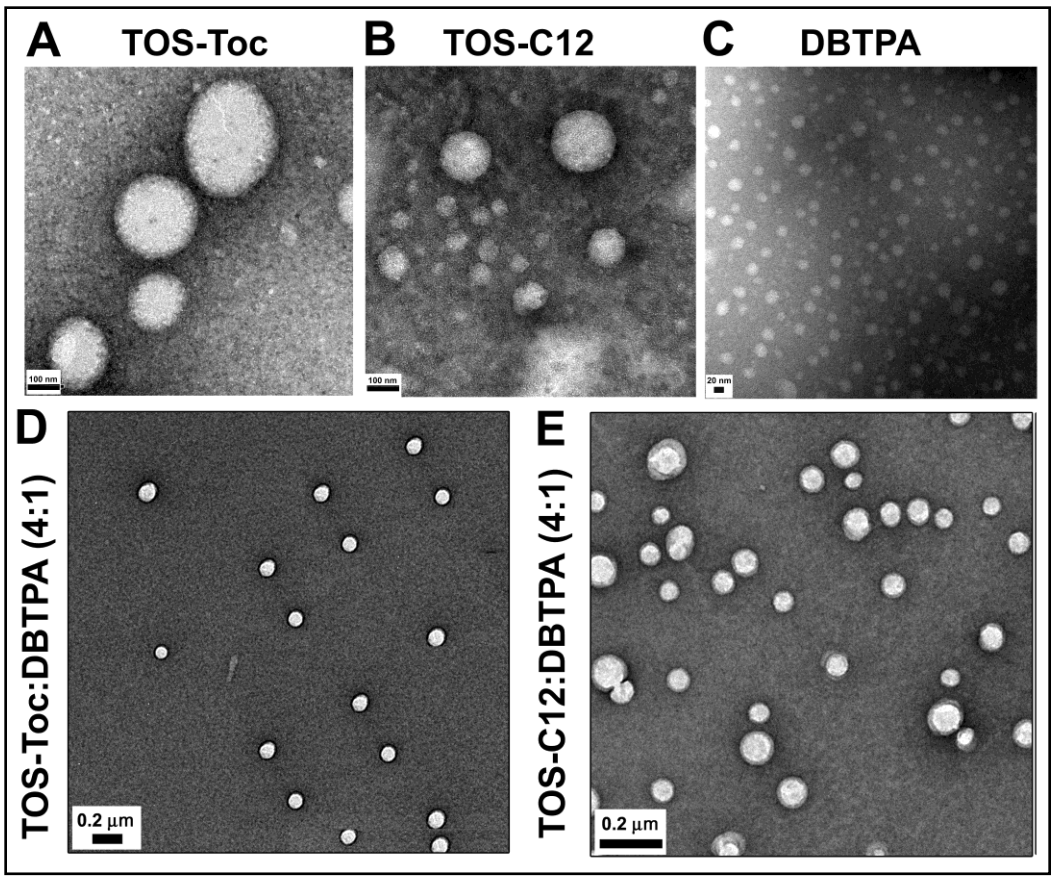

Fig. 9 Transmission electron microscopic images of neat cationic lipid TOS-Toc (A), TOS-C12 (B) and bolalipid DBTPA (C). D) & E) depicts the images derived from mixed aggregates obtained from lipid/bolalipid at transfection optimized molar ratios (4:1) of TOS-Toc and TOS-C12 respectively.

5.2.5 Study of DNA binding interactions of bolaliposomes: The delivering gene efficiencies of artificially prepared membranes are directly correlated to the strength of gene binding that arrives due to charge-charge electrostatic interactions of positive ends of lipid membranes and the negative dipole of nucleic acid. To evaluate these interactions, EtBr displacement and gel electrophoresis assays were conducted, and the results are represented in Fig. 10(A-D). The % drop down of maximum fluorescence value of DNA:EtBr complex upon sequential titration with lipid formulation is measured in EtBr displacement assay, whereas the retardation of mobility of DNA on agarose gel under electrophoretic conditions is observed from gel electrophoresis assay.

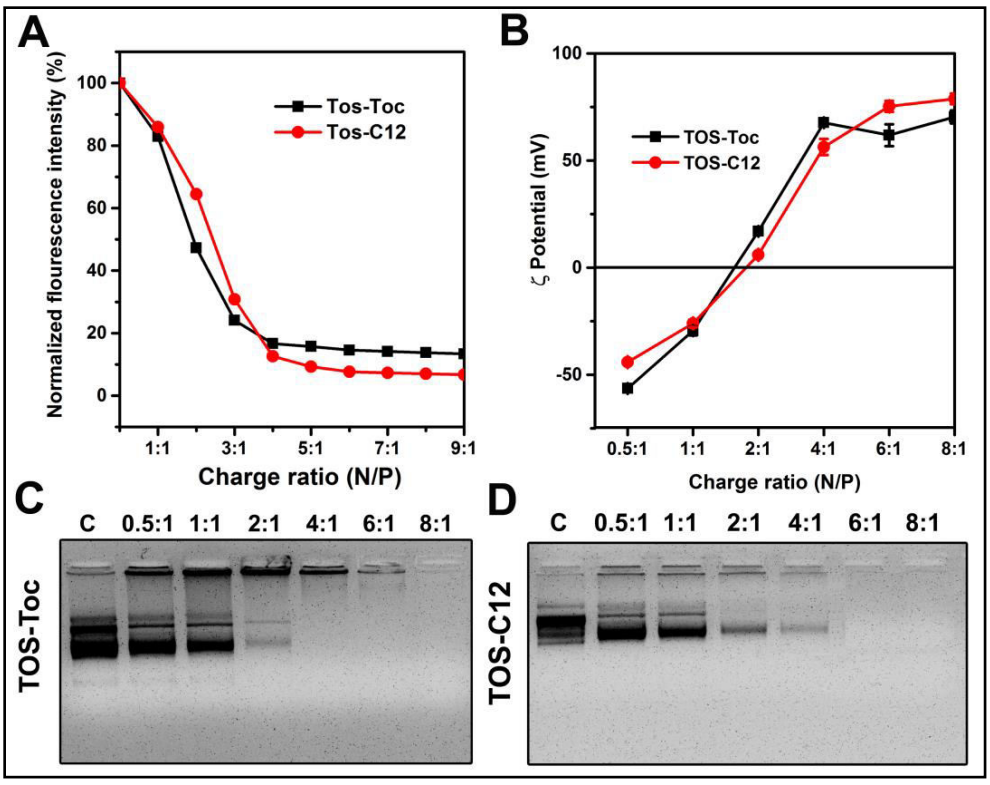

Fig. 10 DNA binding interaction studies of bolaliposomal formulation: A) EtBr displacement from DNA:EtBr complex upon titration of bolaliposome formulation (4:1) of TOS-Toc (square) and TOS-C12 (circle). Normalized fluorescent values across the increased concentration of formulation. B) zeta-potential of pEGFP-N_3DNA complexes derived from each bolaliposome with respect to the N/P charge ratios mentioned at the bottom, incubated in milli-Q for about 25 min prior to the measurements. C) & D) 1% agarose gel pictures captured post electrophoresis of pEGFP-N_3 DNA (0.3 µg/well) complexes derived from TOS-Toc and TOS-C12 respectively according to the charge ratios mentioned on top of each panel. Naked DNA served as control indicated as "C" on top of each panel.

EtBr is a common nucleic acid staining agent, which gains fluorescence properties upon binding with plasmid DNA due to intercalation with base pairs of *ds*DNA with close pi-pi stacking interactions. Progressive addition of bolaliposome suspension to CT-EtBr:DNA could displace the EtBr from the complex and led to a gradual drop in control fluorescence value and eventually leading to saturation. The amount of lipid that could

displace the maximum EtBr has the potential for optimal compaction of DNA, which would be responsible for finest binding of DNA. As the data provided through Fig. 10A shows that, for the lipid TOS-Toc, the fluorescence drop down is observed more than 50% at 2:1 and approximately 80% at 3:1 charge ratio. This was then turned to saturation on increasing the amount of TOS-Toc. However, the other lipid TOS-C12 displaced ~70% of EtBr at the ratio 3:1 (N/P) and also became saturated almost at the N/P ratio of 4:1.

To characterize the electrostatic interactions between the plasmid DNA and the present bolaliposomes as a function of lipid:DNA charge ratio, electrophoretic gel retardation assay is carried out using conventional gel electrophoresis. The electrophoretic mobility pattern of gel retardation assay revealed that the retardation of DNA was initiated even at very low charge ratios, viz. 0.5:1 and 1:1, in case of both the bolaliposomes (TOS-Toc and TOS-C12). It is also observed that for both the lipids, about 90% of DNA mobility was retarded at 2:1 N/P charge ratio and complete retardation of DNA was achieved at 4:1 N/P charge ratio (Figs. 10C & 10D). This was further supported by measuring the zeta potential of complexes derived from the charge ratios mentioned in Fig. 10B, which represents the neutralization of negative charge of DNA with successive addition of bolaliposome. The complexes surface potentials were initially negative, where the DNA was not properly complexed (0.5:1 & 1:1). The negative potential was turned to positive at 2:1 ratio, which was increased up to +60 mV (4:1) upon further addition of cationic suspension; the zeta potential appeared as saturated.

These observations resulted from gel electrophoresis, EtBr intercalation, and complex surface potentials are mutually consistent and provide sufficient justification that the maximum transfection was observed at 2:1 N/P charge ratio based on their optimal DNA compaction ability and complex stability.

5.2.6 Cellular uptake pathway analysis: Transport of extracellular material into the cytoplasm through plasma membrane involves many distinct kinds of pathways, which include participating number of proteins and receptors that complicate the mechanism.[38] The transfection efficiencies of the non-viral gene delivery systems seem to be linked to the internalization (endocytosis) of DNA associated complexes. The better transfection results of complexes derived from the newly formulated lipids (TOS-Toc and

TOS-C12) and their competing potentials with golden formulation (L3K) encourage us to gain insight of their internalization mechanism.

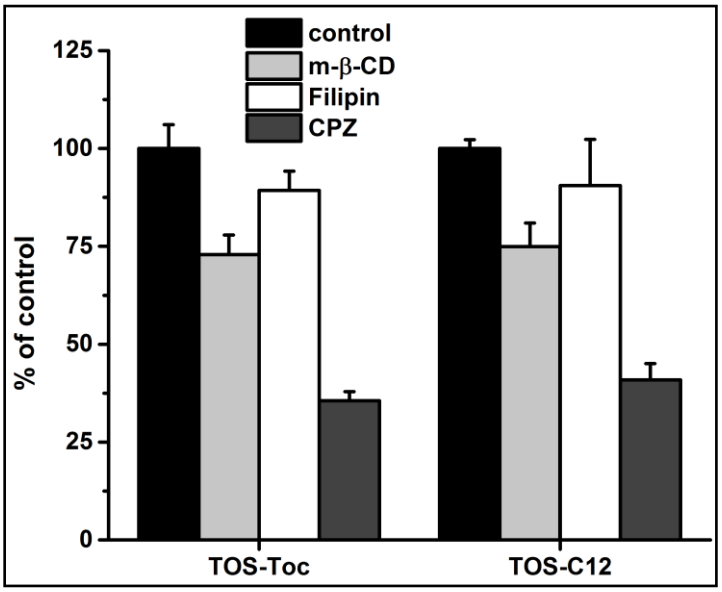

Fig. 12: Transfection using pEGFP-N_3 plasmid (0.8 µg/well) in HEK293 cell line in presence of endocytosis inhibitors: Normalized % of GFP +ve cells were obtained from GFP fluorescent quantification of two individual experiments at 48 h of post transfection. Cells were pretreated with the inhibitors (control: black), methyl-β-cyclodextrin (m-β-CD, light gray), Filipin-III (white) and chlorpromazine (CPZ, gray) for about 1 h before complex addition. Complexes were added to incubate further 4 h.

In order to ascertain internalization mechanism of these bolalipoplexes, we have attempted transfection experiment using the gene *p*EGFP-N_3 in HEK293 cells pretreated with inhibitors.[39] Indeed, the inhibitors are the chemical compounds used to block either some of the functional step or proteins responsible for endocytic mechanism. Initially, the cells were pre-treated with optimized concentrations of different pharmacological endocytosis inhibitors such as chlorpromazine (10 µg mL^{-1}, clathrin pathway inhibitor),[40] filipin-III (5µg mL^{-1}, caveolae pathway inhibitor)[41] and methyl-β-cyclodextrin (10 µg mL^{-1}, cholesterol depletion/clathrin and caveolar pathway inhibitor)[42] for about one hour. Cells were incubated with the complexes for about 4 h, and after the removal of the complexes, the incubation was continued to complete 48 h of

transfection period. The results demonstrated in Fig. 12 indicate that the maximum reduction of activity (~70%) was observed in the presence of CPZ inhibitor, whereas filipin inhibitor reduced ~15% activity, which confirms that the maximum internalization of these bolalipoplexes happens to be the clathrin mediated endocytosis. Significant activity reduction was observed with m-β-CD treated cells, which proved that these complexes were also sensitive towards the cholesterol presence on the plasma membrane. All the observations strengthen the fact that the complexes internalization depends on clathrin coated pits mediated endocytosis.

5.2.7 Cell viability: Toxicity is one of the main drawbacks associated with synthetic non-viral lipid based systems. Until and unless the reagents satisfy the viability issues, better transfection reagents would not be treated as good cytofectins to further *in vivo* experimentation.[43] To this extent, MTT cell based assay[44] was performed using the complexes derived from increasing concentrations (2:1 to 8:1) of both the formulations (TOS-Toc:DBTPA & TOS-C12:DBTPA) with constant DNA to screen their viabilities towards the cell lines, which were used for transfection (HEK293, MCF-7, Neuro-2a and HepG2). The cytotoxicity assay was carried out using neat lipids (TOS-Toc, ToS-C12 and DBTPA) as well in HEK293 and Neuro-2a cell lines (Fig. 13).

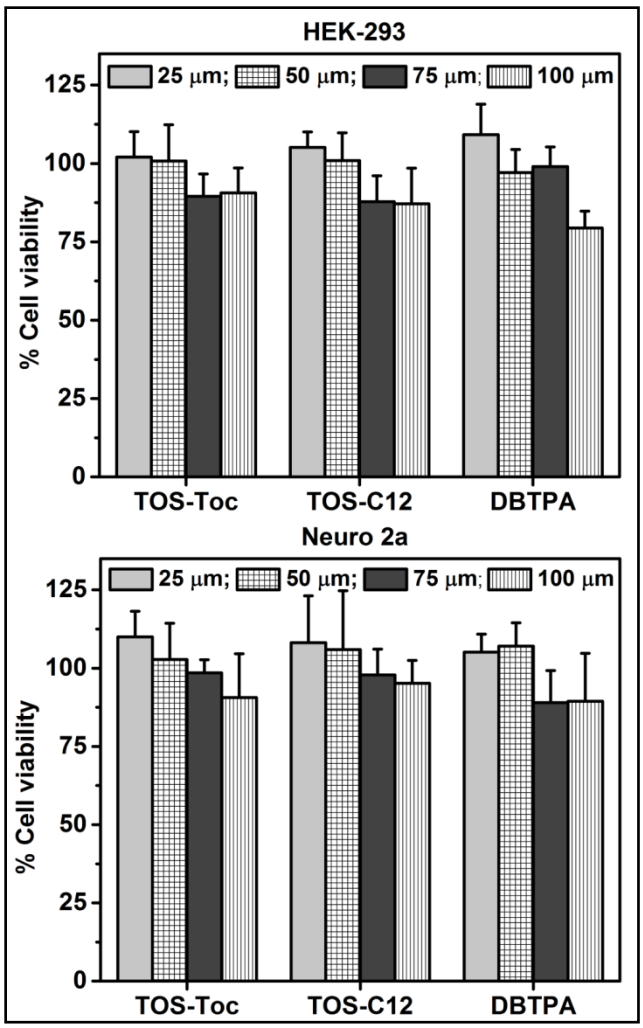

Fig. 13: Cell survival analysis based on MTT assay using neat aqueous suspensions of cationic lipids (TOS-Toc & TOS-C12) and cationic bolalipid (DBTPA). Average of three individual transfections was considered using four different concentrations ranging from 25 μm to 100 μm.

The calorimetric analysis of purple colored formazan granules developed from three individual experiments provided the mean value of percent cell viabilities with respect to the untreated control cells. Fig. 14 shows the results of viabilities of DNA derived complexes conducted across the various cell lines. This indicated that there is no toxicity with transfection optimized N/P charge ratios (2:1) and viabilities are decreasing with increasing charge ratios but not crossing down than the commercial cytofectin (L3K). However, lipid TOS-C12:DBTPA formulation showed comparatively lower

viabilities compared to other lipid formulations (TOS-Toc:DBTPA), particularly at higher N/P charge ratios (6:1 and 8:1). Importantly, the cell viability assay on neat lipids revealed that even at higher concentrations (100µm), these lipids were the least toxic (Fig. 13). Hence, the least cytotoxicities of these lipid formulations may be further exploited for systemic *in-vivo* gene transfection experiments and for designing of new less toxic bolaliposomal formulations.

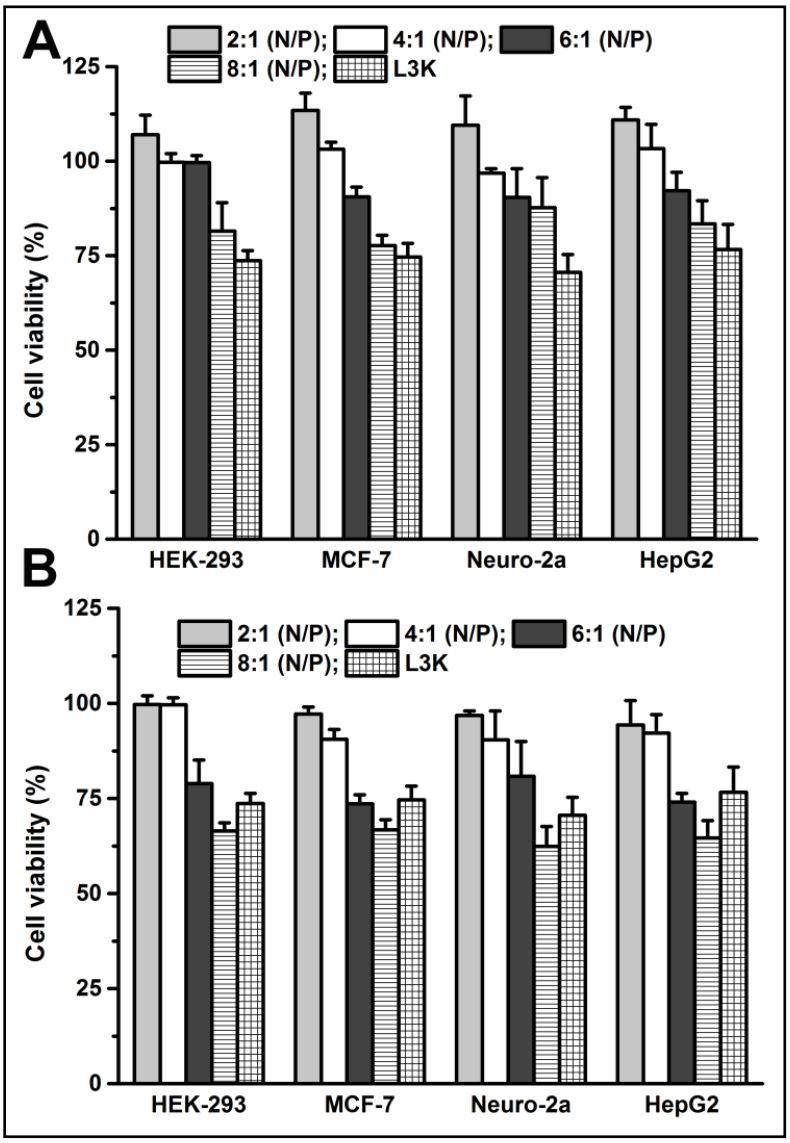

Fig. 14: MTT cell based assay results to represent the viabilities of various cell lines treated with the complexes derived from TOS-Toc:DBTPA (A) and TOS-C12:DBTPA

(B): Complexes of both bolaliposome formulations were prepared using the plasmid pEGFP-N_3 (0.3 µg/well) across the charge ratios ranging from 2:1 to 8:1 in 10% FBS+DMEM and incubated for 4 h.

5.3 CONCLUSIONS

Interestingly, the newly developed mixed lipid formulations of synthesized two distinct cationic surfactants such as tocopheryl succinate based cationic lipids (TOS-Toc & TOS-C12) and 1, 12 dodecane based bolaamphiphile (DBTPA) are giving enhanced transfection activity than their individual neat formulations, named as "bolaliposomes". These new nano-devices were studied with respective their size and morphology to witness their patterns of self assembly and interactions with DNA were elaborated for competing transfection potentials with golden standard L3K. In an attempt to find insight of transfection mechanism, inhibitor assay was done and proved that the DNA derived complexes are involving in clathrin mediated endocytosis while the internalization. Finally, the estimated toxicity results from MTT assay proved that the complexes are lower in toxicity and maintaining the transfection even in 10% serum rendering these formulations suitable for in vivo applications, thus mandating further exploration.

5.4 EXPERIMENTAL SECTION

5.4.1 Materials: All the biological, biochemical experiments and synthesis have been done by using the chemicals, reagents and solvents were procured from Sigma, Alfa Aeser and Spectrochem at highest purity and used directly without further purification. Mass spectral data were acquired by using a commercial LCQ ion trap mass spectrometer (Thermo Finnigan, SanJose, CA, U.S.) equipped with an ESI source. ^{1}HNMR spectra were recorded on Bruker (2001). SAINT (Version 6.28a) & SMART (Version 5.625). Bruker AXS Inc.,Madison, Wisconsin,USA. 3-(4, 5-dimethylthiazol-2-yl)-2,5-diphenyl-2H-tetrazolium bromide (MTT) was purchased from Calbiochem (Merck Millipore, Massachusetts, USA).Lipofectamine 3000 (L3K) was a generous gift from CCMB (Centre for Cellular and Molecular Biology, Hyderabad, India). Endotoxin free plasmid pEGFP-N_3 was obtained from laboratory stocks and purified using the Nucleo Bond Xtra

Midi plus EF (MACKAREY-NAGEL, Duren, Germany). Fetal Bovine Serum (FBS) was procured from Thermo Fischer Scientific (Gibco®).

5.4.2 Chemistry: (Scheme 1) Synthesis of TOS-Ac: To a stirred cooled suspension of alpha-tocopheryl succinate (1.06 g, 2 mmol) in 25 mL of dry DCM were added propargyl amine (0.128 mL, 2 mmol), DIPEA (0.418 mL, 2.4 mmol) and EDCI.HCl (0.46 g, 2.4 mmol) sequentially. After 1 h of stirring at 0 ºC the temperature was raised to the room temperature and continued the stirring until complete conversion of starting materials (~16 h). The reaction mixture was extracted in to excess of dichloromethane (100 mL), and then washed with water (2 X 50 mL) and brine (1 X 50 mL). The solvent was removed under vacuum to afford a crude product, which was further purified by silica gel column chromatography using 1% MeOH: $CHCl_3$ as eluent and yielded a colorless amorphous solid, 0.985 g (1.74 mmol, 87.144%) ^{1}H NMR (400 MHz, $CDCl_3$) δ 5.86 (*s*, 1H), 4.05 (*dd*, *J* = 4 Hz, 2H), 2.99 (*t*, *J* = 8 Hz, 2H), 2.63 – 2.58 (*m*, 4H), 2.21 (*t*, *J* = 4 Hz, 1H), 2.08 – 1.96 (*m*, 9H), 1.82– 1.74 (*m*, 2H), 1.55 – 1.06 (*m*, 25H), 0.87 – 0.83 (*m*, 12H). ESI-MS: 568.43 $[M+H]^+$.

Synthesis of alpha-tocopheryl-2-azidoacetate: To a vigorously stirred solution of alpha-tocopherol (1.075 g, 2.5 mmol) in pyridine (3 mL) and dichloromethane (5 mL) was added a solution of 2-bromoacetylbromide (1 g, 5 mmol) in 5 mL of dichloromethane slowly about 10min. The resulting mixture was then allowed to stir at 0 °C for 3 h, which was diluted using 1 N HCl (50 mL). The diluted aqueous solution was extracted in to dichloromethane. The crude residue was obtained by removing the solvent under reduced pressure after careful washing with saturated $NaHCO_3$ (2 X 25 mL), water (30 mL) and brine (30 mL). The resultant residue was purified by column chromatography with 60-120 mesh silica gel using petroleum ether as the eluent. The obtained bromo derivative (1 g, 1.82 mmol) was further subjected to reflux with stirring using sodium azide (0.59 g, 9.1 mmol) in acetonitrile (10 mL); the solvent was removed under vacuum after 16 h of reflux. The resultant residue was dissolved in water and extracted in to ethyl acetate. The pure azide derivative was obtained as yellowish oil without any further purification by removing the solvent using rotary evaporation. Yield

(0.99 g, 1.93 mmol, 92.86%). ^{1}H NMR (400 MHz, $CDCl_3$) δ 4.16 (*s*, 1H), 2.59 (*t*, *J* = 8 Hz, 2H), 2.10 (*s*, 3H), 2.03 (*s*, 3H), 1.98 (*s*, 3H), 1.84 – 1.73(*m*, 2H), 1.57 – 1.05 (*m*, 24H), 0.87 – 0.83 (*m*, 12H).

Synthesis of 2-azido-*N*-dodecylacetamide: To an ice cooled solution of dodecylamine (0.55 g, 2.97 mmol), K_2CO_3 (2 g, 14.5 mmol) in 25 mL of DCM was added 2-bromoacetylbromide (1.2g, 5.9 mmol) in 25 mL of dichloromethane slowly about 10min and then continued the stirring for 1 h at 0 ºC, the resultant reaction mixture was raised to room temperature and allowed stirring for about 6 h. The crude residue was obtained by removing the solvent under reduced pressure after fine washing with water (30 mL) and brine (30 mL). The resultant residue was purified by column chromatography with 60-120 mesh silica gel using EtOAc: petroleum ether as the eluent. The obtained bromo derivative (0.7 g, 2.29 mmol) was further subjected to reflux with stirring using sodium azide (0.744 g, 11.45 mmol) in acetonitrile (10 mL); the solvent was removed under vacuum after 16 h of reflux. The resultant residue was dissolved in water and extracted in to ethyl acetate; the pure pale yellow colored solid was obtained without any further purification by removing the solvent using rotary evaporation, yield (0.6 g, 2.24 mmol, 97.6%). ^{1}H NMR (400 MHz, $CDCl_3$) δ 6.30 (*s*, 1H), 3.99 (*s*, 2H), 3.28 (*m*,2H), 1.54 – 1.51 (*m*, 2H), 1.28 (*s*, 18H), 0.88 (*t*, 3H).

General method for "click" synthesis: To a stirred solution of acetylene-derivative 1 mmol (TOS-Acetylene) and azide-derivative 1 mmol (alpha-tocopheryl-2-azidoacetate/2-azido-*N*-dodecylacetamide) in THF: *tert*-BuOH: H2O (2:2:1; 20 ml) were added $CuSO_4.5H_2O$ (0.1mmol) and sodium ascorbate (0.4 mmol) simultaneously. The resulting mixture was stirred at room temperature until complete conversion of the starting material, which was diluted with excess of water (100 mL) then extracted in to ethyl acetate (3X 50 mL) and the solvent is dried upon anhydrous $NaSO_4$to remove remained traces of water followed by removal of solvent under reduced pressure. The compound showing the R_f in the range 0.5 – 0.7 in 9:1 $CHCl_3$: MeOH, was purified using column chromatography with the eluent 2-3% MeOH: $CHCl_3$.

Click adduct (I): Pale yellow colored solid was obtained from TOS-Ac and alpha-tocopheryl-2-azidoacetate, yield (0.98 g, 0.91 mmol). ^{1}H NMR (400 MHz, $CDCl_3$) δ 7.72 (*s*, 1H), 6.37 (*s*, 1H), 5.37 (*s*, 2H), 4.55 (*s*, 2H), 2.97 (*t*, *J* = 4 Hz, 2H), 2.62 – 2.55 (*m*, 6H), 2.07 – 1.93 (*m*, 18H), 1.81 – 1.75 (*m*, 4H), 1.57 – 1.07 (*m*, 48H), 0.87– 0.83(*m*, 24H). ESI-MS: 1081.82 $[M+H]^+$.

Click adduct (II): Yellow colored solid was obtained from TOS-Ac and 2-azido-*N*-dodecylacetamide, yield (0.75 g, 0.9 mmol). ^{1}H NMR (400 MHz, $CDCl_3$) δ 7.84 (*s*, 1H), 6.89 (*s*, 1H), 6.51 (*s*, 1H), 5.08 (*s*, 2H), 4.16 (*s*, 2H), 3.16 – 3.19 (*m*, 2H), 2.87 (*t*, *J* = 4Hz, 2H), 2.67 (*t*, *J* = 4 Hz, 2H), 2.41 (*t*, *J* = 8 Hz), 2.08 – 1.86 (*m*, 9H), 1.71 – 1.69 (*m*, 2H), 1.51 – 1.08 (*m*, 42H), 0.87 - 0.83 (*m*, 15H). ESI-MS: 836.66 $[M+H]^+$.

General method for the synthesis of titled lipids: The purified click adducts (0.5 mmol) was refluxed in sealed tube using MeI (10 eq.) and acetonitrile (5 ml) to afford the quaternized triazolium compound after 48 h. Finally the pure title lipid (TS-Toc, TS-C12) was obtained by subjecting the triazolium iodide salt to repeated chloride ion exchange chromatography using amberlyst A-26 chloride ion exchange resin and about 100mLof chloroform as eluent.

TOS-Toc: colorless powder, yield (123 mg, 85%).^{1}H NMR (500 MHz, $CDCl_3$) δ 9.23 (*s*, 1H), 8.30 (*t*, *J* = 5 Hz, 1H), 5.72 (*s*, 2H), 4.73 (*d*, *J* = 10 Hz, 2H), 4.38 (*s*, 3H), 2.93 (*t*, *J* = 5 Hz, 2H), 2.71 (*t*, *J* = 10 Hz, 2H), 2.57 (*t*, *J* = 5 Hz, 4H), 2.07 – 1.94 (*m*, 18H), 1.80 – 1.74 (*m*, 4H), 1.53 – 1.07 (*m*, 48H), 0.87 – 0,83 (*m*, 24H). ^{13}C NMR (101 MHz, $CDCl_3$) δ 172.62, 171.93, 163.19, 150.08, 149.36, 142.34, 140.49, 139.90, 132.79, 126.79, 126.21, 125.11, 117.77, 117.39, 75.35, 75.09, 39.38, 37.79, 32.75, 27.99, 24.81, 24.46, 22.69, 21.03, 20.57, 19.72, 13.16, 12.65, 11.98.ESI-MS (HRMS): Calcd for $[C_{68}H_{111}N_4O_7]^+$: 1095.8447, Found: 1095.8536.

TOS-C12: brownish gummy solid, yield (123 mg, 85%).^{1}H NMR (400 MHz, $CDCl_3$) δ 8.54 (*s*, 1H), 7.40 (*s*, 1H), 7.15 (*s*, 1H), 5.28 (*s*, 2H), 4.61 (*s*, 2H), 4.30 (*s*, 3H), 3.26 – 3.21 (*m*, 2H), 2.97 (*t*, *J* = 4Hz, 2H), 2.67 (*t*, *J* = 4 Hz, 2H), 2.59 (*t*, *J* = 8 Hz), 2.08 – 1.96 (*m*, 9H), 1.78 – 1.75 (*m*, 2H), 1.58 – 1.05 (*m*, 42H), 0.90 - 0.83 (*m*, 15H).^{13}C NMR (101 MHz, $CDCl_3$) δ 172.47, 171.90, 162.74, 149.41, 141.56, 140.50, 131.50, 126.70,

124.99, 123.01, 117.47, 101.83, 75.15, 57.21, 55.41, 50.64, 40.23, 39.37, 38.32, 37.40, 32.79, 31.78, 31.08, 30.05, 29.73, 28.63, 27.98, 27.03, 24.81, 24.46, 22.67, 21.05, 20.58, 19.72, 14.13, 12.95, 12.11, 11.82.ESI-MS (HRMS): Calcd for $[C_{51}H_{88}N_5O_5]^+$: 850.6780, Found: 850.6933.

Scheme 2: Synthesis of (S)-but-3-yn-1-yl 2-((tert-butoxycarbonyl)amino)-3-phenylpropanoate (1a): To an ice cold solution of boc-l-phenylalanine(0.53 g, 2 mmol) in 10 mL of dry DCM, *N, N*-dicyclohexylcarbodiimide (0.5 g, 2.4 mmol), *N, N*-dimethylaminopyridine (0.293 g, 2.4 mmol) were added consecutively. After 5 min of stirring at 0 ºC, but-3-yn-1-ol (0.15 mL, 2 mmol) was added. The resulting reaction mixture was stirred for another 1 h at 0 ºC, then allowed it to raise to the room temperature and continued the stirring for overnight. The solvent was removed under reduced pressure; the resulting residue was redissolved in 50 mL of ethyl acetate and washed with water (3 X 25 mL) and brine (30 mL). The organic layer was dried upon anhydrous Na_2SO_4 and evaporated under vacuum. Finally, the crude was loaded on to the column chromatography using 60-120 mesh silica gel, the compound was eluted using ethyl acetate: pet. ether as eluent. Yield: white amorphous solid, 0.585 g (1.84 mmol, 92.27%). ^{1}H NMR (400 MHz, $CDCl_3$) δ 7.31– 7.24 (*m*, 3H), 7.16 (*d*, *J* = 4 Hz, 2H), 4.99 (*d*, *J* = 4 Hz, 1H), 4.62 (*dd*, *J* = 8, 4 Hz, 1H), 4.22 (*t*,*J* = 4 Hz, 2H), 3.10 (*d*, *J* = 4Hz, 2H), 2.49 (*td*, *J* = 4 Hz, 2H), 2.01 (*t*, *J* = 4 Hz, 1H), 1.42 (*s*, 9H).

Synthesis of 1, 12-diazidododecane (1b): A mixture of 1, 12-dibromododecane (0.33 g, 1 mmol), NaN_3 (0.65 g, 10 mmol) in 5 mL of DMF was refluxed under stirring for about 16 h at 80 ºC. After confirming the reaction progress using TLC, the contents were cooled to room temperature and diluted with 1N HCl (50 mL). The compound was then extracted in to ethyl acetate (3 X 50 mL). All these organic fractions were collectively washed with water (50 mL), saturated $NaHCO_3$ (50 mL) and brine (50 mL). The solvent was dried upon anhydrous $NaSO_4$ and removed the solvent under reduced pressure to obtain the titled compound which was enough pure to proceed further reaction without any further purification. Yield: colorless liquid, 0.24 g (0.95 mmol, 96%). ^{1}H NMR (400 MHz, $CDCl_3$) δ 3.26 (t, *J* = 7.0 Hz, 4H), 1.61 (dd, *J* = 14.4, 7.2 Hz, 4H), 1.39 – 1.26 (m, 16H).

Synthesis of Boc-DBTPA (1c): To a stirred solution of acetylene-derivative 1a (0.5 g, 1.58 mmol) and azide-derivative 1b (0.2 g, 0.79 mmol) in THF:*tert*-BuOH:H_2O (2:2:1; 20 ml) were added $CuSO_4.5H_2O$ (0.04 g, 0.16mmol) and sodium ascorbate (0.079 g, 0.4 mmol). The reaction mixture was stirred at room temperature until complete conversion of the starting material monitored on TLC(~24 h).The reaction mixture was diluted with excess of water (100 mL) then extracted in to ethyl acetate three times (3X 50 mL) and evaporate the solvent under reduced pressure after dried upon anhydrous $NaSO_4$. The compound showing the R_f = 0.5 in 9:1 $CHCl_3$: MeOH, was purified using column chromatography with the eluent 2-3% MeOH: $CHCl_3$. Yield: colorless liquid, 1.285 g (1.45 mmol, 92.44%). ^{1}H NMR (400 MHz, $CDCl_3$): δ 7.29 – 7.22 (*m*, 8H), 7.10 (*d*, *J* = 8, 4H), 4.99 (*d*, *J* = 8, 2H), 4.56 - 4.51 (*m*, 2H), 4.37 (*d*, *J*= 4 Hz, 2H), 4.29 (*t*, 4H), 3.04 (*d*, *J*= 8 Hz, 8H), 1.87 (*t*, *J*= 4 Hz, 4H) 1.41 (*s*, 18H), 1.28 (*m*, 16H).

Synthesis of DBTPA: To a stirred solution of compound 1c (1 g, 1.13 mmol) in 10 mL of dry DCM was added 5 mL of TFA slowly at 0 ºC, and continued the stirring at room temperature by overnight. To remove the excess TFA present in reaction mixture was exposed to repeated rotary evaporations by adding ethyl acetate. Yield: beige solid, 1 g (1 mmol, 99.99%). ^{1}H NMR (400 MHz, DMSO-d_6): δ 8.50 (*s*, 3H), 8.31 (*s*, 3H), 7.88 (*s*, 2H), 7.34-7.26 (*m*, 10H), 7.19 (*t*, *J*= 6.8 Hz, 2H), 4.34 – 4.19 (*m*, 8H), 3.09 (*t*, *J*= 6.4 Hz, 4H), 2.75 (*t*, *J*= 6.8 Hz, 4H) 1.76 (*d*,*J*= 6.4 Hz,4H), 1.20 (*d*, *J*= 6.4 Hz, 16H).^{13}C NMR (100 MHz, DMSO-d_6) δ 144.72 (s), 135.86, 129.97, 129.47, 127.78, 127.54, 122.68, 79.65, 60.90, 54.08, 53.68, 49.57, 48.98, 36.51, 31.15, 30.19, 29.66, 29.33, 28.83, 26.31.ESI-MS (HRMS): Calcd for [$C_{38}H_{55}N_8O_4^{2+}$]: 687.4341, Found: 687.4793.

5.4.3 Preparation of bolaliposomes (lipid: bolalipid): All the newly developed aggregates (bolaliposome) from both the cationic lipids (TOS-Toc & TOS-C12) were prepared by the lipid hydration method as described before (30, 31). The ten formulations of each lipid with bolalipid (DBTPA) were generated with varying molar ratios of lipid: bolalipid ranging from 1:1 to 10:1. Briefly, thin lipid films were produced by mixing appropriate amount of lipid solution from freshly prepared individual chloroform stocks. The resulted volumes were dried uniformly under a thin flow of moisture-free nitrogen

gas and subjected to reduced pressure for a limited time period of four hours. The dried lipid films were hydrated with autoclaved water to a final lipid concentration of 1 mmol and kept for overnight. These rehydrated films were disturbed vigorously by vortexing at room temperature, to produce multi lamellar vesicles which were subjected to probe sonication in an ice bath using a SONICS Vibra cell (25% Amplitude, pulse mode, 9 s on/off) until clarity. These optically clear aqueous suspensions were stored at 4 °C until use, no precipitation was observed even after one month.

5.4.4 Size and surface potential measurements: The suspended nano-aggregates (bolaliposome) of both the lipids TOS-Toc and TOS-C12 in water were characterized in terms of hydrodynamic diameter and zeta potential using a SZ-100 NEXTGEN (HORIBA) instrument, set at 25°C and equipped with a diode-pumped solid-state laser at λ 532 nm. Simultaneously, complexes derived from DNA (pEGFP-N3) and varying range lipid concentrations were analyzed in presence of milli-Q in a quartz cuvette. The instrument was programmed to sum the average of five different measurements done in general mode by using the software SZ-100, HORIBA.

The surface potential of the prepared complexes were also measured in the same instrument using Laser Doppler Electrophoretic Analysis with provided SZ-100 software. Here, Milli-Q served as the blank control for instrument autocorrelation and sample dilutions.

5.4.5 Transmission electron microscopy: The pattern of aggregation and particle size distribution of the cationic bolaliposomes were examined using a JEOL JEM 2100 Transmission Electron Microscope operated at 120 kV. Briefly, a drop (4 µL) of liposomal suspension (1 mmol) was applied on to a standard 300 mesh carbon coated copper grid surface and allowed to adsorb for about 1 min and wicked off with sterile tissue paper. This was followed by negative staining using 2% uranyl acetate to visualize the vesicles under transmission electron beam conditions. Excess stain was removed after 45 sec and the grids were air dried at room temperature before the TEM analysis. The images were acquired on a Gatan camera, Digital Micrograph software.

5.4.6 Gel retardation assay: The electrophoretic mobility retardation of DNA on assembling with new cationic lipid formulations was examined using a typical agarose gel electrophoresis assay. Both the lipid formulations were used to prepare varying range (0.5:1 to 8:1) of lipid:DNA complexes at a constant amount (0.3 µg) of pEGFP-N_3 plasmid, in 20 µL of milli-Q. The complexes were incubated for 30 min at room temperature, prior to the electrophoresis. Samples were loaded onto 1% agarose gel electrophoresis was done for 90 min at 70V in TAE running buffer. Gel images were captured under transillumination at 300 nm using GENESYS imaging software.

5.4.7 Et-Br Displacement assay: The intercalating agent ethidium bromide is used as a probe in the displacement assay to assess the lipid/DNA binding interactions. The fluorescent quantum yield of control EtBr:DNA was decreased gradually on sequential titration of cationic lipid suspension leads to displacement of EtBr from control complex. Fluorescence measurements were recorded using a Hitachi F-7000 fluorescence spectrophotometer at excitation and emission wavelength of 516 nm and 598 nm respectively (slit width 5 nm X 5 nm). Briefly, baseline fluorescence (0%) was established using 0.23 µg EtBr in 20 mM Tris.HCl buffer (pH 7.4). Thereafter, pEGFP-N_3 DNA (2.3 µg) was introduced and mixed to set the instrument at 100% fluorescence value. Constant amount of cationic lipid suspension was added sequentially to vary the N/P ratios from 0.5:1 to 8:1 to the EtBr:DNA solution and measured the resultant retardation in fluorescence after each titration. The fluorescence values were normalized with respect to the EtBr:DNA complex.

5.4.8 Amplification and purification of plasmid DNA: The plasmid *p*EGFP-N_3vector encoding the Enhanced Green Fluorescent Protein was obtained from laboratory stocks. *Escherichia. Coli* DH-5α strain was used as competent cells to do the transformation. Plasmid was amplified in LB broth media at 37 °C overnight. The endotoxin free plasmid was purified using the NucleoBond® Xtra Midi kit (MACKAREY-Nagel). The concentration and purity of the plasmids were quantified using the Nano Drop 2000 and agarose gel electrophoresis that confirmed the plasmid integrity and quality.

5.4.9 Cell Culture: The adherent cell lines (mouse neuroblastoma (Neuro-2a), human hepatocellular carcinoma (HepG2), human embryonic kidney (HEK-293) and Chinese hamster ovary (CHO) chosen for all transfections were used from laboratory maintenance stocks. Cell lines were cultured in 25 cm^2 flasks in 6 mL of DMEM (Dulbecco's Modified Eagles medium, Invitrogen) containing 10% (v/v) Fetal Bovine Serum, 10 mmol $NaHCO_3$, 50 µg/ml streptomycin, 60 µg/mL penicillin, and 30 µg/ml kanamycin respectively.

5.4.10 Transfection Biology: All transfections were performed using pEGFP-N_3 plasmid in various cell lines having different origin. Cell lines were seeded on to 24 well plates maintaining the density 40,000 cells/well before the day of transfection. Complexes were prepared using the bolaliposomal formulations at required ratios using 0.8 µgpEGFP-N_3 plasmid per well in serum free DMEM, followed by incubation for about 30 min. The cells in the wells were washed using PBS 100 µL/well, and were added incubated complex after formulating to –FBS+DMEM and +10%FBS+DMEM transfection complexes using plain and 20XFBS containing DMEM respectively. Subsequently, the cells were allowed for 4 h of incubation with complex containing media, was replaced with fresh 10%FBS+DMEM continued the incubation for another 44 h. The transfection was terminated by removing the media and washed the cells using PBS (100 µL/well), the cells were detached by adding 1X trypsin-EDTA (100 µL/well) and resuspended in to 10%FBS+PBS (400 µL/well). The cells expressing EGFP was quantified using a FACS Calibur flow cytometer (Becton-Dickinson) equipped with an argon ion laser at 488 nm for excitation and detection at 530 nm. 10,000 cells were analyzed for each sample using the software, Cell Quest. Non transfected cells served as live cell controls for gate settings which in turn provided the cutoff thresholds for quantification of fluorescent cell population.

Treatment with inhibitors: For transfection using inhibitors experiment, cells were incubated with chlorpromazine(CPZ, 10 µg ml−1), filipin-III (5 µg ml−1) and methyl-β-cyclodextrin (m-β-CD, 10 mg ml−1) (all from Sigma) in normal cell culture medium for 1 h at 37 °C. Consequently, the lipoplexes derived from the bolaliposomal

formulations were incubated for 4 h. Finally, the cells were trypsinized and collected in 10% FBS containing PBS, followed by analysis using FACS.

5.4.11 Floid cell imaging for GFP expression: The qualitative analysis of transfection of newly developed mixed aggregates were assessed initially using the live cell imaging of cells treated with pEGFP-N3 plasmid derived complexes after 48 h of post transfection. Multiple times of (more than two) transfections was done and imaged separately under microscope (Floid™ Cell Imaging Station) with and without fluorescent light, fine images were selected for qualitative analysis report.

5.4.12 Cell viability assay: Each of the cell lines was transfected with lipoplexes using the efficient bolaliposomal formulations (4:1) at varied range of N/P charge ratios (2:1 to 8:1) with 0.3 µg/well pEGFP-N_3 plasmid and L3K lipoplexes as well after 24 h of cells seeding (10 000 cells per well) in 96 well tissue culture plates. Lipoplexes were incubated with cells for about 4 h. Cell viabilities were analyzed at 48 h from the addition of complexes. The cell viabilities were determined using conventional MTT based assay. The percentage data interpretation was made by taking viabilities of control cells (untreated cells) as 100%.

5.5 REFERENCES

1. Naldini, L., *Nature*. **2015**, *526*, 351.
2. Ginn, S.L.; Alexander, I. E.; Edelstein, M. L.; Abedi, M. R.; Wixon, J. *J Gene Med.* **2013**, *15*, 65.
3. Jin, L.; Zeng, X.; Liu, M.; Deng, Y.; He, N. *Theranostics*. **2014**, *4*, 240.
4. Nayerossadat, N.; Maedeh, T.; Ali, P. A. *Adv Biomed Res.* **2012**, *1*, 27.
5. Yin, H.; Kanasty, R. L.; Eltoukhy, A. A.; Vegas, A. J.; Dorkin, J. R.; Anderson, D. G. *Nat Rev Genet.* **2014**, *15*, 541.
6. Thomas, C. E.; Ehrhardt, A.; Kay, M. A. *Nature Rev Genet.* **2003**, *4*, 346.
7. Mintzer, M. A.; Simanek, E. E. *Chem Rev.* **2008**, *109*, 259.

8. Felgner, P. L.; Gadek, T. R.; Holm, M.; Roman, R.; Chan, H. W.; Wenz, M.; Northrop, J. P.; Ringold, G. M.; Danielsen, M. *Proc. Natl. Acad. Sci. U.S.A.* **1987**, *84*, 7413.
9. Srinivas, R.; Samanta, S.; Chaudhuri, A. *Chem Soc Rev.* **2009**, *38*, 3326.
10. Karmali, P. P.; Chaudhuri, A. *Med Res Rev.* **2007**, *27*, 696.
11. Balazs, D. A.; Godbey, W. T. *J Drug Deliv.* **2010**, *2011*.
12. Du, Z.; Munye, M. M.; Tagalakis, A. D.; Manunta, M. D.; Hart, S. L. *Sci. Rep.* **2014**, *4*, 7107.
13. Fasbender, A.; Marshall, J.; Moninger, T. O.; Grunst, T.; Cheng, S.; Welsh. M. J. *Gene Ther.* **1997**, *4*, 716.
14. Bhattacharya, S.; Bajaj, A. *Chem. Commun.* **2009**, *31*, 4632.
15. Kedika. B.; Patri, S. V. *J. Med. Chem*, **2010**, *54*, 548.
16. Kedika, B.; Patri, S. V. *Bioconjug Chem.* **2011**, *22*, 2581.
17. Gosangi, M.; Mujahid, T. Y.; Gopal, V.; Patri, S. V. *Org. Biomol. Chem.* **2016**, *14*, 6857.
18. Kumar, K.; Maiti, B.; Kondaiah, P.; Bhattacharya, S. *Org. Biomol. Chem*. **2015**, *13*, 2444.
19. Prasad, K. N.; Kumar, B.; Yan, X. D.; Hanson, A. J.; Cole, W. C. *J Am Coll Nutr.* **2003**, *22*, 108.
20. Duhem, N.; Danhier, F.; Pourcelle, V.; Schumers, J. M.; Bertrand, O.; LeDuff, C. S.; Hoeppener, S.; Schubert, U. S.; Gohy, J. F.; Marchand, B. J.; Préat, V. *Bioconjugate Chem.* **2013**, *25*, 72.
21. Noh, S. M.; Han, S. E.; Shim, G.; Lee, K. E.; Kim, C. W.; Han, S. S.; Choi, Y.; Kim, Y. K.; Kim, W. K.; Oh, Y. K. *Biomaterials*, **2011**, *32*, 849.
22. Kang, Y. H.; Lee, E.; Choi, M. K.; Ku, J. L.; Kim, S. H.; Park, Y. G.; Lim, S. J. *Int. J Cancer*, **2004**, *112*, 385.
23. Youk, H. J.; Lee, E.; Choi, M. K.; Lee, Y. J.; Chung, J. H.; Kim, S. H.; Lee, C. H.; Lim, S. J. *J Control. Release*, **2005**, *107*, 43.
24. Akinc, A.; Thomas, M.; Klibanov, A. M.; Langer, R. *J Gene Med,* **2005**, *5*, 657.
25. Sharma, V. D.; Ilies, M. A. *Med. Res. Rev.* **2014**, *34*, 1.

26. Patil, S. P.; Kim, S. H.; Jadhav, J. R.; Lee, J. H.; Jeon, E. M.; Kim, K. T.; Kim, B. H. *Bioconjugate Chem.* **2014**, *25*, 1517.
27. Khan, M.; Ang, C. Y.; Wiradharma, N.; Yong, L. K.; Liu, S.; Liu, L.; Gao, S.; Yang, Y. Y. *Biomaterials,* **2012**, *33*, 4673.
28. Fuhrhop, J. H.; Wang, T. *Chem. Rev.* **2004**, *104*, 2901.
29. Brunelle, M.; Polidori, A.; Denoyelle, S.; Fabiano, A. S.; Vuillaume, P. Y. *Comptes Rendus Chimie*, **2004,** *12*, 188.
30. Jain, N.; Arntz, Y.; Goldschmidt, V.; Duportail, G.; Mély, Y.; Klymchenko, A. S. *Bioconjug Chem.* **2010**, *21*, 2110.
31. Marshall, K. E.; Morris, K. L.; Charlton, D.; O'Reilly, N.; Lewis, L.; Walden, H.; Serpell, L. C. *Biochemistry*, **2011**, *50*, 2061.
32. Tamamis, P.; Adler-Abramovich, L.; Reches, M.; Marshall, K.; Sikorski, P.; Serpell, L.; Gazit, E.; Archontis, G. *Biophys. J.* **2009**, *96*, 5020.
33. Rostovtsev, V. V.; Green, L. G.; Fokin, V. V.; Sharpless, K. B. *Angewandte Chemie*, **2002**, *114*, 2708.
34. Cheng, X.; Lee, R. J. *Adv. Drug Deliv. Rev.* **2016**, *99*,129.
35. Mochizuki, S.; Kanegae, N.; Nishina, K.; Kamikawa, Y.; Koiwai, K.; Masunaga, H.; Sakurai, K. *(BBA)-Biomembranes*, **2013**, *1828*, 412.
36. Dua, J. S.; Rana, A. C.; Bhandari, A. K. *Int. J. Pharm. Stud. Res*, **2012**, *3*, 14.
37. Bajaj, A.; Kondiah, P.; Bhattacharya, S. *J Med Chem.* **2007**, *50*, 2432.
38. Medina-Kauwe, L. K.; Xie, J.; Hamm-Alvarez, S. *Gene Ther.* **2005**, *12*, 1734.
39. Govindarajan, S.; Kitaura, K.; Takafuji, M.; Ihara, H.; Varadarajan, K. S.; Patel, A. B.; Gopal, V. *Int J Pharm.* **2013**, *446*, 87.
40. Vercauteren, D.; Vandenbroucke, R. E.; Jones, A. T.; Rejman, J.; Demeester, J.; De Smedt, S. C.; Sanders, N. N.; Braeckmans, K. *Mol Ther.* **2010**, *18*, 561.
41. Orlandi, P. A.; Fishman, P. H. *J Cell Biol.* **1998**, *141*, 905.
42. Rodal, S. K.; Skretting, G.; Garred, Ø.; Vilhardt, F.; Van Deurs, B.; Sandvig, K. *Mol Biol Cell.* **1999**, *10*, 961.
43. Lv, H.; Zhang,S.; Wang, B.; Cui, S.; Yan, J. *J. Control. Release.* **2006**, *114*, 100.
44. Hansen, M. B.; Nielsen, S. E.; Berg, K. *J Immunol Methods,* **1989**, *119*, 203.

Publications

1) **Mallikarjun, G**., Thasneem, Y. M., Vijaya, G., Srilakshmi, V. P. (2016) Effects of heterocyclic-based head group modifications on the structure–activity relationship of tocopherol-based lipids for non-viral gene delivery. ***Org. Biomol. Chem.*** **14, 6857-6870. (SCI Journal, Impact factor-3.559)**

2) **Mallikarjun, G**., Hithavani, R., Srilakshmi, V. P. (2016) Delocalizable Cationic Head Group based alpha-Tocopherol Derived Gemini Cationic Lipids for Improved Transfection Efficiency of Plasmid Delivery -***Manuscript has been communicated.***

3) **Mallikarjun, G**., Hithavani, R., Srilakshmi, V. P. (2017) Novel 1, 2, 3-Triazolium Based Dicationic amphiphiles Synthesized by using Click-chemistry Approach for Efficient Plasmid Delivery -***MedChemComm., 8,*** **999.**

4) **Mallikarjun, G**., Hithavani, R., Srilakshmi, V. P. (2016) Effect of side chain functionality of head group of a cationic lipid on the gene transfection using newly synthesized α-tocopherol based cationic lipids ***–Manuscript under preparation.***

5) **Mallikarjun, G**., Hithavani, R., Venkatesh, R., Srilakshmi, V. P. (2017) Evolution of New "Bolaliposomes" using Novel α-Tocopheryl Succinate-based Cationic Lipid and 1, 12-Disubstituted Dodecane-based Bolaamphiphile for Efficient Gene Delivery -***Bioconjugate Chem (in press)***

Conferences

1. **Poster: Mallikarjun, G**., Thasneem, Y. M., Vijaya, G., Srilakshmi, V. P. "Effect of Head Group Modifications on the Structure-Activity Relationship of Tocopherol based Lipids" at ***14th FAOBMB Congress & 84th Annual meeting of SBC (I) Current Excitements in Biochemistry and Molecular Biology for Agriculture and Medicine***, from 24th -30th November, 2015.

2. **Poster:** Mallikarjun, G., **Hithavani, R.,** G., Srilakshmi, V. P. "Targeted Gene Delivery to Liver: Tocopherol Based Lipids" at ***International Symposium on Bioorganic Chemistry (ISBOC-10)*** held at IISER Pune, June 11-15, 2015.

3. **Conference attended**: "***International Conference on Chemical Biology Disease Mechanisms and Therapeutics (ICCB-2014)"*** held at IICT-Hyderabad from February 6-8, 2014.